

This electronic thesis or dissertation has been downloaded from the King's Research Portal at <https://kclpure.kcl.ac.uk/portal/>



**Studies Investigating Sub-2 m Particle Stationary Phase Supercritical Fluid Chromatography and Application to Profiling of Natural Products and Drug Discovery Research**

Jones, Michael David

*Awarding institution:*  
King's College London

The copyright of this thesis rests with the author and no quotation from it or information derived from it may be published without proper acknowledgement.

**END USER LICENCE AGREEMENT**



**Unless another licence is stated on the immediately following page** this work is licensed

under a Creative Commons Attribution-NonCommercial-NoDerivatives 4.0 International

licence. <https://creativecommons.org/licenses/by-nc-nd/4.0/>

You are free to copy, distribute and transmit the work

Under the following conditions:

- Attribution: You must attribute the work in the manner specified by the author (but not in any way that suggests that they endorse you or your use of the work).
- Non Commercial: You may not use this work for commercial purposes.
- No Derivative Works - You may not alter, transform, or build upon this work.

Any of these conditions can be waived if you receive permission from the author. Your fair dealings and other rights are in no way affected by the above.

**Take down policy**

If you believe that this document breaches copyright please contact [librarypure@kcl.ac.uk](mailto:librarypure@kcl.ac.uk) providing details, and we will remove access to the work immediately and investigate your claim.



Studies Investigating Sub-2  $\mu\text{m}$  Particle Stationary Phase  
Supercritical Fluid Chromatography and Application to  
Profiling of Natural Products and Drug Discovery Research

Michael D. Jones

A THESIS SUBMITTED IN PARTIAL FULFILMENT OF THE REQUIREMENTS  
FOR THE DEGREE OF DOCTOR OF PHILOSOPHY

Analytical and Environmental Science  
School of Biomedical Sciences

2016

Supervisors:

Dr. Norman W. Smith

Dr. Cristina Legido-Quigley

## **Dedication**

I dedicate this thesis to my parents, David and Michaela Jones. My father instilled in me the importance of education, holding to your convictions, and following through on your commitments. My mother enlightened me about the importance of patience, compromise, and a steadfast mind. If not for all these learnings, this journey would have been far more difficult.

## Acknowledgments

Embarking down the path of doctorate of philosophy degree is one that I thought I would never have taken, particularly at a point in my life when I was settled in with life and family. Interestingly, the spark of scientific research supported by Waters Corporation combined with enlightening remarks from those I look up to, and inspired by the PhD students at King's I have met over the years provided the unique catalyst that persuaded a decision to begin and accomplish such a journey. For this, I am grateful and honoured that I had the opportunity to be guided by Dr. Norman Smith. Norman was my lighthouse 'across the pond' helping me stay on course through these *sometimes* foggy years.

I am forever indebted to Dr. James Heaton, Dr. Cristina Legido-Quigley and Dr. Nicola Gray for initially challenging me to make the commitment to the program at King's College. Their persistent belief in me was refreshing and enabled my self-confidence to capitalize on an opportunity that could have easily been ignored. I truly enjoyed our discussions about chromatography, their companionship, and inclusive camaraderie. I not only learnt a great deal about analytical science, but also a great deal about the importance of fellowships when continuing on such a path

Guidance and mentorship is such an important ingredient to successfully completing an enduring path. I am especially thankful to Dr. Rob Plumb for teaching me how to plan tactically for challenging tasks and Dr. John Langley for teaching me a certain sense of humbleness in science, of which I am still learning.

Many have helped, whether it was in the form of insightful discussion, reviewing written thoughts, or giving me a swift kick of motivation. So, particularly to the last point, special thanks goes to Dr. Paul Rainville and Dr. Sean M. McCarthy.



I would like to thank all my collaborators; Dr. Bharathi Avula (University of Mississippi), Dr. Vladimir Shulaev (University of Northern Texas), Yasah Vezele (University of Rhode Island), and Dr. Giorgis Isaac (Waters Corporation) for working together on such interesting research studies.

I was extremely fortunate to have worked with many at Waters Corporation, particularly for the many insightful conversations about the technology and general SFC principles. I would like to specifically note a special thanks to Warren Potts III, John Van Antwerp, Andrew Aubin, Dr. Paula Hong, Jenifer Simeone, Dr. Jacob Fairchild, and Dr. Uwe Neue.

Finally, I thank my family. My wife Amy and son Austin have maintained patience and endured sacrifices to support the completion of this thesis. Their continuing understanding allowed me to finish this journey. With its completion, I look forward to more time spent with Amy, Austin and our new little girl Kennedy.

## Abstract

The aim of this thesis was to investigate a novel prototype supercritical fluid chromatography instrumentation optimized to exploit the theoretical benefits of sub-2  $\mu\text{m}$  particle stationary phases and determine the benefits of its applied use towards the discovery and early drug development of new chemical entities found in natural products. The prototype supercritical instrument was designed to reduce the system and extra-column volumes in order to reach the theoretical efficiencies of a sub-2  $\mu\text{m}$  particle stationary phase. The system was also designed to decrease baseline noise and drift via design improvements of the  $\text{CO}_2$  solvent delivery by the pump, updated backpressure regulator needle and seat designs, and optimization of UV detector design that accounts for  $\text{CO}_2$  refractive indices rather than typical liquid mobile phases used in reversed phase liquid chromatography. The prototype instrument was also designed to improve the sample introduction to the flow stream, thus to improve the applied use of the instrument allowing the analyst to attain highly reproducible results that would be required for improved qualitative separations, semi-quantitative statistical profiling, and quantitative commercial use determinations. Supercritical fluid chromatography utilizes  $\text{CO}_2$ -based mobile phases with unique properties associated with improving solvation, lowering mobile phase viscosity and exploring a wide range of polarity of solutes. Natural products have a complexity of compounds varying in polarity requiring a variety of analytical techniques resulting in numerous chromatographic profiles. The goal of this research is to prove the benefits of this novel technology to natural product research, specifically in the field of discovering new molecular entities and drug discovery workflows. Establishing the usefulness of a new technology and its potential impact to new therapeutic discovery requires a large gap of experimentation and education to be filled prior to any immediate implementation.

The thesis will study four distinct requirements to validate the benefits of a new technology: Review of the theory and past challenges with SFC, Investigate the proof-of-principle attributes of the prototype instrumentation, assess the practicality of its use relative to analytical scientist's needs when working in a commercial industry, and applicability towards drug discovery and early development workflows when derived from natural products. The proof-of-principle attributes study the theoretical promise of sub-2  $\mu\text{m}$  particle columns when employed with an optimized SFC instrument and overall system performance. The practicality of the novel instrumentation will investigate methodology variables affecting chromatography and approaches interfacing with mass spectrometry. The knowledge gained from these preliminary studies combined with a review of previous research enable the applied use of the novel technology towards the drug discovery workflow as it pertains to necessary lead discovery, lead optimization, process development, and early analytical method development. The applied approaches investigated within this thesis include reaction monitoring of candidate drug substance syntheses' and comprehensive profiling of natural products as these are critical activities in the discovery and early development of commercialized drug products.

In this thesis, insight was provided regarding SFC theory, previous uses, instrument design and reasons why researchers found limitations in terms of performance hindering the progress of their research to be adopted for commercial use. The discussions and studies regarding the new design combined with the results presented in Chapters 1 and 2. They illustrate the key points to these past challenges and how they were addressed with the prototype instrument. The preliminary studies exploring the new designs use with sub-2  $\mu\text{m}$  particle size columns indicated good reproducibility for a mixture of 18 analytes. The preliminary investigation efficiency, retention and peak shape attributes were affected by a multitude of properties related to mobile phase homogeneity, density variations and

insolubility. Two parameters of which are related to instrument design and performance, whereas insolubility is due mostly in part of the analysts knowledge of the analyte solubility. All of which require the necessary education on part of the user in order to increase their success in using a supercritical fluid chromatographic approach. In some comparisons, the results from an optimized instrument design to those previously published with a non-optimized instrument design place into question the conclusions from their results.

Instrument design is important to understand and defines a basis for general expectations of the results to come once it's employed for analytical determinations. The practicality of the instrument design can be better understood when methodology variables are taken into consideration. In chapters 3 and 4, one factor at a time (OFAT) and multivariate approaches are explored to determine the variables that effect chromatographic separations, information rich data, and interfacing with mass spectrometry. In addition, these chapters highlight the importance of troubleshooting techniques that help distinguish system related effects versus chemistry related effects based on experimental observations and reason that could cause retention time drift, peak splitting, peak distortion, and ionization efficiency. More importantly, evidence of the various retention mechanisms affecting the selectivity, retention and resolution of analytes; but more specifically, structurally related small molecule (>1500 Da) analytes analogous to those observed in natural product profiling and reaction monitoring and process optimization syntheses. The examples show how the column choice can greatly impact the selectivity of a mixture of structurally related impurities and the retention behaviour of biologically related molecules such as differing lipid classes and lipid species found in natural product sources.

Natural products have numerous structural analogues with a wide variety of polarity. The discovery and eventual commercialization of any natural product synthetically derived chemical entities require reaction synthesis and process optimization which is monitored

analytically. In the final chapters, the technology is applied to these application areas of chemical substituent profiling and synthesis monitoring. One of the applications is focused on the typical procedures and workflows practiced in the lead optimization and process development groups employed in the pharmaceutical or chemical material industry. The application investigates the reaction synthesis monitoring of three small molecules chosen either for their unique stereochemical properties and relationship to derived natural product entities. The reasoning for this investigation was due in part of proving the sustainability of the technique and novel technology design improvements for use by the industry in terms of post discovery of a new chemical entity. The examples in this chapter show the benefit of a high efficiency separation using the SFC approach when compared to UHPLC, the effectiveness to determine recovery values, the ability to troubleshoot synthetic route issues, and an approach to streamline chiral and achiral screening on a single chromatographic system. One of the highlights demonstrates the optimized SFC instrument as a tool for a column agnostic screening approach to aid process optimization of a synthetic reaction during the clopidogrel experiments.

The final applied approach explores the chemical profiling of two species of chamomile and multivariate analysis of a collection of chamomile commercially available products. Chamomile was chosen due to its long history of being used as a medicinal plant. Chamomile has been reported to contain therapeutic compound classes ranging in polarity and derivatives of sesquiterpenes, flavonoids, polyacetylenes, terpenoids, and coumarins, Due to chamomiles diversity and amount of published content related to the characterization of composition, it was deemed as an appropriate representative test case to use to investigate this new SFC technology and compare to other chromatographic techniques. The chapter highlights the sub 2um SFC technology and the benefits of identification of 6 new chemical entities with the aid of multivariate statistical analysis the separation profile. This was

achieved by the enhanced selectivity benefits of a SFC approach. The results also concluded the use single quadrupole detector was capable to distinguish between authentic and adulterated chamomile commercial products.

## List of Figures

Figure 1.1 Chemical process for natural product discovery [7].....	5
Figure 1.2: Schematic of a modern liquid chromatograph system configured with ultraviolet light detection coupled to mass spectrometry. ....	14
Figure 1.3: Nomenclature of a chromatogram. Adapted from Ettre [24]. ....	15
Figure 1.4: Conceptual representation of a theoretical plate and division within in a column	21
Figure 1.5: van Deemter Plot showing contribution of A, B, and C terms on HETP. Figure courtesy of Waters Corporation .....	24
Figure 1.6: Illustration of a sample loop fitting within the injection valve of a chromatographic system highlighting the ‘gap’ contributing to dispersion and sample carryover. ....	25
Figure 1.7: Phase diagram illustration for carbon dioxide.....	30
Figure 1.8: Two dimensional phase diagram representing a unified region derived from Chester <i>et al</i> [37].....	36
Figure 1.9: Core components schematic of the Waters ACQUITY UPC <sup>2</sup> instrumentation with MS detection and make-up flow. Figure courtesy of Waters Corporation. ....	45
Figure 1.10: Schematic representation of two different commercial designs of pumping mechanism delivering liquid CO <sub>2</sub> . Figure courtesy of Waters Corporation. ....	47
Figure 1.11: Schematic representation of two different injector designs; single (A) and dual (B) valve designs used in autosamplers for SFC instrumentation. ....	49
Figure 1.12: Schematic of a commercially available splitter from Waters Corporation (Courtesy of Waters Corp.).....	54

Figure 1.13: Schematic of a ‘home-made’ splitter designed to minimize make-up flow sample dilution when interfaced to MS in order to maximize sensitivity. ....	55
Figure 2.1: Initial prototype SFC instrumentation design utilizing modified ACQUITY UPLC pump, autosampler and detector designs and Thar modified automated back pressure regulator instrumentation. ....	63
Figure 2.2: Electronic pressure and temperature measuring device. (A) Pressure transducers. (B) Thermocouples. ....	71
Figure 2.3: BEH Technology particle synthesis based on ethylene bridged bonding provided courtesy of Waters Corporation .....	73
Figure 2.4: Prototype SFC instrument analysis of the 18 component test mix. The UV chromatogram is the results of 6 injections overlaid. ....	75
Figure 2.5: Elution volume trend plot for acetone for an isocratic 5% modifier elution method. Column: BEH HILIC 3.0 mm x 100 mm; 1.7 $\mu$ m .....	76
Figure 2.6: Effect of isocratic modifier with decreasing flow rate. ....	78
Figure 2.7: Influence of % modifier using a Sunfire 4.6 x 150 mm; 5 $\mu$ m, 40 $^{\circ}$ C, flow rate was 4.0 mL/min, BPR=200 bar. (Courtesy of J.L. Veuthy, U. Geneva) .....	79
Figure 2.8: Effect of modifier percent on peak shape.....	80
Figure 2.9: Comparison of carbamazepine under isopycnic conditions at different flow rates. ....	82
Figure 2.10: Effect of increased mixing on (a) baseline noise, (b) low %modifier/low flow, (c) varied % modifier, and (d) decreased column i.d.....	84
Figure 2.11: Effect of increasing column length with low volume mixer .....	86
Figure 2.12: Flow rate versus retention factor ( $k$ ) for isobaric and isopycnic evaluations of carbamazepine.....	88

Figure 2.13: Isopycnic trend plot comparison for hybrid 3.0 mm internal diameter columns packed with 5 $\mu\text{m}$ particles and 1.7 $\mu\text{m}$ particles. ....	90
Figure 2.14: van Deemter curve comparing the efficiency differences while running in an isobaric outlet pressure state (classical approach) versus an isopycnic (constant density) state. The results are plotted as plate height versus linear velocity.....	91
Figure 2.15: Van Deemter plots comparing two separate experiments on two prototype instruments.....	93
Figure 2.16: $\text{CO}_2$ + 5% methanol modifier isopycnic plot (reproduced with permission from A. Tarafder) overlaid with operating parameters from Figure 2.6. and Figure 2.13. ....	95
Figure 3.1: Peak distortion comparisons of 0.2 mg/mL 4-HBB standard between polar solvent DMSO and non-polar solvent heptane/IPA 9:1 for 0.5 $\mu\text{L}$ , 2 $\mu\text{L}$ , and 5 $\mu\text{L}$ injection volumes on an ACQUITY UPC <sup>2</sup> BEH, 3.0 mm x 100 mm; 1.7 $\mu\text{m}$ column.....	113
Figure 3.2: CSH Fluoro-phenyl UPC <sup>2</sup> /UV results showing peak distortion of 4-HBB for polar solvents DMA, DMF, NMP, and DMSO including the non-polar solvent heptane/IPA (9:1). ....	114
Figure 3.3: Evidence probe plume pulsation (circled in blue) in MS TIC during a blank injection.....	116
Figure 3.4: Investigating capillary voltage for basic and neutral pharmaceutical compounds .....	117
Figure 3.5: MS TIC sensitivity comparisons of Phosphatidylglycerol (PG) and Phosphatidylethanolamine (PE) lipids when varying capillary voltage .....	118
Figure 3.6: Investigating desolvation temperature.....	119
Figure 3.7: MS TIC comparison of different post-column addition ‘make-up’ flow compositions for an unknown mixture of analytes. The blue box represents benefits of water	



addition. The green box represents similarities of base and weak base addition. The red box represents the benefits of strong base addition to the make-up flow. ....	121
Figure 3.8: Comparison of sensitivity with MS splitter versus full flow into the MS without splitter (n = 3 for each condition for each analyte and the average was reported.) ....	122
Figure 3.9: Column screening results with peak tracking confirmed by MS. The modifier (B) was methanol with 2g/L ammonium formate. 5% to 30% B over 5 min and held at 30% for 1 min. ....	126
Figure 3.10: MS spectral analysis of EP impurity C for the doublet peaks observed when using the UPC <sup>2</sup> CSH Fluoro-phenyl stationary phase. ....	127
Figure 3.11: MS ESI+ TIC of a degraded standard solution of metoclopramide EP impurity F. ....	129
Figure 3.12: Normalized x-axis overlay metoclopramide analyzed with extended 12- and 35-minute gradient run times flattening the slope compared to the 6-minute screening experiments. The original gradient was used; 5% to 30% B. ....	130
Figure 3.13: Highlighted in this overlay, the addition of acetonitrile to the composition of the modifier increased the resolution of the later eluting analytes. ....	131
Figure 3.14: Peaks with hydroxyl (or polyphenols) functionality such as impurity H tend to benefit from the use of only formic acid, as shown in Figure 3.14A. Optimal peak shape observed for compounds with primary, secondary, and tertiary amine functionality trend from the use of ammonium salt-based additives as with impurity F, shown in Figure 3.14B .....	132
Figure 3.15: Injections of an expired metoclopramide sample performed with different additive compositions in the modifier. Combining ammonium formate with formic acid in terms of a “buffer-like” system provided the best peak shape for all analytes in the sample. The modifier used was 50:50 methanol/acetonitrile. ....	133

Figure 3.16: Comparing the effect of chain length on retention between ACQUITY UPC <sup>2</sup> BEH vs. ACQUITY UPC <sup>2</sup> C <sub>18</sub> SB stationary phases. ....	135
Figure 3.17: Comparing the effect of acyl chain saturation on retention between ACQUITY UPC <sup>2</sup> BEH vs. ACQUITY UPC <sup>2</sup> C <sub>18</sub> SB stationary phases. The 18:0/18:0 data points were added from the acyl chain length experiments to illustrate agreement with each trend .....	136
Figure 3.18: Isopycnic results in black versus isobaric results in red. Gradient occurs during the first 3 minutes only. Increased density earlier in the gradient decreased retention for these polar analytes. ....	137
Figure 3.19: MS ESI+ TIC of the separation of lipids Mix 1 showing the retention drifting, loss of resolution and loss of sensitivity over 200 injections.....	138
Figure 3.20: Trend plot for calculating the difference and percent difference between injection #1 and injection #236.....	139
Figure 3.21: Overlay comparison of injections performed over 13 days of injections using the mobile phase with both additives composed of 1 g/L ammonium formate and 1% formic acid .....	140
Figure 4.1: Replicate injections of the system suitability test mix performed using the UPC <sup>2</sup> BEH column.....	152
Figure 4.2: Overlay of the system suitability test mix injected over 16 hours on the UPC <sup>2</sup> BEH 2-EP column.....	152
Figure 4.3: UPC <sup>2</sup> system pressure increase plotted for the system suitability test mix injections on the UPC <sup>2</sup> BEH 2-EP column .....	153
Figure 4.4: System suitability test mix results performed using the UPC <sup>2</sup> 2-EP column and ammonium formate/formic acid methanol modifier conditions. ....	155

Figure 4.5: cLogP versus BEH 2-EP retention time results for the 300 compounds where the colors are represented by stereochemistry and the size of the point is represented by molecular weight.....	158
Figure 4.6: LogSw versus BEH 2-EP retention time results for the 300 compounds where the colors are represented by stereochemistry and the size of the point is represented by the BEH 2-EP tailing factor results.....	159
Figure 4.7: cLog <i>P</i> versus BEH 2-EP tailing results for the 300 compounds where the highlighted yellow colors are represented by clog <i>P</i> values > 3.0. The greater the size of the data point was represented by greater retention.....	160
Figure 4.8: 2-EP tailing results versus BEH 2-EP retention times for the 300 compounds where the increasing size of the data point refers to increasing clog <i>P</i> values.....	161
Figure 5.1: Reaction scheme for route synthesis of rosuvastatin calcium expanded to illustrate the reaction stages (R(#)) monitored by UPC <sup>2</sup> /MS and UPLC/MS.....	170
Figure 5.2: Reaction Scheme for the synthesis of Imatinib expanded to illustrate the reaction stages A thru G monitored by UPC <sup>2</sup> /MS and UPLC/MS. ....	172
Figure 5.3: Reaction scheme for the synthesis of clopidogrel expanded to illustrate the reaction stages (x) monitored by UPC <sup>2</sup> /MS and UPLC/MS.....	174
Figure 5.4: UV/MS chromatographic traces of the nitro pyrimidine intermediate and spectral analysis comparison of the intermediate product and unknown by-product performed at cone voltage = 80 V. Maxplot is defined as photodiode array data collection for a range of 200-400 nm for these experiments.....	179
Figure 5.5: Hydrogenation reaction UPC <sup>2</sup> /MS traces showing the intermediate by-product conversion of the nitro functionality to the nitroso- functionality and finally to the amine functionality and confirmed by MS .....	181

Figure 5.6: Hydrogenation reaction kinetic plot showing a relationship between the nitroso intermediate consumption and the impurity generation.....	183
Figure 5.7: UV/MS chromatographic traces of a hydrogenation reaction mixture time point showing the complete reaction profile of starting material, intermediate product, intermediate by-product, and over-reduced impurities (highlighted in the rectangular box). ....	184
Figure 5.8: Possible sites accounting for observations of over-reduced species in the SFC/MS data. ....	185
Figure 5.9: MS spectral confirmation of the pyridine ring reduction for impurities peaks eluting at 1.02 minutes and 1.14 minutes. ....	186
Figure 5.10: Overlay of UPC <sup>2</sup> / MS total ion chromatogram results for the final clopidogrel reaction step 'U' time point. Oligomer peaks highlighted in the grey box.....	187
Figure 5.11: Oligomer by-product .....	188
Figure 5.12: Overlay of UPC <sup>2</sup> /MS of clopidogrel reaction step 'W' .....	188
Figure 5.13: Bromo-ester starting material results for clopidogrel reaction step 'W' .....	190
Figure 5.14: Reaction kinetics comparison of the bromo-ester SM adjustment with dioxane versus THF as the reaction solvent system. ....	190
Figure 5.15: UPC <sup>2</sup> /MS comparison of synthesized versus purchased thienopyridine starting material used in the clopidogrel reaction step 'W'. ....	191
Figure 5.16: Overlay of UPC <sup>2</sup> UV chromatograms for the achiral and chiral screening results for clopidogrel reaction step 'W'. Achiral column = UPC <sup>2</sup> 2-EP, Chiral column A = Chiralpak ID, and Chiral Column B = Chiralpak IB. ....	192
Figure 5.17: Revised synthetic scheme for the synthesis of clopidogrel based on decision points guided by UPC <sup>2</sup> /MS results. ....	193
Figure 5.18: Separations of rosuvastatin starting materials for reaction step R8 performed using ACQUITY UPC <sup>2</sup> and UPLC with high and low pH mobile phases .....	195

Figure 5.19: Reaction monitoring separations of rosuvastatin R8 reaction step after 90 minutes performed using ACQUITY UPC <sup>2</sup> and UHPLC with high and low pH mobile phases .....	195
Figure 5.20: UPC <sup>2</sup> /PDA chromatographic results overlay of intermediates R9, R10, and R11 final analysis time points. Wavelength was recorded at 254 nm.....	197
Figure 5.21: UV and MS chromatographic traces of the Trefoil chiral separation of 'R12' rosuvastatin reaction product. ....	199
Figure 5.22: QDa MS spectra confirmed with the resulting m/z = 482 Da measurements of both peaks, rosuvastatin and the enantiomer. ....	199
Figure 5.23: Injection linearity exploring injection solvent effects of Rosuvastatin (3R,5S) enantiomer.....	200
Figure 6.1: Structures of some sesquiterpene lactones: A. Germacranolides, B. Heliangolides, C+D: Guaianolides, E: Pseudoguaianolides, F: Hypocretenolides, G: Eudesmanolides .....	205
Figure 6.2: Structures of the standard reference compounds found in chamomile extracts ..	208
Figure 6.3: UPC <sup>2</sup> UV chromatograms of Roman chamomile comparing different gradient profiles (A) 1% to 40% methanol modifier and (B) 5% to 40% linear gradient over minutes eluted with a methanol modifier. ....	217
Figure 6.4: German and Roman chamomile UPC <sup>2</sup> UV Chromatograms. Conditions: UPC <sup>2</sup> column 1.7 $\mu$ m 2-EP 2.1 x 150 mm; . Flow rate was 1.2 mL min <sup>-1</sup> at 40 °C. 1500 psi backpressure. Gradient performed with a slope profile of 5 to 40% modifier. Co-solvent was MeOH: ACN (90:10) with 0.05% H <sub>2</sub> O. $\lambda$ =350nm. ....	218
Figure 6.5: Roman Chamomile UPC <sup>2</sup> UV Chromatogram. Evidence of increasing peak tailing over time highlighted in the rectangular box. See Figure 6.4 for conditions. ....	219

Figure 6.6: UPC <sup>2</sup> UV chromatogram using the 3μL injection of German chamomile extract .....	222
Figure 6.7: UPC <sup>2</sup> UV chromatogram using the 1μL injection of German chamomile extract .....	222
Figure 6.8: Chromatograms of Roman chamomile methanolic extracts labeled (a), (b), (c) show the retention time shift and the increased baseline noise with the increase of temperature for the major compounds found in roman chamomile, where peak 1 is apigenin, peak 2 is apigenin-7-O-glucoside, and peak 3 is chamaemeloside.....	224
Figure 6.9: Comparison of UPC <sup>2</sup> -MS ESI+ base peak intensity chromatogram (BPI) Roman chamomile extracts prepared using different solvents (a) isopropanol/Hexane (b) isopropanol, (c) hexane, and (d) methanol. ....	226
Figure 6.10: Comparison plot of peak ID vs. retention time for the UPC <sup>2</sup> and UHPLC chromatography results for the extracts of German Chamomile. ....	228
Figure 6.11: Zoomed extracted ion chromatograms (XIC) of $m/z = 475$ of German chamomile methanolic extract. An additional isobaric peak was identified in the UPC <sup>2</sup> trace (A) when compared to the UPLC-RP trace (B). ....	229
Figure 6.12: PCA scores plot (PC-1 vs. PC-2) of the authentic German chamomile (GC) and authentic Roman chamomile (RC) extracts .....	231
Figure 6.13: Scatter plot (S-plot) of German and Roman chamomile generated from the OPLS-DA statistical analysis of the dataset .....	232
Figure 6.14: Proposed fragmentation pathways for the two isobaric species, (4a) 1,10-epoxynoblin and (4b) hydroxynoblin.....	233
Figure 6.15: MS Spectral analysis of (5a) 1,10-epoxynoblin and (5b) hydroxynoblin. ....	235
Figure 6.16: Predicted structures of four of the five unknown chemical entities observed in the chromatographic separation profile .....	236

Figure 6.17: PCA scores plot of the commercial tea samples extracts (black) and the extracts from authentic German (blue) and Roman (red) chamomiles .....	237
------------------------------------------------------------------------------------------------------------------------------------------------------------	-----

## List of Tables

Table 1.1: Summary table of Liquid Chromatography Modes .....	11
Table 1.2: Critical temperatures and critical pressures of various substances.....	32
Table 1.3: A comparison of diffusivity and viscosity values for a gas, a liquid and a supercritical fluid [41].....	33
Table 2.1: 18 components used for test mixture .....	67
Table 2.2: Table of observed total system backpressure ( $P_{\text{sys}}$ ) related to flow rate and applied backpressure ( $P_{\text{app}}$ ) from the back pressure regulator. ....	78
Table 3.1: Diluents used in the study.....	104
Table 3.2: Columns and dimensions for diluent study .....	105
Table 3.3: List of metoclopramide impurity standards, peak designation, masses, and European Pharmacopoeia labels. ....	107
Table 3.4: Diluent effects experimental reasoning and design .....	110
Table 3.5: Table of results post column addition make-up flow rates effect on peak area ...	120
Table 3.6: Table of metoclopramide and related substances structures, names and monoisotopic mass.....	125
Table 3.7: Table of masses found in the degraded standard solution of metoclopramide EP impurity F.....	128
Table 4.1 Compounds and concentrations for the system suitability test mixture performed during the cheminformatic correlations experiments .....	147
Table 4.2 Columns and dimensions explored for system suitability study.....	149
Table 4.3: Table of descriptors using for the cheminformatic multivariate trend investigations .....	156
Table 5.1: List of chiral columns used.....	177
Table 6.1: Experimental variables for the method development investigation. ....	212



Table 6.2: Qualitative analysis of German (GC) and Roman (RC) chamomile using UPC <sup>2</sup> /MS, UPLC/MS, and GC/MS. ....	234
---------------------------------------------------------------------------------------------------------------------------------	-----

Table 6.3: Qualitative analysis of the authentic chamomile extracts and commercial tea extracts for the presence of the 11 chemical marker compounds .....	238
---------------------------------------------------------------------------------------------------------------------------------------------------------------	-----

## List of Equations

Equation 1.1: Partition coefficient represented by the logarithmic concentration of the hydrophobic phase divided by the logarithmic concentration of the hydrophilic phase. ....	8
Equation 1.2: Definition of retention factor .....	16
Equation 1.3: Definition of selectivity .....	17
Equation 1.4: Definition of resolution .....	18
Equation 1.5: Purnell Equation for resolution between two adjacent peaks highlighting the physical and chemical aspects of the equation influencing resolution under isocratic conditions .....	18
Equation 1.6: Resolution equation as it pertains to gradient elution[18] .....	19
Equation 1.7: Theoretical representation of efficiency .....	19
Equation 1.8: Practical calculation of column efficiency. ....	20
Equation 1.9: Calculation of peak capacity under isocratic conditions. ....	20
Equation 1.10: Calculation for peak capacity for gradient elution chromatography .....	20
Equation 1.11: Calculation determining the height equivalent theoretical plate .....	22
Equation 1.12: The van Deemter equation .....	22
Equation 1.13: Equation for dispersion variance .....	26
Equation 1.14: Wilke-Chang equation for diffusion .....	27
Equation 1.15: Equation for specific permeability .....	27
Equation 1.16: Efficiency relationship equation for the comparison of open, packed, and packed capillary columns when assuming maximum achievable theoretical plates .....	37
Equation 1.17: Reduced equation from Equation 1.14 when normalizing for mobile phase ..	37
Equation 1.18: Tarafder's reduced equation for retention dependency on density and temperature .....	41

Equation 1.19: Bartmann and Schneider efficiency equation when accounting for the role of density in SFC.....	42
Equation 2.1: Conversion of volts to pressure (psi).....	70
Equation 2.2: Calculation for peak volume .....	75
Equation 3.1: Calculation of equilibration volume as defined by 5 column volumes and calculation of re-equilibration time.....	109
Equation 5.1: Calculation for percent diastereomeric excess .....	198

## List of Terms, Symbols and Abbreviations

$\alpha$	selectivity
$\eta$	viscosity
$\rho$	density
$\Delta p$	pressure drop
4-HBB	4-hydroxybutyl-benzoate
%	percent
$\mu\text{g}$	Microgram
$\mu\text{L}$	Microliter
$\mu\text{m}$	Micrometre
A	Eddy diffusion coefficient
ABPR	Automatic backpressure regulator
ACN	Common name for acetonitrile
ADC	Antibody drug conjugate
ADME	<u>A</u> dsorption- <u>D</u> istribution- <u>M</u> etabolism- <u>E</u> xcretion
ADMET	Absorption, distribution, metabolism, excretion, toxicity
API	Active pharmaceutical ingredient
AZ	AstraZenaca
B	Longitudinal diffusion coefficient
$B_0$	Specific permeability
BEH	Ethylene Bridged Hybrid
BEH 2-EP	Ethylene Bridged Hybrid 2-Ethylpyridine
BI	Boehringer Ingeheim
C	Mass Transfer coefficient
CC	Convergence chromatography
$^{\circ}\text{C}$	Degrees Celcius
CAD	Corona charged aerosol detector
CCM	Convergence chromatography manager
CDER	Center for Drug Evaluation and Research

CDS	Chromatography data management system
CER	Ceramides
CLND	chemiluminescent nitrogen detector
CM-A	Column manager with active heating
CM-Aux	Auxillary column manager
CSH	Charged surface hybrid
cm	Centimetre
CO <sub>2</sub>	Carbon dioxide
cSFC	Open tubular capillary column supercritical fluid chromatography
$d_p$	Particle size
$D_m$	Diffusion coefficient of analyte in mobile phase
$D_s$	Diffusion coefficient of analyte in stationary phase
DAD	Diode array detection
de	Diastereomer excess
DMA	N,N-Dimethylacetamide
DMF	Dimethylformamide
DMPK	Drug metabolism pharmacokinetics
DMSO	Dimethyl sulfoxide
ECD	Electrochemical detector
ee	Enantiomeric excess
ESI	Electrospray ionisation
ESI+	Positive electrospray ionisation
ESI-	Negative electrospray ionisation
$F$	Flow rate
FDA	Food and Drug Administration
FID	Flame ionization detection
FLR	Fluorescence detector
GC	Gas chromatography

<i>h</i>	Peak height
h	Hour
H	Height equivalent to theoretical plate
H2L	Hit to Lead process
H <sub>acc</sub>	Hydrogen bond acceptors
H <sub>don</sub>	Hydrogen bond donors
HETP	Height equivalent to theoretical plate
HIC	Hydrophobic interaction chromatography
HILIC	Hydrophilic interaction liquid chromatography
Hit	A compound with a desired activity via HTS but requires confirmation testing
HPLC	High performance liquid chromatography
HRMS	High resolution mass spectrometry
HTS	High throughput screening
HTS	High throughput screening
i.d.	Internal diameter (in terms of the chromatographic column)
IEX	Ion-exchange chromatography
IND	Investigation new drug application
IPA	Common name for 2-propanol (isopropanol)
Isobaric	Constant pressure
Isopycnic	Constant density
k'	Retention factor (capacity factor)
K	Kelvin
KPa	KiloPascal
kV	Kilovolt
L	Length
LC	Liquid chromatography
LCMS	Liquid chromatography coupled to mass spectrometry
LC/UV	Liquid chromatography coupled to ultraviolet detection
Lead	A compound confirmed to have pharmacological or biological activity

LPC	Lyso-Phosphatidylcholine
LPE	Lyso-Phosphatidylethanolamine
$\log D$	Distribution coefficient
$\log P$	Partition coefficient (also referred as $\log P$ )
$\log P_{oct/wat}$	Octanol-water partition coefficients
$\text{LogS}_w$	Intrinsic water solubility
LSER	Linear Solvation Energy Relationships
mg	Milligram
MeOH	Methanol
mL	Millilitre
mm	Millimeter
min	Minute
MRM	Multiple reaction monitoring
MS	Mass spectrometry
MS/MS	Tandem mass spectrometry
MW	Molecular weight
$m/z$	Mass to charge ratio
$n$	Number of replicates
$N$	Number of theoretical plates
$n_c$	Maximum theoretical plates for a capillary column
$n_p$	Maximum theoretical plates for a packed column
$\text{NH}_4\text{OH}$	Ammonium Hydroxide
ng	Nanogram
NME	New molecular entities
NMP	N-methyl pyrrolidone
NMR	Nuclear magnetic resonance
NPLC	Normal phase liquid chromatography
OFAT	One Factor at a Time
OPLS-DA	Orthogonal partial least squares – discriminate analysis

$P_c$	Peak capacity
$P_C$	Critical pressure
PC	Phosphatidylcholine
PCA	Principal component Analysis
pcSFC	Packed capillary column supercritical fluid chromatography
PD	Pharmacodynamics
PDA	Photodiode array detector
PDT	Product intermediate
PE	Phosphatidylethanolamine
PG	Phosphatidylglycerol
PK	Pharmacokinetics
pKa	Logarithmic acid dissociation constant for an acid or base
pSFC	Packed column supercritical fluid chromatography
psi	Units of measurements for pressure termed as pounds per square inch
Pd/C	Palladium on carbon
QC	Quality control
QQQ	Tandem (triple) quadrupole mass spectrometer
QToF	Quadrupole time-of-flight mass spectrometry
$r$	Radius
RB	Rotational bonds
RD&E	Waters Research, Development, and Engineering group
RI	Refractive index
RP	Reversed-phase
(R#)	Reaction (number) referring to stage during synthesis
RPLC	Reversed-phase liquid chromatography
$R_s$	Chromatographic Resolution
SAR	Structural activity relationships
SEC	Size Exclusion Chromatography
SEF	Silyl ether formation



SFE	Supercritical fluid extraction
SIR	Single ion recording
SM	Sphingomyelin
SM(#)	Starting material (number)
SMARTS	SMILES Arbitrary Target Specification (chemical nomenclature)
SMILES	Simplified Molecular Input Line Entry System
SPE	Solid phase extraction
SQD	Single quadrupole detector
$T$	Temperature
$T_c$	Critical temperature
$t_0$	Void time (or dead time)
$t_r$	Retention time
$t'_r$	Corrected retention time
TCM	Traditional Chinese Medicines
TIC	Total ion count
THF	Tetrahydrofuran
TLC	Thin layer chromatography
TFA	Trifluoroacetic acid
tPSA	Topical polarizable surface area
$u$	Linear velocity
$u_{opt}$	Optimum linear velocity
UPC <sup>2</sup>	Ultraperformance Convergence Chromatography
UPLC	Ultraperformance liquid chromatography
UHPLC	Ultrahigh-performance liquid chromatography
USP	United States Pharmacopoeia
UV	Ultraviolet
$\bar{v}$	Reduced average velocity
$V_0$	System void volume (or dead volume)
$V_r$	Retention volume

$w$	Chromatographic peak width
$w_{0.5}$	Peak width at half height
$w_B$	Peak width at the base
XIC	Extracted ion chromatogram

## Table of Contents

Dedication .....	ii
Acknowledgments.....	iii
Abstract .....	v
List of Figures .....	ix
List of Tables .....	xix
List of Equations .....	xxi
List of Terms, Symbols and Abbreviations .....	xxiii
Table of Contents.....	xxx
CHAPTER 1 .....	2
1 Introduction to Natural Products, Liquid Chromatography and Supercritical Fluids. ....	2
1.1 Natural Product Research.....	2
1.1.1 Role of Natural Products in Drug Discovery .....	4
1.1.2 Impact of Combinatorial Chemistry .....	6
1.2 Liquid Chromatography and Their Principles of Measurement.....	9
1.2.1 Stationary Phases and Chromatography Columns .....	12
1.2.2 Liquid Chromatography System Components.....	13
1.2.3 Nomenclature of a Chromatogram.....	15
1.2.4 Retention Factor ( $k$ ) .....	16
1.2.5 Selectivity Factor ( $\alpha$ ) .....	17
1.2.6 Resolution ( $R_s$ ).....	18
1.2.7 Chromatographic Efficiency ( $N$ ).....	19
1.2.8 Peak Capacity ( $P_c$ ) .....	20

1.2.9	Plate Theory .....	21
1.2.10	Rate Theory.....	21
1.2.11	Extra-column volume and Band Broadening.....	24
1.2.12	Specific Permeability and Diffusion Coefficient.....	26
1.3	Supercritical Fluids .....	28
1.3.1	History of Supercritical Fluids.....	28
1.3.2	Properties of Supercritical fluids .....	30
1.4	Supercritical Fluid Chromatography.....	33
1.4.1	Historical Application of Supercritical Fluid Chromatography.....	34
1.4.2	‘Open Tubular’ versus ‘Packed Column’ Supercritical Fluid Chromatography.....	37
1.4.3	Role of Density for Solute Retention in SFC.....	40
1.4.4	Column Efficiency in SFC.....	41
1.4.5	Recent Theoretical Advancements in SFC .....	43
1.5	SFC Technology and Instrumentation.....	44
1.5.1	SFC Core Components .....	44
1.5.2	SFC Stationary Phases and Mechanisms .....	49
1.5.3	Detection Schemes.....	52
1.5.4	Back Pressure Restriction and Regulation.....	52
1.6	Supercritical Carbon Dioxide Opportunity for Natural Products Research .....	55
CHAPTER 2 .....		62
2	Investigations of a Low Dispersion Prototype SFC Instrument using Sub-2 $\mu\text{m}$ Particle Size Columns .....	62

2.1	Introduction .....	62
2.2	Experimental .....	66
2.2.1	Analyte probes selection study .....	67
2.2.2	Peak Distortion Studies.....	68
2.2.3	Isobaric versus Isopycnic van Deemter Studies.....	69
2.3	Results .....	71
2.3.1	Investigations with Sub-2 $\mu\text{m}$ Particle Stationary Phases .....	71
2.3.2	Peak Distortion Studies.....	76
2.3.3	Isopycnic and Isobaric Pressure Study .....	86
2.4	Conclusions .....	96
CHAPTER 3 .....		98
3	Exploring Method Development and Optimization Variables .....	98
3.1	Introduction .....	99
3.2	Experimental .....	103
3.2.1	Diluent Study .....	103
3.2.2	Mass Spectrometry Interfacing Investigations.....	105
3.2.3	Method Development One Factor at a Time (OFAT) Investigations .....	106
3.2.4	Amphipathic Analysis Investigations .....	108
3.3	Results .....	110
3.3.1	Diluent Study .....	110
3.3.2	Optimizing the Mass Spectrometry Interface .....	115
3.3.3	One Factor at a Time (OFAT) Method Development Investigations .....	123

3.3.4	Analysis of Amphipathic Compounds .....	133
3.4	Conclusions .....	140
CHAPTER 4 .....		143
4	Cheminformatic Investigation of Solute Physiochemical and Structural properties affecting SFC Chromatographic performance .....	143
4.1	Introduction .....	143
4.2	Experimental .....	147
4.2.1	Cheminformatics Experimental .....	147
4.2.2	Cheminformatic System Suitability Test Mixture .....	147
4.2.3	Instrumentation Parameters for the Cheminformatic Study .....	148
4.3	Results .....	150
4.3.1	Development of the chemometric analysis system performance test .....	150
4.3.2	Design of Physiochemical and Structural Correlations .....	155
4.3.3	Results of Chromatographic, Physiochemical and Structural Correlations .....	156
4.4	Conclusions .....	161
4.5	Acknowledgements .....	162
CHAPTER 5 .....		164
5	UPC <sup>2</sup> /MS Applied to Pharmaceutical Drug Substance Reaction Synthesis Monitoring .....	164
5.1	Introduction .....	165
5.2	Experimental .....	168
5.2.1	Reaction Schemes .....	169
5.2.2	Reaction Monitoring Analysis .....	175

5.3	Results .....	178
5.3.1	Monitoring the Synthesis of Imatinib by UPC <sup>2</sup> /MS .....	178
5.3.2	Achiral and Chiral Screening of Clopidogrel Racemates by UPC <sup>2</sup> .....	186
5.3.3	Monitoring the Asymmetric Synthesis of Rosuvastatin .....	194
5.4	Conclusions .....	201
5.5	Acknowledgements .....	202
CHAPTER 6 .....		204
6	Investigating Sub-2µm Particle Stationary Phase Supercritical Fluid Chromatography Coupled to Mass Spectrometry for Chemical Profiling of Chamomile Extracts.....	204
6.1	Introduction .....	204
6.2	Materials and Methods .....	209
6.2.1	Solvents and reagents.....	209
6.2.2	Plant Materials .....	209
6.2.3	Sample Preparation .....	210
6.2.4	Chromatography .....	211
6.2.5	Mass Spectrometry.....	213
6.2.6	Data Analysis .....	214
6.3	Results and Discussions .....	215
6.3.1	Chromatographic method development and optimization .....	215
6.3.2	Effect of Column Temperature .....	223
6.3.3	Summary of Method Optimization .....	225
6.3.4	Sample preparation optimization .....	226

6.3.5	Chromatographic Technique Comparisons.....	227
6.3.6	Statistical Analysis.....	229
6.3.7	Mass Spectrometry Analysis.....	232
6.3.8	Applied Investigation of Commercial Chamomile Teas .....	236
6.4	Conclusions .....	239
6.5	Acknowledgements .....	241
CHAPTER 7	.....	243
7	Conclusions and Future Research.....	243
7.1	Final Conclusions.....	243
7.2	Summary of Thoughts, Peer Interactions and Observations about Future pSFC and UPC <sup>2</sup> Adoption.....	249
7.3	On-going related research .....	254
7.4	Future Research.....	255
References	.....	256
Bibliography	.....	267



# CHAPTER 1:

---

## INTRODUCTION

## CHAPTER 1

### 1 Introduction to Natural Products, Liquid Chromatography and Supercritical Fluids.

#### 1.1 Natural Product Research

Natural products and their derivatives have been employed as therapeutic treatments of ailments and diseases for thousands of years. Early medicines were based on tree-bark, leaves and fruit. Many well-known and commonly used therapeutics have their origins in nature's remedies, Aspirin and digitalis being two common examples. Natural products have been used as the basis of consumer products, are the basis of Traditional Chinese Medicines (TCM), antibiotics, and as the starting synthesis point for the development of blockbuster drugs. More recently these natural compounds have been the starting point for specifically designed Antibody Drug Conjugate (ADCs) 'warheads' [1]. Natural product profiling and characterization has also led to the betterment of food genomics improving quality attributes, environmental resilience, and drought resistance [2]. The practice of natural product research requires collaborative knowledge of analytical, organic, and biological chemistry. Natural products are a decoction of multiple components, some active and some inactive others acting symbiotically. Due to the complexity and diversity of biological moieties, understanding the chemical dynamics of a natural product require data interpretation from biosynthesis, biology, taxonomy, pharmacology, spectroscopy, and separation sciences.

The idea of discovering natural products with therapeutic relevance may seem like a semi-stroke of luck, however a statistical analysis of approved New Molecular Entities (NME) by

the FDA proved otherwise. An analysis performed on NME approvals between 1981 and 2010 by Newman and Cragg showed of the 1355 approved NMEs, 50.63% are natural products or natural product derived semi-synthetics [10]. For the 30 year period, NMEs originating from natural products and natural products derivatives have been predominately developed for the treatments of anticancer and antibacterial indications. Antiviral medicines are dominated by the discovery and development of vaccine-based new chemical entities, which are derived from nature by definition [10, 11]. Further review notes a slight decline of approved small molecules between 1981 and 2010 specifically in the 1990s, however natural product , natural product botanicals, and natural product derived NMEs accounted for a median of 35.2% of the total FDA approved NME's during the 30 year period. The analysis did not conclude any clear and indicative trend of natural products representation from year to year positive or negative, yet subsequent articles suggested a slight decline has occurred [6-8]. Additionally, the decline does not coincide with the FDA's claims to refute the public perception of the Agency approving fewer drugs in recent years [12]. The small molecule approval rate is in the range of 20 to 30 molecules per year. The NME approval rate has not necessarily declined, but the Center for Drug Evaluation and Research (CDER) analysis did indicate fewer NME applications have been submitted. From a natural product NME perspective, drilling down into the data indicates a maximum representation of 50% NME in 2010 and a minimum representation of 12.2% in 1997 have natural products origins [10]. Interestingly, the percentage of NMEs from plant based origins decline steadily as the years progress, yet shift to a greater percentage of NMEs derived from bacterial and fungi origins spanning from 1931 to 2013, thus indicating an inclusion of research diversity in the discovery of NME from natural products [8]. In many of the closing remarks and response articles focused on natural product research, the recognition of natural products significant role in the drug discovery of NMEs clearly stated opportunity residing by expanding the

research for chemically diverse compounds exploration within marine life species [1, 3, 5, 7, 8, 10, 11, 13, 14].

### **1.1.1 Role of Natural Products in Drug Discovery**

Natural products are produced by nature; eukaryotic and prokaryotic, which are extracted from cells, tissues, microorganisms, plants and animals [3]. The environmental and biological diversity found in nature contributes to the novelty of the compounds extracted from the biological source. The natural products used for medicinal purposes are a result of pharmacognostic studies; *Pharmacognosy*. Pharmacognosy is the study of natural products molecules that are useful for their medicinal, ecological, gustatory, or other functional properties that allow for the identification, selection, and processing of the primary and secondary metabolites found in natural products to be bioactive towards a targeted disease[4]. These metabolites *may* evolve to the role of a “lead” candidate for a new pharmaceutical drug. Examples of natural products used as medicines such as aspirin, morphine, quinine, and pilocarpine were derived from plants [5]. Therapeutic natural products are broadly defined as any of the following [6, 7]:

- Unregulated organisms or natural materials;
- FDA-regulated, unmodified natural materials or compounds;
- Naturally occurring compounds that have been chemically modified and referred to as “semisynthetic”; and
- Purely synthetic medicinal compounds inspired by a natural compound.

The analysis of natural products requires intensive investments in time and resources due to the effort needed to isolate and identify the active substances within a comprehensive sample profile [8]. The identification of these components normally employs a combination of chromatography (TLC, GC, HPLC), mass spectrometry and NMR. The task of finding a

bioactive compound from a natural product starts early within the pharmaceutical drug discovery process. The process of discovering new molecular entities (NME) follows a “hit to lead” (H2L) scheme within the pharmaceutical discovery process. A “hit” is the result of a high throughput screening (HTS) exercise discovering bioactivity specific to the target disease. The “hit” is determined a “lead” drug candidate after subsequent structural activity relationship (SAR) testing and generation of pharmacodynamics / pharmacokinetic (PD/PK) information. The progression of a natural product NME from discovery to development highlighting the amount of material required to fulfill the needs of each stage of testing is depicted in Figure 1.1.

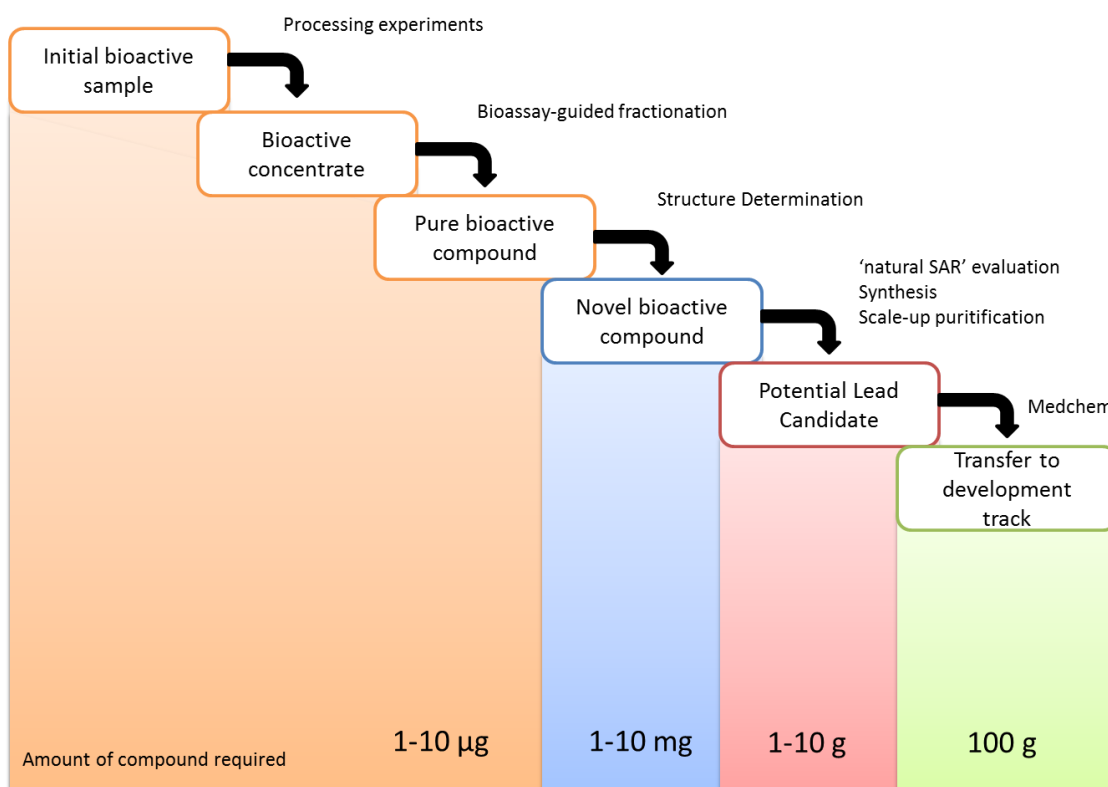


**Figure 1.1 Chemical process for natural product discovery [7]**

The process begins with the natural product being extracted from its source (plant leaves etc), concentrated, fractionated and purified; yielding essentially a single chemical compound. Historically, this process has suffered most often from three major hurdles.

- 1) The rapid identification of known compounds (dereplication) - to avoid the duplication of effort. This step has been greatly facilitated by the availability of reliable HPLC-mass spectrometer (LC/MS) systems, and the general availability of natural-product databases. The correlation of both molecular mass and ultraviolet light (UV) absorption data with known compounds by database searching is ordinarily sufficient to classify sets of compounds [9].
- 2) The de novo structure determination of NMEs - this area has been revolutionized by many advances in high-resolution mass spectrometry and high field NMR spectroscopy. In those cases in which the biological activity profile meets criteria for potency and selectivity, preliminary SAR studies are conducted and the process is scaled up. Once the feasibility of modulating biological response through synthetic modification is established, the hit is declared a lead and proceeds onwards for additional optimization by traditional medicinal chemistry.
- 3) Efficient techniques and capabilities to isolate and purify targets - Utilization of analytical and purification scale liquid chromatographic techniques provide the tools to monitor reactions and isolate constituents of interest such as isomeric compounds. The purification step in the process is rate-limiting and potentially hindered by supply of the source material. Additionally, one must correlate the biological signal of interest with the bioactive compounds. As it can be assumed by this description, a strong basis of knowledge, equipment, techniques, and a *hint of luck* are required to discover natural products for medicinal purposes.

### 1.1.2 Impact of Combinatorial Chemistry

The perceived decline of natural product drug discovery has also been attributed to a number of factors circumstantiating from the advent of combinatorial chemistry, lack of focus on molecular targets as a result of competitive first-to-market timelines, and commercially driven philosophies steering away from treatments for infectious diseases, which are the strength for lead natural product derived compounds. The pharmaceutical industries shift to

combinatorial chemistry and failure to produce a high success of leads in the 1990s ultimately resulted in the disillusionment of combinatorial effectiveness.

Combinatorial chemistry, is an approach facilitated by the use of high throughput screening (HTS) of compound libraries consisting of hundreds of thousands to millions of synthetic compounds designed on the basis of chemical accessibility and maximum achievable size [10]. Although the perception has been acknowledged as a contributed factor to the decline of natural product drug discovery, the HTS approach was regarded as a useful approach to optimizing the development of natural product lead candidates rather than lead identification. In a 2014 review by Butler *et al*, they recognized the counterintuitive mindset of **not** utilizing HTS for natural product lead identification due to their significant role in drug development. Only one *de novo* natural product drug was cited as a result of a combinatorial screening Hit to Lead (H2L) identification campaign, the antitumor compound known as sorafenib from Bayer [11]. Since the turn of the millennium, the pharmaceutical industry has recognized the lack of diversity within their synthetically developed chemical libraries evident by the recent shift to “focused” or “targeted” library screening.

Advances in cheminformatic tools such as Instant JChem (ChemAxon), Spotfire (TIBCO), Vortex (Dotmatics) and “CLEVER”<sup>1</sup> freeware facilitate the visualizing, management and *in silico* techniques of vast chemical libraries to produce smaller (200 to 3000) chemically relevant screening libraries designed to target a disease. Multivariate statistical analysis of natural products and synthetic drugs shows discretely different molecular descriptors in terms

---

<sup>1</sup> Chemical Library Editing, Visualizing and Enumerating Resources (A\*STAR Agency for Science, Technology and Research) Singapore

of the aromatic atoms, solvated hydrogen donors and accepters, molecular rigidity, mass, octanol-water partition coefficients ( $K_{OW}$  or  $\log P_{oct/wat}$ ; expressed by Equation 1.1), number of chiral centers, and number of specific elements such as oxygen, nitrogen, sulphur, and halogens.

$$\log P_{oct/wat} = \log \left( \frac{[solute]_{un-ionized\ octanol}}{[solute]_{un-ionized\ water}} \right)$$

**Equation 1.1: Partition coefficient represented by the logarithmic concentration of the hydrophobic phase divided by the logarithmic concentration of the hydrophilic phase.**

In respect to building focused natural product libraries, the following criteria can be followed [12-14]:

1. Lower ratios of aromatic ring atoms to total heavy atoms,
2. Greater number of chiral centers,
3. Increased steric complexity,
4. Greater amount of oxygen atoms,
5. Greater number of solvated hydrogen-bond donors and accepters and
6. Greater molecular rigidity.

The cheminformatic advancements allow the discovery organizations to customize inclusive of the typical Lipinski rule of five “drug likeliness”; *which natural products structures that violate two or more rules is less than 10%*, but additionally design libraries based attributes such as scaffold architecture and pharmacophore properties [14-16].

The purpose of the targeted or focused library approach seeks to elaborate structural modifications onto existing bioactive natural-product scaffolds in a parallel, systematic fashion in order to improve its inherent biological activity or drug-like properties. This can be



performed either by semi-synthetic modification of the parent molecule, or by fully synthetic natural product inspired methods. This strategy was put into practice by Waldmann *et al.*, who recently developed potent, selective inhibitors against the TIE2 receptor tyrosine kinase by parallel synthesis of a small (74 member) focused library based on nakijiquinone [17]. Although diverse focused libraries can be designed, there is still a requirement to efficiently screen, separate, isolate, and interpret the resulting complexity from any natural product research campaign.

In order to gain a better understanding of how best to address the aspects of natural product research, it has already been identified in the previous sections regarding the significant role of chromatography and mass spectrometry. Additionally, the concepts of supercritical fluids must be reviewed as they present a unique opportunity for topics such as: (i) Sample preparation; by providing selectivity and specificity to discrete analytes of interest. (ii) throughput; by resulting in lower mobile phase viscosity thus reducing compromises and limitations set by system pressure thresholds, and (iii) chromatographic flexibility; by simplifying eluent configurations which are unique for particular stationary phase use.

## **1.2 Liquid Chromatography and Their Principles of Measurement**

This history and invention of chromatography traces back to 1906 to Mikhail Tsvet, an Russian-Italian botanist researching plant pigments. Tsvet successfully utilized liquid-adsorption chromatography to separate chlorophylls and carotenoids, interestingly a natural product application, thus connecting natural product research to the origin of chromatography. Chromatography is the field in which separation techniques allow for an analyte to migrate between different ‘phases’ that move relative to each other.

Chromatography also refers to the analytes affinity to migrate at different velocities [18]. The phases typically consist of a stationary phase and mobile phase, with the exception of countercurrent chromatography which uses two mobile phases in opposite directions. Generally, the stationary phase is a solid and the mobile phase is a liquid, gas, or supercritical fluid<sup>2</sup>. As it can be expected, when the mobile phase is a gas, it is referred to as gas chromatography (GC). When the mobile phase is a liquid, it is referred to as liquid chromatography (LC) and thus for supercritical fluids it is referred to as supercritical fluid chromatography (SFC). The general types of chromatography can elute solutes by either one or a combination of the following mechanisms: (i) Adsorption, (ii) Partition, (iii) Ion Exchange, (iv) Molecular (*size*) Exclusion, and (v) Affinity. Basically, the separation mechanisms are driven by polarity, electrical charge, or molecular size.

Liquid chromatography or High Performance Liquid Chromatography (HPLC) is the most common technique employed today. HPLC uses a variety of separation mechanisms as outlined in Table 1.1. Each chromatographic approach has a unique function and practical purpose in regards to effectively achieving a separation of analytes. For example, Hydrophilic Interaction Liquid Chromatography (HILIC) is very useful for highly polar molecules often found in the pharmaceutical industry such as the separation of Metformin and its related substances[19, 20]. Ion-exchange chromatography (IEX) leverages the ionic strength of buffers for the separation of proteins and biomolecules for the biopharmaceutical industry. Size exclusion chromatography (SEC) utilizes stationary pore size to achieve effective separations of oligomers and larger polymers required in plastics and materials industries.

---

<sup>2</sup> The concepts of supercritical fluid is discussed in section 1.3

**Table 1.1: Summary table of Liquid Chromatography Modes**

LC Mode	Stationary phase (SP)	Mobile Phase (MP)	Targeted mechanism
<b>Normal Phase LC (NPLC)</b>	Polar sorbent (silica, alumina)	Non-polar eluent (hexanes, chlorinated hydrocarbons) /IPA/MeOH	Adsorption.  Interaction of polar functional groups of analyte with polar functional groups of SP
<b>Reversed Phase LC (RPLC)</b>	Non polar silica-based bonded phases  (hydrophobic carbon chains, Si-C18, SI-C8,)	Polar eluents (water, acetonitrile , methanol)	Adsorption, Partition  Dependent on interactions between the SP surface and hydrophobic functionality of the analyte
<b>Hydrophobic Interaction Chromatography (HIC)</b>  (NOTE: RPLC-derived)	Low hydrophobicity sorbent with concentrated buffer  (Si-C4)	Water or dilute buffer	Adsorbed to SP with concentrated buffer and eluted with lower concentrated buffer (good for proteins)
<b>Hydrophilic Interaction Chromatography (HILIC)</b>  (NOTE: NPLC-derived)	Polar sorbent (silica, polar ligand bonded silica)	Aqueous Eluents	Partition driven. Thin aqueous (aq.) film on SP surface and analytes equilibrate between MP and SP aq. layer
<b>Ion-Exchange Chromatography (IEX)</b>	Cation (+) or Anion (-) charged SP surfaces via acidic or basic functionality attached to silica or polymer particles	Strong and weak pka buffers	Ion-exchange, Primarily based on charge, whereas opposite charges attract resulting in retention, a competitive process
<b>Size-Exclusion Chromatography (SEC)</b>	Controlled porosity polymeric SP	Polymers: non-aqueous; Biomolecules: Aqueous buffers	Sieving by analyte size relative to SP pore size; Larger analytes elutes first

As discussed earlier, HPLC is the dominant separation technique, however the opportunity for supercritical fluid chromatography lends to a hypothetical expansion of capabilities that will be discussed in later sections. Gas chromatography is used during natural product research for the analysis of small aliphatic hydrocarbons, essential oils, and natural product lipids research. However, gas chromatography often requires derivatization and is limited to volatile compounds. Since SFC is a form of liquid chromatography derived from Normal Phase Liquid Chromatography (NPLC), many of the same LC measurement principles are utilized and deemed essential to best understand and characterize separations of simple and complex mixtures. Therefore, the basics of chromatographic principles and systems are reviewed in this section to better identify, understand the similarities and differences between general LC and SFC. This information will be used to design experimental procedures appropriate for natural product analysis appropriate for use in pharmaceutical drug discovery and development.

### **1.2.1 Stationary Phases and Chromatography Columns**

The stationary phase particles are the driving influence on the chromatographic separation. The particles can be non-porous, porous, or a combination thereof known as pellicular particles or more recently referred to as superficially porous-based particles[21]. Stationary phase particles can be composed of silica, organo-silica hybrids of different polarity, chiral functionalized, graphite particles, and polymeric particles. Each type has particular uses, benefits and compromises to separation needs and performance. The stationary phase particles are packed into cylindrical tubes called ‘columns’ using processes developed to increase column stability and lifetime during use. There are other manufacturing processes where the silica is ‘grown’ as tubular formations known as monolith columns. In general, column hardware can vary in length, internal diameter, thickness, material composition and

external connection details. All of which should be considered when connecting to a chromatographic system.

### 1.2.2 Liquid Chromatography System Components

A modern day liquid chromatograph system (Figure 1.2) consists of a pump (B) which siphons, compresses, meters, mixes, degases and delivers the mobile phase (A) throughout the fluidic path of the system (blue arrows). The pump typically has the capability to deliver the mobile phase isocratically (*constant composition*) or with gradient elution (*varying composition*) at a constant flow rate. The autosampler (C) consists of an injection mechanism that will collect and aspirate the contents of a sample into the flowing mobile phase stream. The samples are typically located in vials or a well within a sample plate and located in the autosampler. Many autosamplers have the capacity for 2 or more plates. The sample is carried in the flowing stream to a column (1 or 2) of appropriate stationary phase packing material held within the column heating or column management module (D). The column compartment module has two main functions. The primary function regulates the temperature of the column to mitigate solute retention irreproducibility from injection to injection caused by environmental temperature inconsistencies. A secondary function is to manage column selection if a selection valve is installed. The solutes migrate and separate on the column via one or a combination of the modes described in **Error! Reference source not found.**, at the exit of the column they travel through a transfer line to a detector(s) configured either in series or parallel if multiple detectors are used. Different forms of detectors can be chosen based on solute properties. Solutes with chromophores can be detected by UV detection. Solute fluorescence can be detected using a fluorescence detector. Other forms of detectors include corona charged aerosol detector (CAD), evaporative light scattering detector (ELSD), refractive index (RI), electrochemical detector (ECD), chemiluminescent

nitrogen detector (CLND) and a mass spectrometer. In Figure 1.2, a schematic illustrates an ultraviolet light detector (E) and mass spectrometer (F) configured in series with the flow typically split after the UV detector to maximize ionization efficiency of the MS detector. The signal from the detection modules are converted to graphs that are collected, processed and stored by chromatographic software installed on a computer (G). Eluent waste is collected in a sealed container or certified waste collection system (H) for safe disposal. In larger chromatographic laboratories, the waste eluent can either be recycled or piped to an external containment area [22, 23].

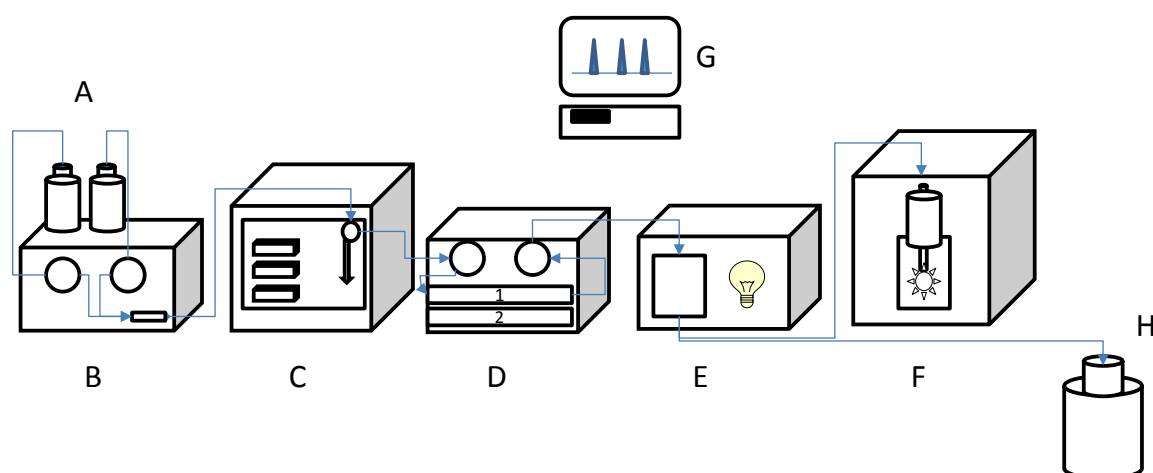


**Figure 1.2:** Schematic of a modern liquid chromatograph system configured with ultraviolet light detection coupled to mass spectrometry.

### 1.2.3 Nomenclature of a Chromatogram

A chromatogram is the representation of the chemical separation in terms of peak response versus elution time. The chromatogram displays numerous parameters that can be used to qualitatively and quantitatively assess the solutes separation results and evaluate system performance. An example of the basic parameters and nomenclature for a chromatogram are described in Figure 1.3.

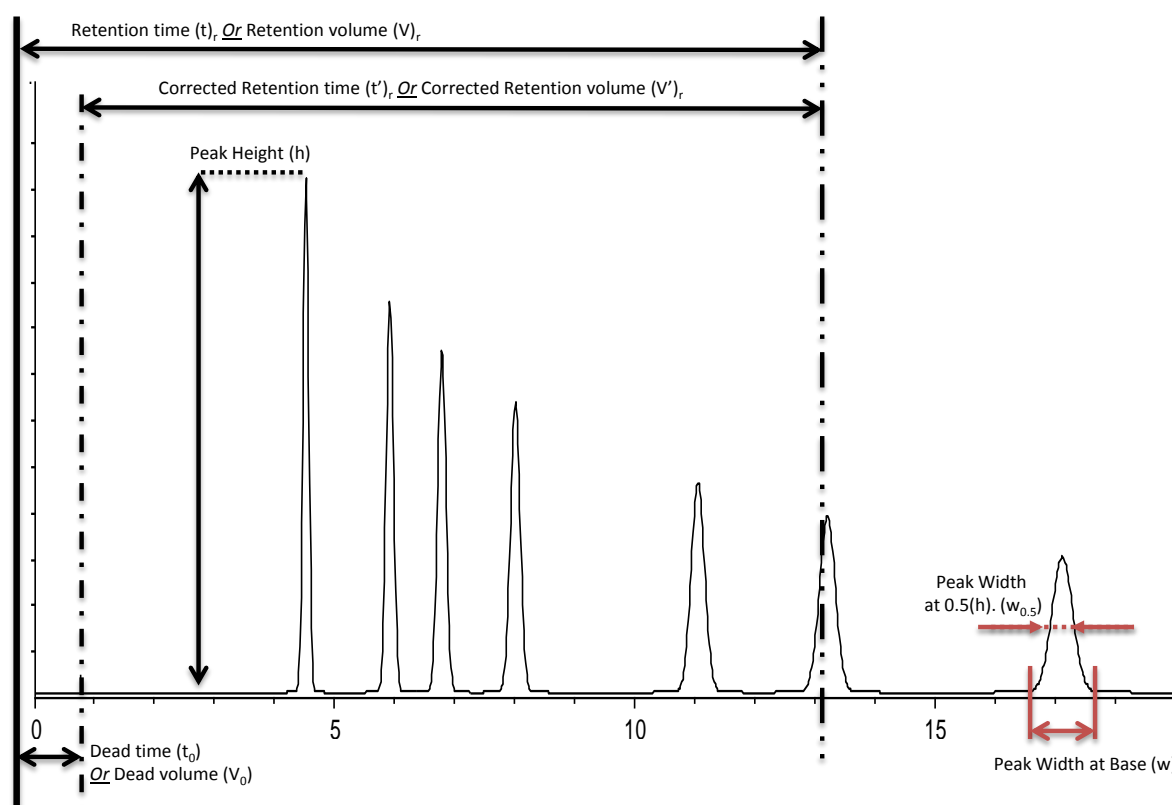


**Figure 1.3: Nomenclature of a chromatogram. Adapted from Ettre [24].**

The baseline is any part of the chromatogram, which represents detection of only the mobile phase. An unretained solute is either represented by time or volume. The ‘dead point’ is the position of the peak maximum of an unretained solute. Dead time or void time ( $t_0$ ) is the time elapsed between the point of injection and the apex of the unretained solute. Dead volume

( $V_0$ ) represents the amount of mobile phase passed through the column from the point of injection and the apex of the unretained solute. The retention time ( $t_r$ ) is a characteristic property of the solute measured from the injection point to the peak apex. Retention volume ( $V_r$ ) is the volume of mobile phase passed through the column between the point of injection and the peak apex. The corrected retention time ( $t'_r$ ) is the time spent by the solute on the stationary phase calculated from measurement of the unretained solute and the apex of the eluted solute. The same determinations can be calculated for the functions of volume. The peak height ( $h$ ) is the distance from the baseline to the peak apex. The peak width ( $w$ ) is the distance between each side of a peak measured at 0.607 of the peak height representing two standard deviations ( $2\sigma$ ) of the Gaussian curve. The peak width at half height ( $w_{0.5}$ ) is the distance measured between each side of the peak at half its maximum height. The peak width at the base ( $w$ ) is the distance between the intersections of the tangents geometrically drawn to the sides of the solute peak and to the peak baseline. The  $w_B$  is representative to four standard deviations ( $4\sigma$ ) of the Gaussian curve.

#### 1.2.4 Retention Factor ( $k$ )

The retention factor ( $k$ ) is a measurement, which is used to determine the solutes affinity to the stationary phase relative to an unretained solute. Retention factors can be calculated from functions of retention times or volumes. The retention factor is defined by the following equation [18, 22, 25]:

$$k = \frac{t_r - t_0}{t_0} = \frac{V_r - V_0}{V_0}$$

**Equation 1.2: Definition of retention factor**



Solutes with retention factors, which are between 2 and 5, are used as probes when determining optimum column efficiency for van Deemter plots [18]. The United States Pharmacopoeia (USP) does not accept chromatographic methods as valid if the  $k$  is less than 2. Retention factors are also used to troubleshoot shifts in solute retention. Chromatographic comparisons resulting in a solutes retention factor varying from injection to injection are typically attributed to column issues. Chromatographic comparisons resulting in constant values of  $k$  for a solute can be attributed to system issues.

### 1.2.5 Selectivity Factor ( $\alpha$ )

The selectivity factor is a measure of the difference in retention of two eluting solutes in a separation. The selectivity is a function of column packing material. Method parameters such as mobile phase composition, mobile phase pH, and column temperature can all affect selectivity. A selectivity value equal to 1 represents no separation between the solutes. Selectivity can be calculated as a function of times, volumes or capacity factors as described by the following equation [18, 22, 25] :

$$\alpha = \frac{t_2 - t_o}{t_1 - t_o} = \frac{v_2 - v_0}{v_1 - v_0} = \frac{k_2}{k_1}$$

#### Equation 1.3: Definition of selectivity

Where  $v_2$  and  $v_1$  represents the retention volume of the respective solute peaks.  
 $k_2$  and  $k_1$  are the capacity factors of the respective solute peaks.

### 1.2.6 Resolution ( $R_s$ )

The measurement describing the degree of separation between two adjacent peaks is calculated as resolution ( $R_s$ ) using the following equation [18, 22, 25]:

$$R_s = \frac{\Delta t_r}{0.5(w_{b,1} + w_{b,2})}$$

#### Equation 1.4: Definition of resolution

Where  $\Delta t_r$  is the difference of the retention times between two adjacent peaks and  $w_{b, (x)}$  are the widths at the peak base for each adjacent peak. Instrument vendors will also report values calculated using widths at various standard deviations and half height when defining instrument specifications and qualification procedures.

The resolution equation can also be represented by the Purnell equation using values of efficiency ( $N$ ), selectivity ( $\alpha$ ) and retention factor ( $k$ ) and represented by Equation 1.5.

$$R_s = \frac{\sqrt{N}}{4} \underbrace{\left( \frac{\alpha - 1}{\alpha} \right) \left( \frac{k}{1 + k} \right)}_{\text{“chemical”}}$$

↑  
“physical”

#### Equation 1.5: Purnell Equation for resolution between two adjacent peaks highlighting the physical and chemical aspects of the equation influencing resolution under isocratic conditions

The Purnell equation can be split to determine the physical or chemical influence on resolution. By breaking down the equation, the ‘physical’ parameters are limited by contributions of extra-column bandspreading thus effecting efficiency ( $N$ ). The physical

parameters can be due to poor column packing, gaps within the connecting fluidic hardware and system volume contributions such as higher volume detector flow cells. These physical limiting factors make it difficult to benefit from the theoretical efficiency provided for example, by the use of sub-2 $\mu\text{m}$  particle stationary phases

The ‘chemical’ influence of the equation is addressed with the introduction of new hybrid stationary phases which are stable at high pH and higher pressures. Factors such as mobile phase composition, pH, and column physiochemical properties will affect selectivity ( $\alpha$ ) and retention factors ( $k$ )

A similar equation can be derived for gradient elution chromatography (Equation 1.6)

$$Rs = \frac{\sqrt{N}}{4} \left( \frac{k_e}{k_e + 1} \right) (\ln \alpha)$$

**Equation 1.6:** Resolution equation as it pertains to gradient elution[18].

### 1.2.7 Chromatographic Efficiency ( $N$ )

Column efficiency is measured and reported as a number of theoretical plates ( $N$ ) calculated by Equation 1.7. Peak width and retention time are key features of the concentration profile that determine the efficiency of a column to resolve two solutes under isocratic conditions.

$$N = \frac{L}{H}$$

**Equation 1.7: Theoretical representation of efficiency**

Where  $L$  is the length of a column and  $H$  is the height equivalent of a theoretical plate, also referred to as HETP. The practical determination of column efficiency is calculated from the chromatographic results using Equation 1.8 [18, 22, 25].

$$N = 16 \left( \frac{t_r}{w_b} \right)^2 = 5.54 \left( \frac{t_r}{w_{0.5}} \right)^2$$

**Equation 1.8: Practical calculation of column efficiency.**

The concepts of quantitating column efficiency are used to communicate two major theories, plate theory and rate theory.

### 1.2.8 Peak Capacity ( $P_c$ )

During gradient elution, the solute band is focused at the front of the column and the peak fidelity is as adversely affected by diffusion as the solute migrates across the length of the column as with an isocratic method. The separating power of a column under a gradient elution profile is determined by a different form of measurement aimed at determining the number of discretely resolved peaks that are eluted per unit time. The efficiency of the column measured from a gradient elution experiment is dependent upon the capacity factor of the last eluting peak ( $k_{max}$ ) and defined by Equation 1.9 [26].

$$P_c = 1 + \frac{\sqrt{N}}{4R_s} \ln(1 + k_{max})$$

**Equation 1.9: Calculation of peak capacity under isocratic conditions.**

When using a gradient elution, peak capacity can be calculated by the following Equation 1.10 where  $t_g$  = time for the gradient and  $w$  is the width of the chromatographic peak

$$P_c = 1 + \frac{t_g}{w}$$

**Equation 1.10: Calculation for peak capacity for gradient elution chromatography**

### 1.2.9 Plate Theory

The theoretical plate model assumes a column of fixed length is equally segregated into a large number of divisions across the column with each division representing a theoretical plate (Figure 1.4). Plate theory assumes the solute is in equilibrium with the stationary phase and mobile phase as it migrates through the column from one plate to the next. A larger number of theoretical plates ( $N$ ) translate to a more efficient column.

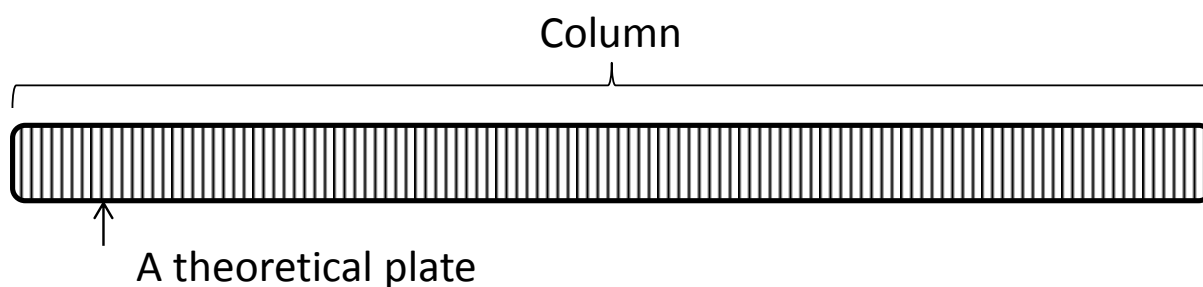


**Figure 1.4: Conceptual representation of a theoretical plate and division within in a column**

Unfortunately, plate theory does not account for additional phenomena occurring within the column affecting the rate of elution and solute band fidelity as it travels the length of the column, hence why the Rate Theory is widely adopted.

### 1.2.10 Rate Theory

Rate theories consider the contribution of flow hydrodynamics and their effect on peak dispersion. The Height Equivalent to the Theoretical Plate (HETP) is the theoretical link between Plate Theory and Rate Theory representing a numerical value equal to the variance per unit length of the column. The HETP is a function of the representative of the properties of the column and the solute. If Equation 1.7 was solved for HETP ( $H$ ) to yield Equation 1.11, then, smaller HETP values indicate more theoretical plates within the column and better

resolution. HETP determinations provide a good measure for dispersion within the column when plotted versus linear velocity.

$$HETP (H) = \frac{L}{N}$$

**Equation 1.11: Calculation determining the height equivalent theoretical plate**

A number of equations have been used to represent the efficiency, flow and peak width dispersion relationship such as the van Deemter equation, the Giddings equation and the Knox equation. The van Deemter equation is the most commonly used and simplest to apply practically to a set of empirical data where the linear velocity ( $u$ ) is known [18].

$$H = A + \frac{B}{u} + C(u)$$

**Equation 1.12: The van Deemter equation**

The van Deemter equation (Equation 1.12) is composed of three independent contributions, which additively represent a curved relationship when plotted (Figure 1.5). The three terms are generally represented by A, B and C.

- The A term represents the contribution of solute eddy diffusion that occurs as a result of varying size and distribution of inter-particle channels in the column. The A term is independent of linear velocity and solely dependent on the column packing. Solute band broadening as a result of eddy diffusion can be minimised by using small diameter packings with a narrow particle size distribution.

- The B term captures the molecular longitudinal diffusion (axial) and is indirectly proportional to the linear velocity. The B term dominates band broadening at low velocities. However, in liquid chromatography where diffusion coefficients are small, the contribution of  $H_{md}$  to the overall plate height is often negligible.
- The C term considers the resistance to all mass transfer contributions as it pertains to the mobile phase and stationary phase interactions inclusive of any adsorption kinetics. The C term increases within increasing linear velocity and increasing particle diameter.

The three terms plotted together indicate a minimum dispersion whereas the optimum linear velocity, or flow rate can be determined to achieve the maximum efficiency (or minimum HETP) for a particular column. This information is essential when developing and optimizing chromatographic method conditions, column vendor selection, and method validation activities. Methods operating in the robust regime of the maximum efficiency range of a column, ensures the resolution achieve between two adjacent peaks will be maintained.

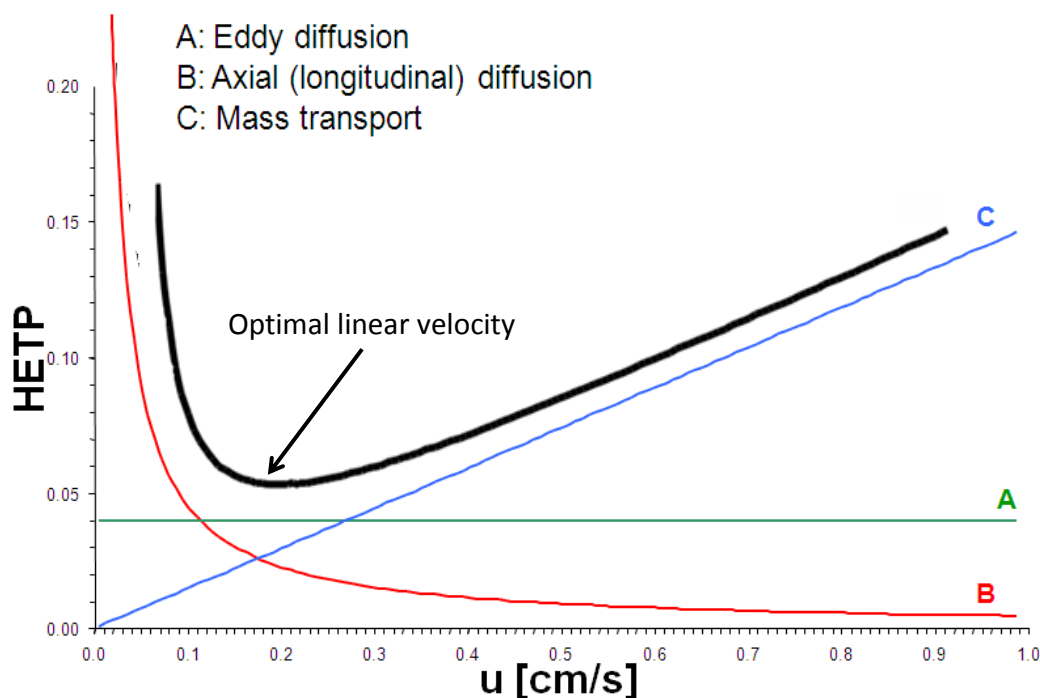


**Figure 1.5: van Deemter Plot showing contribution of A, B, and C terms on HETP. Figure courtesy of Waters Corporation**

### 1.2.11 Extra-column volume and Band Broadening

Measuring the efficiency of columns using any of the rate theories is an excellent approach to making decisions regarding column choice. An analytical scientist can make assumptions on how well a vendor can control their column manufacturing process and provide a quality column with the least occurrence of bandspreading factors adversely affecting overall column efficiency. With that said, the factors affecting column efficiency within the column are controlled by the vendor or the individual choosing to pack stationary phase in the column. Factor controlling those aspects of efficiency are more or less out of the control of the everyday analysts. There are factors that an everyday analyst can control related to the chromatographic systems, which can contribute to decreases in observed efficiency. These extra-column effects are easily controlled and easily identified via system level troubleshooting aimed at investigating erroneous observations and results.



Extra-column volume effects are found within the connections of the fluidic path of the chromatographic system. They are typically identified at the column connections due to the frequent interchanging use of columns. They are also found at valve connections, flow splitters, and detection interfaces. In some instances, improper fittings are causing other complications such as sample carryover from injection to injection in addition to the contribution to dispersion (Figure 1.6).

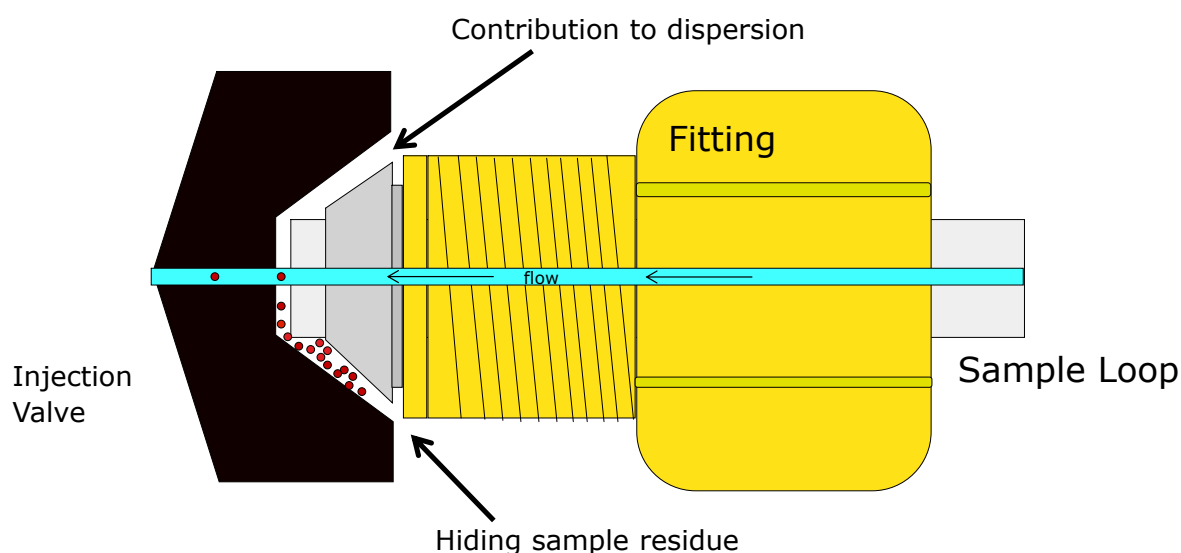


**Figure 1.6: Illustration of a sample loop fitting within the injection valve of a chromatographic system highlighting the ‘gap’ contributing to dispersion and sample carryover.**

All of the aforementioned extra-column dispersion effects are independent and therefore additive variance ( $\sigma$ ) contributions affecting overall observed separation efficiency represented by the following equation:

$$\sigma_t^2 = \sigma_i^2 + \sigma_f^2 + \sigma_c^2 + \sigma_d^2$$

**Equation 1.13: Equation for dispersion variance**

Where (t) is the total variance calculated from the additive contributions from the injector (i), the fluidic path and tubing quality (f), the column internal dispersion (c), and the detector (d).

### 1.2.12 Specific Permeability and Diffusion Coefficient

Solute permeability and diffusion provide an insight into quality when comparing columns with different packing attributes. Derivations of permeability and diffusion coefficient equations allow for theoretical equations focused to measure *separation impedance* [27] or *quality of the separation medium* [18]. They can also help predict theoretical plate assumptions regarding column efficiency comparisons when using mobile phases with different viscosities.

Diffusion coefficients for a solute in the mobile phase must be known to predict HETP or optimal linear velocities. Based on the van Deemter plots, the *slope* of C term is predicted to decrease as a result of the indirect proportional relationship of the increased diffusion coefficient ( $D$ ) to the viscosity of the mobile phase ( $\eta$ ). The diffusion coefficient can be calculated from the Wilke-Chang equation.

$$D = 7.4 \times 10^{-8} \frac{\sqrt{\psi_2 M_2 T}}{\eta V_1^{0.6}}$$

**Equation 1.14: Wilke-Chang equation for diffusion**

Where T is the temperature in Kelvin,  $M_2$  is the molecular weight of the solvent,  $V_1$  is the molar volume of the solute in milliliters, and  $\eta$  is the viscosity in centipoise, and  $\psi_2$  is the association factor for the solvent. An association factor for non-polar solvents would be 1, 1.9 for methanol, and 2.6 for water [25].

If a mobile phase of lower viscosity is used, the “resistance to mass transfer” decreases, and the slope of the C term decreases allowing for a larger range of optimal linear velocity. Dissecting this statement further, the influence of specific permeability ( $B_0$ ) relating to the packing density and flow through properties of the column/particle morphology, can be related to that of the mobile phase viscosity. Permeability is useful to know when exploring the kinetic capabilities of a packing morphology combined with instruments limitations [28-30].

$$B_0 = \frac{F\eta L}{\pi r^2 \Delta p}$$

**Equation 1.15: Equation for specific permeability**

Where  $\Delta p$  is the pressure drop along a column, r is radius of the column and F is the flow rate.

The A term of the van Deemter equation is more or less fixed by the quality of the column packing and thus having a finite minimum HETP value. However, the concepts of the

diffusion coefficient and specific permeability have influence on the B and C terms of the van Deemter and therefore influence the point of optimal flow rate.

### **1.3 Supercritical Fluids**

Supercritical fluids have been primarily a subject of physical chemistry research over the past century [31], specifically with natural products. Particular discoveries have allowed increased capabilities for analytical chemistry, provided profitable improvements when implemented by industry, and heightened the awareness as a viable environmental friendly solution addressing the worldwide initiatives for sustainability. The industry has used supercritical fluid CO<sub>2</sub> to extract essential oils from hops for use in beer brewing. The hop extracts obtained by supercritical extraction (SFE) can solve many industrial problems associated with evaporation during storage. The use of the hops extracts instead of the raw hops would eliminate the need for cooled storage essentially reducing energy costs [32]. Saul Katz from the General Foods Corporation developed a method extracting caffeine from green coffee beans resulting in a more efficient process for batch processing of decaffeinated coffee [33]. Although these are only a few examples, the applicability for supercritical fluid CO<sub>2</sub> are widespread for practical purposes throughout pharmaceutical, food, environmental, and consumer needs industries.

#### **1.3.1 History of Supercritical Fluids**

In the 17<sup>th</sup> and 18<sup>th</sup> centuries, experimentation designed to explore the behavior of fluids in presence of high temperature and high pressure was heightened with Denis Papin's invention of the "steam digester" in 1679. The steam digester, otherwise known as the *Papin Digester*, could retain water in the liquid state at temperatures greater than the boiling point and used to

extract fat from bones or reduce bone to bone meal [34]. The Papin digester was one of many devices used for experiments exploring liquefaction of gases in the late 1700s by Antoine-Laurent de Lavoisier [35] which stemmed from the interest of French baron Charles Cagniard de La Tour. Cagniard de La Tour's experimentation in 1822 using the Papin digester, a quartz ball, and alcohol marking the first reports of an acoustical difference projected by the ball when rolled in the digester as the state of phase was changed with increasing temperature [36]. Further research with a glass tube visually confirmed his hypothesis of a homogeneous mixture and cited observations of a diminished meniscus between the two layers where the gas and liquid meet. He called this phenomena the "*état particulier*" [37]. Later, Mendeleev referred to it as the "absolute boiling point" in 1861 [38]. Cagniard de La Tour's discovery initiated further interest from Michael Faraday years later who began a search for a term to call this continuity behavior [39, 40]. Thomas Andrews studied the pressure-volume curve of carbonic acid homogenous fluid and published his works using the term we currently use today – "*the critical point*" [41].

Historically, supercritical fluids have been defined as substances that are above their critical temperature ( $T_C$ ) and above their critical pressure ( $P_C$ ). Recent theoretical research highlighted in section 1.4 of this chapter discusses extensions of this *historical* definition. Once a substance is above the  $T_C$  and  $P_C$ , equilibrium of vapor and liquids, a common homogenous substance can be observed. Phase diagrams generally are constructed to describe the three states of matter for a substance; *solid, liquid, and gas*, yet provide a visual aid to defining the supercritical nature of that substance. For the example of carbon dioxide ( $\text{CO}_2$ ), the phase diagram in Figure 1.7 highlights the boundaries of each of the three states of matter whereas convergence to the triple point indicates a state of equilibrium for all three states of matter for  $\text{CO}_2$ . Upon following the boiling point boundary between the liquid and

gas states of matter, distinctions regarding the substance density can be observed until a convergence of the densities occurs. The convergence point results in a homogeneous solution occurring beyond the boiling point boundary and is defined as the *critical point*, or Cagnaird de La Tour's "*état particulier*". Changes in temperature or pressure above the critical point do not result in condensation [42].

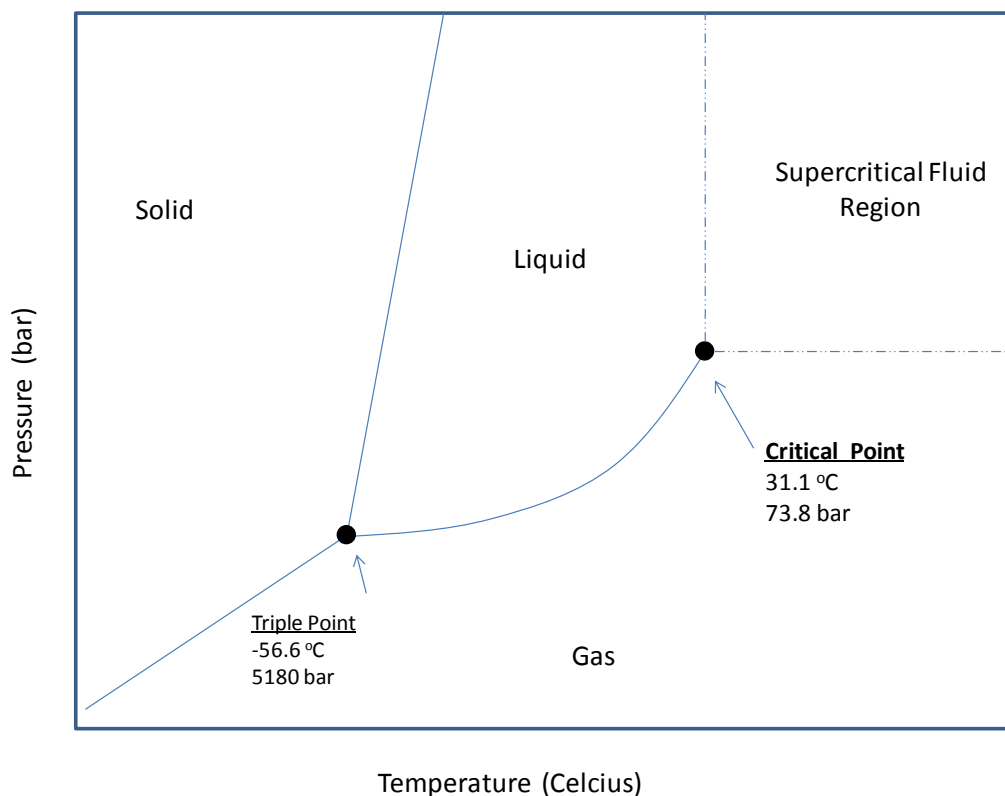


**Figure 1.7: Phase diagram illustration for carbon dioxide**

### 1.3.2 Properties of Supercritical fluids

Supercritical fluids have been pictorially described in phase diagrams, however supercritical fluid is not an additional or new state of matter such as the known states of matter, which are solids, liquids, and gases. The properties of supercritical fluids allow defined changes in the homogenous substance's density that result in advantageous characteristics when compared

to the properties of a liquid. The critical temperatures and critical pressures of many substances are listed in **Error! Reference source not found.**. A gas to liquid state transition is determined by intra-molecular forces. The motional energies of gaseous molecules can overcome the attractive forces that lead to a liquid state when the critical temperatures and critical pressures are reached [43]. An increase in pressure of a gas in a closed container forces the molecules to exist in close proximity to each other which results in frequent molecular collisions. Although a gas, the density approaches that of a liquid. The increased molecular collision rate allows the supercritical fluid to increase the solvating properties; hence it's applicability as an extraction solvent. Hannay and Hogarth published the first account of the solvating properties in 1879 and 1880 [44-46]. Hannay's findings were summarized as stating the solvating property was related to the increased density of the gas and increases in volume would result in decreased solvent action [46]. For example, appropriate manipulations of temperature and pressure of supercritical carbon dioxide (CO<sub>2</sub>) can extract complex mixtures from food, pharmaceuticals, chemicals, fossil fuels and plastics [47].

**Table 1.2: Critical temperatures and critical pressures of various substances**

Substance	T <sub>c</sub> (°C)	P <sub>c</sub> (psi)
Propane	97	616
Ammonia	132	1691
Carbon Dioxide	31	1132
Hydrogen	- 242	294
Nitrogen	-149	514
Oxygen	-118	735
Helium	-268	33
Water	374	3200
Phosphine	51	947
Argon	-122	705
Propane	97	617
Hydrogen Sulfide	102	1306

Interestingly, decreasing the density of the supercritical fluid can result in separation of the solute and from the supercritical fluid if there is a solubility mismatch and the solute and crash out of solution. The reduction in viscosity and increase in diffusivity; *where diffusivity refers to the supercritical fluid's ability to pass through a substance at a measured rate*, when applied to separation techniques, potentially increases the applicability of the supercritical fluid for chromatography but it must be balanced for analyte solubility [48]. The diffusivity and viscosity properties of a gas, a liquid and a supercritical fluid are compared in Table 1.3**Error! Reference source not found..** In terms of a practical perspective, supercritical fluids would be prime candidates for use as a mobile phase in



packed column chromatographic applications, as first suggested by Lovelock in 1958 [49, 50].

**Table 1.3: A comparison of diffusivity and viscosity values for a gas, a liquid and a supercritical fluid [41].**

	Diffusivity (cm <sup>2</sup> /s)	Viscosity (g/cm x s)
<b>Gas</b>	<b>10<sup>-1</sup></b>	<b>10<sup>-4</sup></b>
Supercritical Fluid	<b>10<sup>-4</sup> - 10<sup>-3</sup></b> <b>Liquid Like</b>	<b>10<sup>-4</sup> - 10<sup>-3</sup></b> <b>Gas Like</b>
<b>Liquid</b>	<b>&lt; 10<sup>-5</sup></b>	<b>10<sup>-2</sup></b>

The most commonly used supercritical fluid is carbon dioxide (CO<sub>2</sub>). CO<sub>2</sub> is chemically pure, non-polar, and stable. The physical state of CO<sub>2</sub> can be easily manipulated by commercial instrumentation due to the achievable critical pressure and critical temperature. The use of CO<sub>2</sub> is considered environmentally benign. The waste removal is residue-free, non-toxic (*relative to handling of organic solvents*), and non-flammable. CO<sub>2</sub> is considered a renewable feedstock. The majority of CO<sub>2</sub> collection is produced and collected in processes from the effluent of ammonia plants or derived from naturally occurring deposits [51]. It is also a by-product from commercial processes fermenting sugars from beer and wine making, yet there is no published reference of collection from beer or wine manufacturers for mass collection of CO<sub>2</sub>.

## 1.4 Supercritical Fluid Chromatography

Supercritical fluid chromatography has been researched extensively since the 1960s. The inclines and plateaus of research activity have cycled approximately each decade. During this time frame, three review articles have been published and when read collectively, cover an extremely in-depth overview of the history, theoretical principles, instrumentation innovations, and practical applications. Roger Smith's 1999 review "Supercritical Fluids in Separation Science – the dreams, the reality and the future" is a concise compilation of the 20 years prior to publication and candid perspective on the future direction of supercritical fluid chromatography [31]. Larry Taylor's 2009 review compared the capillary and packed column approaches while highlighting current trends moving forward with SFC [52]. Guiochon and Tarafder's 2011 review, focuses on the main fundamental issues that need to be studied and understood in order to reach a level of knowledge of SFC similar to the one now achieved in preparative GC and HPLC [53]. Lesellier's review in 2009 "Retention mechanisms in super/subcritical fluid chromatography on packed columns" provides a concise general overview, however the review lacks a comprehensive citation diversity of work performed by the scientific community. Berger and Lesellier account for greater than 55% of the bibliography [54]. It should be noted, a more comprehensive review based on packed column SFC providing an overview of theoretical and novel developments in recent years was finally published in 2015 during the writing of this thesis [55]. The 2015 Lesellier and West review provides a new foundation for industry to expand upon and develop new pragmatic uses of packed column SFC.

### 1.4.1 Historical Application of Supercritical Fluid Chromatography

Klesper *et al.* has been credited in the majority of publications as pioneering supercritical fluid to practice as a mobile phase for use in chromatography [56]. They built and employed

an apparatus using chloroflouroalkanes as a mobile phase due to their inertness and low flammability to separate etioporphyrin II, Ni etioporphyrin II, and NI mesoporphyrin IX dimethylester. The porphyrin colored bands was observed to elute down the path of the polyethylene glycol stationary phase lined glass column. They referred to this technique as “*High Pressure Gas Chromatography above Critical temperatures*”.

In the late 1960s, Sie and Rijinders published novel approaches using supercritical CO<sub>2</sub>, gas-liquid and gas-solid separations, and instrument designs for sample introduction and detection [57-60]. They were the first to coin the term supercritical fluid chromatography as they investigated the rapid analysis of compounds deemed heavy for ordinary gas chromatography, using n-pentane and isopropanol as mobile phase fluids under supercritical conditions [61]. In the same decade (1969), J. Calvin Giddings *et al.* expanded on this research by utilizing pressures greater than 2000 bar and reported it “Dense Gas Chromatography” [62]. Giddings insights sparked the ideology transferring the nomenclature from supercritical chromatography to evolve as “Unified Chromatography”. He stated “One of the most interesting features of ultra-high-pressure gas chromatography would be its *convergence* with classical liquid chromatography...” predicting “there ought to be only one theory, or at least one true theory, of chromatography”. 20 years after Giddings findings, Martire and Boehm’s theories link GC, SFC, and LC with a set of general equations reducing the retention expressions with assumptions [63]. They came to the recognition of certain similarities among the equations describing supercritical fluid chromatography (SFC) and several previously derived expressions (based on kindred models) for gas and liquid chromatography (GC and LC, respectively). The end result of this realization is a unified theory of chromatography, encompassing all three types of mobile phases. In further publications Martire expresses the states of phase boundaries are not involved and therefore

forming a “unified molecular theory of chromatography” however, the research was focused mostly on the capillary approaches [64, 65]. Based on similar findings, Ishii and Takeuchi introduced the term “unified fluid chromatography” in which they envisioned changing the separation mode between GC, SFC, and LC by changing temperature and pressure [66]. Chester published unified chromatography theories redefining the representation of the supercritical fluid region specified above the critical point on the phase diagram concepts in Figure 1.8 [67]. The change in perception of the supercritical region is consistent with recent theoretical research by Tarafder and Guiochon whereas the isopycnic plots were constructed to determine how the role of density dictates operating conditions for SFC [68-74].

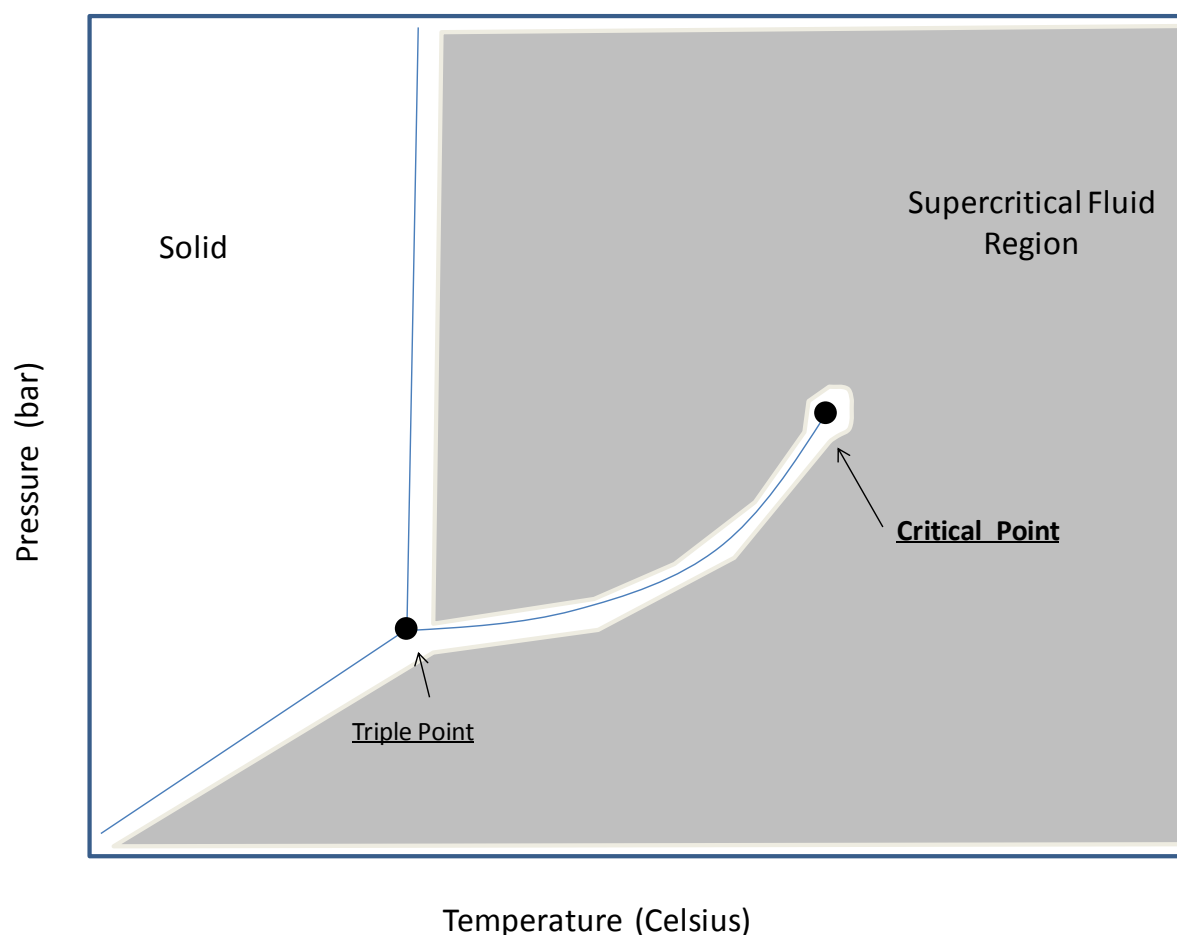


**Figure 1.8:** Two dimensional phase diagram representing a unified region derived from Chester *et al* [37].

### 1.4.2 ‘Open Tubular’ versus ‘Packed Column’ Supercritical Fluid Chromatography

Supercritical fluid chromatography can be performed with open tubular capillary columns (cSFC), packed capillary columns (pcSFC) or with packed columns (pSFC). The techniques are compared most appropriately in terms of maximum number of plates assuming the pressure drop per theoretical plate can be compared and the maximum pressure drop allowable across a column can be determined [75]. Schoenmakers reports an equation (Equation 1.16) seemingly derived from the specific permeability equation and Kozeny-Carmen equations to summarize a comparison of Open, Packed, and Packed-capillary columns:

$$[B_0 \eta n h_r \bar{v} D_M]_c = [B_0 \eta n h_r \bar{v} D_M]_p$$

**Equation 1.16: Efficiency relationship equation for the comparison of open, packed, and packed capillary columns when assuming maximum achievable theoretical plates**

Where ( $\eta$ ) is the viscosity of the mobile phase (Pa.s), ( $h_r$ ) is the reduced plate height, ( $\bar{v}$ ) is the reduced average velocity,  $D_M$  is diffusion coefficient of the solute in the mobile phase ( $\text{cm}^2 \text{s}^{-1}$ ),  $B_0$  is the specific permeability coefficient ( $\text{m}^{-2}$ ). For capillary columns  $B_0 = 32/d_c^2$ ,  $h_r = 4.5$  and  $\bar{v} = 45$ . For packed columns  $B_0 = 1000/d_p^2$ ,  $h_r = 3$ , and  $\bar{v} = 10$ .

The reduced Equation 1.17 considers the same mobile phase conditions on each side of Equation 1.16:

$$n_c = 4.63 \left( \frac{d_c}{d_p} \right)^2 n_p$$

**Equation 1.17: Reduced equation from Equation 1.16 when normalizing for mobile phase**

Schoenmakers summarizes example values in a table within the chapter concluding that very high plates counts are achievable by capillary column SFC, but they come with a cost of a very high run time (i.e. for a 50  $\mu\text{m}$  ID column, a maximum theoretical plate count of 9,260,000, but a 77,000 minute run time) [75].

Open tubular columns are designed with a film of stationary phase coated on the inside walls of the column. Successful implementations of an open tubular SFC are based on three critical parameters:

1. The system must include the column and the detector within the same pressurized value,
2. The system must minimize the contributions to band broadening, and
3. The internal stationary phase films must be optimized to resist long term bleed, yet provide minimal resistance for mass transfer.

This technique was pioneered by Novotny *et al.* premised on the early concern that packed columns produce a pressure drop along the column significantly reducing the chromatographic efficiency of a pSFC approach [76]. Open tubular capillary columns progressed initially in the 1980s based on research focusing on highly efficient separations of non-polar hydrocarbons and flame ionization detection capability. Their internal diameters were typically 50  $\mu\text{m}$  to 100  $\mu\text{m}$ . Unfortunately, enthusiasm dwindled due to lack of reproducibility, blockages due to adiabatic expansion of the  $\text{CO}_2$ , low sample “loadability” leading to poor techniques introducing the solute in small amounts (nL), limited solute applicability (i.e. poor for polar solutes), and lack of commitment from vendors to innovate the technology.

Packed column SFC (pSFC) research began to expand once the limitations of open tubular SFC were realized. The benefits of packed column SFC was realized in terms of improved separation performance, solute flexibility and instrumentation ease of use. Typically, packed columns, which are commonly used for liquid chromatography, with particle sizes ranging from 3  $\mu\text{m}$  – 10  $\mu\text{m}$ , lengths ranging from 50 mm – 300 mm and internal diameters ranging from 3.9 mm – 4.6 mm have been used. The range of usable stationary phases includes normal phase, chiral and reversed-phase columns. The first reports of packed column SFC was performed by Gere *et al.* by modifying a commercial (Hewlett-Packard) HPLC system by adding backpressure regulation, a high pressure UV flow cell, and external chilling [77]. They successfully constructed van Deemter plots comparing packed column SFC and HPLC for columns with 3  $\mu\text{m}$  and 5  $\mu\text{m}$  particle stationary phases, and the results showed that pSFC combined with small particles provide greater chromatographic efficiency and speed. The importance of their findings negated the disputes regarding the effect of the pressure drop on performance for small particle stationary phases from previous reports [61, 76].

The main advantage of packed capillary column SFC (pcSFC) is the higher specific permeability ( $B_o$ ) resulting in a higher number of theoretical plates obtained when compared to a conventional packed column with the same pressure drop. The decreased internal column diameters would require reduced instrument extra-column volumes. For this reason, the reduced internal diameters would be a challenge for detector flow cell design and sample injection designs. In comparison to open tubular capillary SFC, the benefits of packed capillary column SFC are realized in acquisition time and sample loadability.

### 1.4.3 Role of Density for Solute Retention in SFC

The role of density and its impact on supercritical fluid chromatography was first explored by Van Wassen and Scheider where they plotted capacity factors in respect to density rather than pressure, thus concluding isothermal curves were more appropriate to use [78]. Peaden and Lee used open tubular supercritical chromatography to determine similar relationships between the retention factors and density [79]. This led to a general expression for column efficiency derived from the relationship of the solute retention and mobile phase density by Poe and Martire [80].

Understanding the role of pressure, temperature and *more notably* density were determined to be controlling mechanisms for solute retention. However, the factors they controlled were determined to be mobile phase viscosity, solute diffusivity, and solubility. Lou *et al.* plotted the effect of changing temperature and pressure on solute solubility [81]. Lou *et al.* developed methodology to measure the vapor pressure of acenaphthene, anthracene, and chrysene using FID. They measured inflection points suggesting retention factors are inversely proportional to solubility and directly proportional to the affinity for the solute with the stationary phase. The experiments allowed Lou *et al.* to derive an equation to estimate the solute affinity to the stationary phase with changes in temperature. Solubility has also been plotted as a function of pressure, however it was observed by many that trends were difficult to determine [82, 83]. The solubility of different analytes with respect to pressure gave rise to different slopes resulting in crossover points. Yet, the author plots the same data as a function of density and the author observes the solubility to have clear and specific trends [73]. Solubility increases with increasing density under isothermal conditions and increases with temperature under isopycnic conditions.



Mobile phase viscosity changes with particular flow rates and directly affects the pressure drop along a column. Due to these changes in pressure, density gradients occur along the column. Scientists have modeled these viscosity changes in CO<sub>2</sub> with a wide range of pressure and temperature values [84, 85]. The National Institute of Standards and Technology (NIST) uses the equations derived from Vesovic *et al.* experimentation and provides them to researchers learning to understand supercritical fluids through modeling [84]. Together with the NIST values and REFROP software, Tarafder *et al.* [73] derived an equation based on the dependence of retention on density and temperature. Tarafder reduced the equation, Equation 1.18, which resembled the solubility equation derived by Chrastil [86].

$$\ln(k_i) = -(\lambda_i + 1) \ln(\rho) + \ln(f_i(T))$$

**Equation 1.18: Tarafder's reduced equation for retention dependency on density and temperature**

Where  $k_i$  is the retention factor of component  $i$ , where  $\lambda$  is a coefficient depending on the experimental conditions,  $\rho$  is the density of the mobile phase and  $T$  is the temperature.

Although the solute solubility has a dependence on temperature and density, it was the opinion of Tarafder *et al.*; *stating later in section 1.4.5*, that the solute diffusivity dependence was strongly influenced by the mobile phase density alone.

#### 1.4.4 Column Efficiency in SFC

Density plays a critical role in SFC, in terms of solubility, diffusivity, viscosity, pressure drop across a column, and therefore it can be expected that density plays a major role in chromatographic efficiency. The earliest works correlating the role of density and

determinations of column efficiency in terms of height equivalent to a theoretical plate (HETP) was performed by Bartmann and Schneider [87]. Their Equation 1.19 is divided into three terms, all of which are affected when there is a change in density.

$$H = B \frac{\bar{u} d_p \rho}{\eta} + \frac{1.3 D_m}{\bar{u}} + \frac{1.5k}{(1-k)^2} \frac{\bar{u} d_p F}{D_m}$$

**Equation 1.19: Bartmann and Schneider efficiency equation when accounting for the role of density in SFC**

*Therefore:*

$$\text{If } \rho \downarrow, \text{ then } \bar{u} \uparrow \quad D_m \uparrow \quad \eta \downarrow \quad k \uparrow \text{ and } H \downarrow$$

*(whereas  $k$  remains an integer greater than 2 and changes in density are a function of changes in pressure while maintaining constant temperature above the critical point)*

The loss of efficiency, specifically in particular regions of low pressure and low temperature where the mobile phase has a low viscosity and high molecular diffusivity, has been studied and hypothesized for decades. The earliest investigations hypothesized that the loss of efficiency was due to large pressure drops across the column [61, 76]. This theory was later confirmed by various authors, suggesting the low efficiency is attributed to large density gradients [88-90]. A commonality was observed throughout many literature citations, where for the general operating values of 373 K and 80 bar, scientists repeatedly generated low efficiency “poor” chromatograms. Rajendran *et al.* performed experiments near this critical region speculating that the poor chromatographic efficiency was due to adiabatic cooling [91]. Poe and Schroden [92] expanded on this concept and determined the occurrence of radial temperature gradients along the column in which Kaczmariski *et al.* [93] calculated the axial and radial temperature gradients within the column during Poe’s experiments. They experimentally determined radial gradients by evaluating the efficiency of the column during

insulated and air bath configurations. At reduced densities, approaching 1.0, band broadening and peak splitting was far greater with the column residing in the air bath versus the insulated column, suggesting the radial temperature gradient was mitigated, but the axial gradient maintained an influence on the separation. Reducing the particle size only pronounced the band broadening issue, thus leading to the investigations the separation influence due to the temperature drop across a column. During some preliminary experimentation with sub-2  $\mu\text{m}$  particle stationary phases performed on prototype instrumentation, similar peak shape abnormalities were observed and will be discussed further in Chapter 2.

#### **1.4.5 Recent Theoretical Advancements in SFC**

In 2010, the collaborative research from the University of Minnesota-Duluth, University of Tennessee, Oak Ridge National Laboratory, Rzeszow University of Technology (Poland), and Waters Corporation, resulted in significant advance in supercritical fluids theory. The research was focused on explaining the insights of previous works with peculiar results regarding the observed efficiency when using neat  $\text{CO}_2$  in supercritical or subcritical states. The recent theoretical research published by Tarafder *et al.*, correlates the critical role of density, the design of constant density plots (or *isopycnic plots*) and the applied use of the isopycnic plots to determine optimal operating parameters when using SFC. The isopycnic plots are referred in the context of a pressure – temperature plane (P-T plane). Tarafder successfully explains the previously reported phenomena using the isopycnic plots proving or disproving hypothesized claims in the previous works.

## **1.5 SFC Technology and Instrumentation**

For the purposes of this research, the general components of SFC focused technologies such as stationary phases and instrumentation, are discussed in this section enabling the low dispersion system evaluation, systems integration studies, method development strategy development and natural products research performed in Chapters 2 through 6.

### **1.5.1 SFC Core Components**

Instruments used for supercritical fluid chromatography require a core configuration different to conventional liquid and gas chromatographic systems (Figure 1.9) illustrates the essential components for a modern day SFC instrument coupled to mass spectrometry.

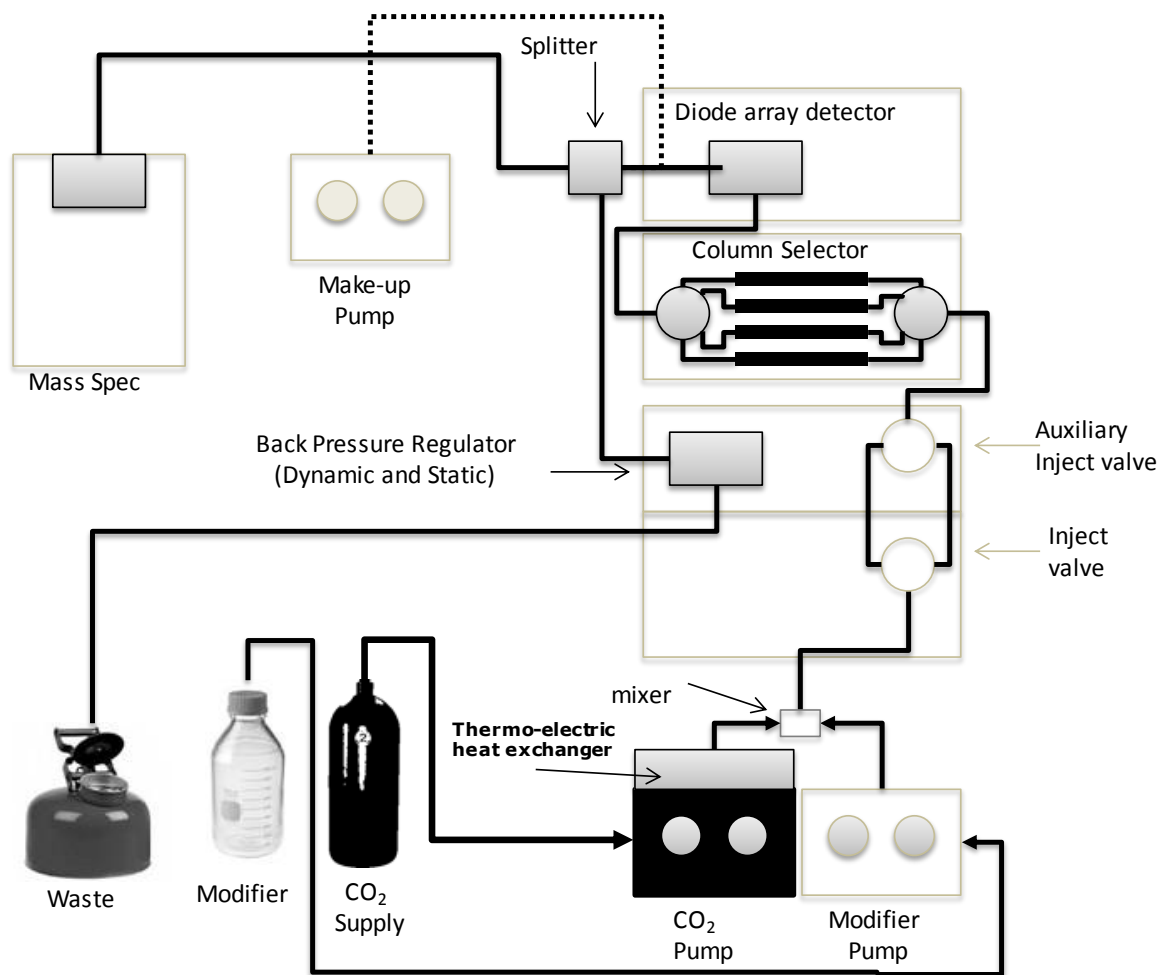


**Figure 1.9: Core components schematic of the Waters ACQUITY UPC<sup>2</sup> instrumentation with MS detection and make-up flow. Figure courtesy of Waters Corporation.**

### 1.5.1.1 Pump Design

Pumping mechanisms are designed in one of two approaches as shown in Figure 1.10. The pumping mechanism is a binary high pressure mixing design.

- *Design 1 - cools the CO<sub>2</sub> using an integrated thermoelectric chilling device that operates as a heat sink located on the piston delivery component of the pump with heat sink cooling coils located at the head of the pump.*
- *Design 2 - utilizes a chilling device between the CO<sub>2</sub> tank and the pumping device, typically performed using a glycol-chilling agent. In both instances, the CO<sub>2</sub> is cooled to maintain a more dense liquid state. Liquid CO<sub>2</sub> is less compressible than supercritical or gaseous CO<sub>2</sub>; therefore cooling the CO<sub>2</sub> fluid to low temperatures allows the pumping mechanism to reproducibly compress and control the density of the CO<sub>2</sub> and delivers the fluid throughout the chromatographic system in a manner comparable to HPLC.*

Although the fluid delivered is in a liquid-like state, super/subcritical properties occur within the column once heat is applied. The design which best controls the temperature, density, and compressibility effectively, should yield improvements in baseline noise and reproducible elution times. In theory, Design 1 allows for a more precise electrically controlled temperature environment within the pump chamber, thus allowing for a reduced baseline drift and reduced baseline noise due to external environment temperature fluxuations. Basically, Design 1 should minimize the amount of density variability of the liquid CO<sub>2</sub> and allow for a more controlled delivery of the mobile phase. The improved solvent delivery would benefit signal to noise ratio measurements and improve the overall sensitivity limits of detection capabilities of the instrument system design.

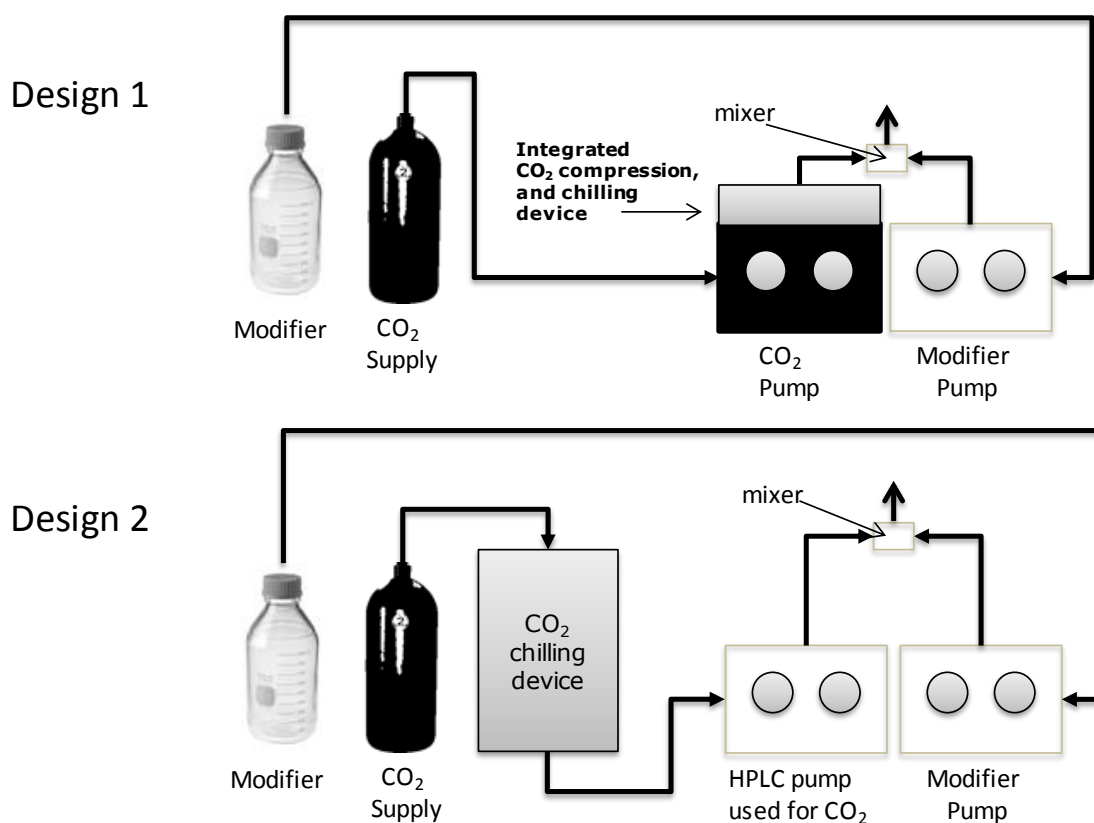


**Figure 1.10: Schematic representation of two different commercial designs of pumping mechanism delivering liquid CO<sub>2</sub>. Figure courtesy of Waters Corporation.**

### 1.5.1.2 Sample Introduction

Historically, traditional SFC instrumentation was simply re-purposed HPLC equipment which used a single valve injection design Figure 1.11 (A). This can lead to irreproducibility from injection to injection. As a result, validation of an SFC method was considered a challenge. The injection sequence performed by a re-purposed HPLC autosampler can result in difficulties maintaining the physical state of CO<sub>2</sub>, therefore leading to poor injector linearity, accuracy and precision. Adiabatic expansion of the CO<sub>2</sub> liquid would occur and vent through the path of least resistance, typically in the path of the needle. The out-gassing of the CO<sub>2</sub> from the needle would create positive pressure at the point of sample retrieval and therefore result in injection-to-injection irreproducibility. As a result SFC could not be

effectively used for quantitative analysis. In order to maintain the physical state of CO<sub>2</sub>, only full loop injections could be performed. As a consequence of only performing full loop injections, sample was wasted due to loop overfills needed to place the sample properly in the loop for injection.

The use of a second auxiliary valve (Figure 1.11 (B)), allows the injection mechanism to maintain the CO<sub>2</sub> physical state and prevent expansion and expulsion of the gas out of the needle. The auxiliary valve also provides expanded flexibility allowing partial loop injections with precision and accuracy. The dual injection design will vent residual pressurized CO<sub>2</sub> in the primary sample loop to waste, enabling the sample to enter the loop under atmospheric pressure while maintaining the closed circuit of the mobile phase flow stream keeping the CO<sub>2</sub> mobile phase in a supercritical phase. The design of the auxiliary valve also allows for reductions in pressure pulsation resulting in adding to the reproducibility of the sampling design when performing partial loop injections. A single valve design would result in positive pressure inside the needle during the sampling from the vial due from the depressureing residual CO<sub>2</sub> escaping through the path of least restriction. this results in irreproducible injections, carry over, and accuracy issues with the methodology.



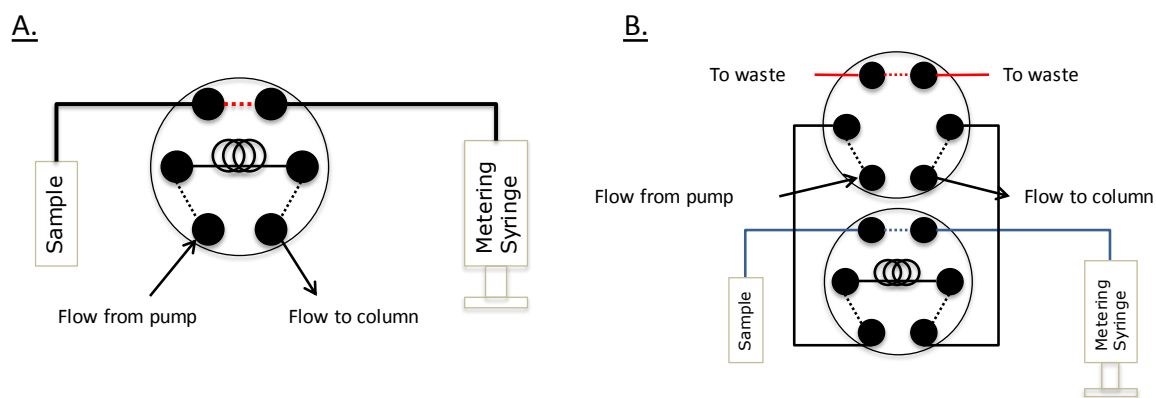


**Figure 1.11: Schematic representation of two different injector designs; single (A) and dual (B) valve designs used in autosamplers for SFC instrumentation.**

### 1.5.2 SFC Stationary Phases and Mechanisms

Supercritical fluid chromatography is referred to as a derivative of normal phase chromatography. Normal phase LC (NPLC) is characterized as an adsorption based retention mechanism and driven by the solute affinity to the stationary phase. This is different to reversed-phase LC (RPLC), which is characterized by a hydrophobic retention mechanism based on the solute partitioning in the stationary phase and the solute elution affinity upon increasing organic in the mobile phase. Many stationary phases can be used with super/subcritical CO<sub>2</sub> mobile phases. SFC which is described to have adsorption retention mechanisms can also have ionic interactions either with the mobile phase or stationary phase. Solute retention can be affected by the addition of an ion-pairing additive increasing the polarity of stationary phase and mobile phase [94]. One of the differences between normal phase and reversed-phase LC are the opposite polarities of the mobile phases used to elute the solute. In SFC, the mobile phase can remain constant regardless of the type of stationary phase; polar or non-polar leading to a ‘stationary phase agnostic’ approach. Column polarity along with the choice of additive [95] can dictate the elution of the solute providing a more “unified” approach to chromatography [96].

The industry has primarily adopted the use of chiral stationary phases for the preferred analysis of enantiomeric racemates. Chiral stationary phases are manufactured either with (i) a polymer coated with an enantiomeric selector or with (ii) an immobilized enantiomeric selector. In terms of which is more effective, a study by Ghanem *et al.* concluded the polymer coated amylose tris-(3,5- dimethylphenylcarbamate) chiral column provided the best separation of the chiral  $\beta$ -blocker probes. However, the immobilized amylose tris-(3,5- dimethylphenylcarbamate) chiral column provided solvent flexibility such as allowing the use of chlorinated organic solvents [97].

Normal phase columns and columns used for hydrophilic interaction liquid chromatography (HILIC) are polar and commonly used for the achiral analysis of polar solutes. These columns are packed with particles such as pure silica and stationary phases with ligand functionality consisting of any of the following: diol, cyano, amino, 2-ethylpyridine (2-EP), amide, and aminopropyl groups. Reversed-phase columns are typically non-polar and include hydrocarbon chains bonded to silica such as octylsiloxane bonded silica ( $C_8$ ) and octadecylsiloxane bonded silica ( $C_{18}$ ). Other typical RPLC columns that are used include phenyl propyl, phenyl-hexyl and penta-flouro phenyl bonded ligands. In a paper by West and Lesellier, they classify 28 commercially available stationary phases based on three types: non-polar, moderately polar and very polar [96]. They evaluated up to 111 solutes using linear solvation energy relationships (LSER) and plotted selectivity characteristics of the solutes, which allowed for a visual representation of the 28 columns in a five-dimensional plot. They conclude by stating, “SFC is a normal phase and a reversed-phase technique depending on which stationary phase was used”. If the mobile phase were more polar than

the stationary phase, as in reversed-phase LC, then a plot of the logarithm of the retention factors ( $\log k$ ) versus the logarithm octanol-water coefficient ( $\log P$ ) would indicate a decreased retention as polarity increased. The reverse is true when plotting  $\log k$  vs.  $\log P$  for stationary phases which are more hydrophilic than the mobile phase, a similar observation to that obtained with normal phase LC. West *et al.* noted that when the stationary phase is bonded with an aromatic ligand, the  $\log k$  vs.  $\log P$  trending for polarity is indiscriminate for the solutes tested, thus eluding to retention mechanism influence from other functionality from the aromatic ligand [96]. Therefore, their LSER models provide a characterization of stationary phases because the equation considers the additional factors that may affect retention such as hydrogen-bonding,  $\pi$ - $\pi$  interactions, and dipole-dipole interactions induced by the bonded ligand.

### 1.5.3 Detection Schemes

Traditional SFC instrumentation has been configured with various types of detection such as Ultraviolet (UV/Vis), Diode Array (DAD) *or Photodiode Array (PDA)*, Evaporative Light Scattering (ELSD) [98], Flame Ionization (FID) [99], Mass Spectrometry (MS), Chemiluminescent Nitrogen (CLND) [100], Fluorescence (FLR) [101], Corona Charged Aerosol (CAD) [102], Acoustic flame ionization [103, 104].

Systems configured with UV based detection (UV, PDA) are one of the most commonly used types of detection for pSFC. Unfortunately, like the other components, the UV based detectors have been repurposed HPLC modules. The flow cells used in these liquid based detectors are designed with the refractive index of typical liquids used with LC analysis. The refractive index for CO<sub>2</sub> (1.000) is quite different than water (1.333) or methanol (1.330). Therefore, the noise observed from a traditional SFC chromatogram would indicate curvature, disturbances or drift in the baseline [105, 106]. Sensitivity would also be impacted therefore challenging the capability to perform trace analysis, such as impurity analysis of pharmaceuticals.

### 1.5.4 Back Pressure Restriction and Regulation

The key functionality to using instrumentation with CO<sub>2</sub> based mobile phases is the ability to maintain conditions that restrict the CO<sub>2</sub> liquid or super/subcritical fluid from endothermic expansion to the gas state. Backpressure restriction can be achieved by using either a static restriction or variable restriction. Static restriction is typically performed using a length of tubing or capillary that applies a restrictive pressure greater than the critical pressure of the component used, such as CO<sub>2</sub>. Static (*or fixed*) restriction cannot control backpressure, and

therefore, cannot control mobile phase density as mobile phase density changes with changing percent modifier and this can greatly impact the separation. Static restriction lacks the flexibility to perform automated approaches toward method development exploring pressure as a variable to aid changes in selectivity.

Instrumentation employing CO<sub>2</sub> based mobile phases utilizes a more practical approach by including a module that can variably control the pressure with software control. This is commonly referred to as an automatic backpressure regulator (ABPR). The general perceptions of the ABPR designs are not favorable by scientists, yet they accept the necessary evil as a tradeoff for flexibility. Reported issues typically cite performance concerns related primarily to baseline noise generation. ABPR modules utilize a “needle and seat” construction that is powered by a stepper motor. The stepper motor applies pressure on the seat mechanism using the needle. The resolution of the stepper motor describes the amount of degrees rotation per pulse. The higher the resolution, then the more refined the stepper motor can make small movements. The benefits of smaller movements by the stepper motor are realized in less pulsation and less baseline noise observed in the chromatogram.

Another applied approach to restriction employs a fixed restrictor with the make-up pump running a reverse flow gradient. This allows the ability to keep the amount of modifier constant to the second detector in parallel and across the restrictor. Unfortunately, like the static approach, the backpressure cannot be variably controlled, and therefore, mobile phase density will vary with changes in modifier. In order to interface with multiple detectors, a flow splitter that allows the control of the column outlet backpressure provides the greatest flexibility.

When coupling UV detection to a destructive based detector such as ELSD or MS, a multiple connection splitter allows for a fixed leak and introduction of make-up flow when also connected to an ABPR or fixed restrictor. This enables control of the mobile phase density. The challenges to this approach are associated with minimizing band spreading when comparing the two detector traces (i.e. UV vs. MS), and maximizing sensitivity for the detector receiving the fixed leak of flow versus diverting the majority of the sample to waste. Schematics of multi-connection splitter configurations are illustrated in Figure 1.12 and Figure 1.13. Figure 1.12 is a commercially available splitter and Figure 1.13 is a splitter designed to utilize a lower amount of make-up flow which results in reduced dilution of the sample and provides a stable flow when introduced into a MS detector.

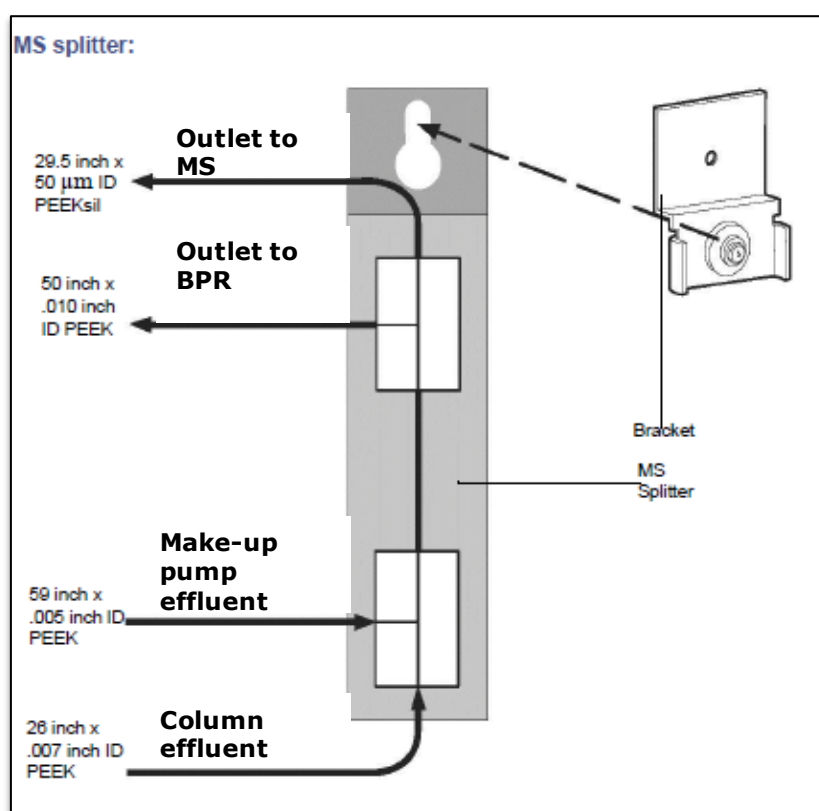


**Figure 1.12: Schematic of a commercially available splitter from Waters Corporation (Courtesy of Waters Corp.)**

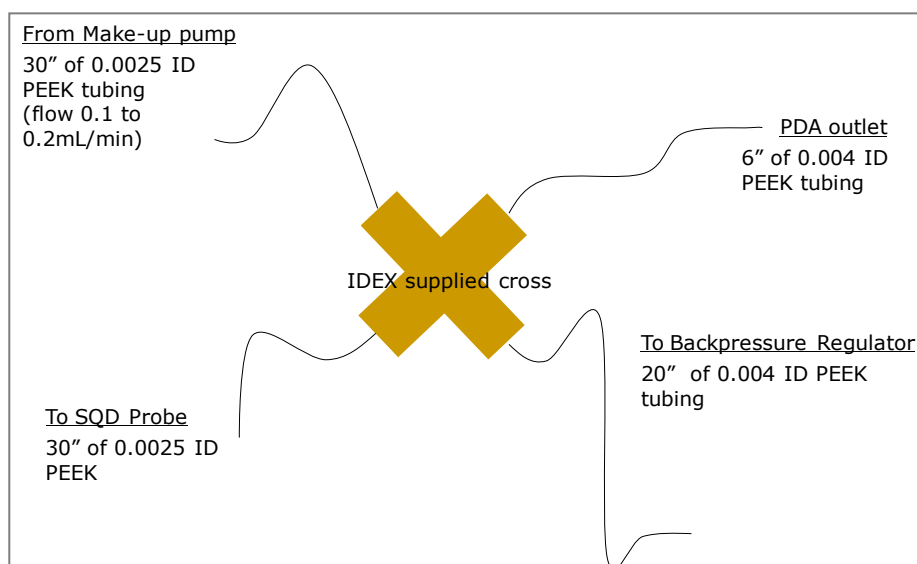


**Figure 1.13: Schematic of a ‘home-made’ splitter designed to minimize make-up flow sample dilution when interfaced to MS in order to maximize sensitivity.**

## 1.6 Supercritical Carbon Dioxide Opportunity for Natural Products Research

As stated earlier, natural product research involves extraction techniques, chromatographic separations, and isolation and scale-up purification tools. Extraction procedures require flexibility for constituent solubility and the range of polarity found in natural products. In practice, scientists utilize a variety of extraction techniques such as microwave extraction, soxhlet extraction, solvent-solvent extraction and solid phase extraction (SPE) to meet the diversity criteria. Supercritical fluid extraction (SFE) uses carbon dioxide ( $\text{CO}_2$ ) as the primary solvator and organic solvents (*protic or aprotic*), as a secondary solvator in order to control the extraction solvating strength. SFE presents an opportunity as a single technique capable of spanning a range of solute polarity and matrix complexity just by manipulating temperature and pressure variables to maximize diffusion or solubility, respectively. Coupling SFE approaches to chromatographic analysis have the potential of simplifying the sample preparation process required to achieve a comprehensive representation of natural product profiles, thus streamlining the time required to attain results.

High throughput screening strategies can benefit from the implementation of supercritical fluid chromatography. The SFC mobile phases are less dense thus resulting in a greater throughput. Historically, SFC has been highly used in drug discovery primarily for chiral screening. The opportunity for achiral use is growing. SFC has the capability of using a single solvent system in terms of elution solvent and dilution solvent. Therefore, time savings exploring selectivity is enhanced due to the range of chromatographic tools compatible with a single solvent system such as polar, non-polar, chiral, and hybrid stationary phases. During recent personal communications with pharmaceutical companies such as AstraZeneca (AZ), Janssen and Janssen, Boehringer Ingeheim (BI), GlaxoSmithKline (GSK), Sanofi Aventis, Eli Lilly, and Dart NeuroSciences, each laboratory manager of medicinal chemistry and supporting separation science divisions indicated a greater use of supercritical fluid chromatographic techniques for achiral analysis. Each group cited the recent improvements of commercially available analytical SFC instrumentation in terms of robustness and reliability, which are *key* to supporting the purification activities. Many of these groups mentioned previous HTS screening activities low success rate, yet they all acknowledged a current shift in practice to re-screen natural products focused based libraries due to recent re-evaluations of natural products and natural products derived drug approval history. This new-found knowledge has allowed companies to intelligently build relevant HTS libraries to increase the H2L success rate. Many of the Medicinal Chemistry laboratories managers cited an improvement in both cheminformatically and analytical performance as a result of these updated technologies. Although these groups are shifting to greater SFC analytical and purification usage, they all commented on the difficulty of implementing a common approach or one-dimensional protocol analogous to the reversed-phase HPLC strategies used in the past two decades. Basically stating, these organizations are looking for guidance regarding method selection parameters for SFC HTS and method



development strategies to aid optimization decisions and workflows within their processes. Currently, a high number of publications cite existing collaborations and continue to grow between industry, academia and vendor providers searching to better characterize and develop the tools needed to progress supercritical fluid techniques for drug discovery.

In this study, the primary aim of this research is to provide a pragmatic approach and expectations when implementing sub-2  $\mu\text{m}$  particle stationary phases for packed column supercritical fluid chromatography for the audience of the pharmaceutical industry. The focus of this study is primarily aimed at the pharmaceuticals audience; however, the information should act as an applicable roadmap for additional industries such as the chemical materials, petroleum, and food research. The aim will be achieved through a step-wise phase driven approach of careful experimental design strategies and application development which integrates the technologies and strategies which are required to discover new molecular entities. The hypothesis is to prove supercritical fluids as a critical requirement for the workflows involved with natural product research and new molecular entity discovery. This hypothesis is inclusive of proving sub-2  $\mu\text{m}$  particle stationary phase packed columns coupled to supercritical fluid chromatography has become a robust approach that has been theoretically nurtured by academia and implemented with fortitude by both instrument and column vendors. The overall hypothesis relies on natural products acting as *the vehicle* to quickly identify unique chromatographic behavior due to their complexity of polarity range and structural diversity.

The objectives that will help determine the aims of this thesis are categorized below and briefly described:

1. Verify the expected theoretical benefits of using sub-2  $\mu\text{m}$  particle stationary phases for packed column supercritical fluid chromatography. The requirement of this verification includes the assessment of prototype low system volume SFC instrumentation, confirming basic van Deemter principles and correlate results to previous and recently published findings. The comparisons of different column formats; sub-2 $\mu\text{m}$  and supra-2 $\mu\text{m}$ ; the chromatographic efficiency can be reviewed and compared with RPLC trends when reducing particle size. This will help determine if the SFC instrumentation design facilitates the use of sub-2  $\mu\text{m}$  particle stationary phases. These findings will be reflected in Chapter 2.
2. The effect of solvents typically used in a synthesis laboratory will be explored to assess their effects on chromatographic performance. Attain method development insights and strategies which are fit-for-purpose for their intended use in discovery HTS and applied pharmaceutical development. This requires a variety of experimentation such as method development of impurity profiles for related substances and biologically related small molecules found in nature such as lipids. The experiments will be designed to help understand and control the primary influential variables that effect selectivity, sensitivity and resolution as it pertains to the relationship of the solutes, stationary phase and mobile phase. Careful observations will be required in terms of identifying secondary interactions or influence on the chromatographic separation. The end result should conclude a simple-to-implement guide and workflow for the industry to implement sub-2  $\mu\text{m}$  particle stationary phases for packed column supercritical fluid chromatography.
3. Explore a chemical compound library of intermediates using generic SFC screening methodology and correlate chromatographic performance to solute physiochemical and structural attributes by use of cheminformatics software provided by ChemAxon. A routine use screening method will be developed to analyze the library. The chromatographic attributes of retention, peak symmetry, peak width, efficiency, peak height, and peak area will be recorded for each column that they analyzed with. These results will be correlated with a variety of physiochemical properties of the molecule (ie:

logP, logS, polarizability, etc) and with the structures number and presence of functional groups (i.e; amines, esters, hydroxyl, etc) . The compound library subset will be selected based on the Lipinski's 'Rule of Five'. A key aspect of this study would be to attain a system suitability method capable of alerting to system level issues affecting chromatographic performance. By utilizing the informatics tools typically used by medicinal chemists and minimizing the occurrence of skewed data entry into the informatics modelling, confidence can be achieved when identifying particular outliers associated with the structural features physiochemical properties of the solute.

4. Develop methodology strategies using the knowledge gained from the previous studies exploring solvents, selectivity variables, and instrument interfacing best practices and apply them to techniques practiced in typical pharmaceutical industry discovery organizations. High throughput screening of chemically diverse compounds will be performed and the results compared with those achieved by reversed-phase LC approaches. The application strategy in this phase will also include the reaction monitoring of three pharmaceutical syntheses from building block scaffolds to final product.
5. Investigate sub-2  $\mu\text{m}$  particle stationary phase supercritical fluid chromatography coupled to mass spectrometry for chemical profiling of chamomile extracts as an orthogonal approach to chromatographic techniques like RPLC and GC. The aim of this phase is to provide insight for future botanicals profiling workflows. It entails comprehensive profiling techniques to discovering unique chemical markers. The application was designed to be validated by previously reported and known reversed-phase results to further validate the use of sub-2  $\mu\text{m}$  particle stationary phase supercritical fluid chromatography and identify additional benefits of utilizing the technique. Aside from providing a continuation of comparative analytical separation techniques, the use of multivariate statistical processing of results will be used to profile the extracts of authentic natural product reference materials for new chemical entities and batch compare commercial products.

6. Summarize the investigations and final thoughts from previous chapters but also provide future insight regarding the impact of supercritical fluid extraction techniques in relation to typically performed solvent-solvent techniques to complete the concept of a fully supercritical fluid workflow for sample preparation and analysis of natural products for new drug discoveries.

## CHAPTER 2:

---

# Investigations of a Low Dispersion SFC Prototype Instrument Using Sub-2 $\mu\text{m}$ Particle Size Columns

## CHAPTER 2

### 2 Investigations of a Low Dispersion Prototype SFC Instrument using Sub-2 $\mu\text{m}$ Particle Size Columns

#### 2.1 Introduction

Limitations in analytical SFC instrument design and column availability have prevented the adoption of small particle pSFC[48]. Earlier attempts at implementing sub-2 $\mu\text{m}$  packed column SFC (pSFC) have resulted in many false starts due to the lack of commercially available instrumentation optimized for sub-2  $\mu\text{m}$  particle stationary phase analysis[48, 75, 92]. As for analytical pSFC, many systems identified in the public domain utilize instrument configurations limited by large system volume and extra column volumes which affect their ability to achieve optimal chromatographic performance[50, 52, 54, 94, 96].

A new generation of SFC technology was designed by the research, development and engineering (RD&E) teams at Waters Corporation. Their design concepts were targeted to address the general issues of traditional SFC commercialized and non-commercialized instrumentation regarding baseline stability, chromatographic sensitivity, and instrument robustness, specifically in regards to the back pressure regulator mechanism. The design explored the different modules; pump, autosampler, detector, and back pressure regulator individually. Additionally, the initial design when based from the ACQUITY UPLC commercialized technologies provides already implemented design changes reducing extra-column volume and system volume. The prototype SFC instrumentation underwent much iteration of optimization and improvement during this study (Figure 2.1). Some improvements were based on the results of this chapter and overall thesis and some were

optimized based on the results of the collaborative efforts from others whom received prototype instrumentation within the Waters organization. Additionally, some brief discussions about the results that led to optimizing the instrument design is touched upon, but the full results will not be shown due to the proprietary nature of the results, specifically pertaining to the autosampler modifications to which this author had generated the results.

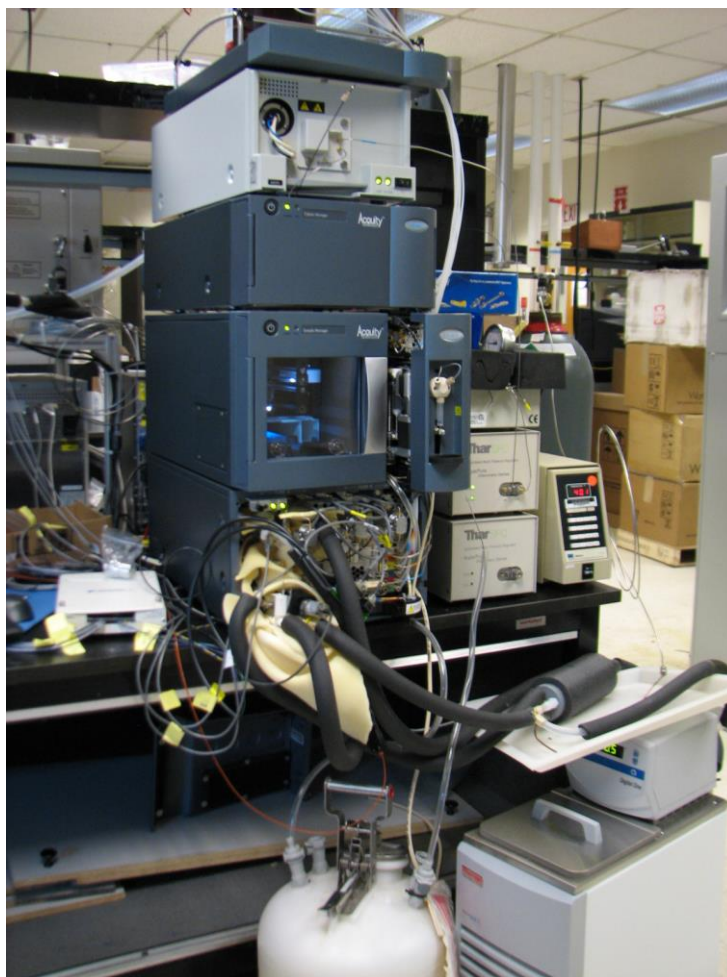


**Figure 2.1:** Initial prototype SFC instrumentation design utilizing modified ACQUITY UPLC pump, autosampler and detector designs and Thar modified automated back pressure regulator instrumentation.

The prototype SFC pump utilized a modified ACQUITY UPLC binary pump. The unit was modified with an external glycol cooling device engineered to cool the primary and actuator of the A side of binary pump heads which was used for the delivery of the CO<sub>2</sub> gas directly

from a 50 lb. tank. This allowed the CO<sub>2</sub> gas from the gas cylinder to be converted to a liquid state for easier and more consistent delivery by the pumping device. The B side of the binary pump, or modifier side, was not engineered with the glycol cooling mechanism. At this time, the temperatures of the CO<sub>2</sub> pump heads were programmed to cool at a maximum of 12 °C. The engineering group used thermal heat sensing technology to determine the efficiency of the cooling device attached to the A side of the pump head. The addition of insulation increased the cooling efficiency but also reduced the number of pressure transducer failures due from condensate penetrating to the electronics of the pressure transducer. Although the actual results are proprietary, it was determined additional insulation was required in order to cool the pump heads to the targeted temperature. Cooling to the targeted temperature allowed for the CO<sub>2</sub> gas to be converted to a liquid state, thus allowing the pumping device to more accurately deliver the solvent with minimal variation arising typically associated with gas compressibility. Mixing of the liquid CO<sub>2</sub> and modifier were not optimized or explored in depth at this point in time. Also, the pumping algorithms were continuously optimized for used with liquid CO<sub>2</sub> delivery as more was understood and modeled by the engineering group at Waters. These modifications to the prototype SFC instrument pump algorithms were uploaded as new firmware on a weekly basis. Therefore, the results in this chapter gave general assumptions to observations obtained from the results and not assumed to be highly reproducible until the SFC instrument design was closer to a commercialization designs. The final commercialized pump used for the later chapters in this thesis employed the electrothermostatically controlled pump where the two pump heads of the CO<sub>2</sub> delivery side are controlled at two different temperatures; 6 °C for the primary and 12 °C for the accumulator, to maintain an optimized gas to liquid conversion and delivery of the CO<sub>2</sub> liquid.



The introduction of the sample by the autosampler was another area of concern. It was assumed that the irreproducibility of results and lack of uptake by the industry; such as the pharmaceutical industry, was due to the inability to meet suitable accuracy and precision results during a validation that were comparable to a 4 or more sigma level of confidence as observed with other chromatographic techniques. Different injection mechanisms such as a flow through needle (FTN) injection design, fixed loop injection design, and finally a dual valve injection design were explored for the prototype SFC instrumentation. The majority of the investigations explored the flow through needle injection design based on the flexibility of this design providing partial loop injection capabilities, a capability not previously provided in typical SFC instrument designs. In summary, the FTN design explored different sampling methods that were compared to 5  $\mu$ L fixed loop injection result used as the benchmark. The final modification to the prototype autosampler utilized a waiting period was implemented after an initial decompression followed by a needle flush just before the sample was aspirated. This approach was deemed successful when the optimization of the wait and flush times resulted in a retention time %RSD for 6 replicate injections to be less than 0.5% and area %RSD to be less than 2%.

The final modifications were to the photodiode array detector. A series of undisclosed modifications were made to the optics bench of the detector. It was communicated by the Waters engineering team that the optics bench was optimized for the refractive index of liquid CO<sub>2</sub> rather than for the refractive index of aqueous liquids as typical for RPLC detectors. The flow cell was redesigned using a 10mm path length. The traditional reduced volume UPLC flow cell constructed of Teflon AF was not compatible with liquid CO<sub>2</sub>.

The automatic back pressure regulator was a new design utilizing a higher resolution stepping motor with a new interface for the needle and seat valve design. The larger and updated motor technology required an updated CPU and power supply for control needs. The materials used for the needle coatings and seat were an ongoing development project by the engineering group at Waters during the investigation within this chapter. The ABPR instrument module was modified with different needle materials during the course of the investigation this chapter.

The goal of this investigative study is to determine the feasibility and functionality of this prototype low system volume instrument configuration for use with sub-2  $\mu\text{m}$  particle stationary phases. The study is designed to:

- Determine instrument design feasibility
- Identify appropriate analyte probes
- Identify and solve any obscure retention behaviors, and
- Confirm similar van Deemter behavior to that of sub-2  $\mu\text{m}$  particle column UHPLC when used with appropriately designed instrumentation.

## **2.2 Experimental**

The experiments within this chapter were performed using a prototype low dispersion SFC instrument produced by the RD&E division at Waters Corporation. There are a multitude of changing experimental parameters explored within this study, therefore an explicit description of additional experimental variables are referenced within the sub-section text and figure captions where appropriate.

## 2.2.1 Analyte probes selection study

### 2.2.1.1 Materials and preparation

An 18 component test mixture (Table 2.1) was selected based on availability and prepared as 1mg/mL stock solutions in methanol. The working standard mixture was prepared such that the final concentration of each analyte was 0.01mg/mL. This concentration was used to achieve a suitable UV signal.

**Table 2.1:** 18 components used for test mixture

Compound name	logS
3-benzoylpyridine,	-2.79
cholecalciferol,	-9.43
6-hydroxyflavone,	-4.10
4-nitroaniline	-1.93
caffeine,	-0.44
theophylline	-4.10
carbamazepine	-3.79
estradiol,	-3.99
4,4'-biphenol	-3.02
cortisone	-3.04
prednisone	-3.38
acetaminophen	-1.14
sulfisoxazole	-2.44
hydrocortisone	-3.09
sulfamethizole	-2.85
prednisolone	-3.43
sulphenazole	-3.70
4-aminophenylsulfone	-2.85

The compounds listed in were purchased from Sigma-Aldrich (Missouri, USA). . The working mixture was prepared adding 1 mL of stock solution to a 100 mL volumetric flask and diluted to volume with methanol. Acetone (HPLC Grade), acetonitrile (Optima™ LC/MS Grade), and methanol (Optima™ LC/MS Grade) were obtained from Fisher Scientific (New Jersey, USA).

### *2.2.1.2 Instrument conditions*

#### *2.2.1.2.1 18 component test mix study*

The analysis was performed using a 2  $\mu$ L sample injection. The flow rate was maintained at 1.2 mL/min. Gradient elution was performed using a linear addition of the methanol modifier from 2% to 16% over 7 minutes. The column temperature was set to 45  $^{\circ}$ C. The outlet pressure was held constant using the ABPR set to 130 bar (approximately 1885 psi). A Viridis<sup>TM</sup> BEH hybrid silica column with dimensions 2.1 mm x 150 mm and particle size of 1.7  $\mu$ m was used for the separation. Detection of the analytes was measured at a UV wavelength of 230 nm.

#### *2.2.1.2.2 Acetone void marker study conditions*

The data was collected using a prototype BEH hybrid silica column with dimensions 3.0 mm x 100 mm, with 1.7  $\mu$ m particle size. The temperature was maintained at 40 $^{\circ}$ C during the isocratic elution with 5% methanol modifier introduced into the CO<sub>2</sub> mobile phase.

## **2.2.2 Peak Distortion Studies**

### *2.2.2.1 Materials and Preparation*

A carbamazepine (Sigma-Aldrich, MO, USA) stock solution was prepared in methanol at a concentration of 1 mg/mL. The working standard solution was prepared using 25 mL of stock solution and diluted to volume in a 100 mL volumetric flask.

### 2.2.2.2 *Instrument Conditions*

The initial exploratory experiments were performed on the prototype low volume SFC analytical instrument configured with photodiode array detection. A BEH HILIC 2.1 mm x 50 mm; 1.7  $\mu$ m column was used for the initial van Deemter study and peak distortion experiments investigating flow rates and percentages of modifiers. The temperature was maintained at 40  $^{\circ}$ C for each set of experiments. The back pressure regulator was maintained at 130 bar.

## 2.2.3 **Isobaric versus Isopycnic van Deemter Studies**

### 2.2.3.1 *Instrument conditions for the van Deemter comparisons*

The mobile phase composition consisted of 95% CO<sub>2</sub> and 5% methanol modifier. Two columns were compared: a prototype BEH HILIC column with dimensions 3.0 mm x 100 mm; 1.7  $\mu$ m particle size column and a prototype BEH HILIC column with dimensions 3.0 mm x 100 mm; 5  $\mu$ m particle size column. Both were maintained at a 40  $^{\circ}$ C. The total system pressure was maintained at 5650  $\pm$  150 psi.

### 2.2.3.2 *Instrument Conditions for the Isopycnic flow rate comparisons*

The mobile phase composition consisted of 93% CO<sub>2</sub> and 7% methanol modifier. The ACQUITY BEH HILIC column with dimensions 2.1 mm x 50 mm; 1.7  $\mu$ m particle size column was maintained at a 40  $^{\circ}$ C. The 0.25 mg/mL standard solution of carbamazepine was used for the 1  $\mu$ L injections.

### 2.2.3.3 *Device to measure the pressures and temperatures of the column inlet and outlet*

An electronic pressure and temperature measuring device (Figure 2.2) was constructed to measure the difference of these values for the mobile phase as it transitions from the column inlet and outlet. Electronic pressure transducers were used to measure inlet and outlet pressures of the column. The pressure transducers were configured on both sides of the column and connected to an electronic board supplied with 110 V analog power supply with probes that were connected to a voltmeter. The pressure transducers transmitted readings that were measured in volts and converted to pressure (in terms of psi) using Equation 2.1:

$$\text{Pressure (psi)} = (6200 * \text{voltage}) - 4650$$

#### **Equation 2.1: Conversion of volts to pressure (psi)**

These constants in Equation 2.1 are provided by the transducer manufacturer to convert the voltage readback to pressure and can vary 0.75 +/- 0.075 resulting in an output of +/- 465 psi. if the readout was equal to zero. The output measurements are linear and should follow the linearity equation of  $y = mx+b$  according to the manufacturer of the transducers. Measurements were recorded using a multimeter tester manufactured by Fluke Corporation. Thermocouples were configured both prior to the inlet pressure transducer and after the outlet pressure transducer. The read-back from the thermocouples was recorded using a high accuracy J/K Input thermocouple thermometer model HH802U and manufactured by Omega Engineering..

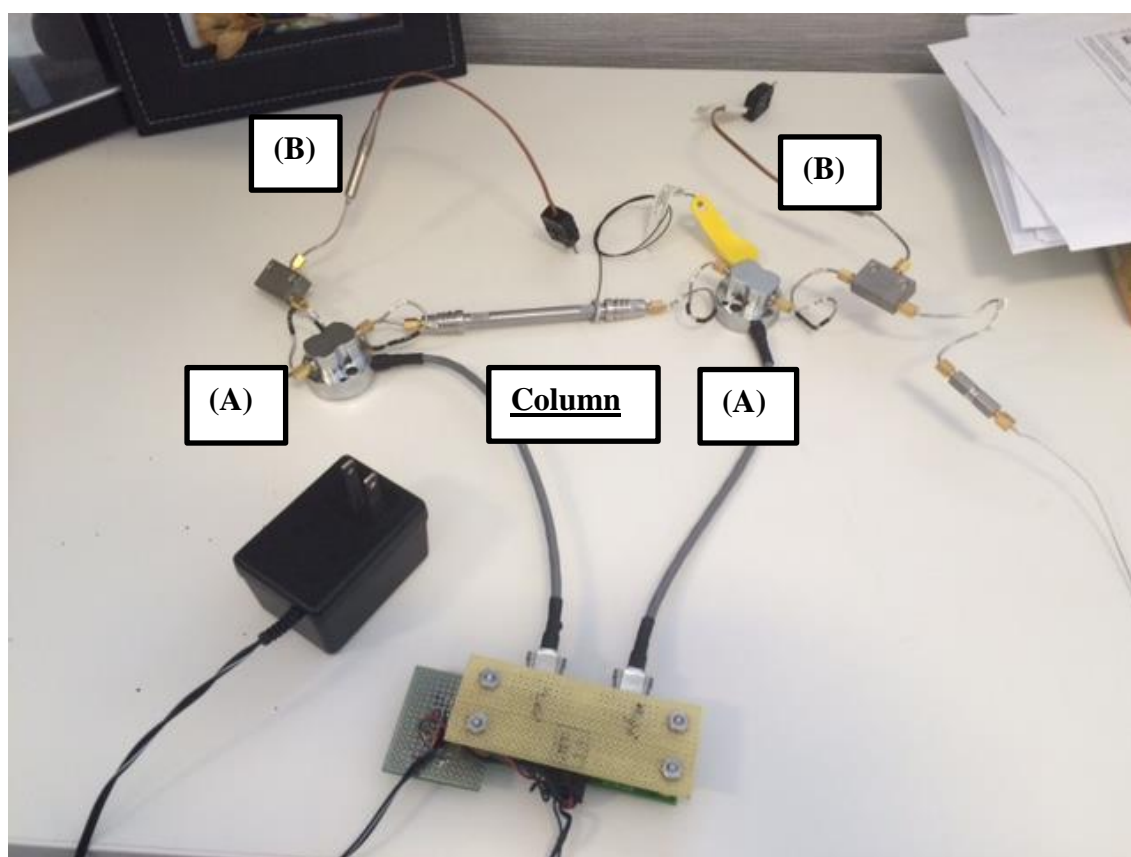


**Figure 2.2: Electronic pressure and temperature measuring device. (A) Pressure transducers. (B) Thermocouples.**

## 2.3 Results

### 2.3.1 Investigations with Sub-2 $\mu\text{m}$ Particle Stationary Phases

In the next sections, preliminary exploratory experiments were performed utilizing commercially available columns that were current at the time of the prototype SFC instrumentation construction. These columns were Viridis™ BEH and ACQUITY UPLC BEH HILIC columns. It should be noted that the stationary phase consists of the same hybrid bridged ethylene base particle. The Viridis™ and ACQUITY naming was a marketing term administered by the manufacturer to denote a classification of column dimensions and scale. Viridis™ denoted analytical and preparatory scale column dimensions that consisted of

stationary phase particles equal to 5  $\mu\text{m}$  and various lengths and internal diameters which were intended for supercritical fluid chromatography applications. ACQUITY UPLC denoted a reference to columns with sub-2  $\mu\text{m}$  particle size stationary phases configured in analytical scale columns typically with 2.1 mm internal diameters and various column lengths.

As the chapter continues and the time progressed throughout the year of experimentation, the preliminary investigations evolved to studies where prototype BEH stationary phase columns with an internal diameter of 3.0 mm were used. The 3.0 mm i.d. columns were determined and formally presented by Jacob Fairchild at the HPLC2012 conference titled “*ACQUITY UPC<sup>2</sup>™: New Capabilities and Possibilities for Separations Science*” to be the appropriate internal diameter for the prototype analytical SFC system. In the HPLC 2012 presentation, he states the 3.0 mm i.d. column was a good compromise between mitigating dispersion and targeting appropriate flow rates which achieve fast linear velocities required to maximize the optimal efficiency for the sub-2 $\mu\text{m}$  particle size. At the time of this research, these columns were considered prototypes due to the supplier’s procedures to pack and reproducibly manufacture the columns had not been validated and refined yet. However, it should be noted that a Viridis™ BEH, an ACQUITY UPLC BEH HILIC, and the prototype BEH HILIC stationary phases are all the same base silica particle. The difference resides in the column dimensions and the particle size and follow the process submitted by U.S Patents 6,686,035; 7,223,473; 7,250,214 and represented by Figure 2.3



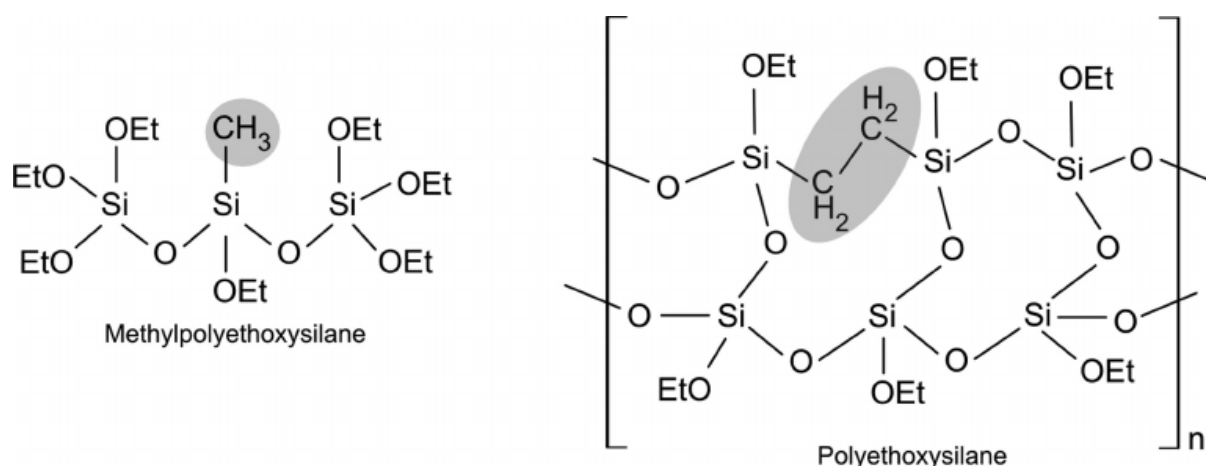


**Figure 2.3: BEH Technology particle synthesis based on ethylene bridged bonding provided courtesy of Waters Corporation**

### 2.3.1.1 Determination of Suitable Experimental Solute Probes

Understanding the benefits of columns packed with sub-2 $\mu$ m particle stationary phases requires comparisons to traditional, larger particle size columns. A series of van Deemter curves were evaluated for each of the different columns with varying particle size using the conditions outlined in section 2.2.3.1. The practical experiments are well documented for LC [107-116], however little has been published to date (*prior to 2011 when this work was performed and presented at HPLC 2011 in Budapest, Hungary*) regarding particle size efficiency for pSFC with smaller particles [76, 77, 117-119]. To determine the effect of particle size on column efficiency for pSFC, various preliminary requirements for the construction of van Deemter curves were addressed, including:

- Explore a selection of analyte probes with different polar, non-polar, acidic, basic and neutral properties
- Empirically determining a probe with  $k = 4$  with Gaussian peak shape
- Finding a suitable representation of the void time ( $V_0$ )

- Considering sample diluents to mitigate external influences on peak shape and efficiency
- Exploring isobaric vs. isopycnic conditions
- Determining relative performance of sub-2  $\mu\text{m}$  particles vs. 5  $\mu\text{m}$  particles in pSFC

The critical factors listed above need to be addressed prior to performing the van Deemter determinations. The analyte probe is the key factor for success. The key characteristics of a good chromatographic test mixture for this purpose include:

1. An unretained/poorly retained analyte for the determination of the void volume
2. An analyte with appropriate  $k$
3. An analyte(s) of low molecular weight to facilitate fast mass transfer
4. Additional probes with a smaller  $k$  can facilitate troubleshooting during the experiment.
5. It must exhibit a Gaussian peak shape

In addition to determining appropriate analyte probes, a void marker must be used to determine the volume of the column. This is generally measured chromatographically using the retention time of an unretained analyte. An appropriate void volume marker can be defined as a probe with the lowest elution time possible, with a retention time that does not change regardless of elution conditions. It must not be influenced by other internal or external variables, such as temperature. Acetone was determined to be unretained and eluting in the injection void of the chromatographic run when injecting the probe during a 5% modifier isocratic experiment. The results in Figure 2.5 show that acetone is unaffected by increasing flow rate. If non-linearity was observed, conclusions regarding the effect of frictional heating or adiabatic cooling of the  $\text{CO}_2$  liquid phase exiting the column as the flow rate increased. The peak volume was calculated using the following Equation 2.2.

$$\text{Peak volume (mL)} = [\text{Flow rate } (\frac{\text{mL}}{\text{minute}})] * [\text{Peak Width (minutes)}]$$

### Equation 2.2: Calculation for peak volume

An 18 component test mix was prepared and analyzed using the gradient method outlined in 2.2.1.2.1(Figure 2.4). The mixture represents a series of acidic, basic, and neutral compounds

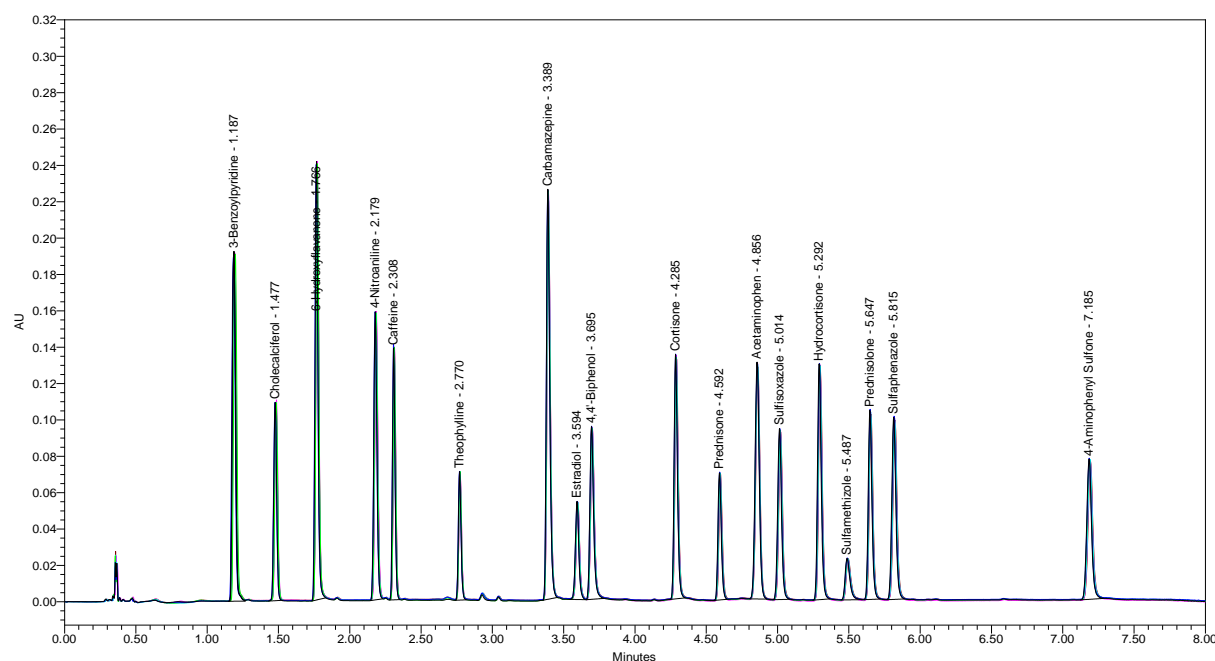


**Figure 2.4: Prototype SFC instrument analysis of the 18 component test mix. The UV chromatogram is the results of 6 injections overlaid.**

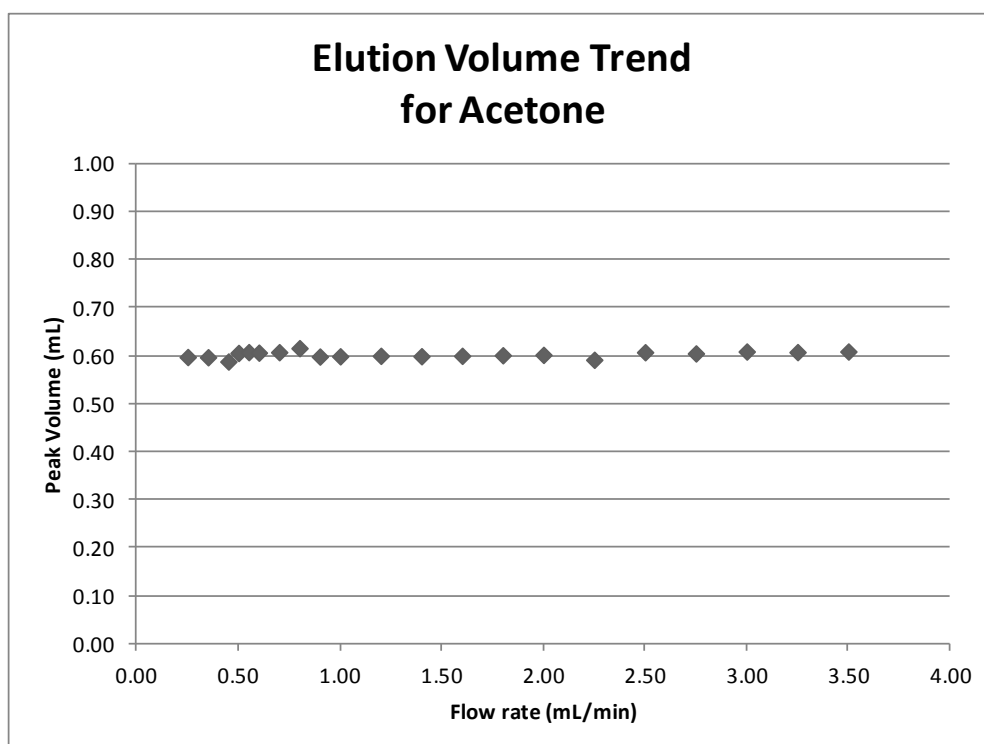


**Figure 2.5: Elution volume trend plot for acetone for an isocratic 5% modifier elution method. Column: BEH HILIC 3.0 mm x 100 mm; 1.7  $\mu$ m**

Based on the results from the experiments shown in Figure 2.4 and Figure 2.5, two analytes were selected as appropriate candidate probes in order to construct van Deemter plots. Based on the critical factors listed earlier, the analytes chosen were:

- Acetone - void volume marker ( $V_0$ )
- Carbamazepine - Target probe for van Deemter measurement because the retention factor was approximately  $k = 4$ .

## 2.3.2 Peak Distortion Studies

### 2.3.2.1 Complications from initial van Deemter study

The van Deemter study was initially performed, but peak distortion was observed for the lower flow rates effecting proper measurements for the van Deemter plot. Lower flow rates

resulted in peak splitting Figure 2.6). The prototype instrument back pressure regulator for these experiments did not have automated control. The back pressure had to be manually adjusted for each of the flow rates. Variations in the observed “total system” pressure were observed to increase with higher flow rates (Table 2.2). The peak splitting issue was hypothesized to be due to an increased pressure drop and a large density gradient effecting the migration of the solute band on column. “Total system pressure” is defined as the pressure readback from the pressure transducer monitoring pressure at the pump heads. This readback would be inclusive of all exerting pressures on the instrument, pre- and post-column. As the outlet pressure is held constant by the back pressure regulator and the inlet pressure increases with increasing flow rate, it can be assumed there is a variation of pressure drop across the length of the column for each experiment.

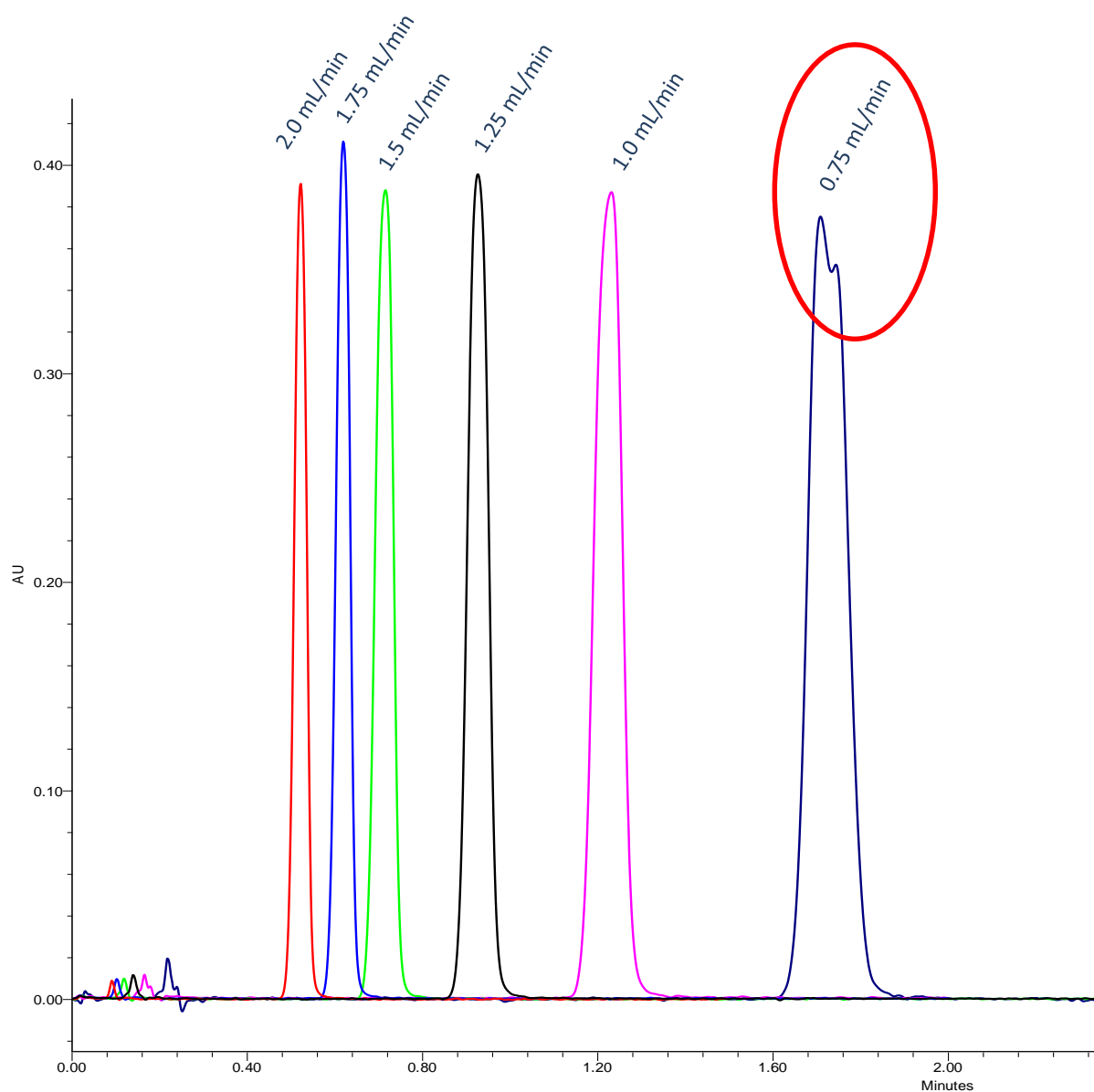


**Figure 2.6: Effect of isocratic modifier with decreasing flow rate.**

**Table 2.2: Table of observed total system backpressure ( $P_{\text{sys}}$ ) related to flow rate and applied backpressure ( $P_{\text{app}}$ ) from the back pressure regulator.**

Flow (mL/min)	$P_{\text{sys}}$ (psi)	$P_{\text{app}}$ BPR (bar)	$P_{\text{app}}$ BPR (psi)
0.75	2439	122	1769
1.00	2720	127	1842
1.25	2990	127	1842
1.50	3263	127	1842
1.75	3568	127	1842
2.00	3835	124	1798

A similar observation by Professor J.L Veuthy and team showed peak deterioration at low modifier strengths in their experiments and presented at the HPLC Symposium in 2010 (Figure 2.7). Interestingly, their observations were performed on a larger particle size column.

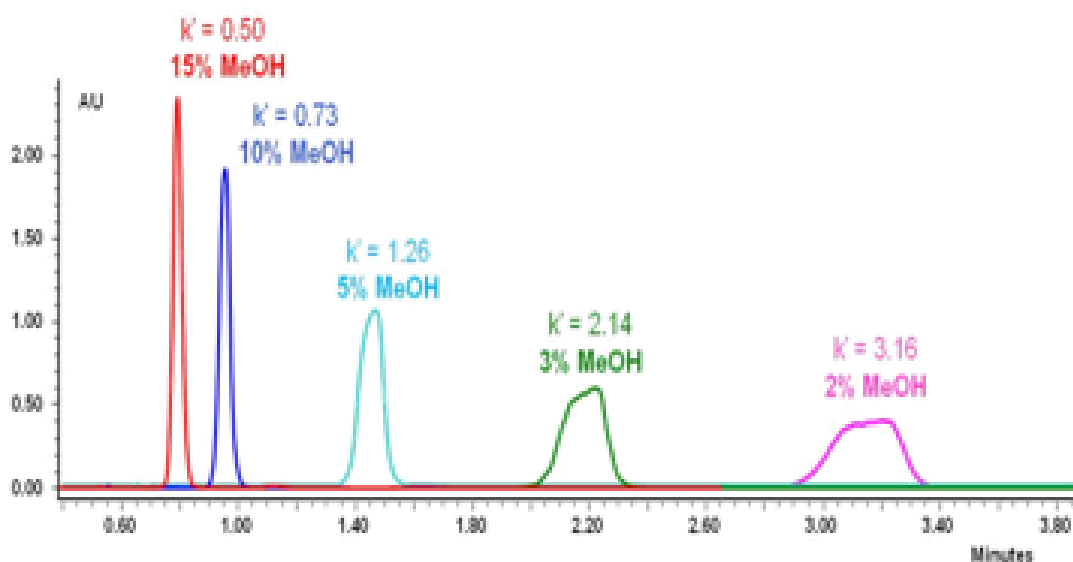


**Figure 2.7: Influence of % modifier using a Sunfire 4.6 x 150 mm; 5  $\mu$ m, 40  $^{\circ}$ C, flow rate was 4.0 mL/min, BPR=200 bar. (Courtesy of J.L. Veuthy, U. Geneva)**

The results of the initial van Deemter attempt combined with the results of Veuthy's HPLC 2010 presentation suggest multiple effects causing the peak shape distortion. A range of co-solvent percentages were explored in order to determine a suitable retention factor ( $k$ ) using carbamazepine as a standard. Interestingly, it was found that at very low isocratic additions of modifier when using an ACQUITY BEH HILIC column with dimensions of 2.1 mm x 50 mm, the peak shape deteriorated as the percentage of co-solvent decreased and  $k$  increased (Figure 2.8).

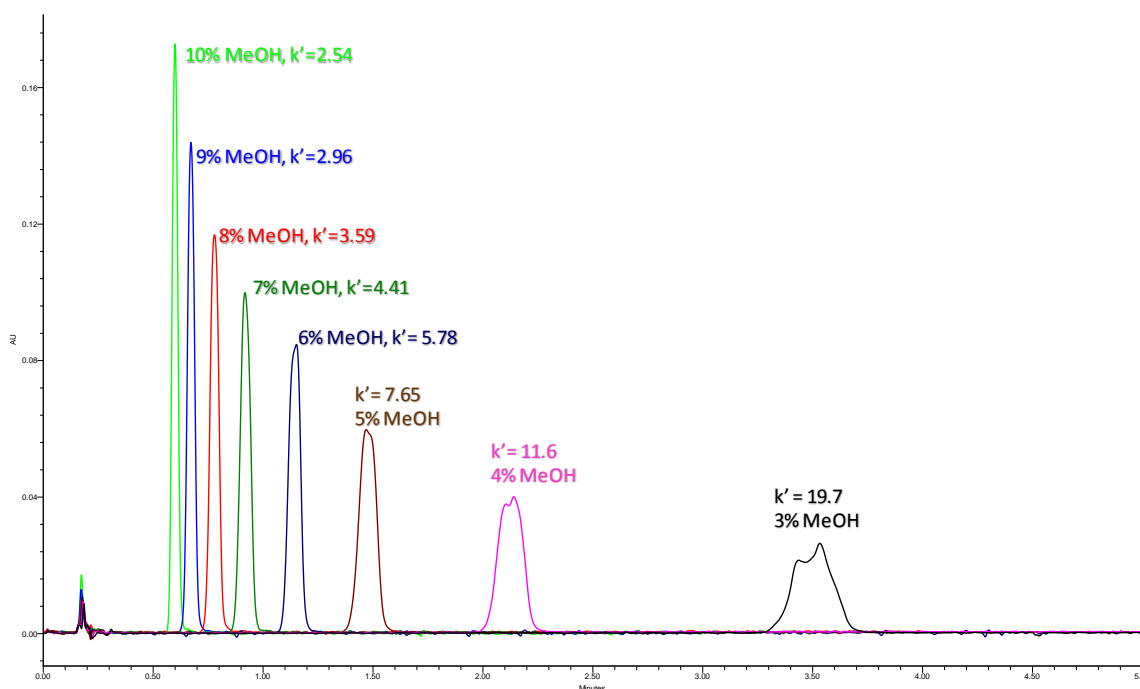


**Figure 2.8: Effect of modifier percent on peak shape.**

In the initial attempts of the van Deemter study that vary flow rate, it was assumed that mobile phase homogeneity of the CO<sub>2</sub> and modifier could be the cause of the peak splitting. The pressure drop across the column could also be contributing to extreme mobile phase density gradients across the column, thus effecting the solute band dispersion. In Veuthy's results, the peak shape distortion was hypothesized by the author to be related to insolubility. The carbamazepine standard was injected and eluted using different percentages of modifier.

Upon a further review of the literature, similar research by Donald Poe *et al.* reported peak shape abnormalities [92]. They concluded the peak shape distortion was due to the effects of pressure drop and temperature drops across radial axis the column, which ultimately affected the density of the CO<sub>2</sub> within the column, inducing band broadening of the solute. This is basically a solubility problem because the solubility is density dependent He proposed that van Deemter experiments should be carried out with "isopycnic" conditions, which is defined



as *constant density* conditions. For these experiments, it is understood that the linear velocities across the column are not equal between a constant pressure studies (isobaric) versus a constant density study (isopycnic). Therefore, in summary, three factors appear to affect peak distortion and require investigation:

- Mobile phase homogeneity
- Density variations or density gradients
- Insolubility

Mobile phase homogeneity can be explored by experimenting with larger mixers on the chromatographic system. Density variations and pressure drops can be measured with temperature and pressure probes on the inlet and outlet of the column. Solubility issues are a bit more difficult to investigate due to supercritical properties of the mobile phase occurring on-column and relating it to the solubility of the solute. The solubility studies would require specialized instrumentation that would not be achievable on the prototype analytical SFC instrument and better studied using specialized pressure containment vessels with a viewing window to observe for insolubility.

#### 2.3.2.2 *Investigating Isopycnic Conditions at Constant Modifier Composition*

The isopycnic conditions resulted in symmetrical Gaussian peak shapes observed at 2.0 mL/min with an overall observed system pressure measured by the transducers at the pump head being held at 4000 pound per square inch (psi), *or approximately 275.8 bar*. The instrument read backs were in “psi” units, and therefore reported as such. At the lower flow rate where the peak shape was observed to be splitting, the back pressure regulator was adjusted to exert an increased pressure on the outlet of the column such that the total system pressure was equal to that observed at 2.0 mL/min and 4000 psi experiments. It can be seen

in Figure 2.9, the peak shape (and baseline noise) at the lower flow rate was not suitable for constructing an optimal van Deemter plot.

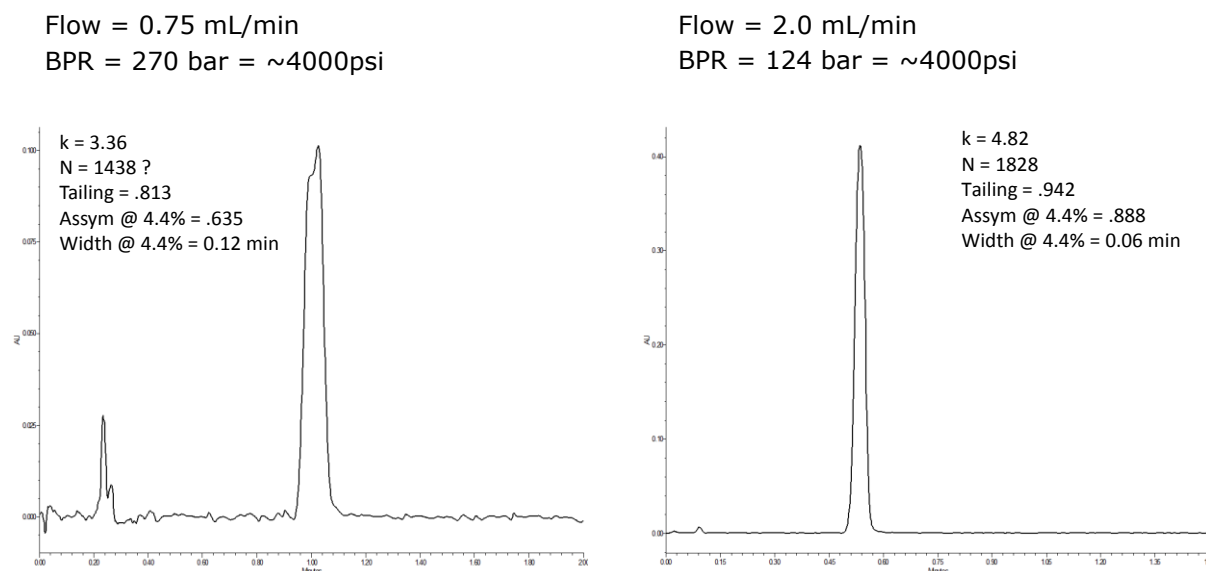


**Figure 2.9: Comparison of carbamazepine under isopycnic conditions at different flow rates.**

The successful experiments that produced the original van Deemter generated by Aubin and Neue [120] utilized a column with internal diameter (i.d.) of 3.0 mm rather than the 2.1 mm i.d. column used in the previous sections of this chapter. It should be noted that Aubin and Neue modeled the empirical data to determine the efficiency benefits of sub-2  $\mu$ m particles for use with SFC. To understand if the column i.d. was a contributing factor, experiments that produced the poor peak shape on the 2.1 mm i.d. column were repeated on a prototype 3.0 mm i.d. column. Again, peak splitting was observed for the low flow and low percentage modifier conditions.

In an effort to rule out volume and mass overloads, the 0.25 mg/mL carbamazepine standard solution was injected at a lower injection volume of 0.2  $\mu$ L. Subsequent experiments with a

diluted standard of 0.1 mg/mL were also explored. The results yielded the same odd and unpredictable peak shapes for the lower flow rates. Based on these results, it was concluded that another effect was contributing to the peak shape distortion.

In previous experiences, mixing has been a point of concern, particularly the miscibility of CO<sub>2</sub> and methanol modifier. Therefore, a larger mixer with a 425 µL of volume was installed on the pump after the piston heads. A decrease in baseline noise was observed and pressure fluctuations appeared to be lower (Figure 2.10 (a)). An experiment was performed using the larger mixer and 3.0 mm i.d. column using the same instrument conditions from Figure 2.6. but with a specific focus on the conditions using the flow rate of 0.75 mL/min and 7% methanol modifier composition. The experiment resulted in a Gaussian and reproducible peak shape with the 3.0 mm column ID (Figure 2.10(b)). The next set of experiments explores the larger mixer and larger column i.d. using the experimental conditions used for Figure 2.8. The results in Figure 2.10(c) resulted in Gaussian peak shapes down to 3% modifier addition. Although this looked promising, sufficient mixing was thought to solve the peak splitting issue due to low flow rate and mobile phase homogeneity. The results of the 2.1 mm i.d. column still looked less than ideal as seen in Figure 2.10(d), therefore mobile phase homogeneity is not the only contributor and larger mixers are not the single solution. However, it is hypothesized that sufficient (or insufficient) mixing is a major contributing factor and a homogenous delivery of mobile phase can be a beneficial contributor to peak shape.

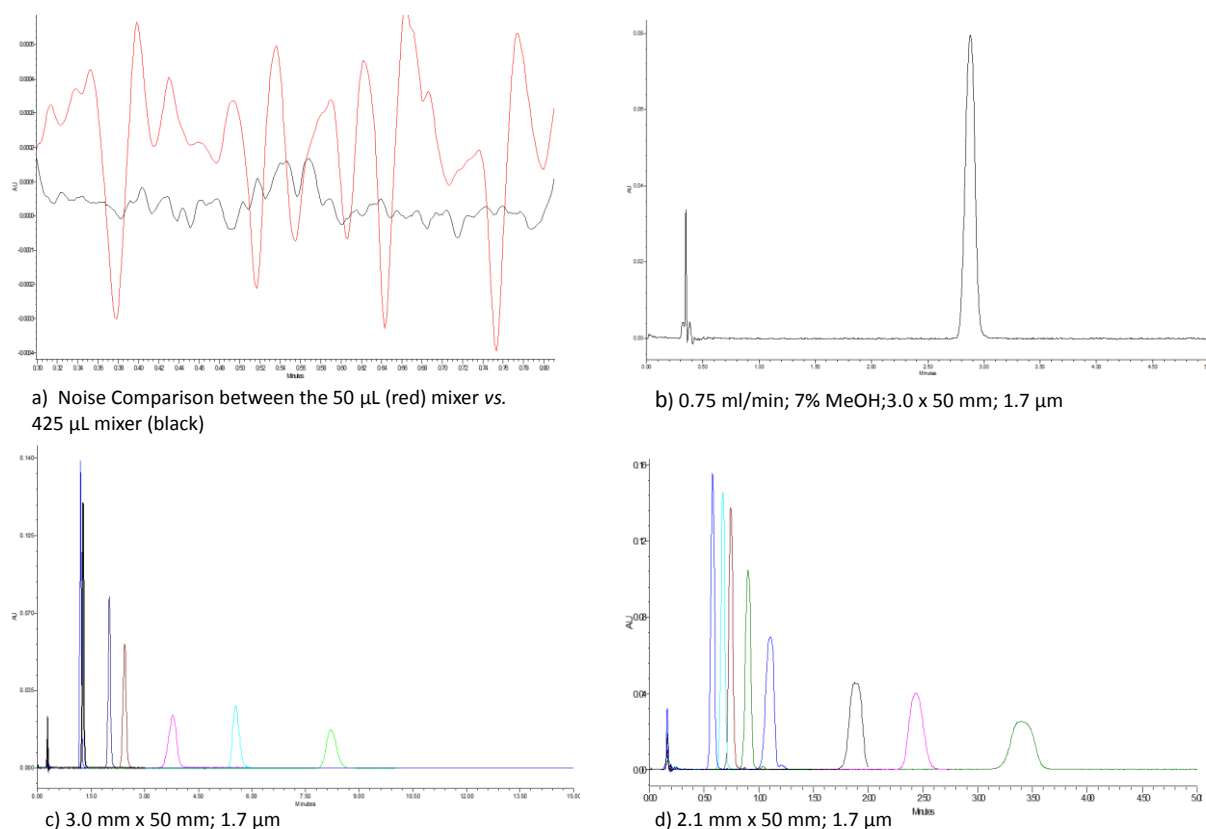


**Figure 2.10: Effect of increased mixing on (a) baseline noise, (b) low %modifier/low flow, (c) varied % modifier, and (d) decreased column i.d.**

### 2.3.2.3 Investigating the Effect of Mobile Phase Mixing

The previous experiments suggested mobile phase inhomogeneity with the modifier and supercritical CO<sub>2</sub> mobile phase at low flow rates. It was then hypothesized that increasing column length would improve peak shape, based on the essential concept that a column is essentially another mixing device within the chromatographic system. Injections of carbamazepine standard solution were injected on to the prototype instrument with the 50 µL mixer configuration.

It was hypothesized the re-insertion of the 50  $\mu\text{L}$  mixer would help differentiate between two factors:

- Peak shape improvement due to an increase in mixing represented by a total increase of system volume in addition to increased column length
- Is the peak shape improvement due to an increase of system volume alone? This would represent the effects of more mixing volume thus facilitating better mobile phase homogeneity and resulting in more optimal peak shapes.

The investigation explored a longer column of dimensions 2.1 mm x 100 mm; 1.7  $\mu\text{m}$  particle size and maintained at a 40  $^{\circ}\text{C}$ . The stationary phase was consistent with previous experiments consisting of ACQUITY BEH HILIC particle. The 0.25 mg/mL standard solution of carbamazepine was used for the 1  $\mu\text{L}$  injections. The mobile phase composition consisted of 93%  $\text{CO}_2$  and 7% methanol modifier. The back pressure regulator was set to 130 bar. The 50  $\mu\text{L}$  mixer and longer column length resulted in improved peak shapes when the percentage of modifier was decreased. Baseline noise was equivalent to that from the 425  $\mu\text{L}$  mixer, and most importantly the peak shapes were reproducible (Figure 2.11).

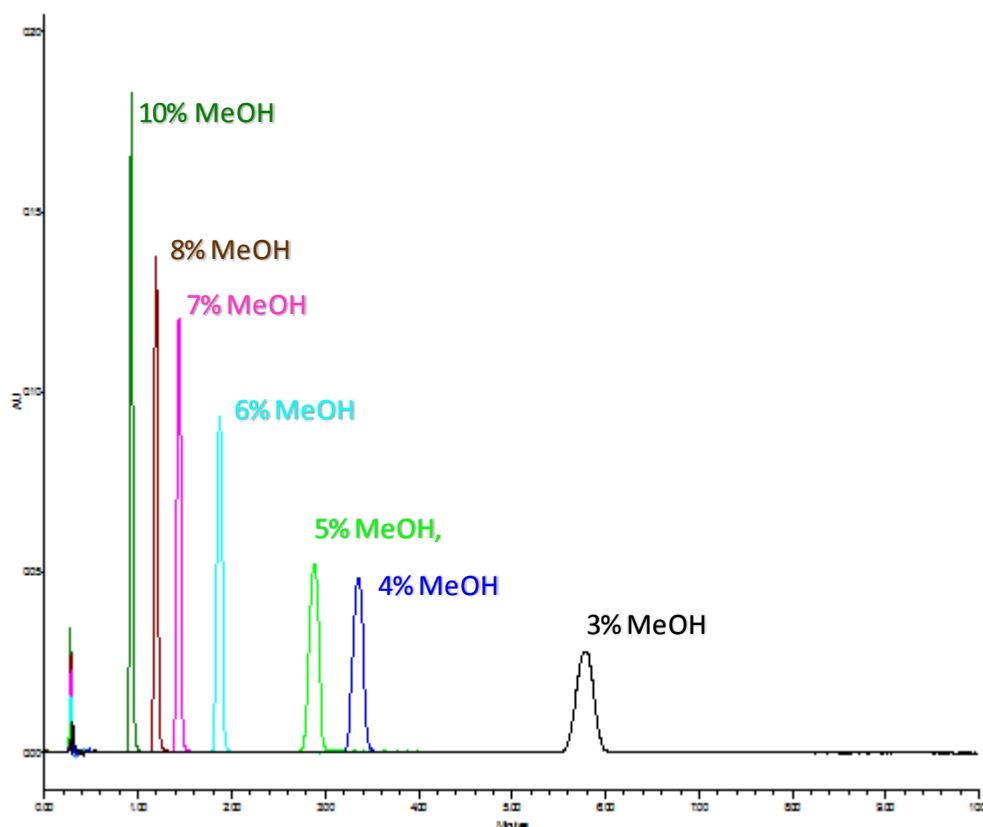


**Figure 2.11: Effect of increasing column length with low volume mixer**

### 2.3.3 Isopycnic and Isobaric Pressure Study

#### 2.3.3.1 Comparing Column Efficiency using Isopycnic versus Isobaric Backpressure Conditions

Retention factor ( $k$ ) and column efficiency ( $N$ ) were investigated using the probe analyte carbamazepine under isobaric and isopycnic conditions. Isobaric conditions use a constant backpressure regulator outlet pressure which results in a change in total system pressure and changing densities as different flow rates are used. Isopycnic conditions vary outlet pressure inversely to inlet pressure in order to maintain a constant density (as determined by measurement of a constant system pressure with changing flow rates). The prototype instrument has upper pressure and flow rate limiting thresholds. The maximum permissible flow rate is 2.0 mL/min, and the maximum pressure is approximately 400 bar, (or an

instrument setting limit of 6000 psi). The thresholds determine the design of the achievable isopycnic experiments. For experimental purposes, the maximum pressure observed for the highest allowable flow rate determines the set point for total system pressure to maintain throughout the isopycnic experiments. There is concern that there could possibly be a density differences between the inlet of the column and outlet of the column, however there is no practical method to determine this experimentally during the experimental run of an analyte. The measurement readings for the pump pressure transducers, backpressure transducers, column inlet and outlet pressure transducers (Figure 2.2) all register the same apparent pressure for the entirety of the closed system. It can be assumed that the average density or apparent constant density is maintained by this technique of adjusting backpressure during varied flow rates and therefore considered ‘isopycnic’.

The plot of  $k$  versus mobile phase flow rate (mL/min) for the two techniques (isobaric vs. isopycnic) is used to generalize the combined effect that the variables such as temperature, pressure, and density have on efficiency. The retention factor for carbamazepine changed with flow rate in different ways, depending upon the experimental conditions (Figure 2.12). When comparing the lower flow rate experiments such as the 0.5 mL/min and 1.0 mL/min experiments, it is hypothesized that the decreased density and lower viscosity of the isobaric results facilitated increasing solute diffusivity and interactions with the stationary phase. In terms of the isopycnic experiments, the mobile phase density is likely to have been maintained closer to ‘liquid’ densities,, thus contributing less to changes in diffusivity of the solute with the stationary phase and consequent lower  $k$ . The  $k$  decreases with higher flow rates for the isobaric conditions, whereas the  $k$  increases when the flow rate increases for the isopycnic experiments. In order to hold density constant during the isopycnic experiments, the backpressure exerted on the outlet of the column is increased for the lower flow rate

measurements of  $k$ . This could be affecting the solubility of the test probe in the mobile phase and inhibiting the interaction with the stationary phase. In terms of the observations of the isobaric test results, possible factors decreasing  $k'$  include (a) radial and axial temperature and pressure gradients resulting in adiabatic cooling, causing an increased linear velocity as the band approaches the column outlet, and (b) performing the experiments too close to the critical density. As the gas expands due to adiabatic cooling, an increased diffusion and retention of carbamazepine occurs as per Equation 1.19. Additionally, since the pressure is a function of the density of the mobile phase, the reduced pressure would affect  $k$  to decrease.

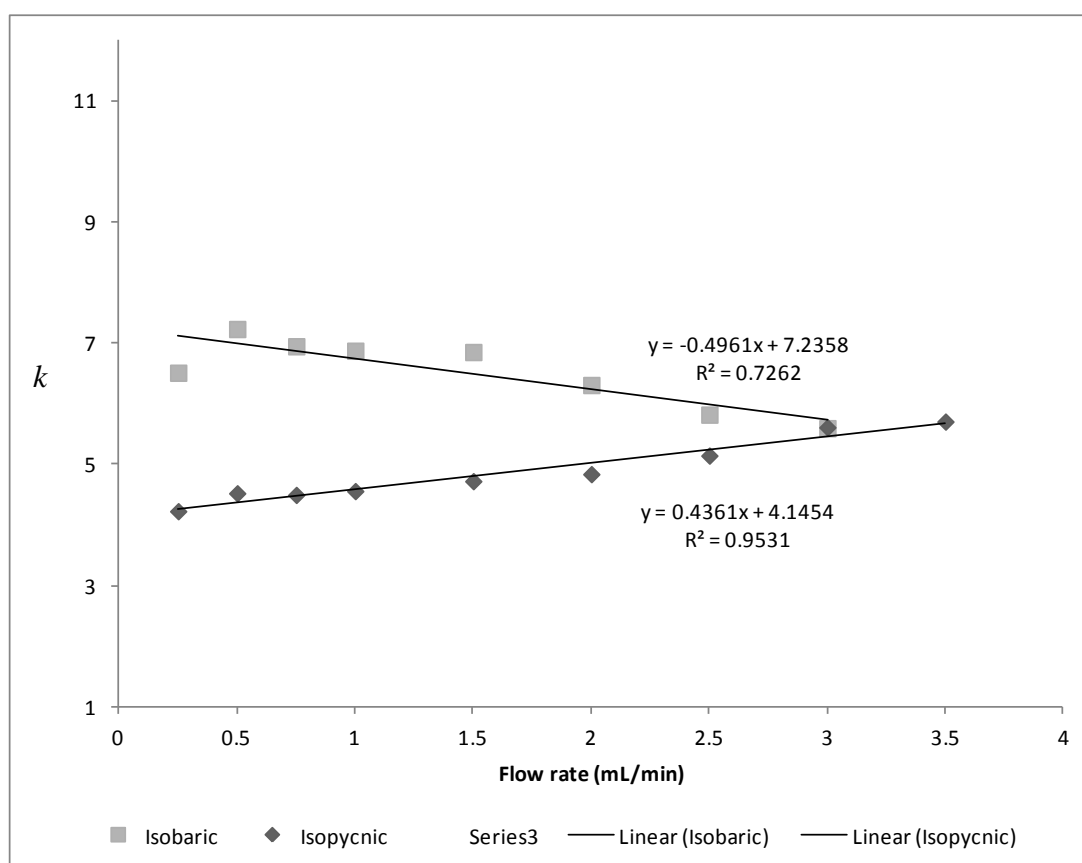


**Figure 2.12: Flow rate versus retention factor ( $k$ ) for isobaric and isopycnic evaluations of carbamazepine.**



### 2.3.3.2 *Isopycnic Comparisons using Different Stationary Phase Particle Sizes*

When the particle sizes are compared under isopycnic conditions, the  $k'$  for the 5  $\mu\text{m}$  particle remained relatively constant. At flow rates above 1.5 mL/min,  $k$  increased for sub-2 $\mu\text{m}$  particles (Figure 2.13). It is possible that the increased  $k'$  for isopycnic results reflect (a) an increase in frictional heating resulting in an increased on-column temperature and therefore allowing temperature to play a role as a function in density, and thus consequently increase in  $k$  [121]. Another explanation could indicate a lower percent molar volume of modifier in the mobile phase, causing  $k$  to increase. The latter would be very difficult to experimentally determine and is unlikely unless an instrument flaw was determined such as a leaking modifier pump seal. System diagnostics were initiated to test the leak rate from the pump seals. The test passed according to the instrument diagnostics control panel, therefore the molar volume explanation was dismissed.



**Figure 2.13: Isopycnic trend plot comparison for hybrid 3.0 mm internal diameter columns packed with 5  $\mu$ m particles and 1.7  $\mu$ m particles.**

### 2.3.3.3 Isobaric versus Isopycnic van Deemter determinations

Rajendran *et al.* have shown that under isobaric conditions, decreases in efficiency are observed when operating at lower outlet pressures (130 bar) and low modifier percentages (<7%) [91]. The apparent optimal linear velocity for maximum column efficiency for the 3.0 mm x 100 mm; 1.7  $\mu$ m column approaches 0.4 cm/sec (Figure 2.14). The isopycnic plate height results in Figure 2.14 suggest the observed optimal linear velocity is 2.2 times greater to reach the maximum efficiency when compared to that of the isobaric experiment. However, it also seems that the optimal linear velocity was not reached for the isopycnic experiments due to flow rate and pressure restrictions of the instrument. Interestingly, the

efficiency for the isobaric experiment was the same as the isopycnic experiment when using at a linear velocity of 1.1. The system pressure read back from the instrument control software at these two experimental points were equivalent. For all practical and research purposes, if plate heights are to be used to categorize performance, then the details of the experimental conditions and more specifically the average density predicted within the instrument which can be guided by the overall observed system pressure and viscosity of the mobile phase composition should be considered when comparing and reporting column comparisons between commercial suppliers.

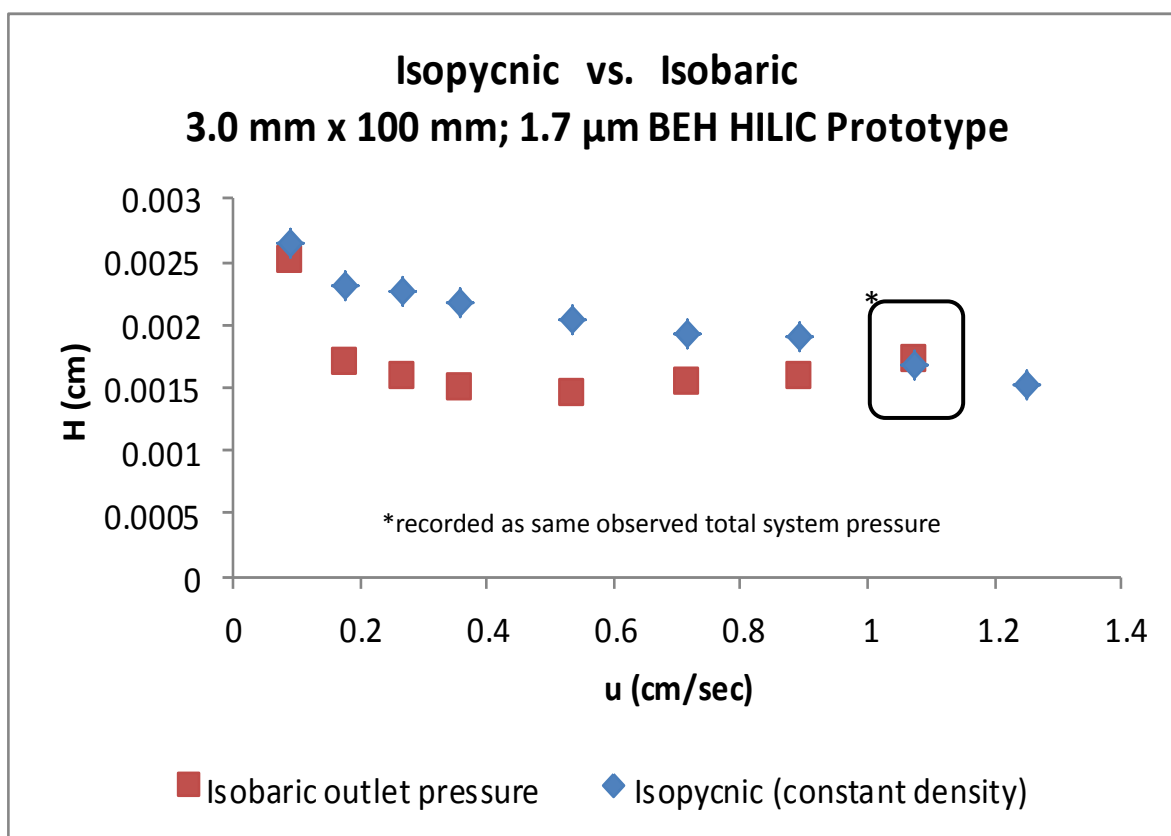


**Figure 2.14: van Deemter curve comparing the efficiency differences while running in an isobaric outlet pressure state (classical approach) versus an isopycnic (constant density) state. The results are plotted as plate height versus linear velocity.**

#### 2.3.3.4 *van Deemter plots Comparing Different Isopycnic Settings*

The experiments used for the generation of data for the van Deemter plots in Figure 2.15 were conducted at 5500 psi and 5700 psi constant total system pressures. These two experiments were performed by two separate analysts. Any variations which are observed might be influenced by the fact that the two systems are prototype instrumentation and manufacturing controls are not established. These variations have the potential to have a greater impact than those of the separate analysts' technique towards the analysis, therefore the results of this experiment are purely qualitative. It is undetermined if the decreased plate height observed for the sub-2 $\mu$ m particle column experiments was caused by the increase in total system pressure. A difference of 200 psi does not appear to have a great effect on column efficiency for the larger particles for the two experiments. It is interesting to observe a decrease in efficiency for the 5  $\mu$ m particles as the linear velocity increases beyond 0.2 cm/sec, a comparable trend to typical RPLC results. This trend is not observed for the sub-2  $\mu$ m particle column experiments, thus suggesting the instrument pressure and flow limitations are inhibiting the capability to determine the optimal linear velocity and maximum efficiency attainable for that column when using this instrument. Regardless of the limitation, the sub-2  $\mu$ m particles yielded greater column plate counts than larger particles. Interestingly, the overall set of results show similar trending for both the sub- and supra- 2  $\mu$ m particles for the two experiments by the two analysts.

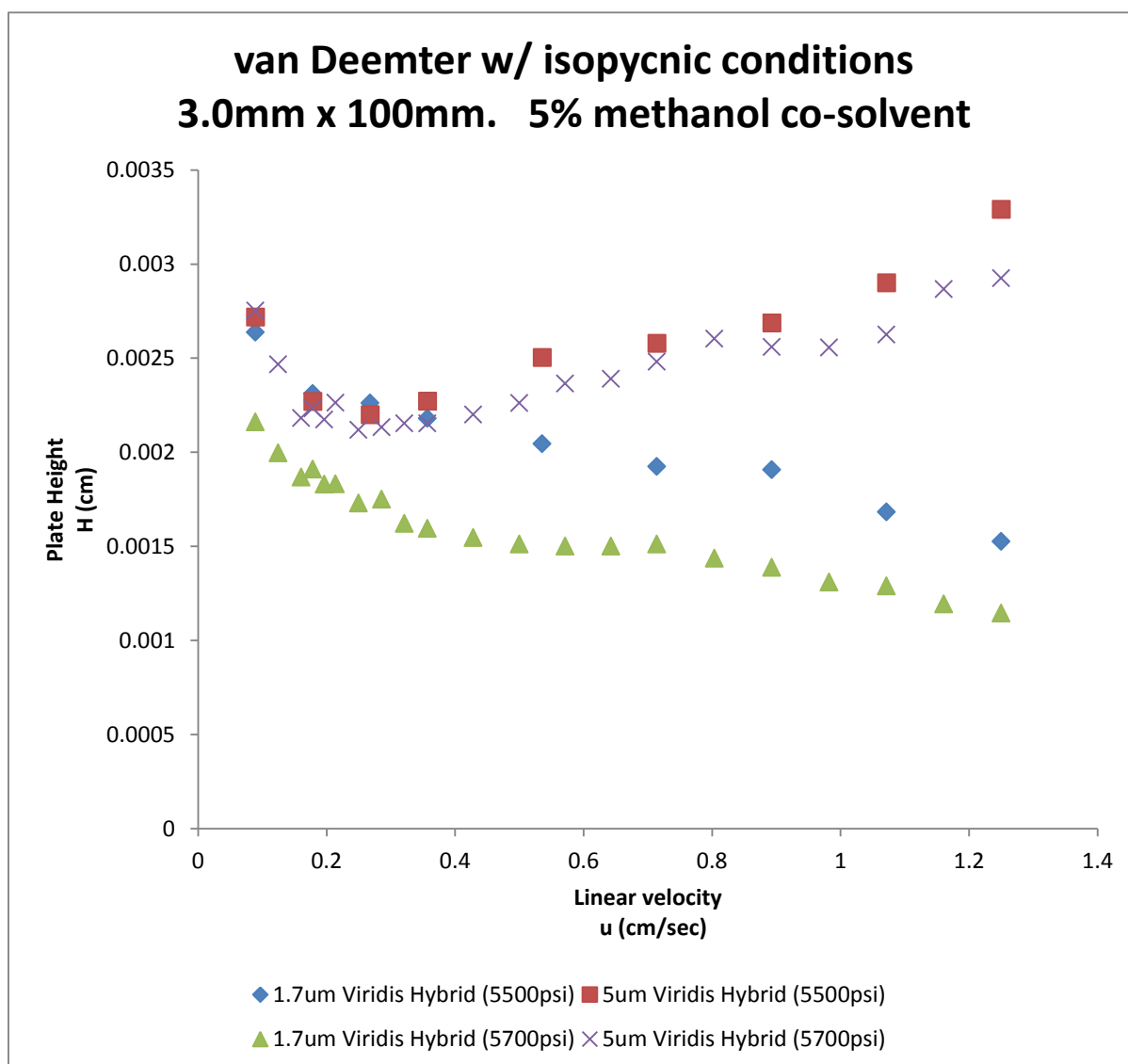


**Figure 2.15: Van Deemter plots comparing two separate experiments on two prototype instruments.**

### 2.3.3.5 Comparison to Previously Published Results

The recent works of Tarafder, Guiochon, Ranger, Kaczmariski, and Poe have provided information that facilitates the understanding of super-/sub-critical fluid compressibility [68-74]. Their series of publications have provided estimates about the viscosity variation when density increases, estimates on solubility variation when plotted versus pressure, and

variations when plotted versus density. The design and use of their isopycnic plots provide the most practical way of identifying problem zones and determining why variations in efficiency have occurred for a given set of experiments. In their reports, a series of isopycnic plots were constructed for CO<sub>2</sub> with the addition of 5%, 10%, 15%, and 20% modifier which result in different critical temperatures and critical pressures.

Based on their reports, the data presented here can be correlated and superimposed on their plots to determine the relative effects of temperature and pressure changes exerted during previously mentioned experiments. Figure 2.15 indicated a slight increase in efficiency with a 200 psi difference in pressure. When plotted on the isopycnic pressure – temperature plane, the density of the fluid changes slightly (Figure 2.16). The operating parameters from Figure 2.8 were plotted on the CO<sub>2</sub> + 5% modifier isopycnic plot indicating a density drop of approximately 0.06 g/mL and a pressure drop approximately 140 bar at the highest flow rate and 46 bar at the lowest flow rate. These results can now be used for future experiments to investigate an allowable range of density differences without affecting chromatographic fidelity. Another conclusion, suggests that as the mobile phase density approaches 0.84 g/mL, peak splitting is observed.

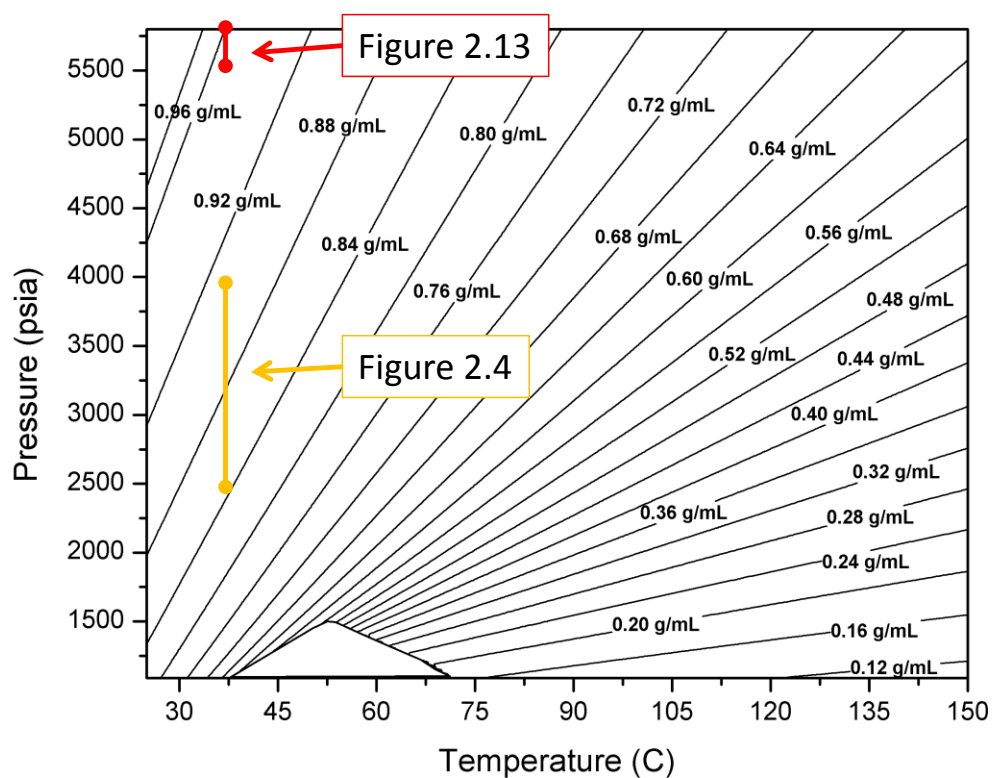


**Figure 2.16:** CO<sub>2</sub> + 5% methanol modifier isopycnic plot (reproduced with permission from A. Tarafder) overlaid with operating parameters from Error! Reference source not found. and Figure 2.15.

## 2.4 Conclusions

In conclusion, the investigation of sub-2  $\mu\text{m}$  particle columns yielded a vast amount of practical approaches to consider when developing SFC methodologies. The higher density  $\text{CO}_2$  yields more robust results, but at the cost of higher pressures. Acetone was determined as a suitable void marker to calculate retention factors for the probe analyte carbamazepine. The retention factor should be kept constant when experimentally determining accurate plate counts for varied particle sizes. Isobaric conditions may be suitable for plate count determinations for practical purposes, but isopycnic experiments could indicate the *potential maximum efficiency* for a given column. Either technique, isobaric or isopycnic would be appropriate to compare columns; however the experiments must be consistent when compared. The apparent plate counts yielded by using an isobaric outlet pressure are not represented accurately due to the changing density as pressure is increased with increased modifier, and thus generating a larger pressure drop across the column. The van Deemter plots prove that sub-2  $\mu\text{m}$  particles yield a better plate count than larger particles regardless of experimental approach. Insight to the phenomenon might be explained using the isopycnic plots published by Tarafder [68, 69, 72, 74].

It was clearly evident that further experiments outside of the scope of this preliminary evaluation using prototype instrumentation and columns should be repeated on final design instrumentation to improve confidence in the conclusions regarding the observed chromatographic phenomena. In terms of utilizing this system in practice, these experiments and investigations described within this chapter provided a basis of some expectations of system level SFC performance when using sub-2 $\mu\text{m}$  particles columns.



## CHAPTER 3:

---

# Exploring Method Development and Optimization Variables

## CHAPTER 3

### 3 Exploring Method Development and Optimization Variables

In the previous chapter, the prototype low volume supercritical fluid chromatography system was proven to take benefit of the sub-2  $\mu\text{m}$  particle stationary phases. The prototype instrumentation was refined and a pre-commercialized instrument was provided by Waters Corporation. The final instrument design was commercialized and introduced at the Pittsburgh Conference in 2012 and marketed by Waters as UltraPerformance Convergence Chromatography™ (UPC<sup>2</sup>). Waters defined “Convergence Chromatography” as a category of separation science that provides orthogonal and increased separation power, compared to liquid or gas chromatography, in order to solve separation challenges. The term Convergence Chromatography was derived from J. Calvin Giddings concepts of a ‘unified chromatography’, a term used by Giddings to describe the unification of liquid, supercritical, and gas chromatography [122]. Instrument design is important to understand and defines a basis for general expectations of the results to come once it’s employed for analytical determinations. The practicality of the instrument design can be better understood when methodology variables are taken into consideration. In the next two chapters, ‘one factor at a time’ (OFAT) and multivariate approaches are explored to determine the variables that effect chromatographic separations, information rich data, and interfacing with mass spectrometry. In addition, these chapters highlight the importance of troubleshooting techniques that help distinguish system related effects versus chemistry related effects based on experimental observations and reason that could cause retention time drift, peak splitting, peak distortion, and ionization efficiency. More importantly, evidence of the various retention mechanisms affecting the selectivity, retention and resolution of analytes; but more specifically,

structurally related small molecule (>1500 Da) analytes analogous to those observed in natural product profiling

### **3.1 Introduction**

Many new chemical entities can either be extracted and purified from natural product sources or synthesized based on previous characterization and understanding of the natural product moiety. The chromatographic screening analysis of new chemical entities relies on appropriate sample preparation and methodology variables which do not adversely affect the chromatographic results and interpretation of the data. Techniques which provide selectivity, specificity, and orthogonality deliver insight about the underlying chemistry of the compounds under investigation, or the chemical reactions creating the molecules.

Synthetic reactions are carried out using a wide range of solvents the properties of these solvents could well effect the performance of the chromatography when loaded onto the system, a well-known effect in HPLC. Documented knowledge of the effect of sample diluent on supercritical fluid chromatography is not as well characterized. When analyzing reaction mixtures, in an ideal scenario, the chemist would favor injecting the reaction mixture directly onto a chromatographic instrument without any dilution. However, when considering the high concentration of a reaction mixture, this is not always practical, and simple dilutions are therefore recommended. In many cases, when analyzing a reaction by reversed-phase LC, the sample aliquot must also be diluted with a suitably comparable RPLC injection solvent to minimize detrimental effects on observed chromatographic peak shape [123-127]. It is normal practice to dissolve the analyte in a solvent with an eluotropic strength significantly lower than the strength of the chromatographic elution solvent thus allowing the

analytes to be focused on the head of the LC system and produce a sharp LC peak [18]. In RPLC the scientist would ideally dilute the sample in water, as it is a weak eluter, however DMSO is often used to ensure analyte solubility. DMSO's strong eluotropic nature is often circumvented by employing a low injection volume for these HTS applications. By the definition above, a non-polar solvent such as hexane would be an optimal diluent for supercritical fluid chromatography due to its low eluotropic strength compared to that of the methanol elution solvent (typically referred to as co-solvent or modifier). However, using hexane can be challenging for the analysis of polar compounds due to its immiscibility with the polar component of the solvent and solubility of the analyte.

Using CO<sub>2</sub> as a primary mobile phase for chromatographic separations provides an orthogonal approach, aiding discovery of unknown impurities when compared to reversed-phase LC. While method development strategies in liquid and gas chromatography are well-defined, that is not the case for CO<sub>2</sub>-based chromatography. Although to say they are not well defined, that is not to say they are not well understood. West and Lesellier have published the most extensive research in this field of SFC and analyte retention [54, 55, 96, 128-135], however there is a need for a well-defined, strategic approach for method development in SFC. In order to streamline this process, a systematic approach to achiral SFC method development requires research and additional practical examples from the pharmaceutical industry to validate the feasibility of the technique.

In pharmaceutical development it is important to understand the impurity profiles of the potential drug substance material in order to allow accurate assessment its toxicological profile. Assessing the purity of the sample allows pharmaceutical companies to make

decisions during drug development and commercialization of the drug. Impurity profiles are dictated by route synthesis pathways, raw material quality from vendors, final drug quality and safety, finished product shelf life, and also provide intellectual protection from counterfeiting. Orthogonal comparisons of the chromatography profiles provide the ability to make the best educated decisions throughout the entire drug discovery, development and commercialization process.

In this chapter, the following investigations explore the applied use of newer technologies composed of sub-2  $\mu\text{m}$  particle size achiral stationary phase columns and the optimized analytical scale low volume pre-commercialized SFC instrumentation for the task of complex sample analysis. The pre-commercialized instrument differed from the prototype in many of the modules. The pump was no longer cooled using Design 2 in Figure 1.10 and utilized the thermostatically controlled schematic in Design 1 of Figure 1.10. The prototype utilized an initial design of the back pressure regulator that was controlled by manual entry of specific code to apply pressure settings. The pre-commercialized backpressure regulated was controlled through the software control console, optimized for appropriate materials that prolong the robustness of the needle and seat components, and included additional static pressure regulation to stabilize pressure irregularities of the dynamic regulation of backpressure. The photodiode array detector optics bench was modified during the experiments performed in section 3.3.3 in order to reach the sensitivity required to perform impurity analysis profiling. The particularity of the details pertaining to many of these changes are proprietary to the manufacturer and thus not described in greater detail.

The sub-2  $\mu\text{m}$  particle columns are primarily explored because they provide the potential for greatest increases of efficiency, sensitivity and resolution. The dispersion of the

prototype and commercial instrument were calculated to be about  $25 \mu\text{L}^2$  at 2 mL/min. This compares with other binary high pressure mixing UHPLC systems ( $1 \mu\text{L}^2$ ), quaternary low pressure mixing UHPLC ( $10 \mu\text{L}^2$ ), the first commercially available UHPLC systems ( $16 \mu\text{L}^2$ ), and traditional HPLC systems ( $40 \mu\text{L}^2$ ) [136]. The question now is “Which column format?, Should 2.1 mm i.d, 3.0 mm i.d. or 4.6 mm i.d. be used?”. The presentation reported 3.0 mm i.d. column formats are the best compromise between mitigating dispersion effects and maximizing the utilization of the instrument based on the upper pressure and flow rate limits of the instrument. However, it was reported the 2.1 mm i.d column format is minimally affected by the slightly higher extra column volume yielding very high efficiencies and a fast analysis [136].

Due to the importance of mass spectrometers role in aiding the identification of new chemical entities in natural product profiles, confirmation of reaction synthesis completions and high throughput screening for potential lead candidates, experiments which explore the optimization of the interface with mass spectrometry detection were investigated. A short study was designed to obtain a better understanding of peak distortion effects when using polar and non-polar organic diluents for sample preparation specifically during reaction synthesis. Generally, the analytical methods performance is the critical aspect to successfully identifying, characterizing, quantitating and controlling new chemical entities for further development. In an effort to build SFC methodology expectations, changes in method variables affecting selectivity and resolution will be investigated using One Factor at a Time principles (OFAT). This will be applied to a commercially available compound and amphipathic compounds commonly found and associated as the matrix of natural products. Results of the study will provide guidance when performing synthetic chemical reactions common to the earlier stages of the medicinal chemistry workflow.

## 3.2 Experimental

The experiments within this chapter were performed using a pre-commercialized low dispersion SFC instrument. Due to the nature of changing method development variables with an aim to deliberately alter selectivity, there are a multitude of changing experimental parameters explored within this study. Therefore an explicit description of all the experimental variables will not be included in this experimental section, but rather referenced within the sub-section text and figure captions where appropriate.

### 3.2.1 Diluent Study

#### *3.2.1.1 Diluent study materials and preparations*

HPLC grades of methanol, acetonitrile, tetrahydrofuran, and 2-propanol were purchased from Fischer Chemical (New Jersey, USA). n-Heptane and n-hexane was purchased from VWR International (Pennsylvania, USA). Reagent grades of dimethylsulphoxide, N,N-Dimethylacetamide, N-methylpyrrolidone, and dimethylformamide were purchased from Fischer Scientific (New Jersey, USA). The probe analyte 4-hydroxybutylbenzoate (4-HBB) (Sigma Aldrich, MO, USA) was prepared as a 0.2 mg/mL solution in a range of polar and non-polar solvents as shown in Table 3.1.

**Table 3.1: Diluents used in the study**

Heptane/IPA 9:1	Tetrahydrofuran (THF)
Heptane/IPA 7:3	N,N-Dimethylacetamide (DMA)
Methyl-t-butyl ether (MTBE)	Dimethyl sulfoxide (DMSO)
Methanol	N-methyl pyrrolidone (NMP)
Acetonitrile	Dimethylformamide (DMF)
2-Propanol (IPA)	

### 3.2.1.2 Diluent Study Instrument Conditions

The separations were performed using the columns outlined in Table 3.2 on an ACQUITY UPC<sup>2</sup> system configured with PDA detection (Waters® Corporation, MA, USA). Each of the columns outlined in Table 3.2 were acquired from Waters Corporation (Milford, USA). Each column was maintained at 45 °C to minimize any external environment effects such as varied room temperature. The analyte was eluted isocratically at 2.0 mL/minute with a mobile phase composition of 97% medical grade CO<sub>2</sub> and 3% methanol. The backpressure was maintained at 2000 psi. The injection volume was 2.0 µL while the samples were maintained at 18 °C in the autosampler. Detection was monitoring at a single wavelength 254nm and a wavelength range from 210 nm to 500 nm.



**Table 3.2: Columns and dimensions for diluent study**

Stationary Phase	Dimensions
ACQUITY UPC <sup>2</sup> Charged Surface Hybrid (CSH) Fluoro Phenyl,	3.0 mm x 100 mm; 1.7 $\mu$ m
ACQUITY UPC <sup>2</sup> BEH silica,	3.0 mm x 100 mm; 1.7 $\mu$ m
ACQUITY UPC <sup>2</sup> BEH 2-Ethyl Pyridine,	3.0 mm x 100 mm; 1.7 $\mu$ m
ACQUITY UPC <sup>2</sup> High Strength Silica (HSS) C <sub>18</sub> Stable Bond (SB), , <i>*This column showed no retention so it was eventually excluded from the study.</i>	3.0 mm x 100 mm; 1.8 $\mu$ m

### 3.2.2 Mass Spectrometry Interfacing Investigations

#### 3.2.2.1 MS Interface Materials and Preparations

Acetonitrile (Optima™ LC/MS Grade), 2-propanol (Optima™ LC/MS Grade), and methanol (Optima™ LC/MS Grade) were obtained from Fisher Scientific (New Jersey, USA). The analytical reference standards clopidogrel hydrogensulfate, lidocaine, tolbutamide, omeprazole, alprazolam, warfarin, and ranitidine hydrochloride were purchased from Sigma-Aldrich (Missouri, USA). The mobile phase and make-up flow additives were formic acid and ammonium hydroxide and purchased from Sigma-Aldrich (Missouri, USA). A seven component mixture was prepared to a concentration of 100 ng/mL for each component and diluted in methanol. A working mixture solution composed of a concentration of 100 ng/mL for each of the seven reference standards listed above; clopidogrel hydrogensulfate, lidocaine, tolbutamide, omeprazole, alprazolam, warfarin, and ranitidine hydrochloride diluted in methanol and labeled as ‘MS Test Mix’.

### 3.2.2.2 *Mass Spectrometry*

The optimization investigation experiments were performed using a Waters Xevo TQ-S triple quadrupole mass spectrometer (Waters Corporation, Manchester, UK) and controlled using Masslynx™ V4.1 software (Waters Corp., Milford, USA). The experiments were performed using positive ES ionization mode. The multiple reaction monitoring(MRM) transitions for each compounds was determined by infusion of standards of each analyte. Infusion could not be performed with SFC mobile phase flow due to issues with the on board MS/MS valve compatibility for use with supercritical fluid solvents. Leaks would occur. The optimizations of temperature and gas flows were determined using a series of injections at varied conditions. This experimental record pertains to investigations and therefor references to MS conditions are noted in the experimental results of the pertain sections in this chapter.

## 3.2.3 **Method Development One Factor at a Time (OFAT) Investigations**

### 3.2.3.1 *Metoclopramide and related substances materials preparations*

Methanol was purchased from Fisher Scientific (Pittsburgh, PA, USA) and USP grade CO<sub>2</sub> from (AirGas, MA, USA). Formic acid and ammonium formate (Sigma-Aldrich, St. Louis, USA) were used in the mobile phases. Standards of metoclopramide and related substances (LGC, UK) were used for the method development experiments. A resolution solution; defined as a mixture of the API and related substances, was prepared with metoclopramide and eight related impurities, as shown in Table 3.3. The impurities were prepared at 0.1% w/v % concentration of the metoclopramide standard. The metoclopramide was prepared by weighing approximately 100 mg of standard and each of the impurities were prepared by weighing approximately 10 mg of standard and dissolved in 100mL of methanol. The resolution solution was used for the chromatographic method development. Investigations of

impurity C and impurity F standards were prepared in methanol and explored at 0.1 mg/mL concentrations.

**Table 3.3: List of metoclopramide impurity standards, peak designation, masses, and European Pharmacopoeia labels.**

Peak #	Name	FW	EP ref.
7	Metoclopramide (4-amino-5-chloro-N-(2-(diethylamino)ethyl)-2-methoxybenzamide	299.8	
1	4-amino-5-chloro-2-methoxybenzoic acid	201.6	(EP C)
2	4-(acetylamino)-2-hydroxybenzoic acid	195.2	(EP H)
3	4-amino-5-chloro-N-2-(diethylaminoethyl)-2-methoxybenzamide N-oxide	315.8	(EP G)
4	4-amino-5-chloro-N-2-(diethylaminoethyl)-2-hydroxybenzamide	285.8	(EP F)
5	4-(acetylamino)-5-chloro-N-2-(diethylaminoethyl)-2-methoxybenzamide	341.8	(EP A)
6	Methyl 4-(acetylamino)-2-methoxybenzoate	223.2	(EP D)
8	Methyl 4-(acetylamino)-5-chloro-2-methoxybenzoate	257.7	(EP B)
9	Methyl 4-amino-2-methoxybenzoate	181.1	

#### 3.2.3.1.1 Instrumentation Configuration for Metoclopramide Analysis

A Waters ACQUITY UPC<sup>2</sup> (Waters Corporation, Milford, USA) equipped with a binary solvent management system capable of four solvent selection for the modifier delivery mechanism, Convergence Manager (CCM) to variably control the outlet backpressure of the

system, four column management system controlled by a Waters CM-A and CM-Aux. Detection was achieved with a Waters UPC<sup>2</sup> photodiode array detector (UPC<sup>2</sup> PDA) and a Waters ACQUITY SQD mass spectrometer using electrospray ionization (ESI+/-) switching. Full scan data was collected with a range of 150 – 1200 Da. The cone voltage was set to 20 V and the capillary voltage set to 3.0 kV. The source temperature was set to 150 °C and the desolvation temperature set to 500 °C. The desolvation gas flow was set to 1000 L/hr. The system control and data acquisition were undertaken using Waters Empower 3® CDS. The eluent was split using the Waters UPC<sup>2</sup> splitter (as described in Chapter 2) *via* post PDA detection but before the CCM allowing for a leak of flow to the MS probe. The splitter was modified to eliminate use of the make-up pump flow by taking out the first tee splitter in the UPC<sup>2</sup> MS splitter containment device while re-plumbing for the flow from the PDA directly to the second tee splitter in the MS splitter device.

### 3.2.4 Amphipathic Analysis Investigations

#### 3.2.4.1 Amphipathic Solution Materials and Preparations

Samples and standards were purchased from Avanti Polar Lipids. Stock 1 and Stock 2 were Brain (porcine) extracts except for lysophosphatidylcholine (LPC) and phosphatidylglycerol (PG) which were egg (chicken). Stocks were prepared in 50:50 chloroform/methanol. Working lipid mixtures were prepared to the specified concentration.

- **Stock 1:** Ceramide, SM, (0.05mg/mL) and PG, PE, PC, (0.1mg/mL)
- **Stock 2:** LPC, LPE, (0.05mg/mL)
- **Mix 1:** 1:1 of [mix 2] and [mix 3]
- **Mix 2:** Phosphatidylcholine (PC) acyl chain length 5 component mix (0.1 mg/mL): 14:0/14:0, 16:0/16:0, 17:0/17:0, 18:0/18:0, 23:0/23:0
- **Mix 3:** Phosphatidylcholine (PC) Saturation 3 component mix: 18:1( $\Delta^9$  cis)/18:1 ( $\Delta^9$  cis), 18:2( $\Delta^9,12$  cis)/18:2 ( $\Delta^9,12$  cis), 18:3( $\Delta^9,12,15$  cis)/18:3 ( $\Delta^9,12,15$  cis)

### 3.2.4.2 Instrument Conditions for the Amphipathic Experiments

The chromatography was performed using an ACQUITY UPC<sup>2</sup> system coupled to an ACQUITY single quadrupole (SQD) mass spectrometer. CO<sub>2</sub> was used as the super critical fluid as mobile phase component A. A modifier co-solvent was used as mobile phase B which consisted of 2 g/L ammonium formate dissolved in methanol. The column for the analysis was a 3.0 x 100 mm UPC<sup>2</sup> BEH column with 1.7 µm particles. The injection volume was optimized for 1 µl. The samples were eluted with an optimized flow rate of 1.9 mL/min. The column temperature was optimized and maintained at 60 °C. The peaks were eluted under gradient elution initially beginning with 15% modifier. The modifier was increased to 50% over 3 minutes and held at 50% for another 2 minutes. Prior to the next injection, the gradient was re-equilibrated at initial conditions for 2 minutes. General re-equilibration times recommended from column manufacturers for RPLC utilizing gradients that extend from 5% to 95% organic are 8-10 column volumes. For this UPC<sup>2</sup> method, the gradient is increased to only 50% elution modifier. It assumed an equilibration of 5 column volumes at initial conditions equating to 1.86 minutes for equilibration time, would be suffice. The time for equilibrating 5 column volumes for this method was calculated by Equation 3.1:

$$\begin{aligned}
 & \text{Total Volume for Equilibration } (V_{\text{equil}}) \\
 &= (\pi r^2 L)(\# \text{ of recommended column volumes } (C_v)) \\
 &= \pi (0.150 \text{ cm})^2 (10 \text{ cm}) (5) = 3.53 \text{ cm}^3 = 3.53 \text{ mL} \\
 \\ 
 & \text{Equilibration time} = \frac{(V_{\text{equil}})}{\text{Flow rate}} = \frac{3.53 \text{ mL}}{1.9 \text{ mL min}^{-1}} = 1.86 \text{ min}
 \end{aligned}$$

**Equation 3.1: Calculation of equilibration volume as defined by 5 column volumes and calculation of re-equilibration time**

The re-equilibration time was verified by observing the pressure profile displayed on the instrument software diagnostic console panel. The diagnostic console for monitoring pressure indicated that the total system pressure after the re-equilibration was equal to that of the total system pressure at the start of the gradient profile. The matching total system pressures are a good indication of appropriate re-equilibration time. The back pressure was regulated using the automated backpressure regulator to maintain isopycnic conditions. The initial back pressure setting was 3000 psi which resulted in an overall system pressure of 5600 psi. For the isopycnic versus isobaric comparisons, the back pressure was automatically decreased to 1500 psi over the 3 minute span of the programmed gradient of the automatic backpressure regulator and held at 1500 psi for 2 minutes. This allowed the observed overall system pressure to be maintained at approximately 5600 psi  $\pm$  30 psi for the duration of the analysis. System control and data collection was achieved using Empower® 3 CDS.

### 3.3 Results

#### 3.3.1 Diluent Study

The goal of this study was to obtain a better understanding of peak distortion effects when using polar and non-polar organic solvents for analysis with the ACQUITY UPC<sup>2</sup> System based on the experimental reasoning specified in Table 3.4. The study included a range of solvents (Table 3.1) that span a range of polarities and relative eluotropic strengths. Results of the study provided guidance for diluent selection when performing synthetic chemical reactions in a medicinal chemistry laboratory. Table 3.4: Diluent effects experimental reasoning and design

Question?	Importance?	Test Case
<b>What is the injection range for common diluents at each end of the polarity spectrum?</b>	To understand loadability and strong solvent effects on peak shape to aid scale-up processes.	Effect of injection volume with polar vs. non-polar diluents on a silica column
<b>Are the results different for different columns?</b>	To understand expected retention for low k' analytes	Effect on different columns

	to aid method selection	
<b>Are other diluents retained? and how would they interfere with the results</b>	To understand the interferences when this technique is implemented in a medchem environment	Investigated DMA, DMF, NMP, <i>etc.</i>
<b>What if the optimal diluent results in poor solubility?</b>	To understand what the limitations and expectations when compositional diluent mixtures are used	Systematic exploration of increasing addition of problematic diluents with optimal diluents.

A test probe analyte with a low retention factor ( $k$ ) is good to study the effect of diluents when injected because it will be more susceptible to peak distortion effects. 4-hydroxy butylbenzoate (4-HBB) was chosen as a suitable probe analyte because of its high solubility in the solvents used in the study and low retention factor. Different injection volumes were investigated to evaluate loadability and strong solvent effects on peak shape. Comparisons of the chromatographic peak shape obtained for the non-polar diluent of heptane/IPA (9:1) and the polar diluent DMSO are shown in Figure 3.1. Peak distortion was observed for the probe analyte on all columns when DMSO was used as the diluent for injections greater than 2  $\mu\text{L}$ . Conversely, the peak shape of the probe analyte was Gaussian when heptane/IPA (9:1) was employed as the diluent. However, when the injection volume was increased to 5  $\mu\text{L}$ , peak distortion occurred irrespective of diluent. It is hypothesized that either strong solvent effects or the mass load of the sample is the major contributor to peak shape distortions at the larger injections rather than the elutropic strength of the diluent. In both cases, mass overload and strong solvent effects, the peak touchdown point would be the same as injection volume is increased, yet the liftoff point of the peak would shift to an earlier time point. Mass overloading is historically seen as a ‘shark fin’ peak shape whereas the tailing factor would be measured and represented as a larger positive integer, which is not seen in the chromatograms in Figure 3.1. The 2  $\mu\text{L}$  and 5  $\mu\text{L}$  injections of DMSO, the mass analysis of

the hump at the beginning of the probe peak indicated retention interference of the DMSO solvent. It was concluded that DMSO is retaining on the column but is also contributing to strong solvent effects at the larger injection volumes which are contributing to the distortion of the peaks.



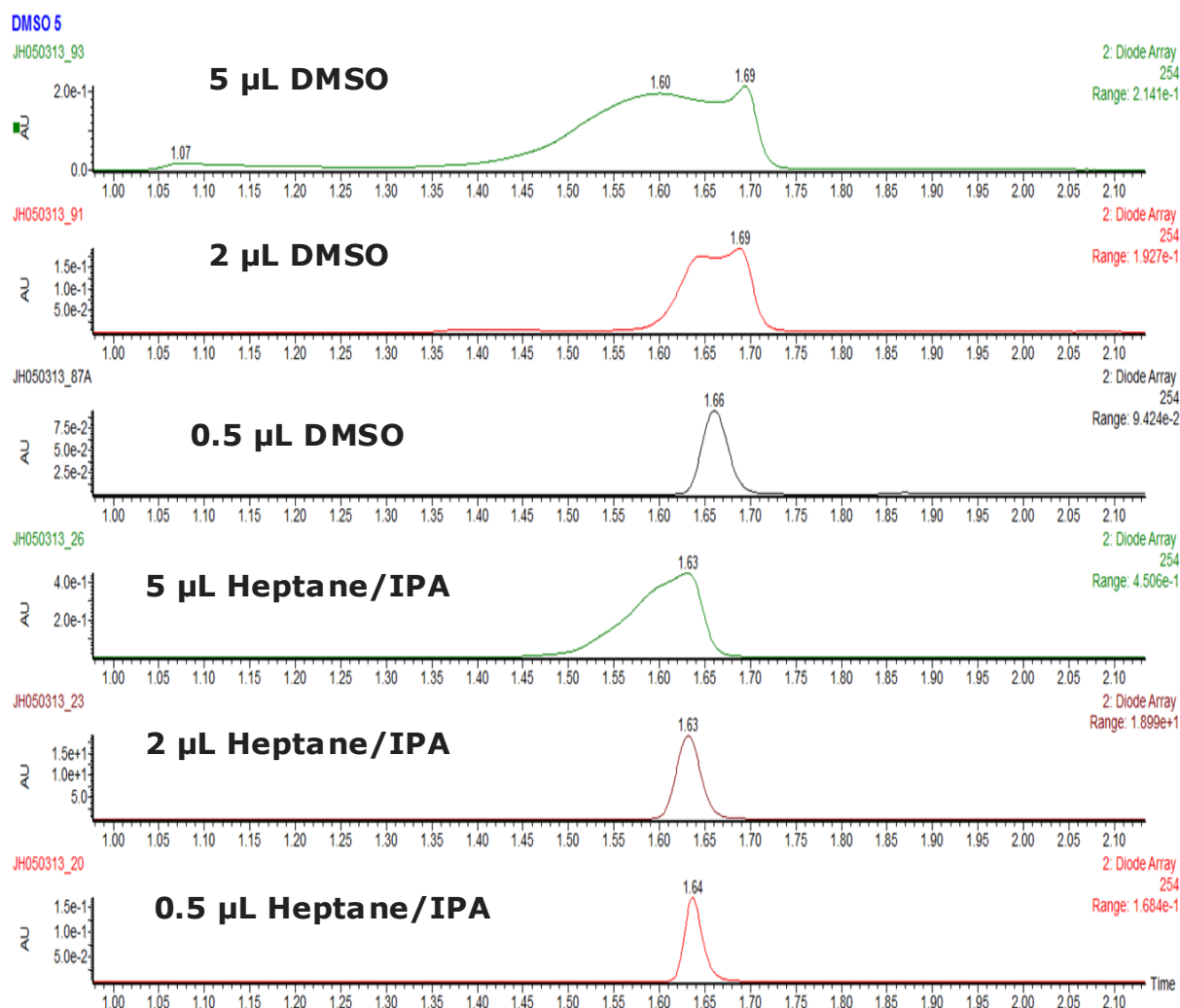


**Figure 3.1: Peak distortion comparisons of 0.2 mg/mL 4-HBB standard between polar solvent DMSO and non-polar solvent heptane/IPA 9:1 for 0.5 µL, 2 µL, and 5 µL injection volumes on an ACQUITY UPC<sup>2</sup> BEH, 3.0 mm x 100 mm; 1.7 µm column.**

Reaction synthesis commonly uses a wide range of polar solvents such as DMA, DMF, NMP, and DMSO. These solvents were used as diluents and compared to the non-polar diluent heptane/IPA (9:1) for the same analyte probe 4-HBB. Each injection resulted in peak shape distortion for the 4-HBB probe. The injections using the DMA and DMF diluent showed retention of these diluents on the column interfering with the 4-HBB probe analyte. A similar result was observed for NMP, however NMP exhibits low absorbance at 254 nm. Therefore extra considerations should be adhered to when using NMP as a diluent at lower wavelengths

as a possible diluent, yet the peak width was observed to be greater than the peak width for the injections of the heptane/IPA (9:1).

The experiment performed for Figure 3.2 was repeated by injecting the 4-HBB probe analyte on the CSH Fluoro-phenyl column. The extent of the 4-HBB peak distortion was observed to be much more severe for this column when compared to the results obtained on the ACQUITY UPC<sup>2</sup> BEH column (Figure 3.1).

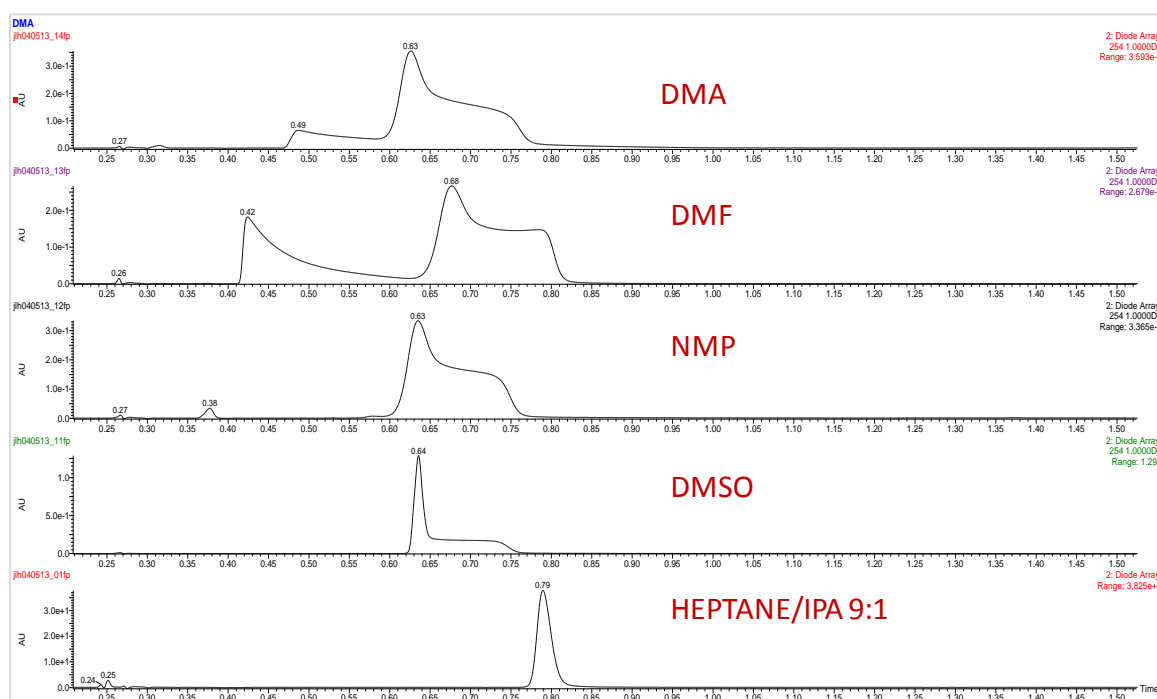


**Figure 3.2: CSH Fluoro-phenyl UPC<sup>2</sup>/UV results showing peak distortion of 4-HBB for polar solvents DMA, DMF, NMP, and DMSO including the non-polar solvent heptane/IPA (9:1).**

Further investigations to help explain this phenomenon would have to consider solubility compatibility and loadability studies. However for the purpose of this chapter and future work described in this thesis, the goal of attaining general expectations regarding sample diluent retention interferences and effects on peak shape due to strong solvent effects and

increasing injection volume has been achieved allowing us to begin general HTS experiments and reaction monitoring of pharmaceutical compounds.

### **3.3.2 Optimizing the Mass Spectrometry Interface**

#### *3.3.2.1 Effects of MS probe exit solvent plume instability*

Prior to beginning any analysis, the instrument was set-up at initial conditions of 5% modifier at a flow rate of 1.5 mL/min with a make-up flow of 0.2 mL/min. The modifier composition was 100% methanol. Make-up flow is defined as the post-column addition of solvent used to aid ionization of the analytes in the mass spectrometer. For this experiment, the composition of the make-up flow was 100% methanol with 0.1% formic acid. The gradient program was initiated to increase to 30% modifier over 7 minutes. Blank injections of methanol were performed to monitor the baseline. Baseline ripples or excessive baseline noise was observed and highlighted in the blue circle of Figure 3.3. Upon further investigation of a subsequent injection, the ripples coincided with pulsation of the spray as it exited the mass spectrometer probe. The ripple was not observed during single ion recording nor detected in the PDA chromatographic trace. As the modifier composition increased, the gradient, the ripple disappeared indicating that the effect was due to poor nebulization at low organic solvent compositions. In an effort to mitigate the increased baseline noise and probe pulsation, make-up flow rates were increased to 0.6 mL/min until the gradient composition increased to greater than 15% modifier.

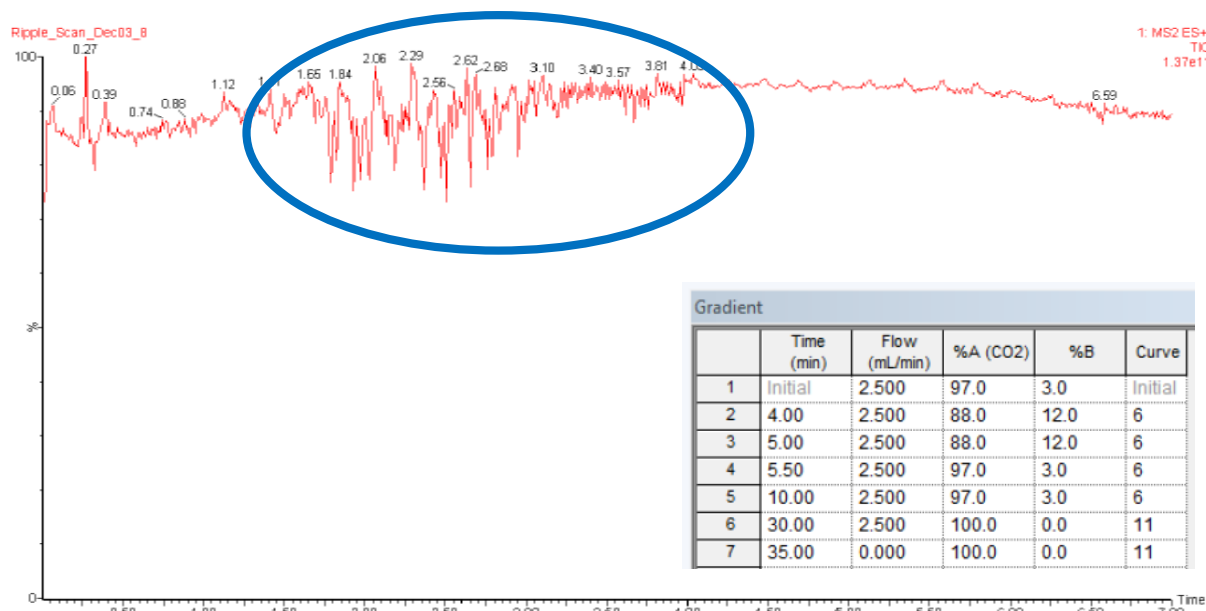


**Figure 3.3: Evidence probe plume pulsation (circled in blue) in MS TIC during a blank injection**

### 3.3.2.2 Investigating capillary voltage parameters

Capillary voltages were explored in order to understand their effect on sensitivity for the probe analytes in the mixture described in section 3.2.2.1. The optimal capillary voltage for the majority of the compounds resulted in a value of 1.0 kV as seen in the plot shown in Figure 3.4. The make-up flow consisted of 0.2% ammonium hydroxide in methanol with a flow rate of 0.4 mL/min. The analysis was performed using an ACQUITY BEH column with a flow rate of 1.5 mL/min and gradient elution programmed at a starting composition of 2% modifier increasing to 45% modifier over 5 minutes. The modifier was prepared with 0.2% ammonium hydroxide in methanol.

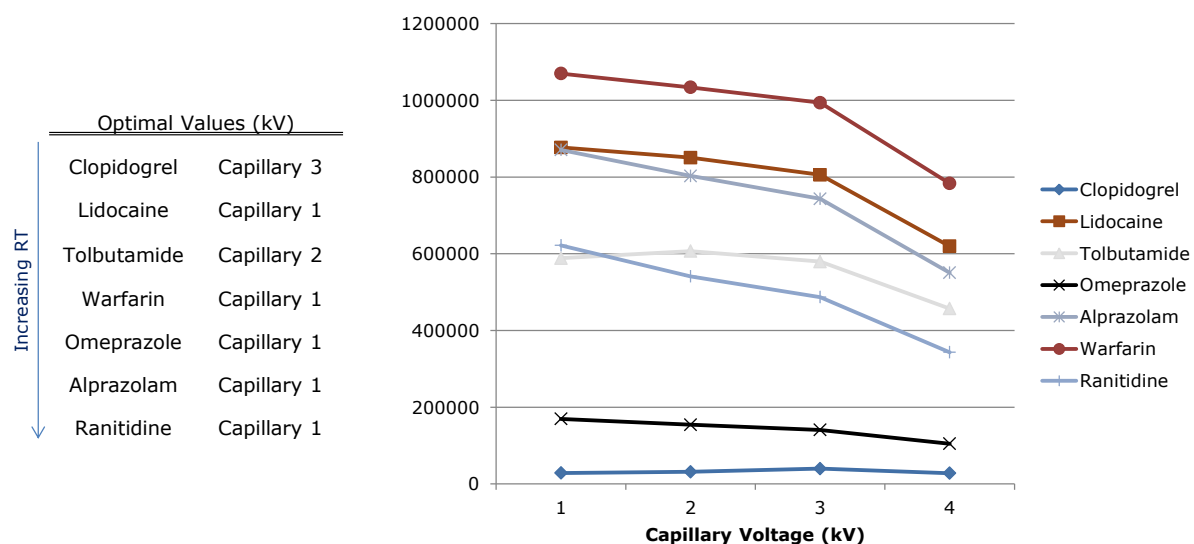


**Figure 3.4: Investigating capillary voltage for basic and neutral pharmaceutical compounds**

Interestingly, different optimal capillary voltages were observed for the analysis of Phosphatidylglycerol (PG) and Phosphatidylethanolamine (PE) lipids (Figure 3.5). The optimal capillary voltage was observed to be 4.0 kV for these amphipathic compounds. It was concluded, the capillary voltage optimal parameters are analyte dependent and not specifically technique dependent.

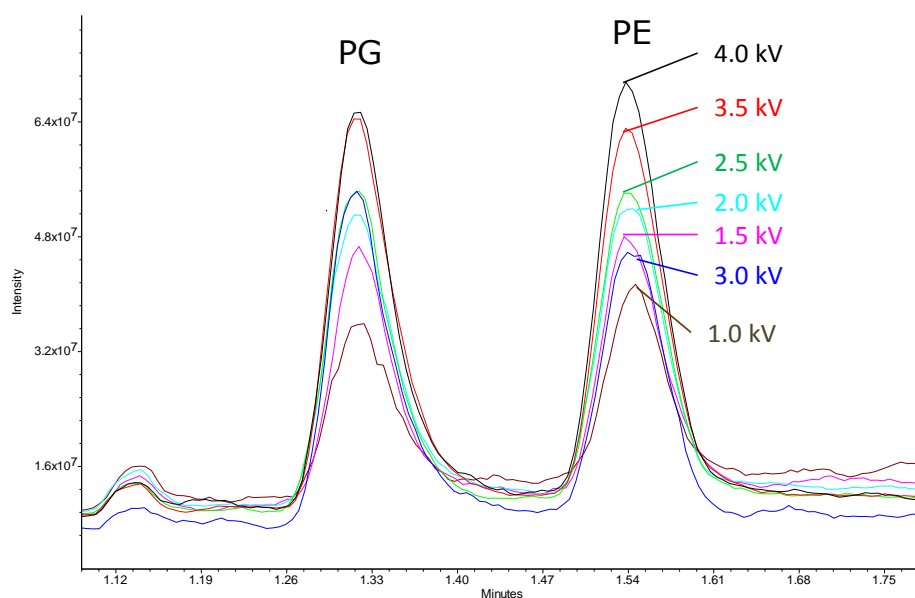


**Figure 3.5: MS TIC sensitivity comparisons of Phosphatidylglycerol (PG) and Phosphatidylethanolamine (PE) lipids when varying capillary voltage**

### 3.3.2.3 Investigating mass spectrometry desolvation parameters

Desolvation temperature was briefly investigated. According to the results plotted in Figure 3.6, ranitidine hydrochloride was the only compound that increases in sensitivity with higher desolvation temperature. It is assumed that the mass spectrometer requires more heat at the point of elution of ranitidine due to the higher amount of modifier, or liquid present in the source of the mass spectrometer.

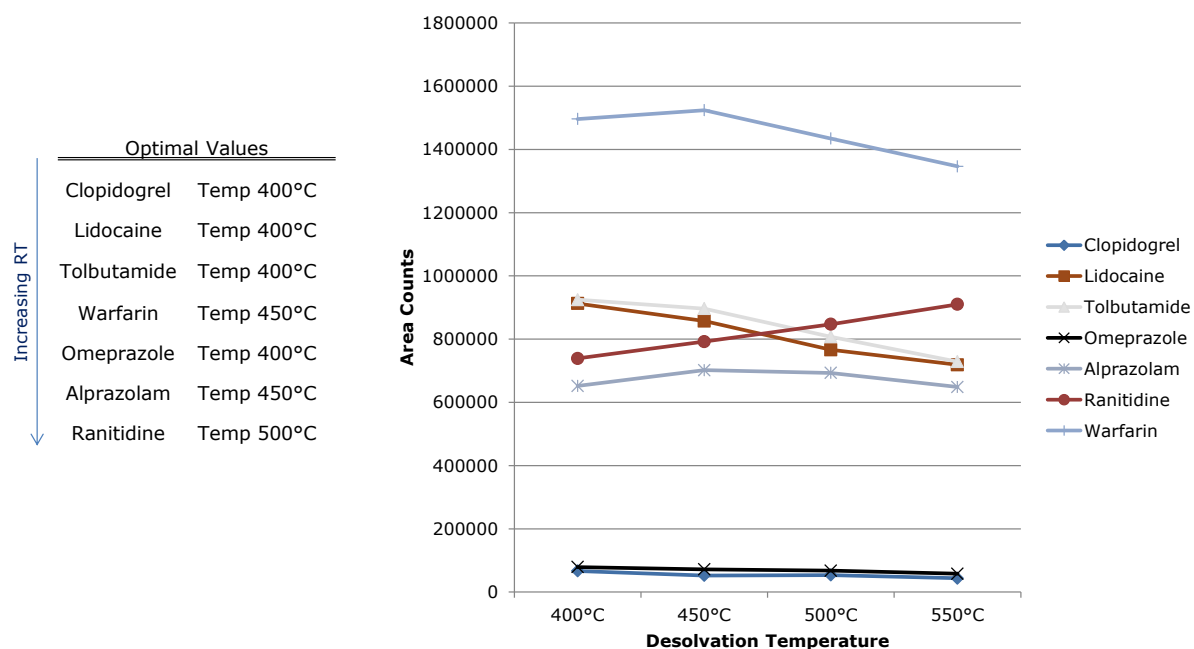


**Figure 3.6: Investigating desolvation temperature**

#### 3.3.2.4 Investigating the effects of post column addition solvent composition and flow rate

Three different post column addition solvent compositions were investigated. Acidic and basic additives in methanol and isopropanol were chosen. Additionally, four different post column addition flow rates were explored. The results in Table 3.5 suggested isopropanol was a better ionization solvent than methanol, specifically when the basic additive is used. A flow rate of 0.2 mL/min worked well for the compounds eluting in the middle of the gradient elution program. However, early eluting peaks ionized better at higher post column addition flow rates and late eluting peaks ionize better at lower post column addition flow rates.

**Table 3.5: Table of results post column addition make-up flow rates effect on peak area**

Make-up Flow Composition	Rate	Area Counts						
		Clopidogrel	Lidocaine	Tolbutamide	Omeprazole	Alprazolam	Warfarin	Ranitidine
0.2% NH <sub>4</sub> OH in Methanol		0.2% Ammonium Hydroxide in Methanol						
	0.1	8761	542871	517700	135327	654177	1224909	1100792
	0.2	8418	547265	618103	132973	711599	1234078	962816
	0.3	9613	506205	655874	131585	644136	1260202	864364
	0.4	8188	465379	593954	117559	614515	1200658	759458
0.2% NH <sub>4</sub> OH in Isopropanol		0.2% Ammonium Hydroxide in Isopropyl Alcohol						
	0.1	16154	562763	654389	137596	683221	1328870	1134824
	0.2	46801	541635	740471	147503	709307	1405293	994782
	0.3	51675	655067	723001	136335	697943	1376285	890588
	0.4	41527	824640	657317	130456	665118	1296238	849088
0.2% Formic Acid in Isopropanol		0.2% Formic Acid in Isopropyl Alcohol						
	0.1	22667	584204	355010	84938	508417	929392	1040988
	0.2	26018	460535	321338	86027	525280	1028658	909494
	0.3	17018	479268	322825	81374	492126	989344	820017
	0.4	19893	627858	300963	74636	484784	906409	756484

During the execution of other experiments that will be discussed in Chapter 4, particular observations pertaining to post column addition were observed and included in this section of Chapter 3 due to the relevance to this section. For the experiments that were investigated in Chapter 4, water was explored as a post-column addition solvent additive as part of the methodology for the QC check analysis that was periodically performed throughout the HTS cheminformatics study. The blue box represents analytes that benefit from the addition of 5% water / 95% methanol as the post column solvent. The green box represents similarities of base and weak base addition. The red box represents the benefits of strong base addition to the make-up flow (Figure 3.7).



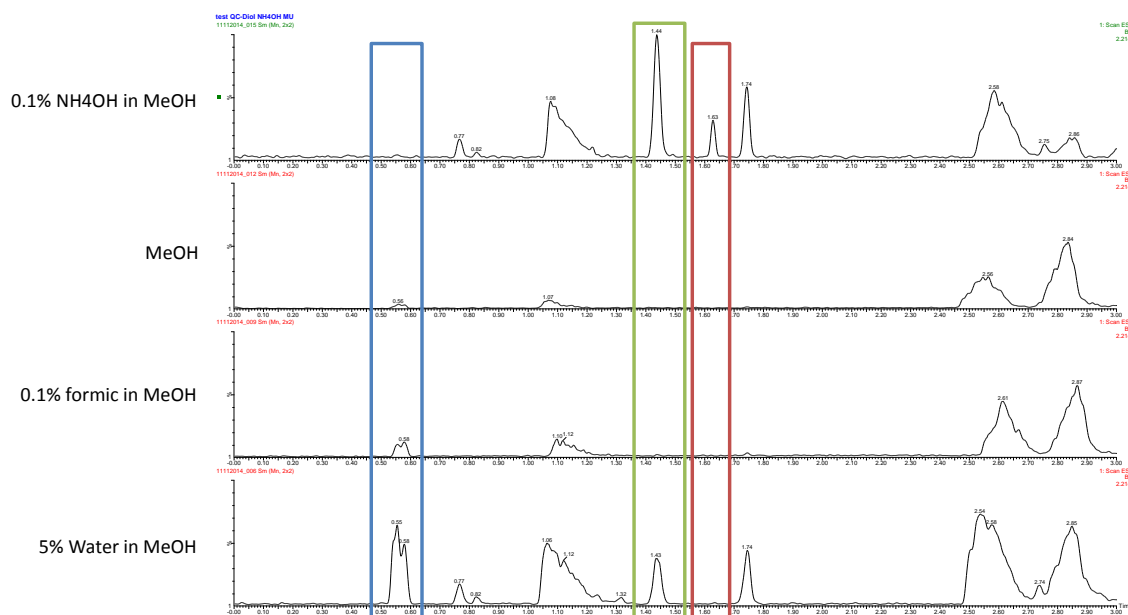


**Figure 3.7: MS TIC comparison of different post-column addition ‘make-up’ flow compositions for an unknown mixture of analytes. The blue box represents benefits of water addition. The green box represents similarities of base and weak base addition. The red box represents the benefits of strong base addition to the make-up flow.**

### 3.3.2.5 Comparison of MS sensitivity for full flow versus split flow

In order to perform this experiment appropriately, the pressure profile of the system in presence of the MS splitter device and automatic back pressure regulator device must be determined. For the analysis of the MS Test Mix using the conditions described in section 3.3.2.2., the observed starting pressure was determined to be 2600 psi with a max pressure of 4200 psi. Based on these pressure determinations, a transfer line designed to by-pass the MS splitter can be made such that they match the pressure profile. The pressure profile was varied based on the transfer line dimensions. The transfer line is the tubing connecting the outlet of the column (or UV flow cell) to the MS which continues to maintain an appropriate amount of backpressure so as not to compromise the phase change composition in the mobile phase as it pertains to the liquid CO<sub>2</sub> converting to gaseous CO<sub>2</sub>. This configuration also by-passed the automatic back pressure regulator; which is a variable pressure regulating device,

to a more static pressure regulating device. The transfer line in this instance was also designed to maintain an average density of mobile phase similar to that of the mobile phase used for the system using the splitter and back pressure regulator. The results observed show a consistent increase in sensitivity when allowing the full flow of mobile phase into the mass spectrometer (Figure 3.8).

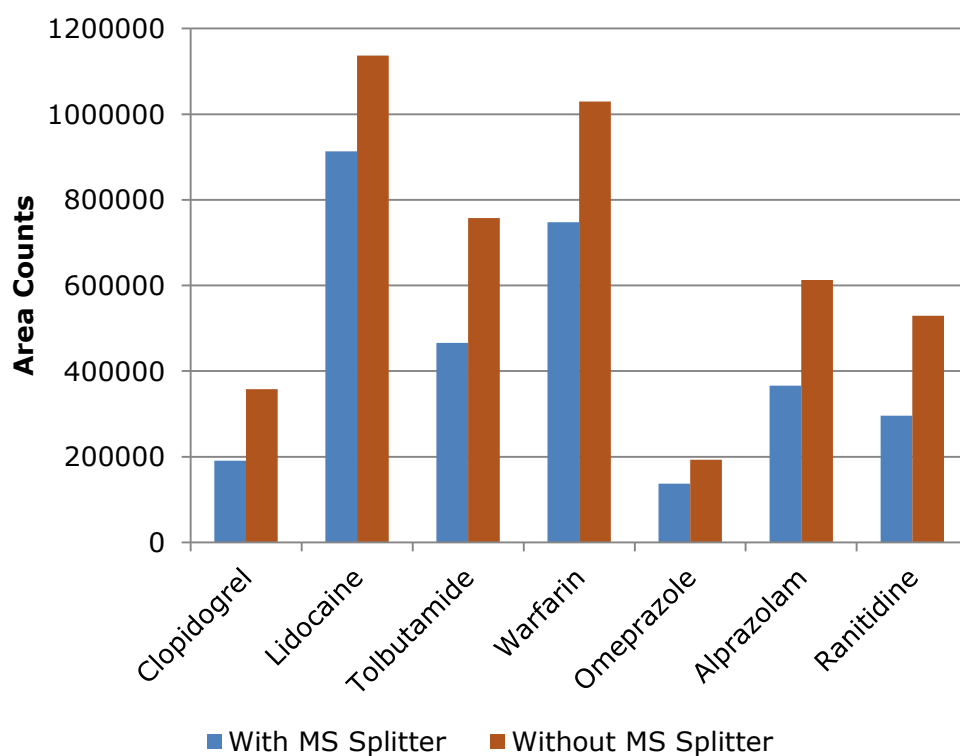


**Figure 3.8: Comparison of sensitivity with MS splitter versus full flow into the MS without splitter (n = 3 for each condition for each analyte and the average was reported.)**

### 3.3.3 One Factor at a Time (OFAT) Method Development Investigations

#### 3.3.3.1 Systematic Screening

The method development process employed systematically screened columns, modifiers, and modifier additives to achieve the best separation for the analytes under test. The initial configuration screened four UPC<sup>2</sup> columns with four modifiers. A “modifier” is the strong solvent mobile phase component that facilitates elution of the analytes increasing in polarity. The four modifiers used were: i) methanol, ii) methanol with 0.5% formic acid, iii) methanol with 2 g/L ammonium formate, and iv) methanol with 0.5% triethylamine. The screening process was performed with a generic 5% to 30% B gradient over 5 min, holding at 30% for 1 min before returning to the initial composition. The total screening time was achieved in just over two hours. The methanol with ammonium formate provided the best overall peak shape compared for each column, as shown in Figure 3.9. The peak tracking during the method screening process was achieved by reviewing the MS spectra provided by the mass spectrometer. The selectivity ( $\alpha$ ) for the more polar analytes varied greatly. Since the same screening method was utilized for these comparisons, the results of changing selectivity were hypothesized to be primarily related to the stationary phase – solute interactions.

The structures of metoclopramide and the related substances are given in Table 3.6. It was clear the first three components; impurities B, 9, and D, did not change selectivity during the column screening most likely due to neutral or polarity likeness. Interestingly, as the polarity increased and the increased composition of modifier was required to elute the polar compounds, the selectivity of the analytes changed dramatically for each of the column comparisons. Impurity F, Impurity A and metoclopramide increased retention on the HSS C<sub>18</sub> SB column, concluding more hydrophobic and possible steric retention mechanisms

between the stationary phase ligand and the diethyl (propyl)amine side chain which many of the other impurities did not have. Impurity A and Impurity C changed elution order on the BEH 2-EP column which was concluded as a result of the greater amount of aliphatic amine functionality of Impurity A versus Impurity C. Impurity A has 2 secondary amines and 1 tertiary amine within the structure. Impurity C has 1 primary amine within the structure. The number of amines could possibly be related to the  $pK_a$  of the BEH 2-ethylpyridine stationary phase. The shift in retention selectivity might also be attributed to solubility. Primary amines are more soluble in water and highly polar functional groups, thus resulting in a greater retention time on the silica columns. The greater retention of Impurity A could be explained by increased hydrogen bonding with the silanols of the stationary phase. Impurity H has a carboxylic acid and hydroxyl group located 5 and 6 on the benzene ring. The same hydrogen bonding retention mechanism could also explain the increased retention of Impurity H on the highly polar BEH column. Impurity C splits into 2 peaks. The retention mechanism for impurity C is hypothesized to be related to pi-pi interactions with the fluorine electron shells of the CSH pentafluorophenyl stationary phase and the conjugated bonds of the analyte structure. If the mixture consisted of constitutional (structural) isomers, separations of the isobaric species could be observed. This will be investigated later in the chapter. Because so many retention mechanisms are recognized with this technique, it becomes very difficult to deduce the dominating retention mechanism within a given separation or comparison of separations screened across columns with different properties.

**Table 3.6: Table of metoclopramide and related substances structures, names and monoisotopic mass.**

Structure	European Pharmacopeia Name	[M + H] <sup>+</sup> or [M - H] <sup>-</sup>
	Metoclopramide	300.14
	Impurity A	342.16
	Impurity B	258.05
	Impurity C	200.03 (negative ion)
	Impurity D	224.09
	Impurity F	286.13
	Impurity G	316.14
	Impurity H	194.06 (negative ion)
	Impurity #9 Methyl 4-amino-2-methoxybenzoate	182.08

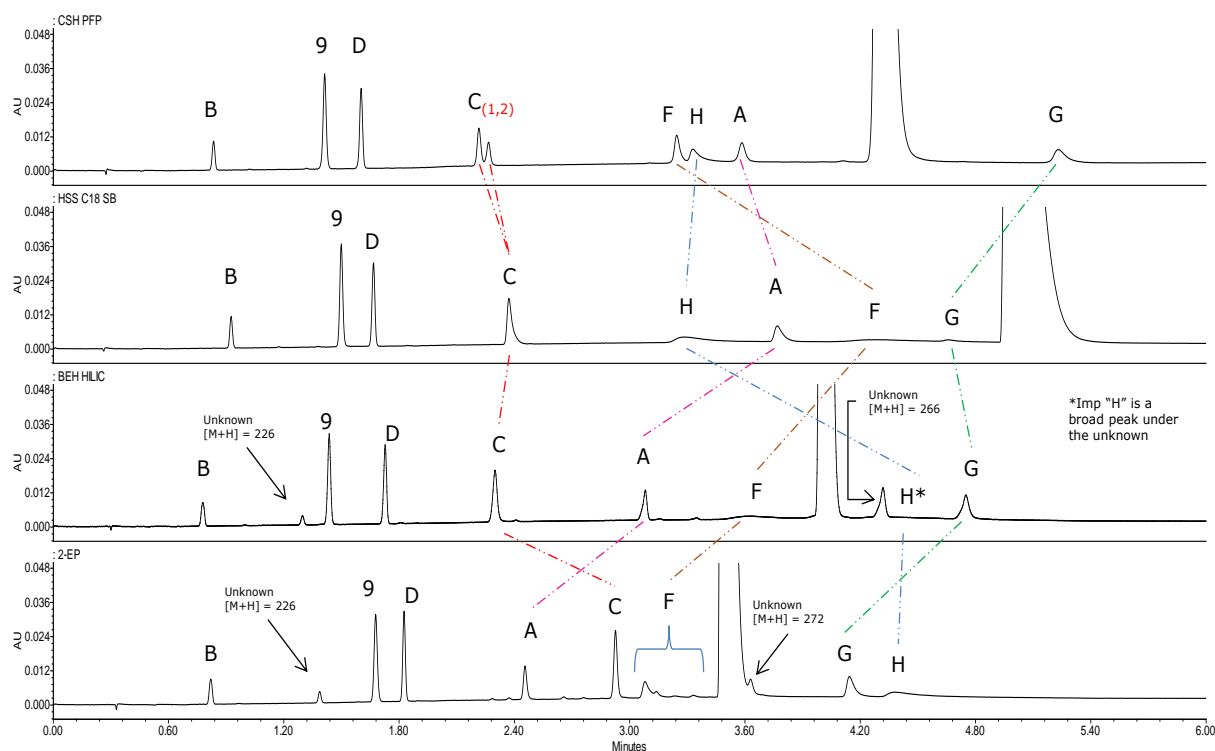


**Figure 3.9: Column screening results with peak tracking confirmed by MS. The modifier (B) was methanol with 2g/L ammonium formate. 5% to 30% B over 5 min and held at 30% for 1 min.**

Based on these results, the UPC<sup>2</sup> 2-EP stationary phase was the optimal column of choice providing Gaussian peak shapes and greatest average resolution for the majority of the analytes. The UPC<sup>2</sup> CSH Fluoro-Phenyl column provided good selectivity and peak shape, with impurity C unexpectedly separated into two peaks. Additionally, the impurity F appeared to separate as a number of peaks on the 2-EP column. However, this is suspected as being due to a stability issue for that particular compound.

#### 3.3.3.1.1 MS Investigation of reference standard Impurity C

During the screening process, two peaks were separated during the injection of the impurity C standard using the ACQUITY UPC<sup>2</sup> CSH Fluoro-phenyl column. This phenomenon was

not observed with the other stationary phases. MS spectral analysis of the two peaks showed similar spectra. The MS spectra in Figure 3.10 indicates possible dimerization of the analyte. Based on this information, it was determined the two peaks were related to each other rather than the second peak being a contaminant. The rapid determination of this relationship provided direction for scoping future analysis by MS/MS and accurate mass MS. The data generated with higher MS resolving techniques or MS fragmentation capabilities to discriminate closely related structures will be more useful in determining the purity of the standard.

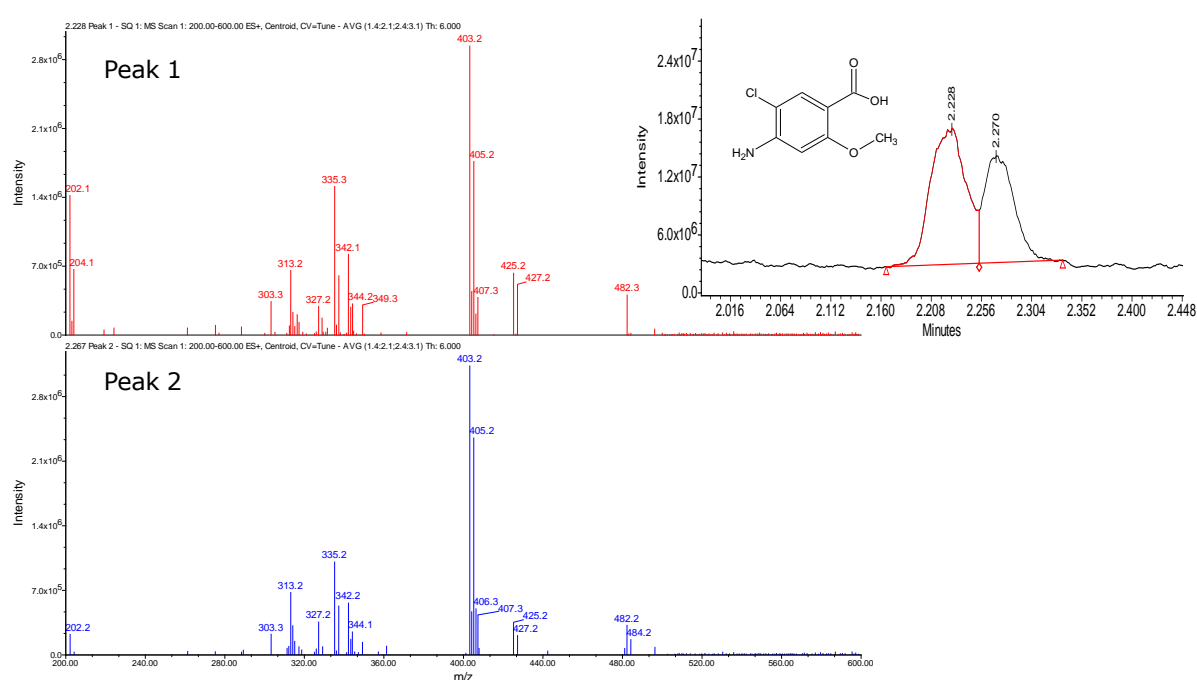


**Figure 3.10:** MS spectral analysis of EP impurity C for the doublet peaks observed when using the UPC<sup>2</sup> CSH Fluoro-phenyl stationary phase.

### 3.3.3.1.2 Investigation of Impurity F working standard solution stability

The peak shape of impurity F was observed to degrade over time during the method development process (Figure 3.11). Unknown peaks would appear in the chromatogram within the course of seven days of investigative analysis. In addition, the color of the

standard solution changed from a clear solution to a solution with a brownish tint. MS interrogation revealed the masses listed in Table 3.7. The masses were correlated to those found to be significant to the UV trace (*not shown*) between retention time 2.0 minutes and 3.5 minutes. XIC of  $m/z = 330$  and  $m/z = 296$  resulted in multiple peaks.

**Table 3.7: Table of masses found in the degraded standard solution of metoclopramide EP impurity F.**

Name	Rt (min)	Observed $m/z$	$\Delta$ Mass $m/z$ (Da)	Proposed transformation
<b>EP Impurity F</b>	<b>2.92</b>	<b>286</b>		
Unknown 1	2.27	344	+ 58	methoxylation + methylation
Unknowns 2 & 4	2.30 & 2.61	330	+ 44	methoxylation
Unknowns 3 & 6	2.68 & 2.89	296	+ 10	hydrolysis + two methylations
Unknown 5	2.86	356	+ 70	unknown
Unknown 7	3.11	252	- 34	Loss of $\text{Cl}^-$
Unknown 8	3.29	258	- 28	Loss of two $\text{CH}_3$ groups

The working standard was prepared in methanol and left standing when left standing unprotected from light for 1 week. Many of the impurity peaks were products of methylation or methoxylation. Based on this information, methanol as a diluent has the potential to be problematic for compounds susceptible to these methylation and methyloxidative degradative reactions. As a result of these observations, the working standard solution shelf life has been



decreased to 3 days until a suitable diluent study can be performed. Further studies would have to be explored to determine if colder storage conditions would increase the shelf life of the solution. For all practical purposes for this investigation, 3 days shelf life was suffice. The unknown peak #8 in Table 3.7 with  $m/z = 258$  has the same mass of methyl 4-(acetylamino)-5-chloro-2-methoxybenzoate which is commonly referred to as “impurity B”. This unknown peak found in the impurity F working standard was determined not to be identical to EP impurity B due to differences in retention time, whereas impurity B eluted approximately at 0.48 minutes. The other impurities origins were still undetermined. They were hypothesized to be products of solution instability with methanol rather than degradants present in the reference material.

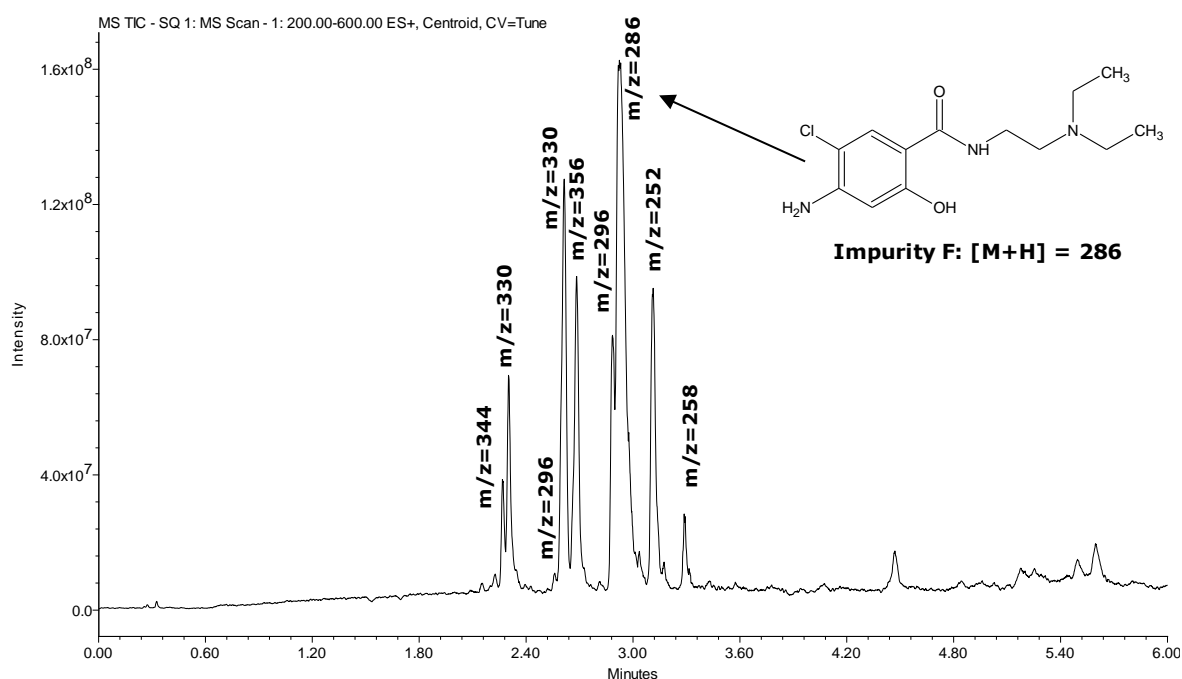


**Figure 3.11: MS ESI+ TIC of a degraded standard solution of metoclopramide EP impurity F.**

### 3.3.3.1.3 Effect of Gradient Slope

In reversed-phase LC, gradient slope is a common tool to manipulate the chromatographic separation, specifically in terms of increasing resolution between a critical pair of peaks. Using the UPC<sup>2</sup> 2-EP stationary phase, the gradient slope was decreased by extending the overall gradient run time. The change in slope had little to no effect on the chromatographic profile with the exception of a selectivity change between peaks 6 and 7, as shown in Figure 3.12.

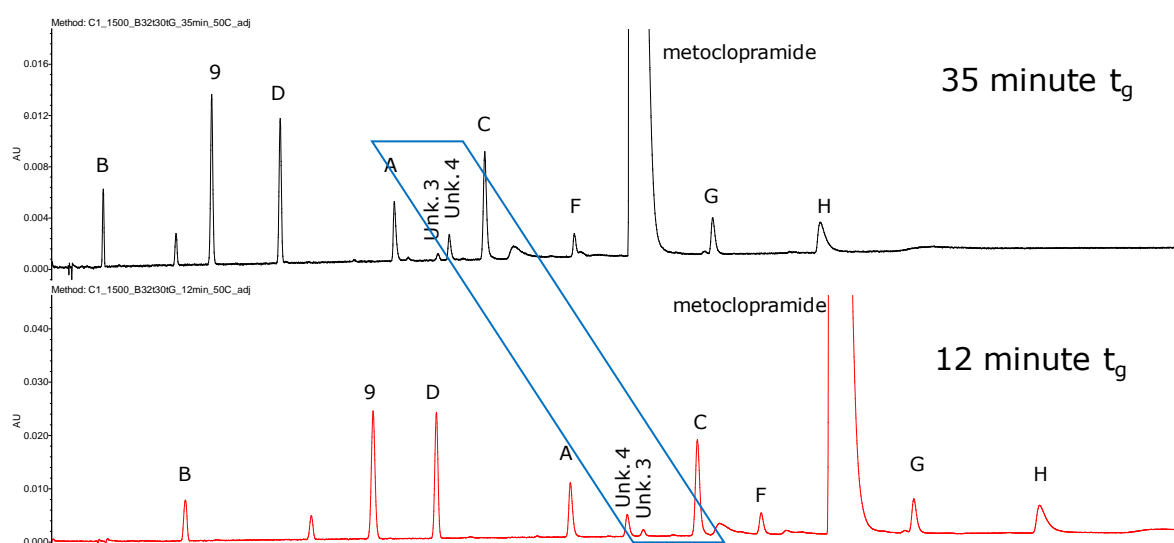


**Figure 3.12: Normalized x-axis overlay metoclopramide analyzed with extended 12- and 35-minute gradient run times flattening the slope compared to the 6-minute screening experiments. The original gradient was used; 5% to 30% B.**

### 3.3.3.1.4 Effect of Different Elution Solvents

Inducing a shallower gradient did not increase resolution between peaks. To increase resolution, a less polar aprotic organic solvent (acetonitrile) was mixed at different compositions with methanol, the stronger elution solvent. The addition of acetonitrile increased resolution, uncovered co-elutions, and spreading the separation between the peaks

within the retention time windows of 2.8 minutes and 3.5 minutes, as well as the effecting the separation of the peaks with the metoclopramide API and the later eluting impurity peaks between the retention window between 3.8 and 5.0 minutes in Figure 3.13. Based on these observations, this technique proves to be a powerful tool when developing methods.

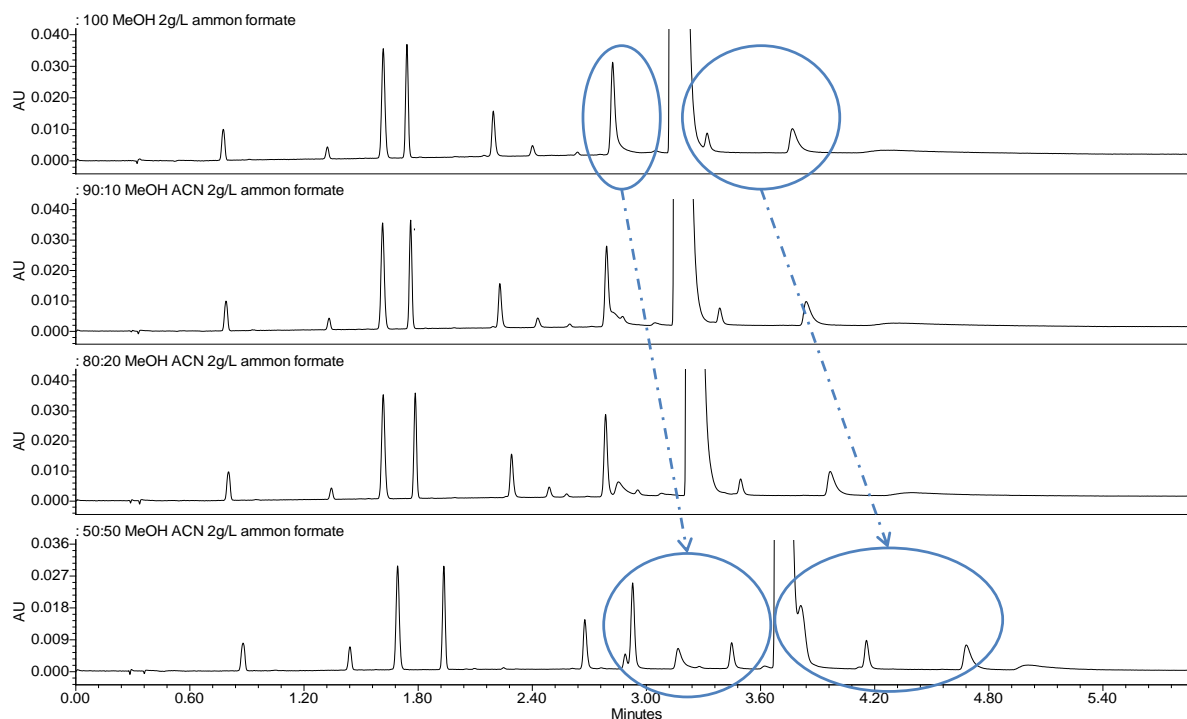


**Figure 3.13: Highlighted in this overlay, the addition of acetonitrile to the composition of the modifier increased the resolution of the later eluting analytes.**

#### 3.3.3.1.5 Effect of Additive

The effect of additives can either enhance or mask analyte interactions with the stationary phase, thus impacting peak shapes. The metoclopramide impurities have many different side group functionalities. The related impurities shown in Table 3.3 and Table 3.6, indicate amines, carboxylic acids, and hydroxyl groups. Therefore, choosing a suitable additive is challenging. Individual standards of each of the impurities were explored during the additives screening. Formic acid achieved acceptable peak shape for impurity H; however, the chromatographic performance of the other related substances; for example when

compared to Impurity F which did not improve significantly. Increasing the concentration of the formic acid yielded further improvements in peak shape for impurity H, as shown in Figure 3.14A. Unfortunately, the peak shape for impurity F was compromised, as seen in Figure 3.14B. Conversely, when 2 g/L of ammonium formate was used as the additive, the peak shape for impurity F was suitable and the peak shape for Impurity H was compromised.

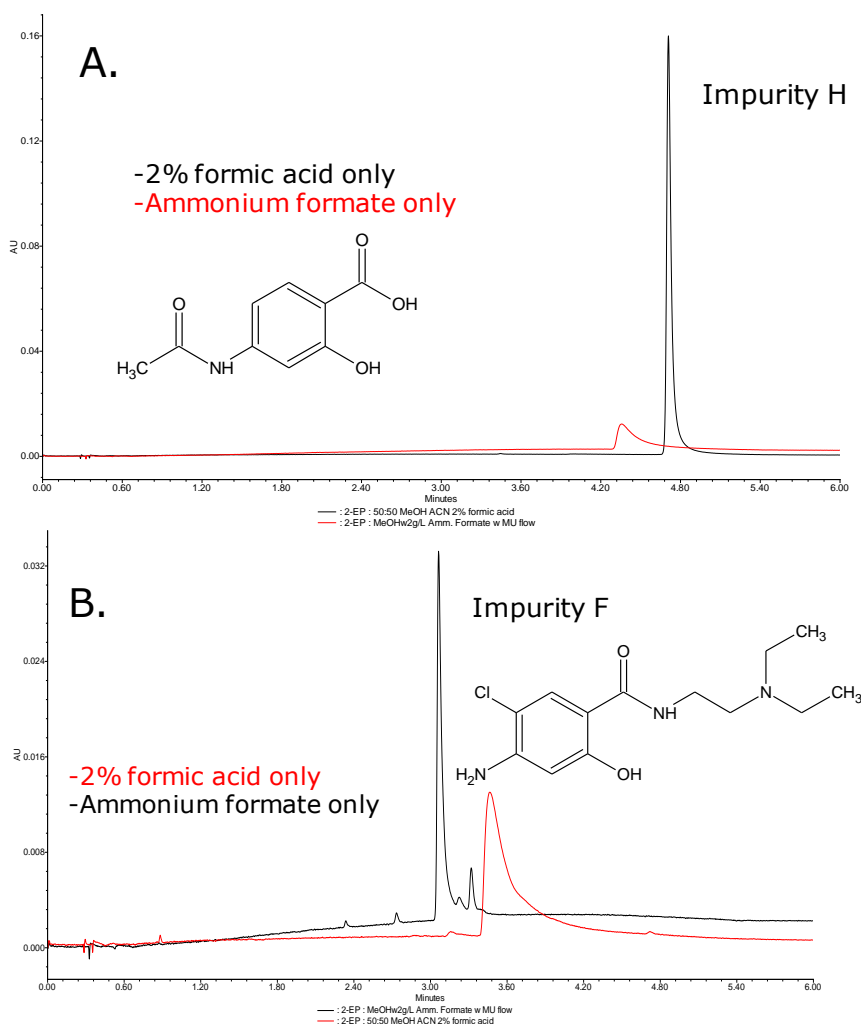


**Figure 3.14: Peaks with hydroxyl (or polyphenols) functionality such as impurity H tend to benefit from the use of only formic acid, as shown in Figure 3.14A. Optimal peak shape observed for compounds with primary, secondary, and tertiary amine functionality trend from the use of ammonium salt-based additives as with impurity F, shown in Figure 3.14B**

Combining formic acid and ammonium formate provided the benefits of each additive, resulting in optimal peak shape for the entire separation. The results of the formic acid, ammonium formate, and combination of additives in the modifier for the expired sample are shown in Figure 3.15. By using the expired sample in this comparison, it was observed that the selectivity and peak shape of the known impurities in the presence of the unknown impurities.

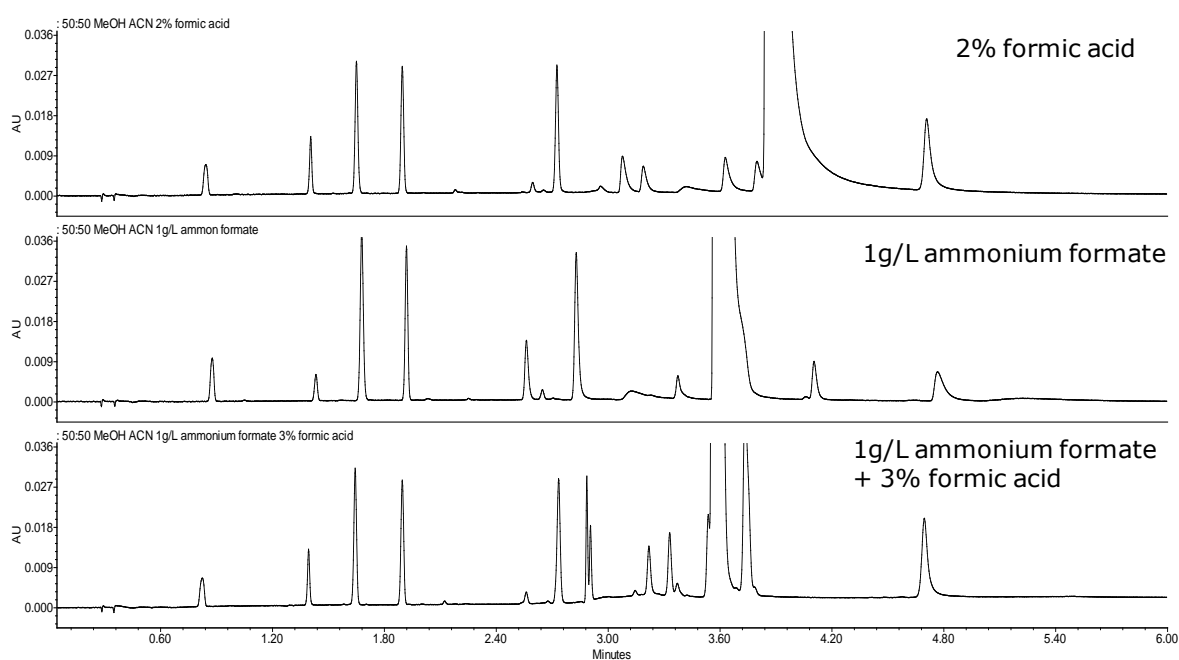


**Figure 3.15: Injections of an expired metoclopramide sample performed with different additive compositions in the modifier. Combining ammonium formate with formic acid in terms of a “buffer-like” system provided the best peak shape for all analytes in the sample. The modifier used was 50:50 methanol/acetonitrile.**

### 3.3.4 Analysis of Amphipathic Compounds

The following sections explored the effects of acyl chain length and saturation for a set of lipid single moieties which are commonly found in natural products. The experiments explored two stationary phases; the ACQUITY UPC<sup>2</sup> BEH which exploits polar retention

mechanistic behavior and the ACQUITY UPC<sup>2</sup> HSS C<sub>18</sub> SB to promote hydrophobic mechanistic behavior. The hypothesis of utilizing the polar and non-polar stationary phase was based on the premise of promoting hydrophobic retention interactions such as those observed when using RPLC, as previously reported by West[134]. For the analysis of lipids, insights could be attained for class and species separations. Both results will be compared to understand dimensionality and selectivity resulting from the distinctly different mechanisms provided by each stationary phase.

#### *3.3.4.1 Effect of Acyl Chain Length*

The PC acyl chain length Mix 2 was used for the comparison of the two stationary phases. The separation of the different chain lengths via the BEH column resulted in a retention window range of 0.2 minutes, whereas the elution order increased with decreasing length. The HSS C<sub>18</sub> SB material resulted in an increase in selectivity. A retention window of approximately four minutes for the separation of the five analytes was observed. Increasing retention is proportional to increasing chain length. Unfortunately, the peak shape obtained using the C<sub>18</sub>-based stationary phase is less desirable with increased tailing proportional to increasing chain length (Figure 3.16). The poor peak shapes are due to the increased interaction with competing polar and non-polar retention mechanisms between the stationary phase and amphipathic analyte.

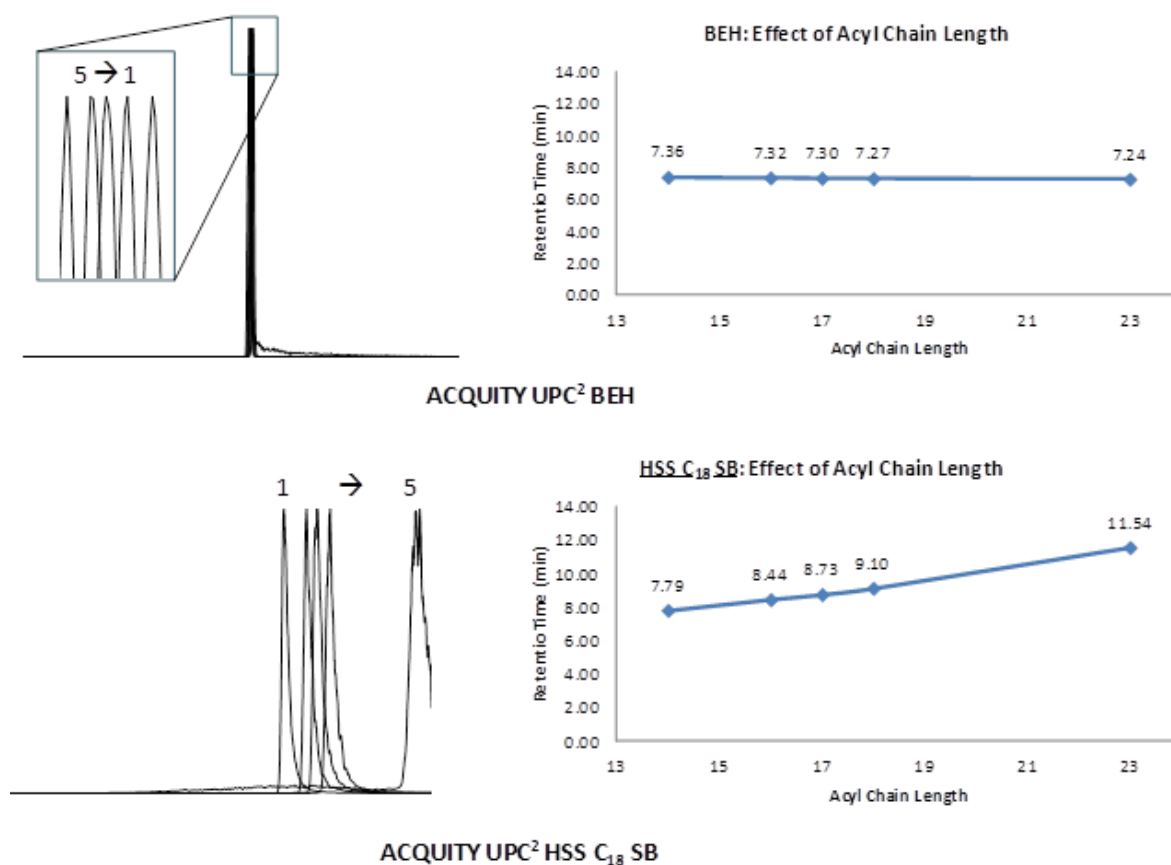


**Figure 3.16: Comparing the effect of chain length on retention between ACQUITY UPC<sup>2</sup> BEH vs. ACQUITY UPC<sup>2</sup> C<sub>18</sub> SB stationary phases.**

### 3.3.4.2 Effect of Acyl Chain Saturation

The PC acyl chain saturation mixture (Mix 3 in section 3.2.4.1) was used to explore the effect that double bonds have on retention in an effort to identify trends with retention and lipid chain length.. The BEH column continued to maintain a narrow retention window separation for the probe analytes. The elution order increases with increasing degrees of unsaturation (Figure 3.17). Retention is similar to the acyl chain length experiment such that retention decreases in respect to molecular weight. The HSS C<sub>18</sub> SB column provided increases in separation for the probe analytes with reverse elution order to that observed on the BEH column, as was also observed in the previous experiments. Again, peak shape is not as favorable on the hydrophobic C<sub>18</sub> stationary phase to that observed on the polar BEH

stationary phase, hence leading to a hypothesis of increased analyte - stationary phase interaction activity for the hydrocarbon based ligand perhaps due to an increased occurrence of hydrogen bonding between the ligand and the solute.

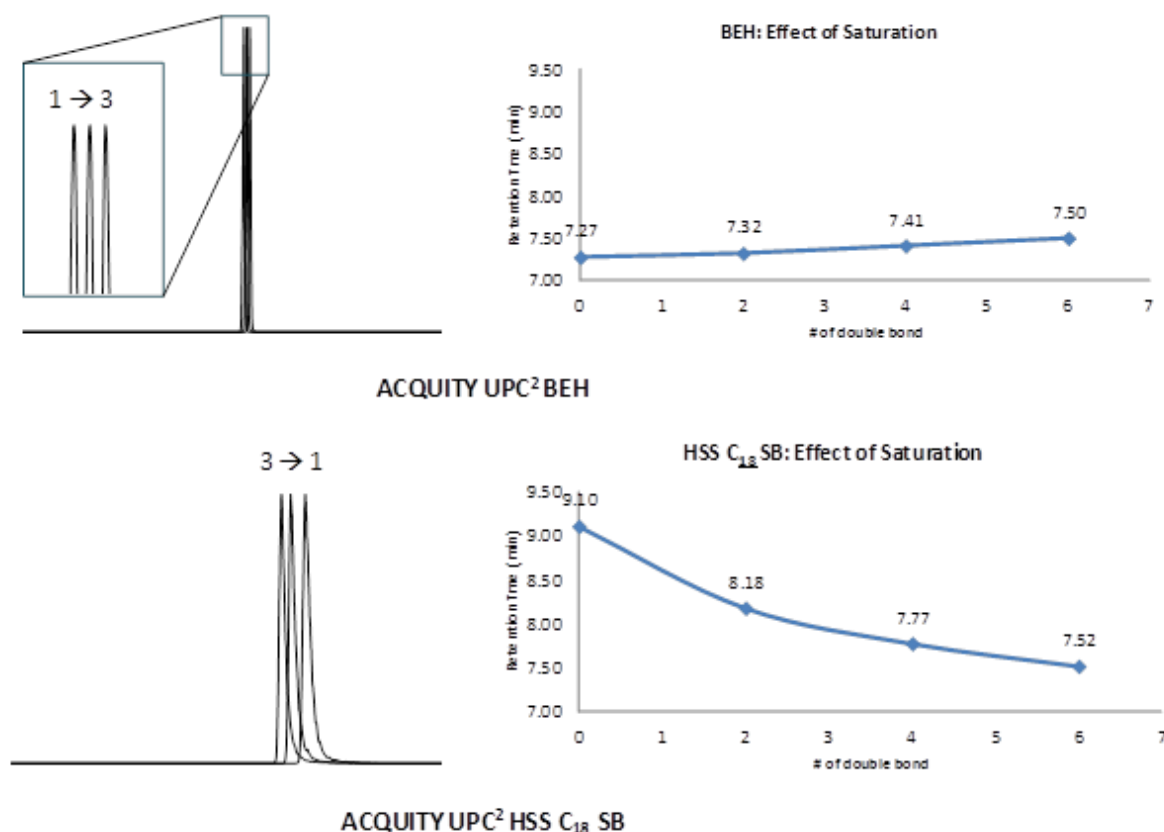


**Figure 3.17: Comparing the effect of acyl chain saturation on retention between ACQUITY UPC<sup>2</sup> BEH vs. ACQUITY UPC<sup>2</sup> C<sub>18</sub> SB stationary phases. The 18:0/18:0 data points were added from the acyl chain length experiments to illustrate agreement with each trend**

### 3.3.4.3 Isopycnic vs. Isobaric Conditions

Injections of Mix 1 (from section 3.2.4.1) were performed to explore any differences when running an isobaric experiment versus an isopycnic experiment. The automatic backpressure regulator pressure value was set isobarically to 1500 psi. The isopycnic conditions were generated using a reverse pressure gradient from 3000 psi to 1500 psi so as to match the pressure generated by the increase of %B. The overall system pressure of 5600 psi was



maintained across the pressurized system, hence constant density. The MS ESI+ single ion recording (SIR) traces of the isobaric (red) and isopycnic (black) UPC<sup>2</sup> automatic backpressure regulator settings were overlaid (Figure 3.18). For the isopycnic conditions during the solvent gradient resulted in the faster elution of the first four peaks with slightly greater peak heights, suggesting an apparent reduction in dwell volume or more efficient mixing due to the higher applied pressure and mobile phase density during the programmed gradient. However, the peak widths were observed to be in a range of 1-2 seconds wider than the isobaric conditions when integrated and measured by the chromatographic software. The isopycnic conditions during the 50% co-solvent hold resulted in identical peak shapes.

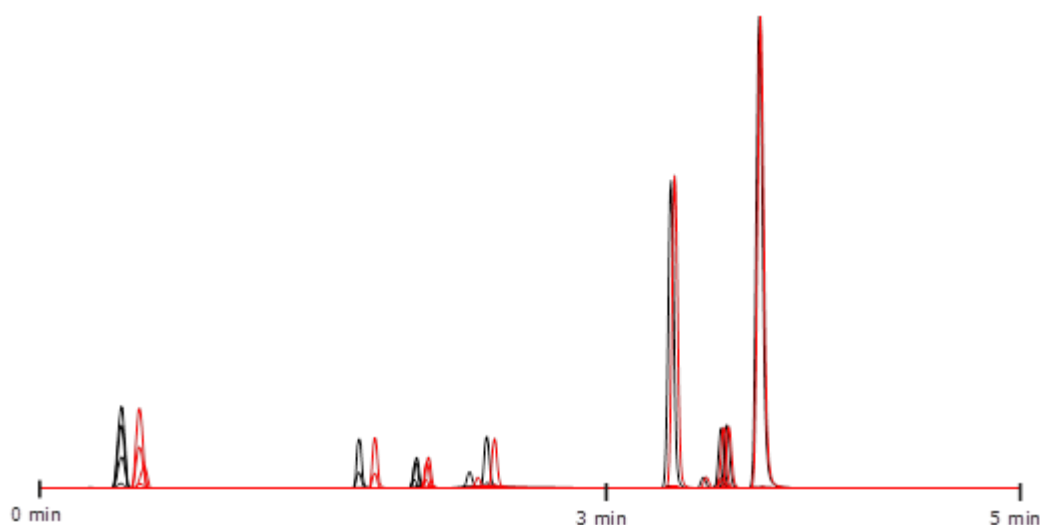


**Figure 3.18: Isopycnic results in black versus isobaric results in red. Gradient occurs during the first 3 minutes only. Increased density earlier in the gradient decreased retention for these polar analytes.**

#### 3.3.4.4 Column lifetime investigations

Retention times were observed to be shifting with shorter elution times over the course of two weeks of using the developed methodology for the class separation of lipids. The methodology that was originally developed used a modifier composition of 100% methanol with 2 g/L ammonium formate. The separation was performed on a 3.0 mm x 100 mm; 1.7

$\mu\text{m}$  UPC<sup>2</sup> BEH column held at 50 °C in the column oven. The flow rate was 2.0 mL/min programmed with a gradient elution of the modifier from 5% to 50% over 12 minutes. The backpressure regulator was maintained at 1600 psi. The phenomenon was observed on two systems and four columns over time prompting an investigation. A sampling of 200 injections of the lipid Mix 1 was performed. A new mobile phase was prepared after 100 injections. It was observed for injection #200 of the lipid mix 3, the polar lipids eluting later had decrease in retention time from 8.56 minutes for phosphatidylcholine (PC) during injection #10 to 6.59 minutes during injection #200 (Figure 3.19). Additional to the retention time shifting -28.5% as shown in Figure 3.20, the intensity of the PC peak had decreased from  $3.98\text{e}^5$  to  $1.82\text{e}^5$  resulting in a 54% decrease in sensitivity. Resolution of many peaks was also observed to decrease between injection #10 and injection #200 (Figure 3.19).

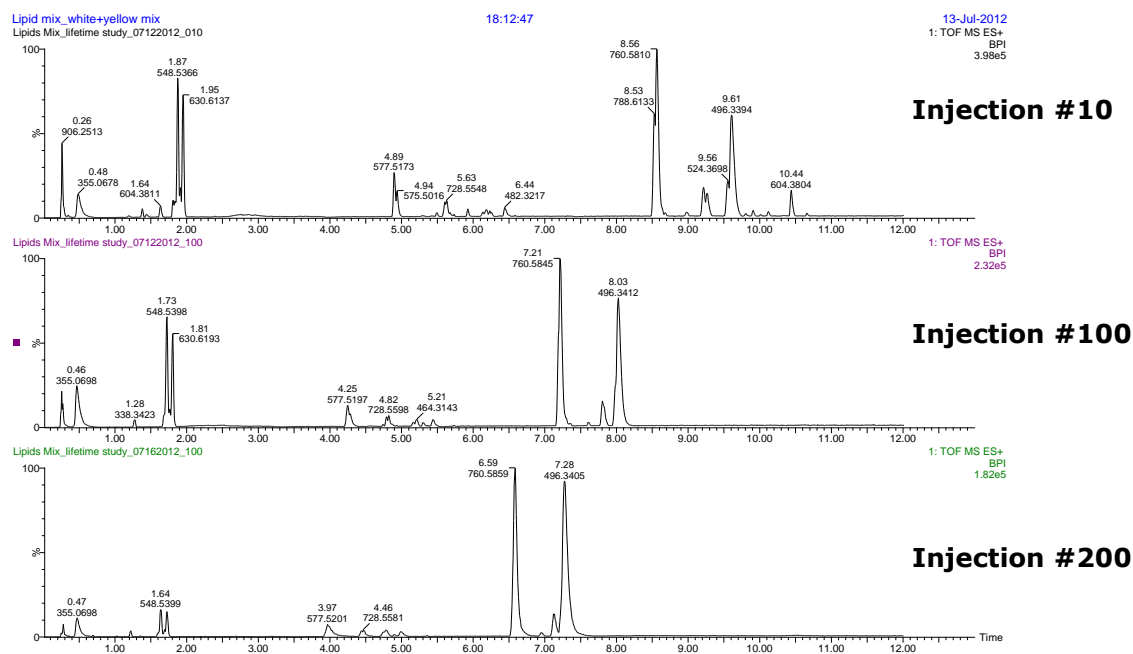


**Figure 3.19: MS ESI+ TIC of the separation of lipids Mix 1 showing the retention drifting, loss of resolution and loss of sensitivity over 200 injections.**

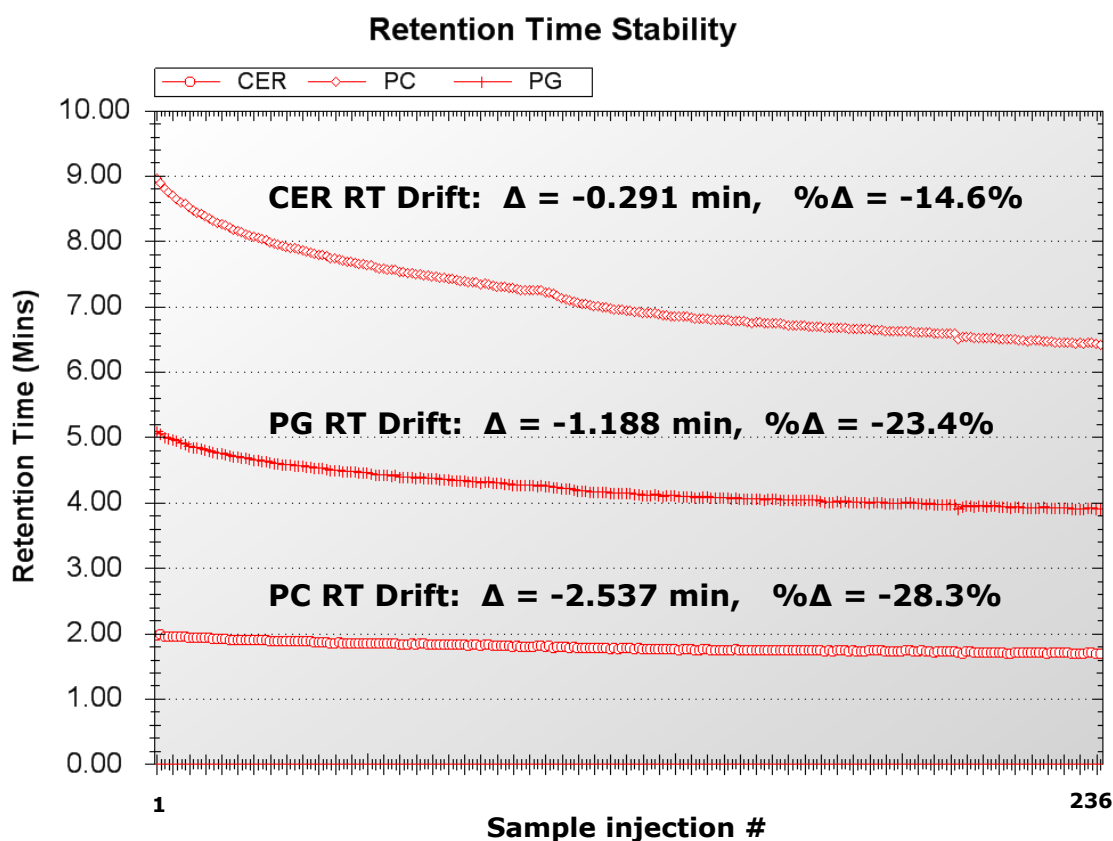


**Figure 3.20:** Trend plot for calculating the difference and percent difference between injection #1 and injection #236.

Based on these findings, communications were relayed back to the Consumables Group organization in Waters Corporation. They further researched the phenomenon and determined evidence of silyl ether formation (SEF) equilibrium reactions between the alcohols on the particle of the surface and in the mobile phase solvent [137]. Their findings stated the silanols of the column can be hydroxylated to their original state upon exposure to water. The regeneration of the column was attempted using this recommendation, however this was not achieved. Therefore, an alternative approach was used to mitigate the decaying chromatographic performance by utilizing a similar buffered mobile phase used in the method development experiments in section 3.3.3.1.5. The results of using the modifier with ammonium formate and formic acid additive stabilized the retention time shifts and

minimized any further decreases in sensitivity, except in the case when it was determined that the sample stock solutions had degraded Figure 3.21.

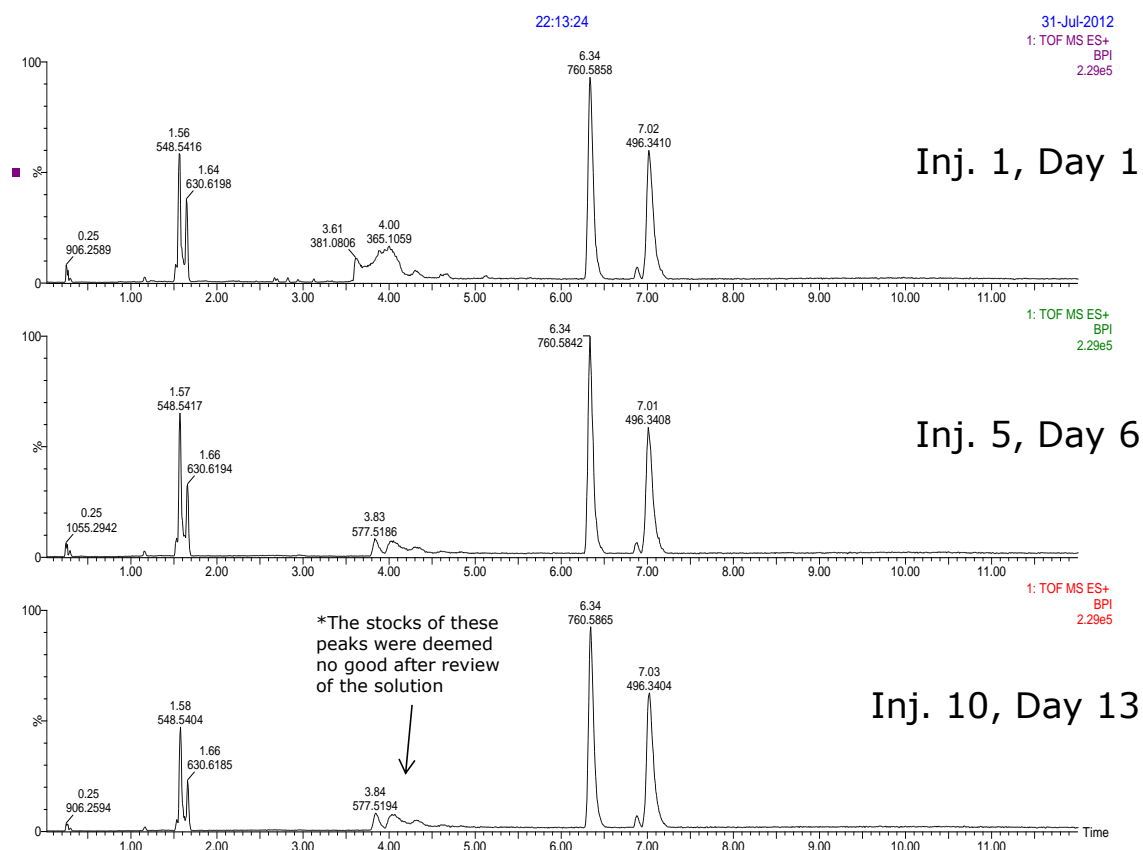


**Figure 3.21: Overlay comparison of injections performed over 13 days of injections using the mobile phase with both additives composed of 1 g/L ammonium formate and 1% formic acid**

### 3.4 Conclusions

The general objective of this chapter was to attain general observations and expectations of sample preparation techniques, mass spectrometry optimization guidelines, and varied method development variables effects on chromatographic performance when utilizing SFC. The diluent study revealed retention of typical solvents used in chemical synthetic reactions that may result as problematic interferences if determining yield of a reaction intermediate or final product.

The investigation of the effect of method development variables on peak shape and retention was correlated to some of the properties of the impurity structures. The analysis of metoclopramide provided a nice example of solute diversity due to the impurities structure functionality of amines, hydroxyl groups, esters, and carboxylic acids. The primary method variables that influenced selectivity, resolution, and peak integrity were stationary phase, modifier elution strength, and additive composition, respectively. The addition of additives resulted in better peak shapes and the addition of weaker elution solvents in the modifier aided resolution between analytes. The addition of a weak acid with its conjugate base as additives in the modifier to create ‘buffered-like’ properties to the mobile phase aid and improve the peak shape for the majority of peaks for the metaclopramide separation. The method development process uncovered multiple (stationary phase – analyte) interactions during the comparison of the column screening process. This was clearly observed with the hypothesized pi-pi interactions of the PFP stationary phase and Impurity C splitting into two peaks and with the example of 2-EP pKa properties affecting the elution order of basic solutes differing in primary, secondary, and tertiary amine functionality. Further research, in addition to and guided by those previously published need to be explored in the next chapter [54, 81, 94, 96, 128-132, 135, 138-140]. Understanding the influence of these interactions with method variables will help build an appropriate method development approach.

Lastly, the observation of the silyl ether formation (SEF) poses a problem in regards to column stability, as well as method repeatability and robustness. Although there seems to be an approach published to regenerate a deteriorated column, the results of these studies suggest using a ‘buffered-like’ modifier composition to prevent retention time shifts and decreases in sensitivity was a better alternative.

## CHAPTER 4:

---

# Cheminformatic Investigation of Physiochemical and Structural Properties Affecting Chromatographic Performance

## CHAPTER 4

### **4 Cheminformatic Investigation of Solute Physiochemical and Structural properties affecting SFC Chromatographic performance**

In the previous chapter, sample diluent, columns, and mobile phase effects were explored to determine the susceptibility to interferences and adverse effects on peak shape. Additionally, “One Factor at a Time” (OFAT) principles explored methodology parameters that manipulate selectivity, sensitivity, and resolution of the packed column supercritical fluid chromatographic results. The aim of this present chapter is to explore a diverse compound library of intermediates and final compounds and employ a multivariate approach to visualize, confirm or identify additional factors that could potentially affect SFC chromatographic results.

#### **4.1 Introduction**

Many new chemical entities can either be extracted and purified from natural product sources or synthesized based on previous characterization and understanding of the natural products structural composition.. The screening analysis of new chemical entities relies on appropriate sample preparation and method variables for analysis which do not adversely affect the chromatographic interpretation of the data. Diluent studies provided knowledge of solubility and interferences whereas if chosen inappropriately can affect the discovery of a positive ‘Hit’ for a new lead candidate. Additionally, natural product profiling experiments yield a high number of new chemical entities that are explored for drug-likeness[141-147]. Cheminformatic data interpretation tools are commonly used to distill information from large screening data sets based on physiochemical properties and their susceptibility to reacting with targeted diseases. The cheminformatic tools for chemical library management and

assessments utilize digital representations of molecules referred to as ‘languages’ for describing molecular patterns referred to as SMILES and SMARTS. SMILES (Simplified Molecular Input Line Entry System) is a line notation (a typographical method using printable characters) for entering and representing molecules and reactions. SMARTS is a language that allows you to specify substructures or describe molecular patterns using rules that are straightforward extensions of SMILES. In fact, almost all SMILES specifications are valid SMARTS targets. Using SMARTS, flexible and efficient substructure-search specifications can be made in terms that are meaningful to chemists [148]. If the cheminformatic tools can provide direction towards lead candidates, could the cheminformatic tools provide insight to chromatographic trends and behavior based on knowledge of physiochemical or structural attributes of the entire chromatographic system which involves solutes, stationary phases and mobile phases? Each of these factors, diluent choice, methodology, and data visualization and interpretation play important roles in the success of moving forward with lead candidates.

General perceptions exist within the scientific community familiar with pSFC suggest a correlation between  $\log P$  and pSFC retention of analytes. Other reports have explored physiochemical attributes to predict ‘best use’ columns for screening exercises and method development activities[55, 128, 132-135, 140, 149, 150]. Examples investigate SFC retention behavior correlations with analyte pKa, polarizability, dipole-dipole moment values, and hydrogen donor-acceptor properties. The authors de la Puente *et al.* has explored these concepts from a discovery HTS objective. West and Lessellier have explored Linear Solvation Energy Relationships (LSER) with an objective to provide method development guidance. In each instance, the authors typically investigate correlations using a list of test probes which are commonly purchased by chemical standards and reagent providers. Many



of the correlations are in regards to retention, yet equally important chromatographic attributes which are ignored in these reports are peak symmetry and peak widths.

Medicinal chemists utilize cheminformatic tools to sort through extensive compound libraries; internally and externally provided, and filter the libraries to build smaller targeted libraries aimed to explore in vitro activity towards chosen therapeutic targets [151-155]. Since medicinal chemists currently utilize these tools to manage the creation of HTS libraries based on physiochemical properties, with the addition of chromatographic results within the cheminformatic tools could allow for trends and correlations to be rapidly identified. The trends and correlations could aid in predicting chromatographic behavior and thus aid in building better screening methods. Examples of similar research in this area has been explored with an objective of developing analytical SFC/MS screening protocols [140]. The authors construct trend plots for 55 compounds versus physiochemical characteristics such as pKa, dipole moment, and electron density to help generalize column selection for SFC/MS HTS. The research described in this present chapter was designed to expand on previously reported results by incorporating structural functionality and library diversity for drugs exhibiting drug likeliness.

In this chapter, the following investigations explore the applied use sub-2  $\mu\text{m}$  particle size achiral stationary phase columns and the optimized analytical scale low volume SFC instrumentation. Post purification QC; (commonly referred to as library QC in the pharmaceutical industry), typically utilize 96, 384, or 1536 well plates of compounds dissolved in dimethyl sulfoxide (DMSO). A cheminformatic tool provided by ChemAxon will be used to investigate trends with the supercritical fluid chromatography

chromatographic peak attributes in relationship to the physiochemical and structural chemistry of the molecules using SMILES and SMARTS notations for describing molecular patterns. The study will explore a compound library and cheminformatics tools will be explored to visualize physiochemical and structural functionality parameters based on SMILES/SMART notations and modeled against retention times, peak width and USP peak tailing values. The objectives of these following experiments were to investigate a diverse, yet drug-likeness set of compounds as defined by Lipinski's 'Rule of Five' that would similarly exist within pharmaceutical company compound libraries. The acquired compounds theoretically exist as building blocks or scaffolds that can be used as intermediates for further targeted HTS screening and catalysis studies thus creating additional new molecular entities. For large dataset screening, it is prudent to routinely test for system performance or system suitability. A system suitability test can defend the validity of system performance influence, positively or negatively, with the conclusions of the investigation. Therefore, an appropriate system suitability test mix and procedure had to be developed to support the investigative observations of the compound library plate. The objective of this preliminary experimental plan was to record the chromatographic attributes for each of the analytes as they are analyzed on different columns using a generic screening method. Once the chromatographic attributes were entered into the cheminformatic software, general observations and trends were explored when plotting chromatographic attributes versus physiochemical or structural functionality of the analyte.

## 4.2 Experimental

### 4.2.1 Cheminformatics Experimental

A chemical library was purchased (ChemBridge, San Diego, USA). Physiochemical parameters were predicted values calculated within the cheminformatic software based on structure. SMILES notations were used to calculate the quantity of structural functional groups such as ketones, aldehydes, primary amines, secondary amines, tertiary amines, halogens, conjugated oxygen containing groups, carboxylic acids, phenols, and enols. . The selected compounds were also filtered based on Lipinski's 'Rule of Five' which evaluates the drug likeness of a chemical compound with a certain pharmacological or biological activity described with physiochemical properties that would make it a likely orally active drug in humans[156]. The dataset filters include compounds with a water-octanol partition coefficient ( $\log P$ ) less than 5, no more than 5 hydrogen bond donors, no more than 10 hydrogen bond acceptors, and a molecular mass less than 500 Da. Cheminformatic modeling was performed using Instant JChem and JChem for Office. (ChemAxon, Budapest, Hungary).

### 4.2.2 Cheminformatic System Suitability Test Mixture

A QC test solution was used to determine system performance during the course of the extensive compound screening. The test solution consisted of a mixture of analytes (Table 4.1) designed to elute over a gradient of 0% to 50% modifier composed of 100% methanol or methanol with additives to improve peak shape.

**Table 4.1 Compounds and concentrations for the system suitability test mixture performed during the cheminformatic correlations experiments**

Compound	Molecular Weight (Da)	Formula	Concentration (mg/mL in MeOH)
benzophenone	182.2179	C <sub>13</sub> H <sub>10</sub> O	0.1
glybenclamide	494.0035	C <sub>23</sub> H <sub>28</sub> ClN <sub>3</sub> O <sub>5</sub> S	0.25
4-hydroxybenzaldehyde	122.1210	C <sub>7</sub> H <sub>6</sub> O <sub>2</sub>	0.25
carbamazepine	236.2686	C <sub>15</sub> H <sub>12</sub> N <sub>2</sub> O	0.25
sulfanilamide	172.2049	C <sub>6</sub> H <sub>8</sub> N <sub>2</sub> O <sub>2</sub> S	0.25
procaine	236.3101	C <sub>13</sub> H <sub>20</sub> N <sub>2</sub> O <sub>2</sub>	0.25
protryptiline	263.3767	C <sub>19</sub> H <sub>21</sub> N	0.25
metoclopramide	299.7964	C <sub>14</sub> H <sub>22</sub> ClN <sub>3</sub> O <sub>2</sub>	0.25

### 4.2.3 Instrumentation Parameters for the Cheminformatic Study

The system suitability separations were initially performed using various columns outlined in Table 4.2 on an ACQUITY UPC<sup>2</sup> system configured with PDA detection (Waters® Corporation, MA, USA). The column was maintained at 45 °C. Gradient elution was performed using a linear addition of the modifier from 5% to 50% over 5 minutes. The backpressure was maintained at 2000 psi. The injection volume was 2.0 µL while the samples were maintained at 18 °C in the autosampler. Detection was monitoring at a single wavelength 254 nm and a wavelength range from 210 nm to 500 nm.

**Table 4.2 Columns and dimensions explored for system suitability study**

Stationary Phase	Dimesions
ACQUITY UPC <sup>2</sup> CSH Fluoro-phenyl,	3.0 x 50 mm; 1.7 $\mu$ m
ACQUITY UPC <sup>2</sup> BEH,	3.0 x 50 mm; 1.7 $\mu$ m
ACQUITY UPC <sup>2</sup> BEH 2-Ethylpyridine,	3.0 x 50 mm; 1.7 $\mu$ m
ACQUITY UPC <sup>2</sup> HSS C18 SB, , <i>*This column showed no retention so it was eventually excluded from the study.</i>	3.0 x 50 mm; 1.8 $\mu$ m

The final separations were performed using a 3.0 mm x 50 mm ACQUITY UPC<sup>2</sup> 1.7  $\mu$ m BEH 2-EP column using an ACQUITY Ultra Performance Convergence Chromatography (UPC<sup>2</sup>) System (Waters<sup>®</sup> Corporation, MA, USA). Gradient elution was performed using a linear addition of the modifier from 5% to 50% over 15 minutes. The modifier composition was 15 mM ammonium formate dissolved in 100% methanol and spiked with 10 mL of formic acid. The achiral columns were maintained at 50 °C. The backpressure regulator was maintained at 1800 psi. The system injected 1.0  $\mu$ L of sample. The post column make-up flow prior to the entry into the MS composed of 0.1% ammonia in methanol flowing at 0.4 mL/minute. The mass spectrometer was an ACQUITY SQD2 (Waters<sup>®</sup> Corporation, MA, USA). The experiment was performed using positive ESI mode. The cone voltage was set to 25 V and a capillary voltage set to 3.0 kV

## 4.3 Results

### 4.3.1 Development of the chemometric analysis system performance test

A variety of acids, bases and neutral compounds were screened and evaluated using a generic UPC<sup>2</sup> method. The method conditions used a 5% to 50% modifier gradient elution profile flowing at 2.0 mL/minute over 6 minutes. The temperature was maintained at 45°C with a backpressure setting of 1800 psi. The method profile allowed for an assessment of analyte elution diversity. The analytes were also chosen in terms of peak shape. A selection of test probes with Gaussian peak shapes and tailing peak shapes were chosen. Tailing analytes were selected as part of the final test mix to determine if any silanol interaction activity changes within the column over time. The resulting system suitability test mix is listed in

Table 4.1.

The system suitability test mix was injected and screened on the four different achiral UPC<sup>2</sup> columns listed in Table 4.2. Methanol was screened initially, but the chromatograms resulted in severely tailing peaks and peak splitting. Retention time shifts were also observed over time for the later eluting peaks on all four columns. Examples are shown for the BEH results in Figure 4.1 whereas the worst peak distortions were observed for protryptiline, procaine, and metoclopramide eluting respectively and retention times were confirmed by mass upon review of the MS spectra. The elution order for protryptiline and procaine swapped for the BEH 2-EP column; however the peak shapes were less abnormally distorted. The polar analytes did result in severe tailing on the BEH 2-EP column shown in Figure 4.2. System pressure was observed to increase on each column over time from 5171 psi to 5946 psi over 9 hours of injections, whereas Figure 4.3 shows the pressure increase for the BEH 2-EP

column. This can be observed when SEF is occurring on-column. It is unclear what is causing the peak shape distortion and retention time shifts on the BEH column, but it is hypothesized that the column chemistries are altering over time effecting the active silanol sites and possible the properties of the ligand. The basic properties of the BEH 2-EP column could be contributed to improved Gaussian peak shapes for the polar, yet basic analytes protryptiline, procaine, and metoclopramide. It was observed that the polar analytes shifted while the more neutral analytes eluted with a consistent retention over the 16 hours. Another hypothesis would suggest solubility issues with the analytes and thus causing precipitation on the head of the column, thus creating changes in the mobile phase density. Additionally to that hypothesis, suspicion of the operating conditions within the sub-optimal conditions outlined in the Tarafder and Poe publications due to the similarity of the peak anomalies reported [68-74, 80, 92]. The later hypothesis is not as suspect due to the high composition of modifier in the gradient profile where the problematic peaks are eluting. Solute precipitation is moderately suspected as the issue. However, when solutes crash out due to the mobile phase upon injection and onto the inlet of the column filter frit, the system pressure would return to normal when the filter frit is replaced. The return to initial pressures did not occur when the filter frit was replaced. Although the replacement of the column frit could alleviate pressure issues that may be caused by precipitation building at the head of the column, the frit replacement does not exclude the possibility of precipitation within the column bed.

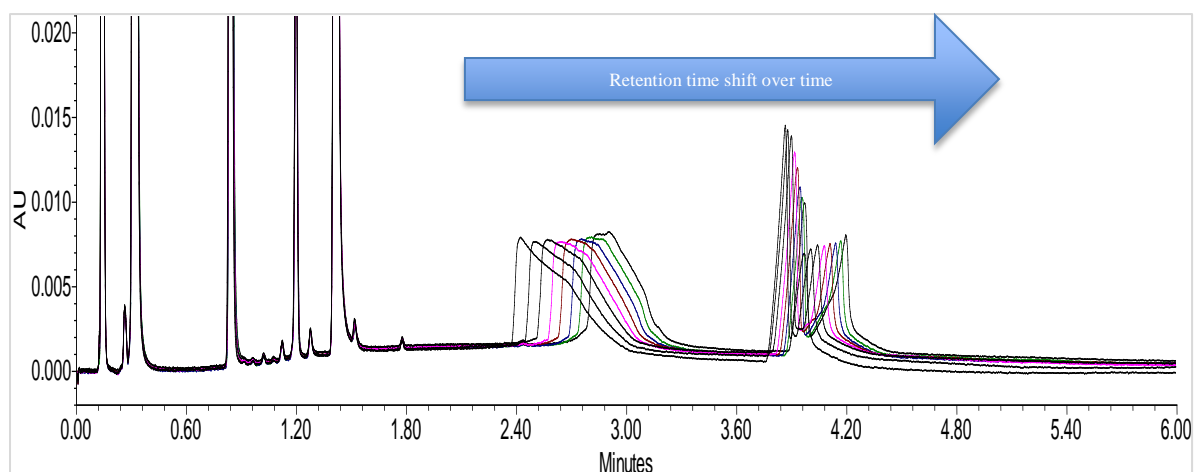


**Figure 4.1:** Replicate injections of the system suitability test mix performed using the UPC<sup>2</sup> BEH column.

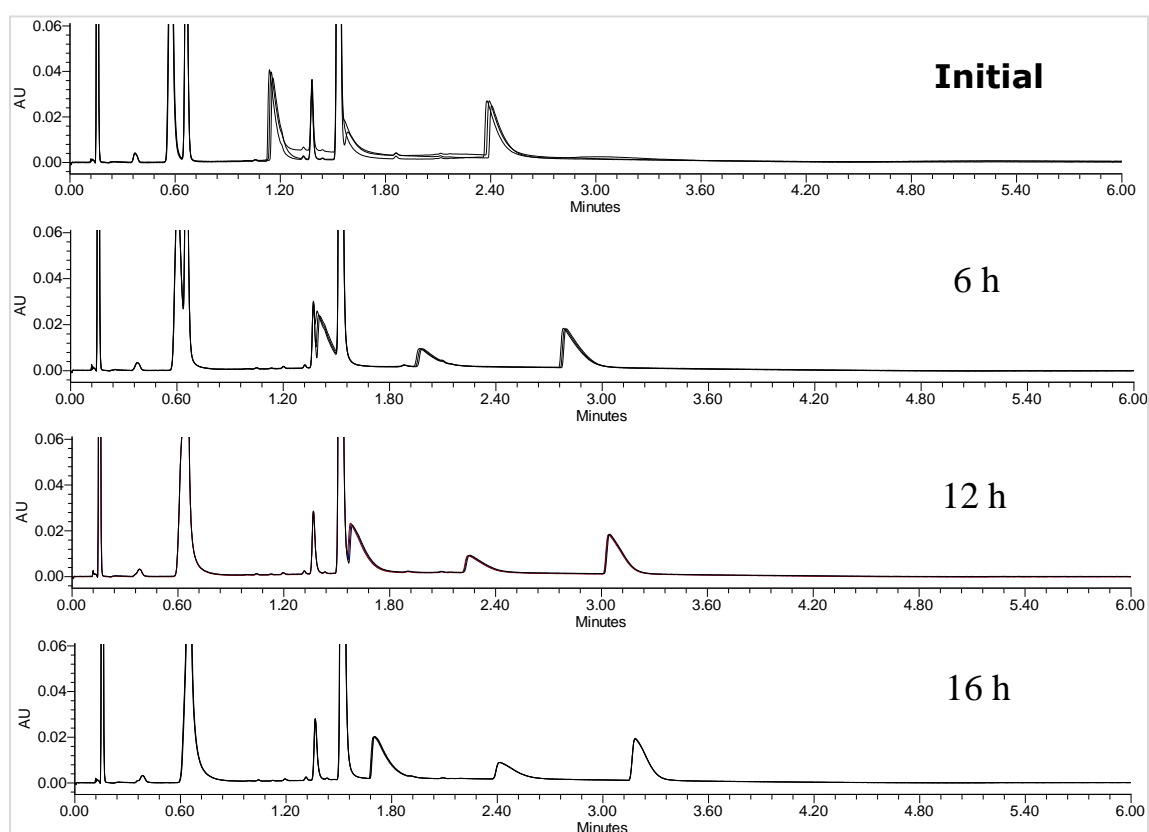


**Figure 4.2:** Overlay of the system suitability test mix injected over 16 hours on the UPC<sup>2</sup> BEH 2-EP column.



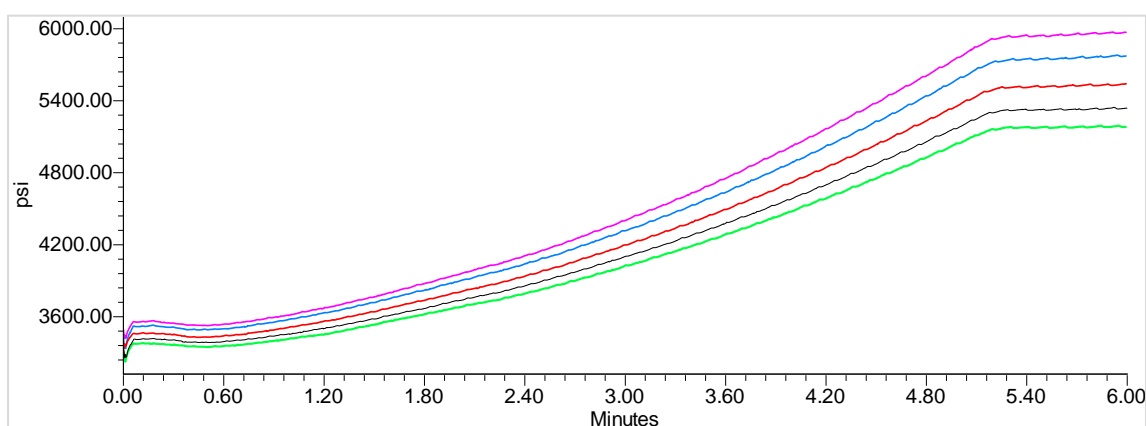


**Figure 4.3: UPC<sup>2</sup> system pressure increase plotted for the system suitability test mix injections on the UPC<sup>2</sup> BEH 2-EP column**

Due to the problematic issues occurring with chromatographic peak shape and retention time, the modifier was changed from 100% methanol to 100% methanol spiked with 10 mM ammonium formate and 1% formic acid based on the previous method development experimentation performed and discussed in Chapter 3. The peak shape and retention time shifts previously observed with the system suitability test mix dramatically improved for all columns. The final methodology for the system suitability test mix was chosen with UPC<sup>2</sup> BEH 2-EP results shown in Figure 4.4. The UPC<sup>2</sup> BEH results were excellent in terms of peak shape and reproducibility; however the separation lacked any critically resolved pairs to be used as a diagnostic. Additionally, the last eluting peak retained in a range of 45-48% of the gradient elution profile. The UPC<sup>2</sup> 2-EP has two critical pairs of tightly resolved peaks and less retention for the last eluting polar metoclopramide peak. The resolution of the first critical pair of peaks; 4-hydroxybenzaldehyde and carbamazepine, decrease with increasing column injections, while the resolution increased for the second critical pair of glybenclamide and sulfanilamide. It is believed this is due to column equilibration steady state issues that were observed for the lipids reproducibility experiments discussed in Chapter 3. Column

equilibration readiness may impact critical pair separations positively or negatively in terms of resolution based on the properties of the analytes shifting in retention time. For this particular system suitability mixture, it was believed to be advantageous to have two sets of critical pairs of analytes showing increases and decreases in resolution, thus utilizing any changes in observed resolution due to slight issues with column or system equilibration. These two criteria allow for quick determinations of system or column performance issues and allows for unpredicted late eluting retention of highly polar compounds that may exist in the screening plate.

It has been previously shown that the high  $pK_a$  properties of a BEH 2-ethylpyridine column provides the best peak shape for the analysis of alkaline pharmaceutical compounds [157]. For this cheminformatic investigation, utilizing the 2-EP column; in combination with a modifier with additives, is a suitable choice for controlling unexpected influences affecting peak shape during the preliminary screening experiments with the compound library. The basic properties of the column and the buffering-like capabilities of the additive based modifier typically yields Gaussian peak shapes for basic, acidic, and neutral analytes. Therefore, it is hypothesized utilizing this particular column and modifier combination will mitigate complications in questionable data inputs into the cheminformatic software assisting with the trending analysis, thus simplifying the data analysis.

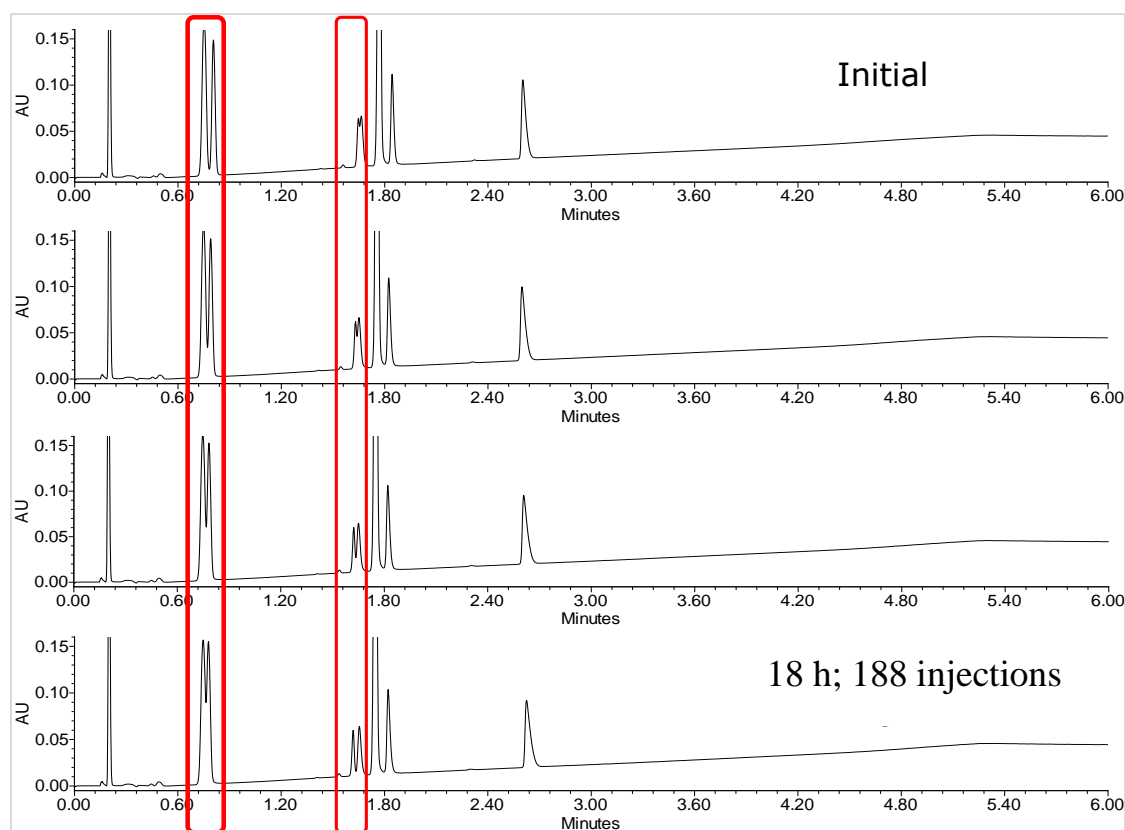


**Figure 4.4: System suitability test mix results performed using the UPC<sup>2</sup> 2-EP column and ammonium formate/formic acid methanol modifier conditions.**

### 4.3.2 Design of Physiochemical and Structural Correlations

SMARTS notations were used to create the compound structural descriptors and the physiochemical descriptors and calculated for each compound in the cheminformatic software. SMARTS notations were either created or downloaded as templates from the internet [158] in order to calculate the number of functional groups per compound such as aldehydes, carboxylic acids, enols, however, the compounds procured by the vendor and tested were found not have some of these structural attributes. The compounds in this library sample plate were found to have a variety of ketone, esters, ethers, halides and hydroxylated functionality described in Table 4.3. The calculated values were tabulated in a single table with the physiochemical descriptors and chromatographic results. Each of the various types

of descriptors (y) was plotted against the chromatographic results (x) for each compound. Additional plots were created to visualize third and fourth dimensional descriptors to identify additional trends. When added, the third and fourth dimensional descriptors are represented by color and size of the data point in the plots.

**Table 4.3: Table of descriptors using for the cheminformatic multivariate trend investigations**

Chromatographic Result Descriptors	Functional group using SMART pattern descriptors	Physiochemical descriptors
Stationary phase	-COOH	clogP
Tailing	# of -OH	log
Retention time	-OH due only from carboxylic acids	logS <sub>w</sub>
Peak doublet or splitting	-OH from phenol groups	H bond accepters
Peak width	# of Primary amines	H bond donors
	# of Secondary amines	Rotational bonds
<b>Other Descriptor labels</b>	# of Tertiary amines	tPSA
Molecular formula	aldehydes	
Molecular weight	Ketones, esters, ethers	
stereochemistry	halides	
	Intramolecular h-bonding	

### 4.3.3 Results of Chromatographic, Physiochemical and Structural Correlations

Using the same method developed for the system performance test, 300 compounds purchased from ChemBridge Inc. were injected. Retention times and tailing factors were recorded and plotted in the cheminformatic software. Descriptors for each of the analytes were generated by the ChemAxon software once the ChemBridge SDF file of compounds

was imported. It was clear after the first set of experiments and data entry, the method needed to be extended to 10 minutes to allow for more discrimination in retention times between the analytes when performing the cheminformatic correlations.

Trends were not observed when plotting the physiochemical descriptor values [such as rotational bonds (RB), hydrogen bond acceptors (Hacc) and donors (Hdon), topical polarizable surface area (tPSA), logarithm of the distribution coefficient ( $\log D$ ), and molecular weight] against the retention time or peak tailing chromatographic results attained on the UPC<sup>2</sup> 2-EP column. Similarly, correlations were not observed for functional group descriptors when plotting the number of primary amines, secondary amines, and tertiary amines against the retention time or peak tailing chromatographic results attained on the UPC<sup>2</sup> 2-EP column. Interestingly, the most notable correlation expectation is retention time in relationship to  $\text{clog}P$  of the analyte, yet Figure 4.5 shows no observable correlation between  $\text{clog}P$  and retention time. With the close relationship to  $\text{clog}P$ , the log solubility of water (LogSw) was plotted versus retention time (Figure 4.6). No trend was observed, yet the data point size was included to represent the tailing factor of the peak and a slight relationship or trend can be identified with this peak shape attribute. The larger the data point, the greater the tailing value.

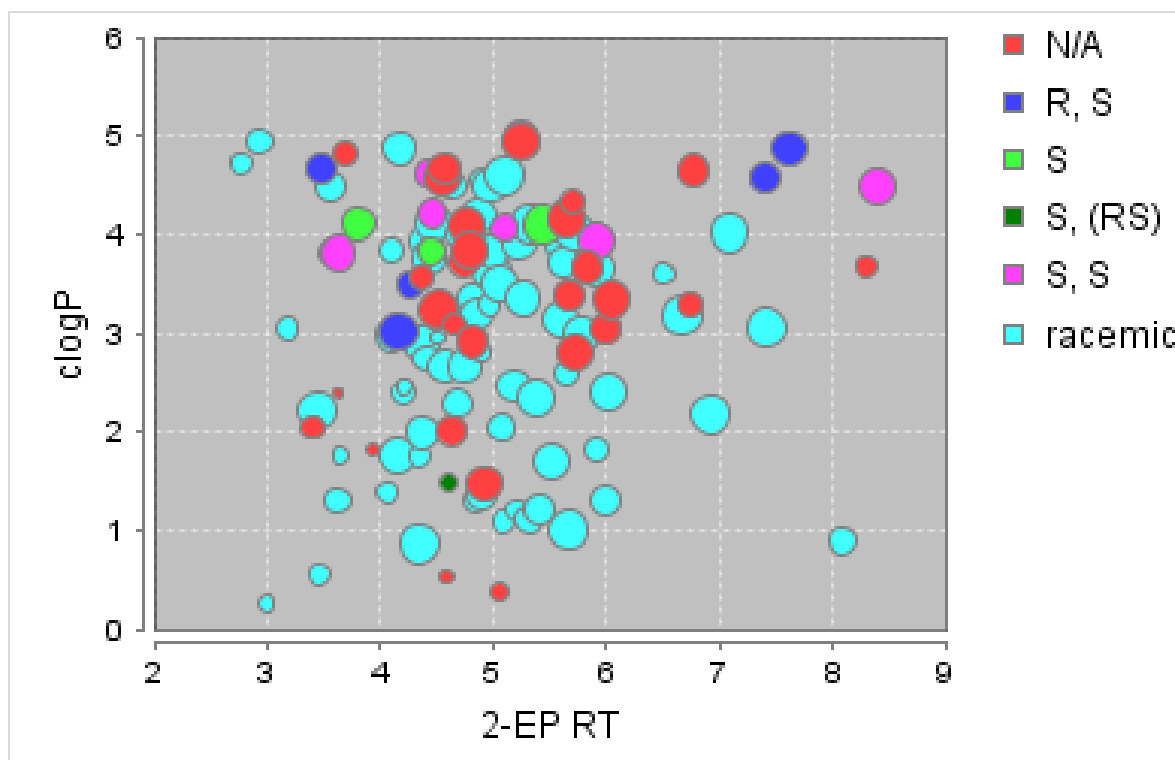


**Figure 4.5:** cLogP versus BEH 2-EP retention time results for the 300 compounds where the colors are represented by stereochemistry and the size of the point is represented by molecular weight

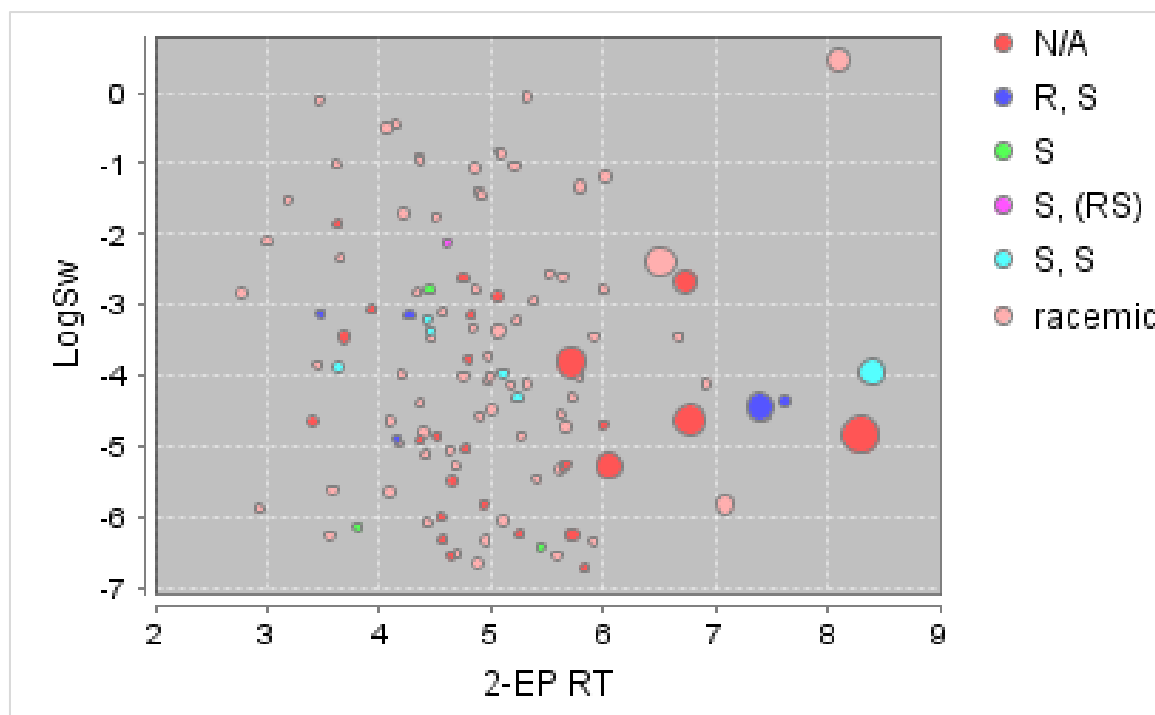


**Figure 4.6: LogSw versus BEH 2-EP retention time results for the 300 compounds where the colors are represented by stereochemistry and the size of the point is represented by the BEH 2-EP tailing factor results.**

As stated, trends rather than conclusive correlations were observed in some instances. Based on the discovery of a relationship to tailing and LogSw, a plot of  $\text{clog}P$  versus BEH 2-EP tailing showed a relationship with  $\text{clog}P$  values greater than three (Figure 4.7). Out of 300 compounds, 69 had a  $\text{clog}P$  value greater than 3.0. About 23% of those compounds had tailing factors greater than 1.5. The majority of compounds with a tailing factor of 3.0 or greater contained an ether group, hydroxyl group or both. In 50% of those instances, the compound also had a pyrrolidine-based ring structure in the molecular scaffold. Due to the results experienced with the system suitability test mix where the later eluting peaks were observed to have greater tailing factors, BEH 2-EP tailing results were plotted versus BEH 2-EP retention times (Figure 4.8). Although there seems to be a tailing factor and  $\text{clog}P$  correlation, there also seems to be a correlation between later eluting peaks and tailing

factors. Yet, there was no conclusive evidence between retention time and  $\text{clog}P$ . The tailing versus retention time plots could be an indication of a poorly performing system at high modifier compositions of the gradient. If so, the system suitability test mix did not indicate this to be an issue. Additionally, system level diagnostic tests provided by the UPC<sup>2</sup> software diagnostic tools indicated the system was working properly. The assumption is that neither the system suitability mix nor the diagnostic level testing can identify the issue with enough accuracy. Newer tools will have to be developed that will indicate issues, whether column related or system related, that are acute to higher organic modifier compositions in the overall mobile phase.

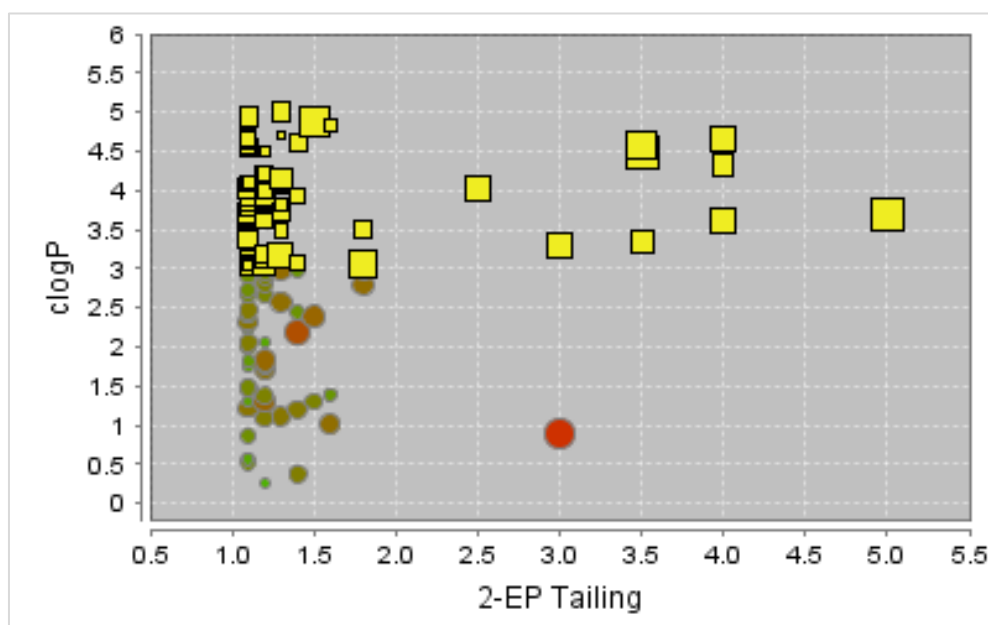


**Figure 4.7:  $\text{cLog}P$  versus BEH 2-EP tailing results for the 300 compounds where the highlighted yellow colors are represented by  $\text{clog}P$  values  $> 3.0$ . The greater the size of the data point was represented by greater retention.**



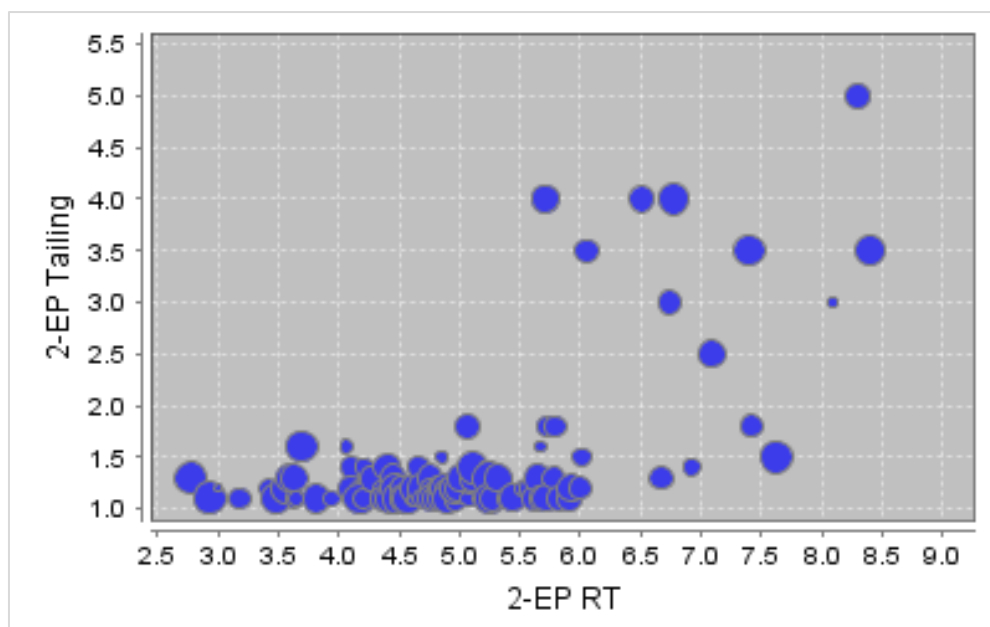


**Figure 4.8:** 2-EP tailing results versus BEH 2-EP retention times for the 300 compounds where the increasing size of the data point refers to increasing  $\log P$  values.

#### 4.4 Conclusions

The results from this cheminformatic study highlight the importance of having a system suitability test with test probes capable of identifying subtle changes in chromatographic separations resulting from the system to reach steady state equilibrium. The system suitability test mix is suitable to determine slight changes in column performance for the UPC<sup>2</sup> 2-EP column. It looks to be suitable for the UPC<sup>2</sup> BEH column, but for different purposes that might be suitable for method development or training activities. The development of the test mix allowed for proper decisions when moving forward with a method for the cheminformatic study of correlating chromatography associated with analyte properties. The cheminformatic analysis revealed little to no correlations or trends between many of the physiochemical or structural attributes of an analyte to that of the retention of that analyte by supercritical fluid chromatography. Interestingly, there seems to be some

trends related to tailing factors. In future investigations, it is recommended to design experiments with  $n \geq 10$  constituents with each of the structural attributes, specifically focused on ethers, hydroxyls, ketones, and pyrrolidine structural functionality. Expanding the investigation to newer column technologies would also be recommended as future work.

#### **4.5 Acknowledgements**

I would like to thank and acknowledge Aurora Costache and Douglas Drake from ChemAxon for their assistance and direction using the ChemAxon Instant JChem product which was required to perform the cheminformatics analysis.

## CHAPTER 5:

---

Applied to Pharmaceutical Drug

Substance Reaction Synthesis

Monitoring

## CHAPTER 5

### 5 UPC<sup>2</sup>/MS Applied to Pharmaceutical Drug Substance Reaction

#### Synthesis Monitoring

The aim of Chapters 3 and Chapter 4 focused on providing insight to scoping experimental planning and chromatographic expectations when utilizing sub-2 $\mu$ m particle columns on the optimized pSFC instrumentation technologies. The scope highlighted considerations pertaining to the sample preparation considerations, methodology, interfacing with destruction detection devices and diagnostic system performance approaches. These applications are focused on the typical procedures and workflows practiced in the lead optimization and process development groups employed in the pharmaceutical or chemical material industry. The application investigates the reaction synthesis monitoring of three small molecules chosen either for their unique stereochemical properties and relationship to derived natural product entities. The reasoning for this investigation was due in part of proving the sustainability of the technique and novel technology design improvements for use by the industry in terms of post discovery of a new chemical entity. The examples in this chapter show the benefit of a high efficiency separation using the SFC approach when compared to UHPLC, the effectiveness to determine recovery values, the ability to troubleshoot synthetic route issues, and an approach to streamline chiral and achiral screening on a single chromatographic system. One of the highlights demonstrates the optimized SFC instrument as a tool for a column agnostic screening approach to aid process optimization of a synthetic reaction during the clopidogrel experiments.

## 5.1 Introduction

Implementing a novel technology into the everyday workflow of a pharmaceutical environment must be cautiously thought through, especially when it involves the fast paced discovery laboratory. Instrument requirements include robustness, ease of use, and throughput and are assessed through a comprehensive evaluation in order to determine the usefulness and ‘fit for purpose’ implementation [159]. A comprehensive investigation should explore the different facets of the medicinal chemistry workflow, from single sample reaction monitoring submission, purification, HTS library QC, and reaction optimization [160, 161]. The synthesis of the natural product derived drugs begins with basic molecular scaffolds which can be attained or synthesized. For example, the scaffolds are typically coupled with additional molecular functionality to create small molecule building blocks which are analyzed and recovered by liquid chromatography coupled to mass spectrometry [162]. Understanding the route synthesis of drug candidates facilitates the expedition of optimizing reaction rates, product yield, product purity, and thus the overall synthetic process as lead compounds progresses from discovery, through to early development.

Multiple “walk-up” systems typically analyze greater than 40,000 samples per month in an analytical high throughput pharmaceutical discovery laboratory [163]. Utilizing these walk-up LC/MS systems, chemists routinely and rapidly obtain molecular weight information of their samples, monitor reaction progress, purify target analytes, and evaluate the purity of resulting intermediates and products. The simple workflow enables a chemist to login to the computer system, assign an identification code to the sample, and select from a menu the type of LC/MS experiments to be performed. The automated sample analyses can be performed rapidly using short LC columns and fast gradients, typically with runs of 5 minutes or less. The evolution of walk-up LC/MS environments has occurred industry wide in recent years.

In fact, dedicated open-access software packages are now available from most instrument manufacturers [164-166].

Chromatography instrument configurations include variations with analytical scale and chromatographic separation technique, such as walk-up purification and supercritical fluid chromatography, respectively. Packed column supercritical fluid chromatography (pSFC) has proven usefulness within discovery research by providing orthogonal techniques to those commonly practiced, such as thin layer chromatography (TLC) and reversed-phase liquid chromatography (RPLC) [140, 167-174]. Purification scale pSFC provide the ability to purify achiral and chiral compounds with fractions that require less dry down time than the commonly used purification scale liquid chromatographs[175]. Yet, the challenges with supercritical fluid chromatography reside with the lack of robust supporting analytical scale instrumentation, efficient screening workflows, and analyte solubility challenges particularly with scale-up purification applications [140]. Additionally, the poor performance of analytical scale pSFC supporting technologies traditionally contributed to the pitfalls of wider adoption and use of pSFC for purification.

In this chapter, the following investigations explore the applied use of newer technologies composed of achiral and chiral sub-2 $\mu$ m particle size stationary phase columns, optimized analytical scale low volume SFC instrumentation, and a novel ‘zero user interfacing’ compact single quadrupole mass detector for a walk-up high throughput screening environment. This optimized pSFC instrumentation is analogous in design and use to that of ultrahigh-performance LC (UHPLC) with extra-column volumes measuring approximately 30 $\mu$ L and system volumes measuring less than 400  $\mu$ L. Pharmaceutical syntheses were performed for

imatinib, rosuvastatin, and clopidogrel. The reactions for each synthesis were monitored, and scaled up as part of the process of investigating this technology in a ‘real world’ synthetic environment. Purification was performed for various stages of the pharmaceutical API synthesis experiments, however the purification overviews will be excluded from this chapter to maintain focus on the analytical evaluations of the sub-2  $\mu\text{m}$  particle stationary phases and low bandspread analytical supercritical fluid chromatography system. It is hypothesized that liquid chromatography might be required as an appropriate path and vice versa, therefore comparisons to reversed-phase LC will highlight these specific instances.

Chiral analysis is an important part of drug discovery and natural product research [176-183]. It would be difficult to ignore the implications that a low-bandspread pSFC instrument would have on the chiral analysis activities which are typically columns with particle sizes greater than or equal to 2.5  $\mu\text{m}$ . Although the focus of this thesis is achiral, chiral chromatography will be performed and evaluated. The diversity each case study provides a suitable example for investigating the applicability, benefits and challenges of implementing packed column SFC/MS, and the newly developed chiral column technologies. The combined results are aimed to provide a comprehensive assessment of overall feasibility, robustness, and flexibility currently questioned by the pharmaceutical discovery and development organizations. Hypothetically, the investigations discussed in these studies should build scientific confidence in the approach, define guidelines for use, and add to the existing knowledgebase about packed column supercritical fluid chromatography use in the public forum.

## 5.2 Experimental

The compounds were chosen based on them meeting a combination of the following criteria:

- Relevance pertaining to overall number of prescriptions and worldwide revenue,
- Compound complexity for achiral and chiral conformations,
- Diversity of reaction schemes and solvents used,
- Relationship to natural products (derived, extracted, or synthesized.)

Imatinib met the criteria for solvent diversity in terms of organic solvents required for synthesis, clopidogrel met the criteria for chiral attributes and rosuvastatin met criteria for natural product origins. Interestingly, statins are derived from the natural product discovery compactin, commonly known as mevastatin, which was isolated from the mold of *Penicillium citrinum* by a Japanese biologist Akira Endo in the 1970s. Although not marketed as a therapeutic drug to treat cholesterol, Merck filed the first cholesterol reducing statin referred to as lovastatin, a derivative of mevastatin. Rosuvastatin is classified in this family of therapeutics[184, 185]. The overall aims of including these ‘applied use’ investigations were to assess the applicability of a low volume instrument with sub-2 $\mu$ m particle stationary phase pSFC as a valuable solution for reaction monitoring activities performed in medicinal chemistry.

The chiral analysis investigates the synthesis of clopidogrel and rosuvastatin. Specifically, rosuvastatin is derived from a class of six-membered heterocyclic ring compounds, specifically pyrimidine scaffolds, reported to lead to a high percentage of top marketed drugs [183]. The therapeutic form of rosuvastatin is a (3R,5S) diastereomer enantiomer and requires enantiomeric determinations. The rosuvastatin asymmetric synthetic route includes a multi-step synthetic pathway including commonly practiced reaction mechanisms such as



cyclocondensation, dehydrogenation, and modified Wittig reactions, thus leading to an enantiomeric product with the potential for a variety of impurities with each reaction intermediate.

### 5.2.1 Reaction Schemes

#### 5.2.1.1 Rosuvastatin Reaction Scheme

The synthetic route developed by Hirai and Watanabe [186, 187] was followed for the asymmetric synthesis of rosuvastatin calcium (Figure 5.1). A key intermediary step of this synthetic pathway uses an aldehyde functionalized pyrimidine intermediate that allows the introduction of a modified Wittig reaction (R8) known as a Horner-Wadsworth-Emmons (HWE) reaction to lock in the *E*-alkene stereochemistry of the rosuvastatin intermediate. By locking in the *E*-alkene stereochemistry as part of the reaction scheme, the protecting group provides access to a high purity yield of the desirable (3R, 5S)-rosuvastatin enantiomer by desilylation of the intermediate (R9) followed by a Narasaka reduction (R10), thus producing the resulting rosuvastatin (3R, 5S) enantiomeric methyl ester. The methyl ester (R10) intermediate follows a two-step process *via* saponification producing a sodium salt form of the rosuvastatin free base (R11) which is then converted to the calcium salt form (R12) which is more commonly used for formulated products. Aliquots from the reaction mixtures were diluted in methylene chloride or methanol and submitted for each reaction monitoring time point.

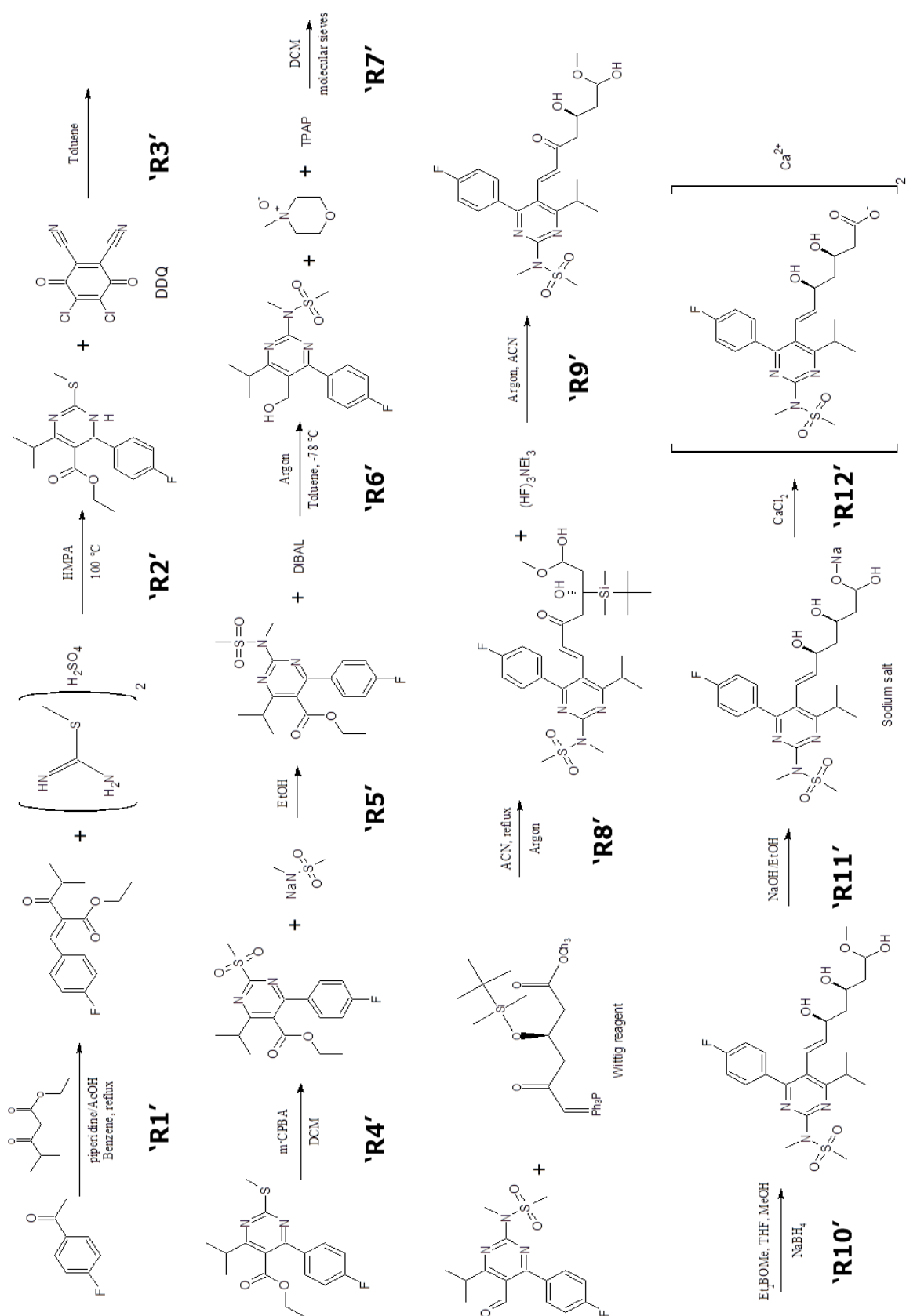


**Figure 5.1: Reaction scheme for route synthesis of rosuvastatin calcium expanded to illustrate the reaction stages (R(#)) monitored by UPC<sup>2</sup>/MS and UPLC/MS**

### 5.2.1.2 *Reaction Scheme for Imatinib*

Zimmerman's synthetic route (Figure 5.2) was followed for the synthesis of imatinib [10]. The aldol product (Stage A) undergoes a condensation reaction with guanidine (Stage B) in basic media to give the 2-aminopyrimidine (Stage C). After generating the functional pyrimidine core a Pd/C catalyzed hydrogenation of the nitro group to the amine group was performed (Stage D). The acid side chain was prepared from 4-(chloromethyl)benzoic acid and condensed with 1-methylpiperazine (Stage E) and converted to the acid chloride using  $\text{SOCl}_2$  (Stage F). Amide formation with 4-chloromethylbenzoyl chloride and a direct displacement of the benzylic chloride with pyridine (Stage G) completes this synthesis of imatinib.

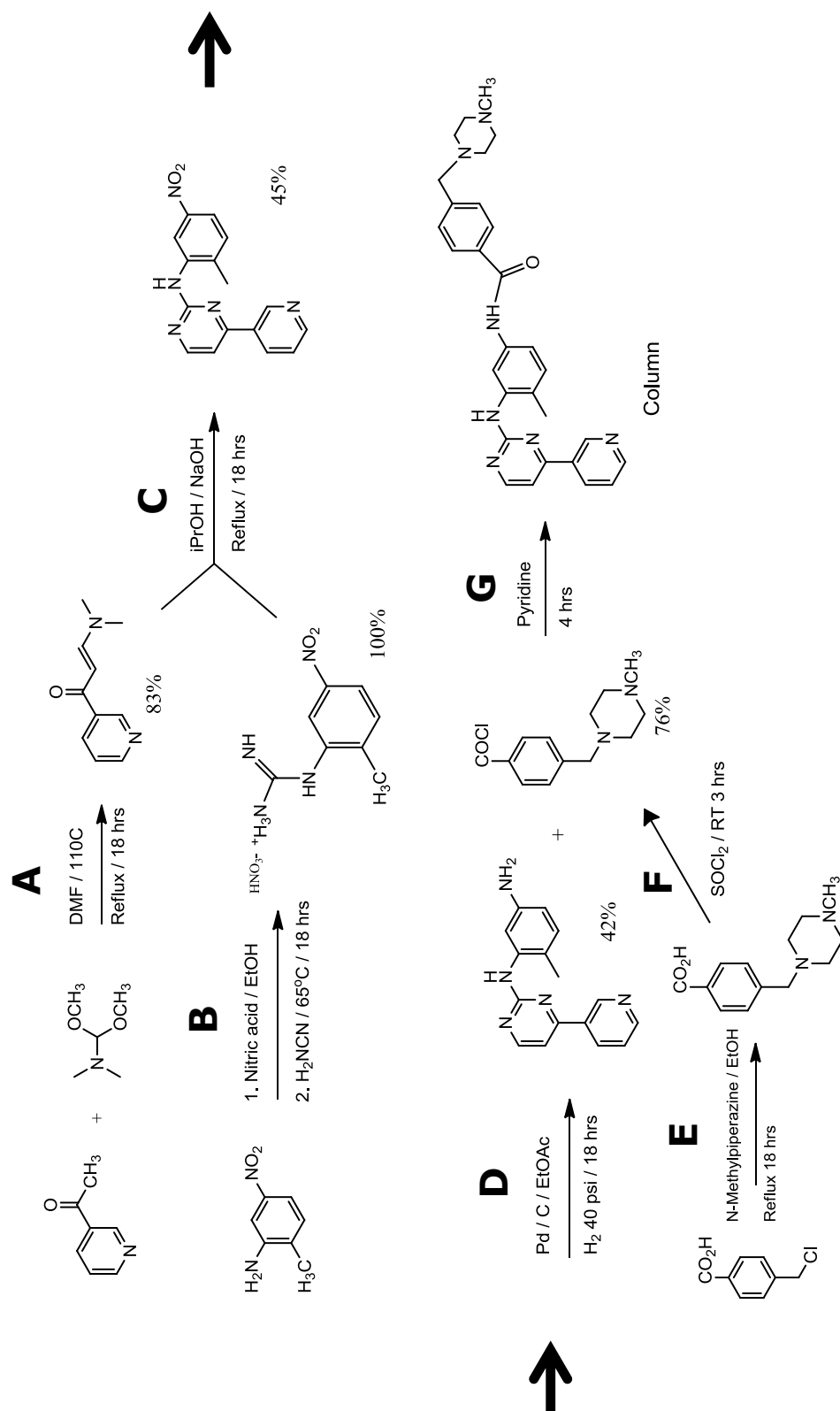


**Figure 5.2:** Reaction Scheme for the synthesis of Imatinib expanded to illustrate the reaction stages A thru G monitored by UPC<sup>2</sup>/MS and UPLC/MS.

### 5.2.1.3 Reaction Scheme for Clopidogrel

The reaction scheme for clopidogrel is outlined in Figure 5.3. The preparation of clopidogrel began from 2-chlorobenzyl cyanide building block [188]. Bromination of the 2-chlorobenzyl cyanide intermediate using bromine at elevated temperature produces the  $\alpha$ - bromo cyanide compound (Stage V), which was condensed with tetrahydro-thieno pyridine (synthesized via coupling an amino thiophene and dioxane compound (Stage U) in the presence of  $\text{NaHCO}_3$  to obtain the functionalized cyano intermediate (Stage W). The obtained cyano compound was converted into the racemic carboxylic acid intermediate (Stage X) which was methylated to yield the racemic clopidogrel ( $\pm$ ) (Stage Y). The requisite isomer of clopidogrel was separated from the racemic compound using L - camphorsulfonic acid as resolution agent (Stage Z), thus the obtained CSA salt was treated with  $\text{NaHCO}_3$  followed by  $\text{H}_2\text{SO}_4$  to yield clopidogrel.

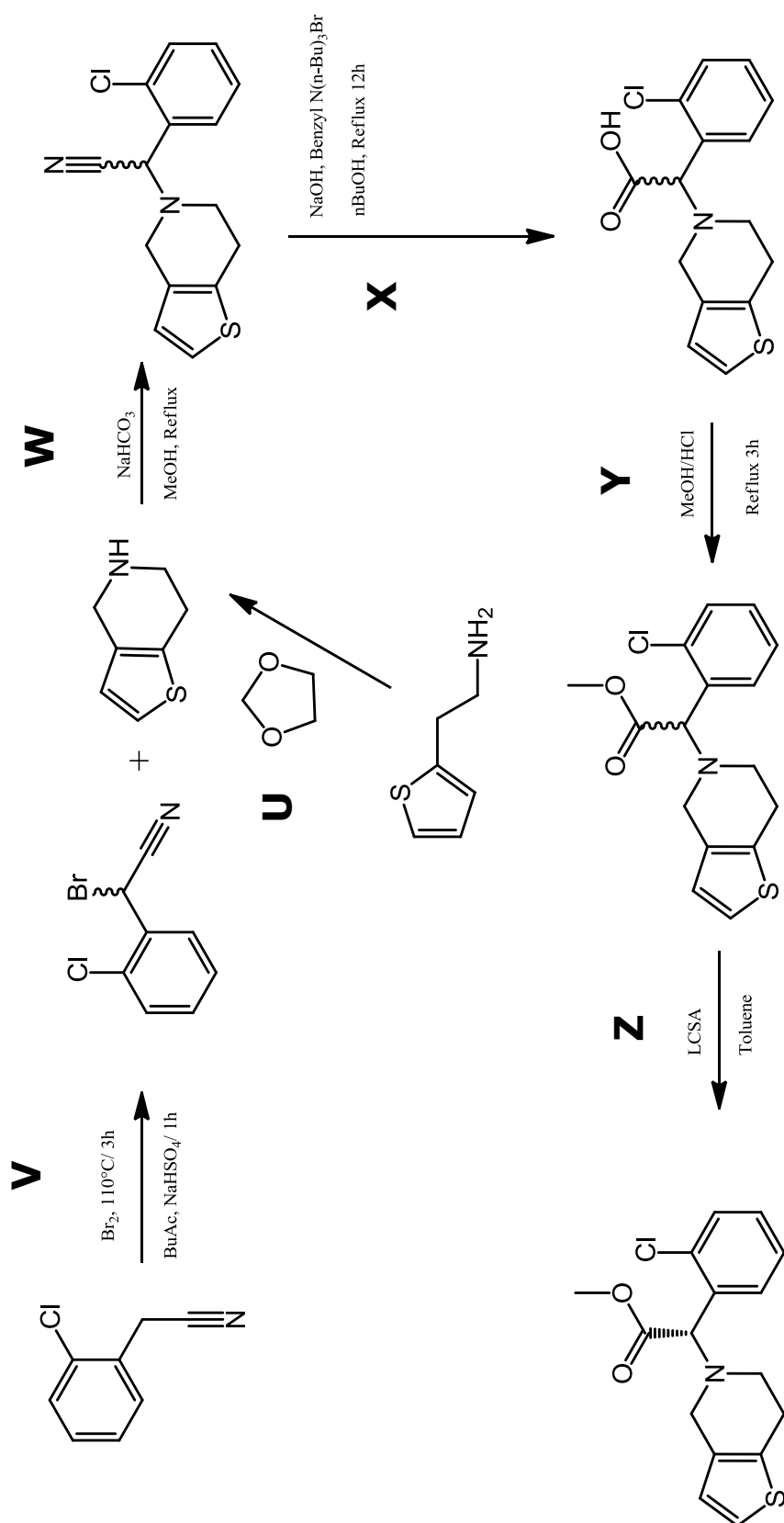


**Figure 5.3:** Reaction scheme for the synthesis of clopidogrel expanded to illustrate the reaction stages (x) monitored by  $\text{UPC}^2/\text{MS}$  and  $\text{UPLC}/\text{MS}$ .

## 5.2.2 Reaction Monitoring Analysis

### 5.2.2.1 Achiral pSFC Screening

The reactions were monitored using ACQUITY UPC<sup>2</sup> configured with a PDA (Waters Corp., Milford, MA, USA), column manager and two auxiliary column managers increasing the column screening capability to 6 columns with independent temperature control. The system was also coupled to ACQUITY QDa (Waters Corp., Milford, MA, USA) for mass measurements with positive and negative polarity electrospray ionization mode (ESI<sub>±</sub>). The ACQUITY QDa was used in ‘standard mode’ with a 0.1 μm aperture. The system was configured with the stationary phases shown in

Table 3.2 with the internal diameter and length dimensions changed to 3.0 mm x 50 mm respectively for rapid screening. Gradient elution was performed using a linear addition of the modifier from 0% to 50% over 2.5 minutes at a flow rate of 2.0 mL/min. The modifier composition was 15 mM ammonium formate dissolved in 100% methanol and spiked with 10 mL per liter of formic acid. The achiral columns were maintained at 50 °C. The backpressure regulator was maintained at 1885 psi. The system injected 0.5 µL of sample. The post column make-up flow prior to the entry into the MS composed of 0.1% ammonia in methanol flowing at 0.4mL/minute.

#### 5.2.2.2 Chiral pSFC Screening

The chiral analysis was performed using the same system configuration described in section 5.2.2.1 using the chiral columns listed in Table 5.1. The immobilized Chiralpak columns were used for the reaction monitoring screening and the Waters Trefoil columns were used for optimization experiments. The chiral screening columns were maintained at 35 °C with a flow rate at 1.5 mL/minute. The rosuvastatin enantiomeric excess experiments in section 5.3.3.3 explored the newly commercially available Trefoil chiral columns (Waters, MA, USA) finalizing on optimized parameters utilizing the ACQUITY UPC<sup>2</sup> Trefoil CEL1 column. The optimized conditions used a 1.4 mL/minute flow rate with an isocratic elution profile of 20% modifier and 80% CO<sub>2</sub>. The elution modifier composition was methanol/isopropanol (1:1) with 20 mM ammonia additive.

#### 5.2.2.3 Achiral Reversed-Phase LC Screening Analysis

The separations were performed using a 2.1 mm x 50 mm; 1.7 µm ACQUITY UPLC BEH C<sub>18</sub> column using an ACQUITY Ultra Performance LC Chromatography™ (UPLC) System



(Waters<sup>®</sup> Corporation, MA, USA). The column was maintained at 40 °C and eluted with a linear acetonitrile – aqueous gradient over 1.0 minute at 800 µL/minute, starting at 5 % acetonitrile and rising to 95 % over the course of the gradient. The aqueous mobile phase was either 0.1 % v/v formic acid for low pH screening or 0.1 % v/v ammonium hydroxide for high pH screening. The column eluent was directed to the mass spectrometer for analysis.

**Table 5.1: List of chiral columns used**

Stationary Phase	Dimesions	Manufacturer
<b>Chiralpak IA</b>	2.1 x 150 mm; 3 $\mu$ m	Chiral Technologies Inc, PA, USA
<b>Chiralpak IB</b>	2.1 x 150 mm; 3 $\mu$ m	Chiral Technologies Inc, PA, USA
<b>Chiralpak IC</b>	2.1 x 150 mm; 3 $\mu$ m	Chiral Technologies Inc, PA, USA
<b>Chiralpak ID</b>	2.1 x 150 mm; 3 $\mu$ m	Chiral Technologies Inc, PA, USA
<b>Chiralpak IE</b>	2.1 x 150 mm; 3 $\mu$ m	Chiral Technologies Inc, PA, USA
<b>Chiralpak IF</b>	2.1 x 150 mm; 3 $\mu$ m	Chiral Technologies Inc, PA, USA
<b>ACQUITY Trefoil Amy1</b>	2.1 x 150 mm; 2.5 $\mu$ m	Waters, MA, USA
<b>ACQUITY Trefoil CEL1</b>	2.1 x 150 mm; 2.5 $\mu$ m	Waters, MA, USA
<b>ACQUITY Trefoil CEL2</b>	2.1 x 150 mm; 2.5 $\mu$ m	Waters, MA, USA

### 5.3 Results

Three active pharmaceutical ingredients (API) were synthesized by the organic chemist staff at Prime Organics, Inc (Waltham, MA, USA). Each reaction was monitored and assessed in terms of identifying any benefit of employing the pSFC technology. Particular examples were observed and are highlighted within the next sections.

#### 5.3.1 Monitoring the Synthesis of Imatinib by UPC<sup>2</sup>/MS

An intermediate step for the synthesis of imatinib requires a condensation coupling reaction between N-(2-methyl-5-nitrophenyl)guanidine (C<sub>8</sub>H<sub>10</sub>N<sub>4</sub>O<sub>2</sub>; mass = 194 Da) and (2E)-3-(dimethylamino)-1-(pyridin-3-yl)prop-2-en-1-one (C<sub>10</sub>H<sub>12</sub>N<sub>2</sub>O; Mass = 176 Da) in the presence of hydroxide and isopropyl alcohol to produce the intermediate product N-(2-methyl-5-nitrophenyl)-4-(pyridin-3-yl)pyrimidin-2-amine. In Zimmerman's approach, the nitro pyrimidine intermediate was added to ethyl acetate and reduced to produce 6-methyl-N1-[4-(pyridin-3-yl)pyrimidin-2-yl]benzene-1,3-diamine (C<sub>16</sub>H<sub>15</sub>N<sub>5</sub>; mass = 277 Da) in the presence of 10% palladium on carbon (Pd/C) to catalyze the reaction. These previously described reactions will be reviewed in the following sections 5.3.1.1 to 5.3.1.3.

##### 5.3.1.1 Monitoring the Condensation Reaction

The reaction was monitored using ACQUITY UPC<sup>2</sup> coupled to ACQUITY QDa with positive and negative polarity electrospray ionization mode (ESI<sub>±</sub>). Detection of the intermediate product eluting at 0.66 minutes and an unknown impurity peak eluting at 0.94 minutes was observed on an ACQUITY UPC<sup>2</sup> 2-EP column in the negative mode total ion chromatographic trace (TIC). Initial assumptions presume the unknown at 0.94 minutes observed with ESI- m/z = 304 Da suggests a reduced by-product impurity with origins to the

intermediate product observed at ESI-  $m/z = 306$  Da. By employing an additional experiment performed using an elevated MS cone voltage, in-source collision induced dissociation (CID) occurs, thus creating fragmentation. The CID experiment will confirm or disprove the hypothesis of the origin relating the intermediate product *via* common fragment analysis. Interestingly, the higher applied voltage confirmed an unlikely event of reduced by-products and relationship to the intermediate product. The MS ESI- spectra did not result in any common fragment ions nor did it result in any form of fragmentation pattern trends (Figure 5.4).

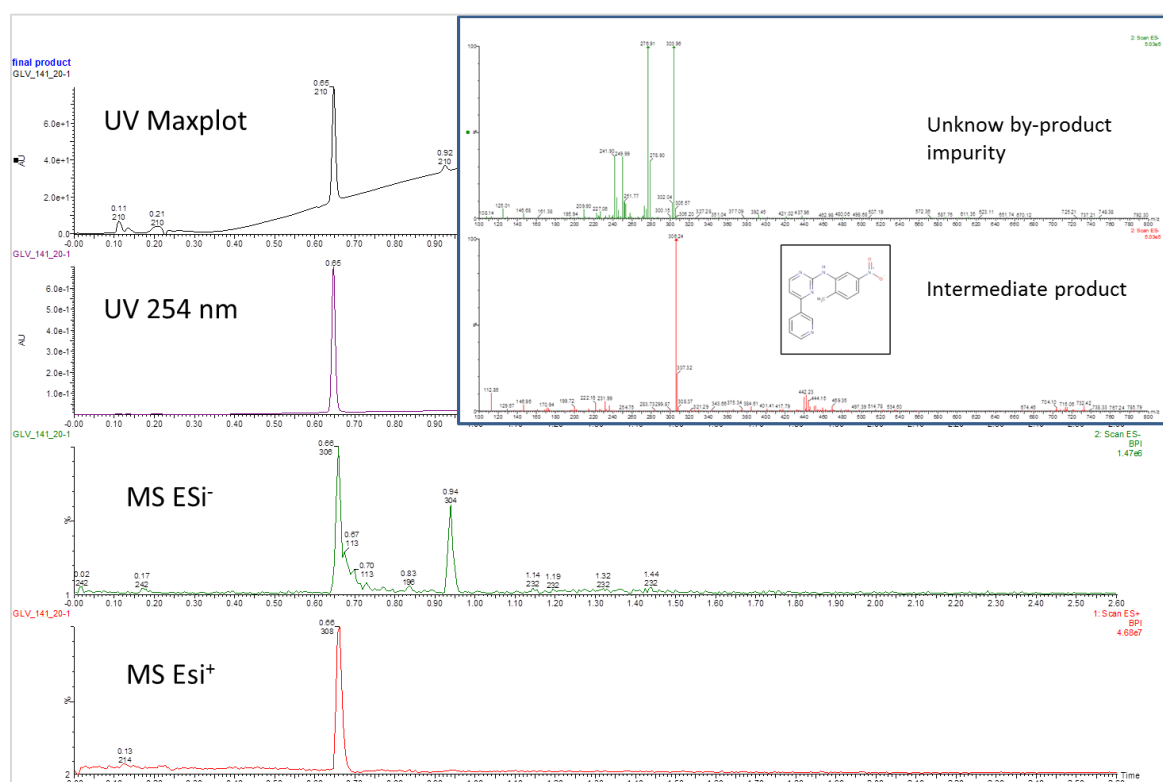


**Figure 5.4: UV/MS chromatographic traces of the nitro pyrimidine intermediate and spectral analysis comparison of the intermediate product and unknown by-product performed at cone voltage = 80 V. Maxplot is defined as photodiode array data collection for a range of 200-400 nm for these experiments.**

The unknown by-product did not result in catalytic inhibitions of further reactions, but the importance of this observation illustrates the requirement to couple chromatography with a mass detection device. Infusion approaches typically performed on standalone benchtop MS instrumentation would not have been as simple to characterize the unknown chemical entities which are structurally similar or isobaric related species to the targeted synthetic products [189, 190]. Additionally, standalone approaches would impede the detection of potentially genotoxic impurities (PGI) at earlier stages of the development process, thus affecting the efficiency of the production of drug at industrial scale.

#### 5.3.1.2 *Interpreting the Nitroso-intermediate Formation*

There were difficulties repeating Zimmerman's synthesis approach as reported in literature. The insolubility of the nitro pyrimidine inhibited the progress of the reaction and therefore the dilution solvent was altered to a ratio of 2:1 ethyl acetate to ethanol rather than 100% ethyl acetate. The data confirmed the positive affect of adding ethanol to the solvent to enhance solubility of the starting materials. Upon review of the chromatography, the results showed peak co-elutions and peak 'bridging' between the run time of 0.55 minutes and 1.10 minutes. The bridging from one intermediate peak to another major intermediate peak during a reaction mechanism is analogous with on-column degradation of solutes observed in literature [191] or during the production of structurally unstable intermediates. The observation in Figure 5.5 results in peculiar chromatography during the production of the nitroso intermediate. The extracted ion chromatogram (XIC) for the nitroso intermediate indicated the related isobaric species with  $m/z = 292$  Da. The 'bridging' in this instance is hypothesized as an indicator that reaction is not quenched and possibly occurring while on-column and . The starting material ( $m/z = 308$  Da), the product intermediate ( $m/z = 278$  Da), and various unknown peaks were identified using the MS spectra extracted from MS ESI+

chromatographic traces. The major unknown peaks observed were  $m/z = 282$  Da and two isobaric peaks with  $m/z = 292$  Da. It was determined from the MS data, the two isobaric peaks observed with  $m/z = 292$  Da were chromatographic observations of nitroso-based intermediates as the nitro pyrimidine converts to the amine based intermediate product (Figure 5.5). The conversion results show two peaks due to the ambiguity of which conjugated oxygen was reduced from the nitro- functional group. Monitoring the time points of this reaction provided insight to the reaction chemistry behavior and kinetics during the entire reaction.

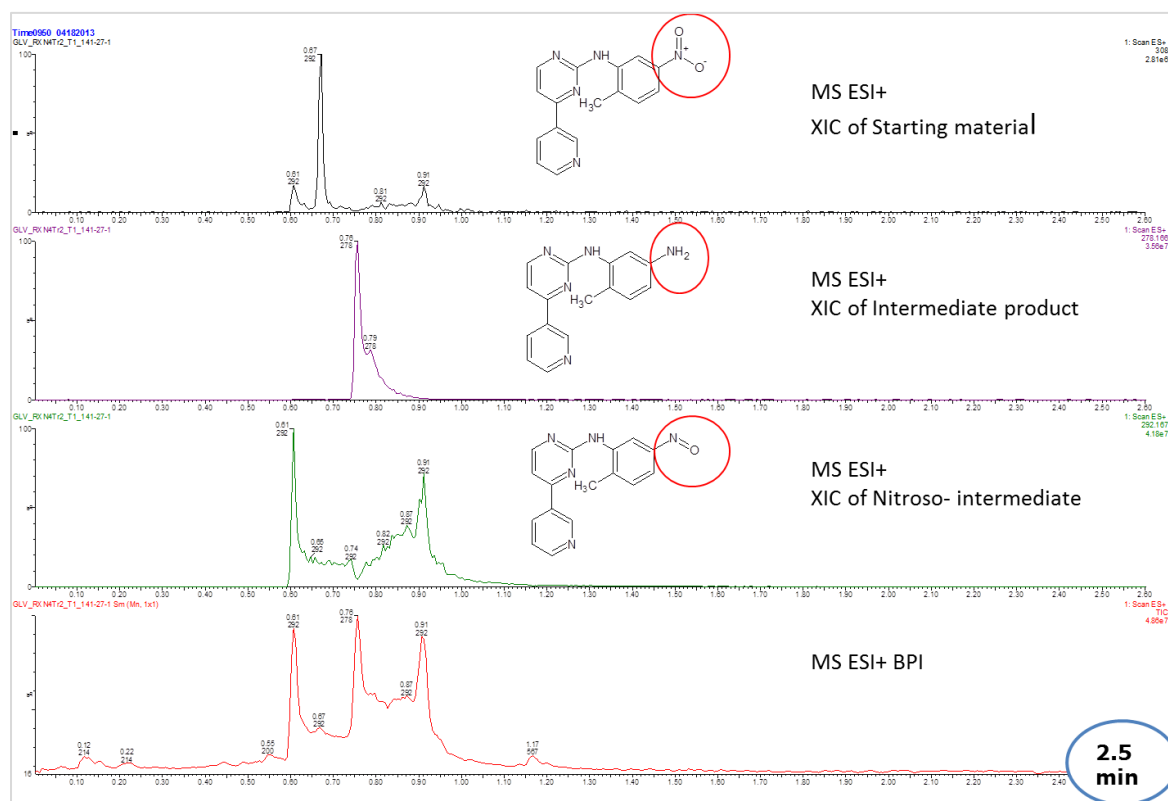


**Figure 5.5: Hydrogenation reaction UPC<sup>2</sup>/MS traces showing the intermediate by-product conversion of the nitro functionality to the nitroso- functionality and finally to the amine functionality and confirmed by MS**

### 5.3.1.3 *Reduction Reaction: Facilitating Identification and Elucidation of Over-reduced Impurities*

Kinetic plots were constructed from the UV data and reviewed for the hydrogenation reaction time points (Figure 5.6). The kinetic plots also revealed peculiarities concerning impurity formation as the nitroso- intermediates are consumed, thus affecting the overall purity and yield of the final intermediate product. When performing Pd/C hydrogenation reactions, it is common to observe reductions of additional unsaturated conjugated nitrogens which are difficult to control within the reactant solution. After the reaction was completed and worked up, several over reduced species were observed. Post reaction analysis of the MS data identified the unknown impurity with  $m/z = 282$  Da, however additional peaks were observed in the MS ESI<sup>+</sup> TIC with observed  $m/z = 284$ ,  $m/z = 567$  Da and another isobaric species with  $m/z = 282$  Da (Figure 5.7). The impurities are hypothesized to be over-reduced species related to the final intermediate as +6 [H], +4[H], and a dimerized over-reduced species. The sample was washed several times in an effort to isolate the desired product and eliminate the catalyst filtrate. The reaction was performed several times with different additions of ethanol and reduction catalyst, however eliminating the over-reduced impurities was unsuccessful, although controlling them was moderately successful.

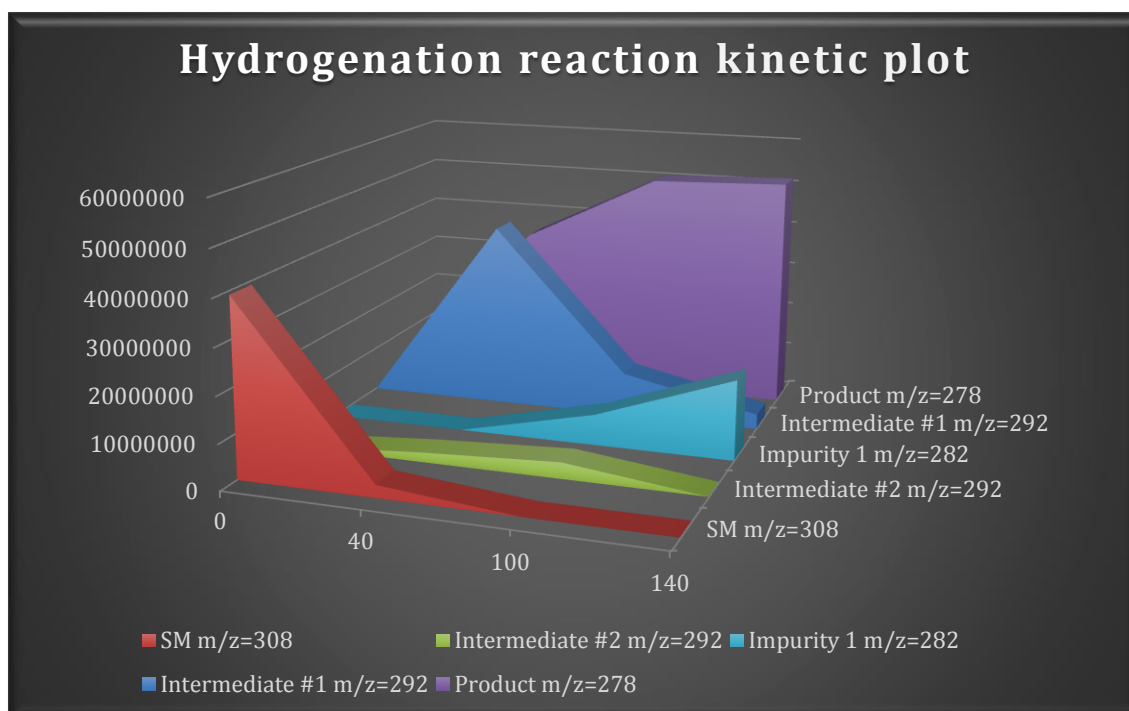


**Figure 5.6:** Hydrogenation reaction kinetic plot showing a relationship between the nitroso intermediate consumption and the impurity generation.



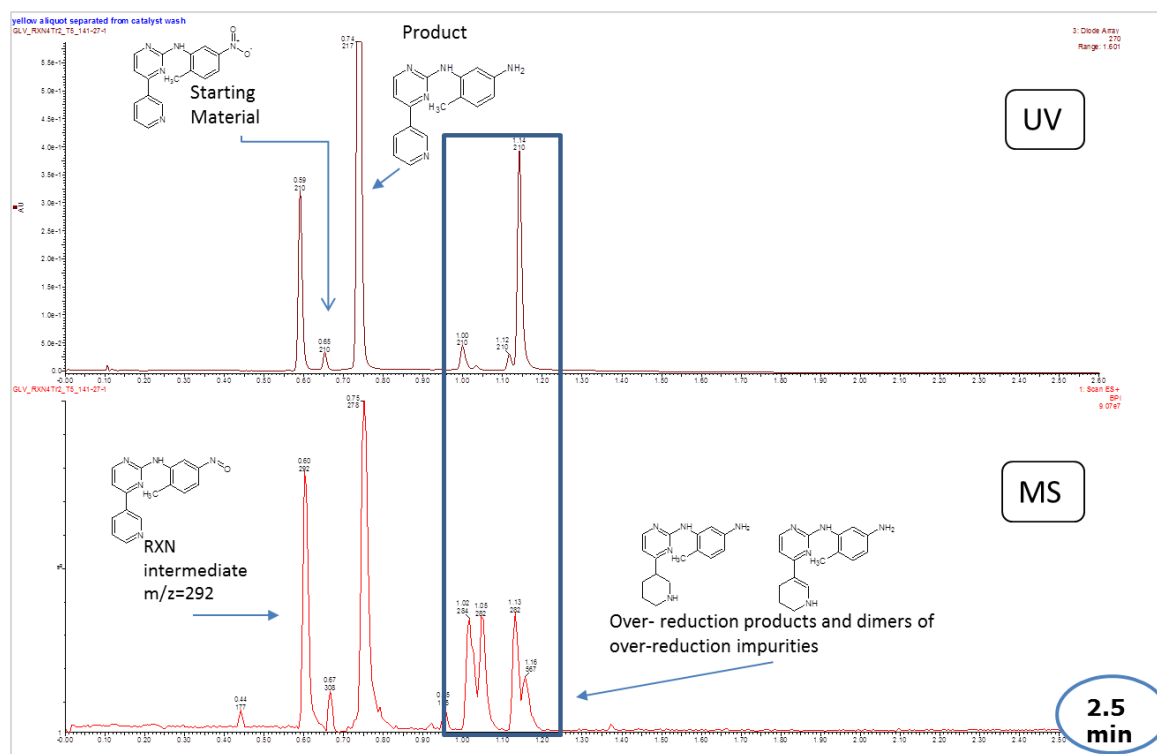


**Figure 5.7: UV/MS chromatographic traces of a hydrogenation reaction mixture time point showing the complete reaction profile of starting material, intermediate product, intermediate by-product, and over-reduced impurities (highlighted in the rectangular box).**

In-source collision induced dissociation was performed to determine the location of the over-reduction. The hypothesis assumes two scenarios, reduction of the pyridine ring or reduction of the pyrimidine rings (Figure 5.8). A seasoned organic chemist may instinctually know the likelihood of where the over-reduction could occur, however the experienced organic synthetic chemists should rely on the analytical data to help interpret, direct, and control the stages of a chemical reaction to confirm assumptions.

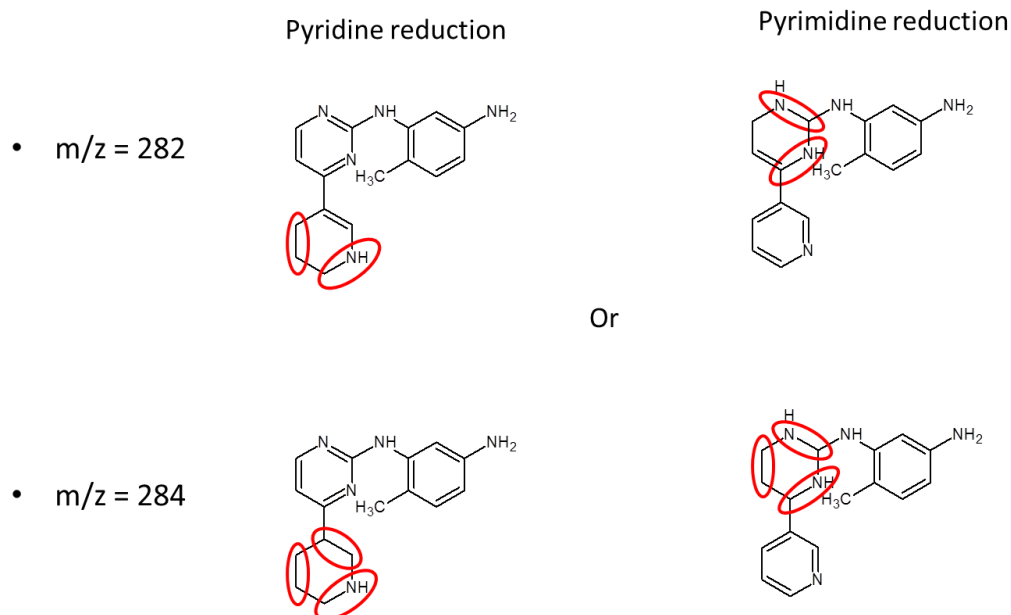


**Figure 5.8: Possible sites accounting for observations of over-reduced species in the SFC/MS data.**

Review of the MS spectra and fragmentation pattern from the in-source CID experiments confirmed the reduction of the pyridine ring. Fragments with  $m/z = 200$  Da and  $m/z = 214$  Da account for the presence of unsaturated bonds in the pyrimidine structure of the product intermediate scaffold (Figure 5.9).

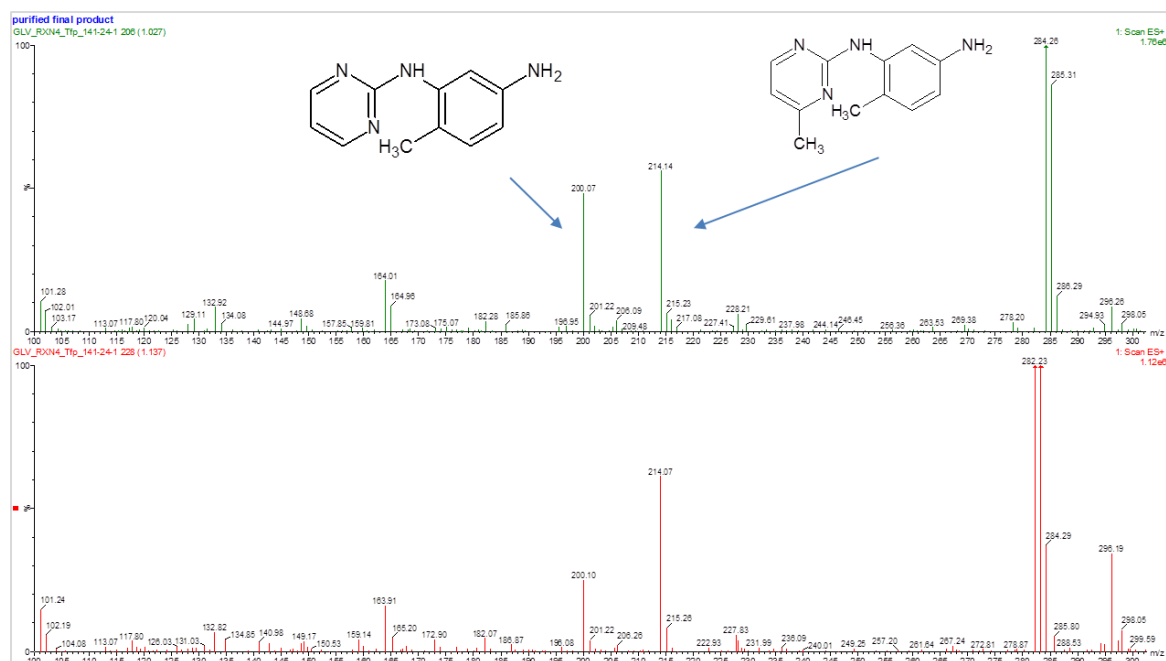


**Figure 5.9:** MS spectral confirmation of the pyridine ring reduction for impurities peaks eluting at 1.02 minutes and 1.14 minutes.

### 5.3.2 Achiral and Chiral Screening of Clopidogrel Racemates by UPC<sup>2</sup>

During the initial start of monitoring the synthetic reactions of clopidogrel, the occurrence of process impurities during the synthesis of reaction step ‘U’ were observed in the UPC<sup>2</sup>/MS screening data but not in the UPC<sup>2</sup>/UV data (Figure 5.10). It was unclear how they would affect the synthesis downstream. Therefore, parallel reactions with different starting materials were explored in order to determine conditions to optimize the synthetic route. The oligomers were identified in the MS trace but not observed in the UV trace. The monomer has a mass of 74 Da, therefore it was determined that it was a by-product formed from the 1,3 dioxolane starting material used in reaction step ‘U’ (Figure 5.11). It was also determined adjustments were required to the gradient methodology to be more specific to this compound. The generic 0% B to 50% B modifier screening gradient was adjusted to 0% B to 20% B modifier gradient elution to allow for a better separation of the oligomers and greater retention of the intermediate reaction products. With this, an additional set of shallow

gradients were added to the open access walk-up methods for purposes of accounting for hydrophilic compounds. These shallow gradient methods were used for the clopidogrel and rosuvastatin reaction monitoring experiments.

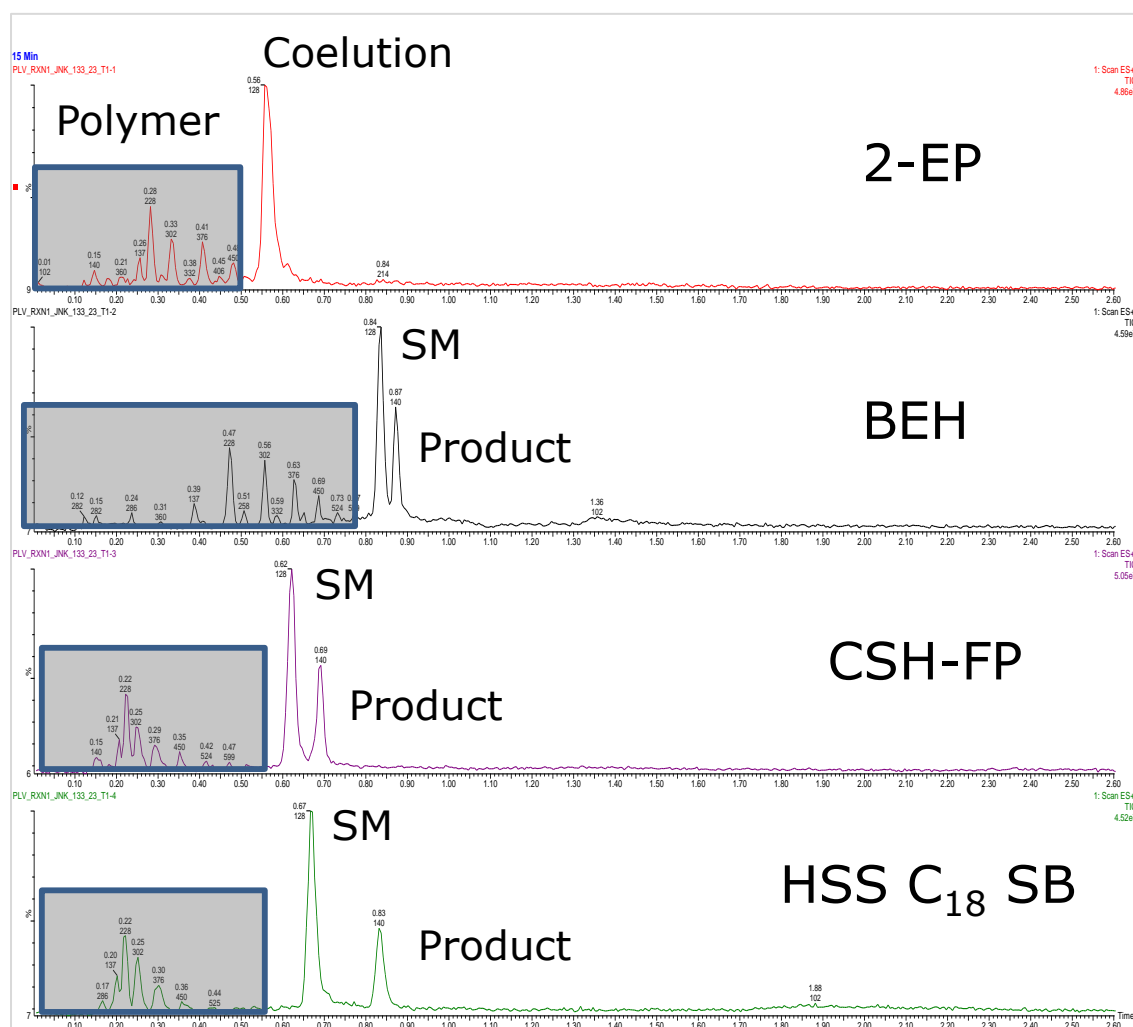


**Figure 5.10: Overlay of UPC<sup>2</sup>/MS total ion chromatogram results for the final clopidogrel reaction step 'U' time point. Oligomer peaks highlighted in the grey box.**

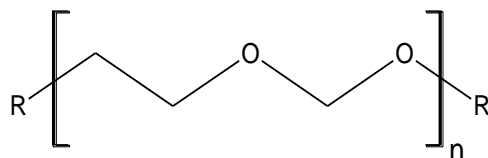
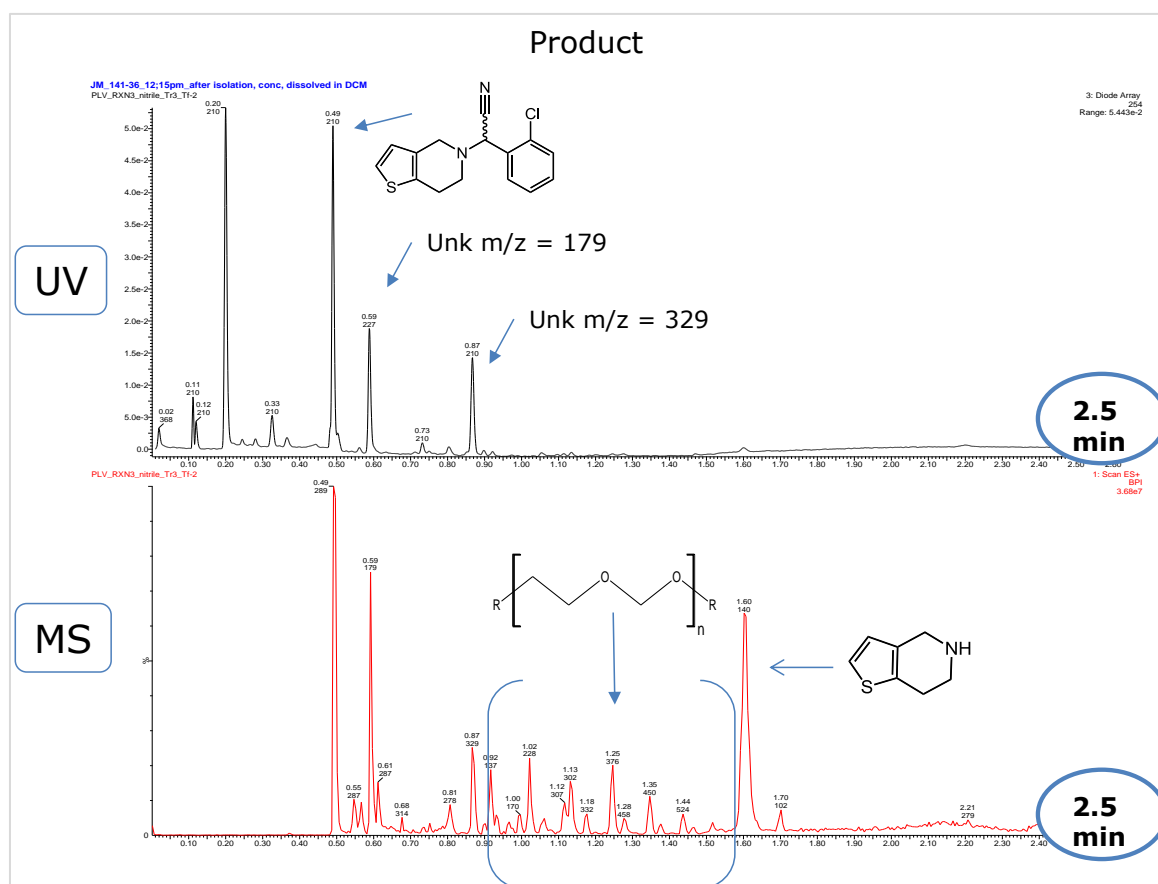


Figure 5.11: Oligomer by-product

Analyzing the reaction with the adjusted method and moving forward with the impure oligomerized starting material for the clopidogrel synthesis step 'W', the oligomers were still observed with less interference, and two new unknown impurities were observed in the UV and verified by mass spectrometry as  $m/z = 179$  Da and  $m/z = 329$  Da (Figure 5.12).

Figure 5.12: Overlay of UPC<sup>2</sup>/MS of clopidogrel reaction step 'W'

In an effort to improve the synthetic route, alternative starting materials based on a bromo-ester material (SM2) rather than a bromo-nitrile starting material (SM) were explored. The thiophene-based material was purchased rather than synthesized to determine if the additional peaks were a result of the chromatographic technique. A systematic experimental plan was formulated to better control the process impurities. The single experimental changes are underlined and described below. Single experimental changes were employed to control the influence of multiple changes upon final conclusions:

1. Substitute the bromo-ester SM2 for the bromo-nitrile SM and use the synthesized thiophene-based SM1
2. Use the bromo-ester SM2 and synthesized thiophene-based SM1 with dioxane to alter the boiling point and reaction kinetics
3. Use the bromo-ester SM2 and a purchased thiophene-based SM1 to eliminate the occurrence of the oligomers.
4. Revisit the bromo-nitrile SM2 using the purchased thiophene-based SM1

#### 5.3.2.1 Investigating the bromo-ester starting material

Upon substitution of the bromo-nitrile starting material with the bromo-ester starting material, the over reduced species and unknown impurities were eliminated. The oligomers were still present, but that was to be expected because the impure thienopyridine -based starting material rich with oligomers was still being used (Figure 5.13). Although the bromo-ester starting material showed promise, the yield was not optimal. The use of dioxane in place of THF allowed for a lower boiling point thus providing improved reaction kinetics decreasing the rate from 22 hours to 3.4 hours with a 29% increase in yield (Figure 5.14).

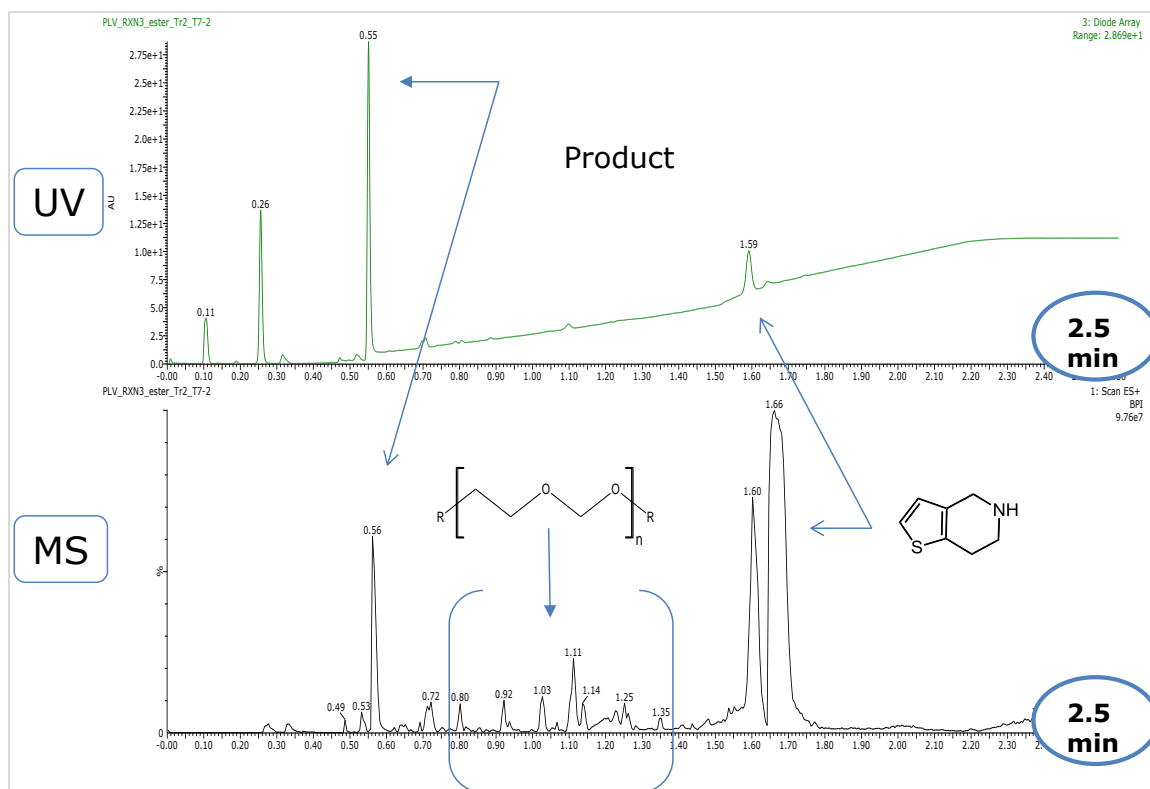


Figure 5.13: Bromo-ester starting material results for clopidogrel reaction step 'W'.

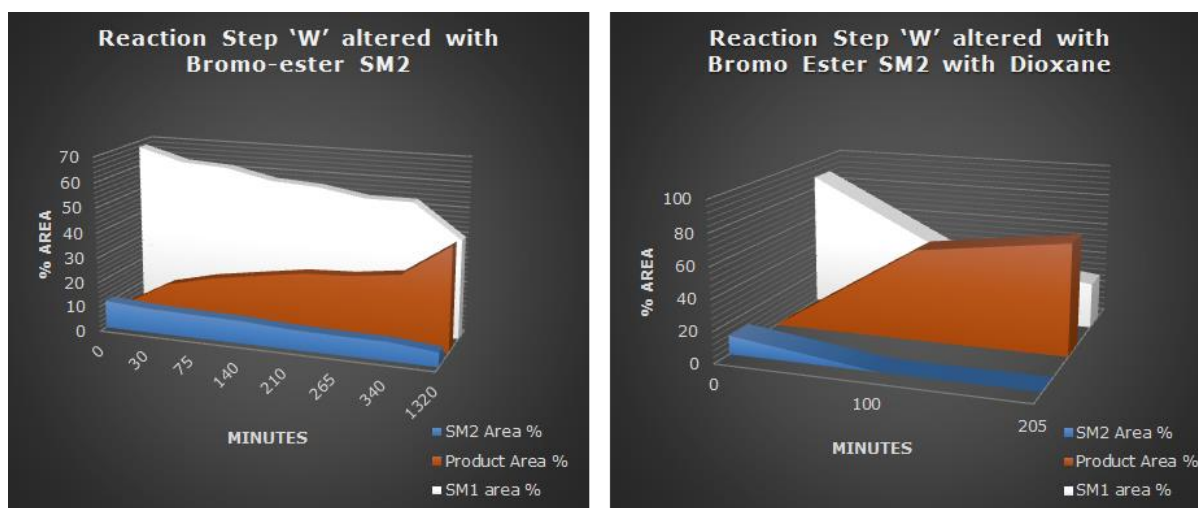
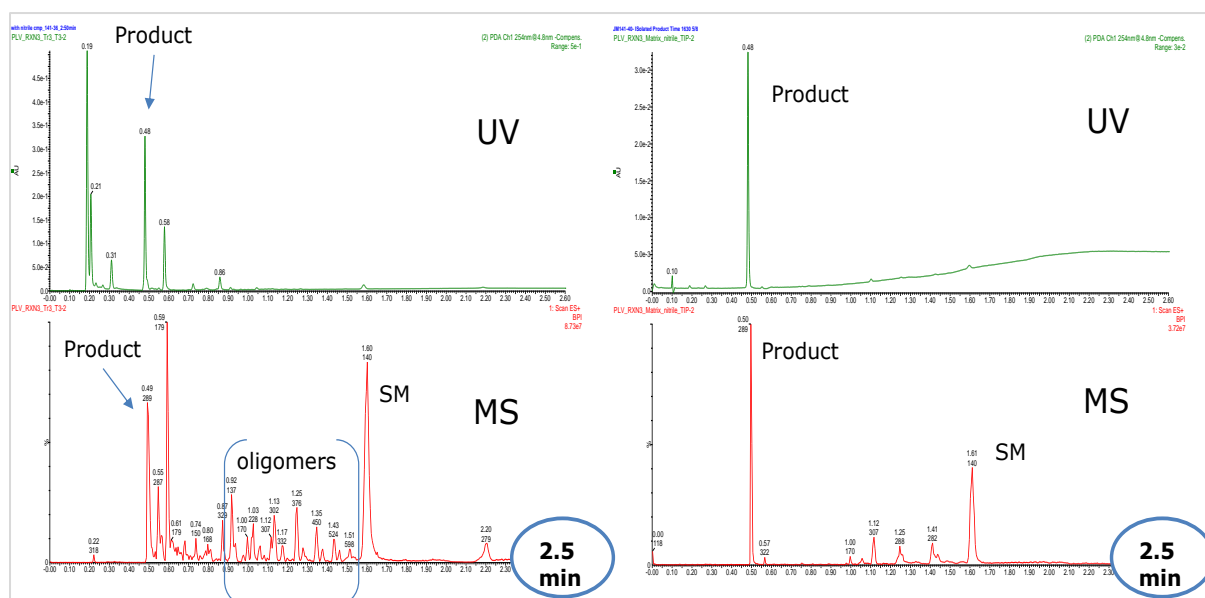


Figure 5.14: Reaction kinetics comparison of the bromo-ester SM adjustment with dioxane versus THF as the reaction solvent system.

### 5.3.2.2 Effect of pure thiophene-based starting material

The purchased thienopyridine starting material was used for both approaches and compared to the original data. In Figure 5.15, comparisons of the bromo-nitrile based approach were performed using both starting materials. The data clearly shows a decrease in oligomers and impurities.



**Figure 5.15: UPC<sup>2</sup>/MS comparison of synthesized versus purchased thienopyridine starting material used in the clopidogrel reaction step ‘W’.**

### 5.3.2.3 Chiral and Achiral Screening of Clopidigrel Synthesis

Chiral and achiral separations can be accomplished with the same solvent system used for the sample diluent mobile phases without swapping instruments. A different chiral column was needed to separate the chiral enantiomers of the product for the clopidogrel intermediate reaction step ‘W’. The achiral UPC<sup>2</sup> BEH 2-EP column provided the best results based on the number of peaks separated and peak shape in comparison to the other achiral columns screened. The entire set of immobilized chiral technologies columns was screened. Chiral



column 'A' (Chiralpak ID) in Figure 5.16 which successfully separated the enantiomers of the intermediate reaction product, failed at separating the enantiomers of the starting material. Whereas, the chiral column 'B' (Chiralpak IB) labeled in Figure 5.16 successfully separated the enantiomers of the starting material, but not the intermediate reaction product enantiomers.

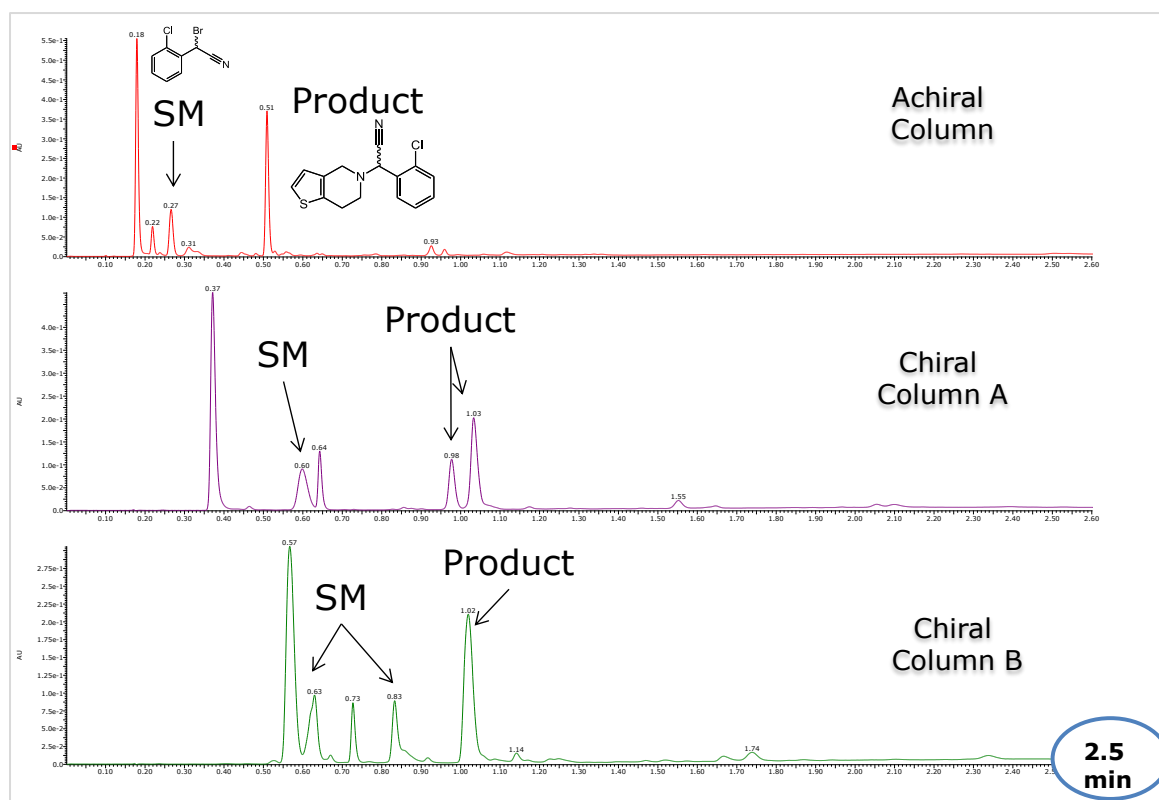


**Figure 5.16:** Overlay of UPC<sup>2</sup> UV chromatograms for the achiral and chiral screening results for clopidogrel reaction step 'W'. Achiral column = UPC<sup>2</sup> 2-EP, Chiral column A = Chiralpak ID, and Chiral Column B = Chiralpak IB.

#### 5.3.2.4 Optimized Synthetic Reaction for Clopidogrel

The final synthetic route summarize in Figure 5.17, the revised reaction scheme provided a 45% increase in yield and 11x reduction in synthesis time.

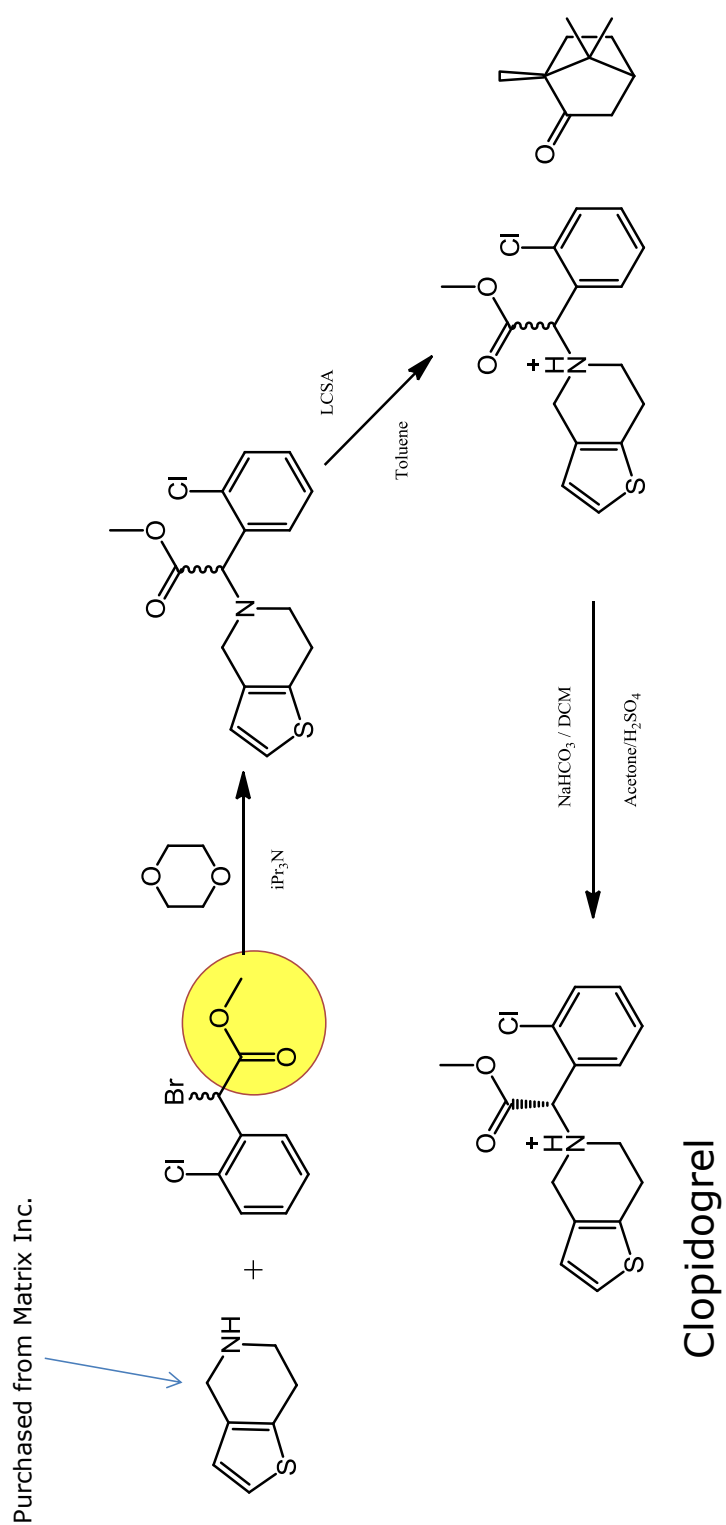


**Figure 5.17: Revised synthetic scheme for the synthesis of clopidogrel based on decision points guided by UPC<sup>2</sup>/MS results.**

### 5.3.3 Monitoring the Asymmetric Synthesis of Rosuvastatin

#### 5.3.3.1 Comparisons to Reversed-Phase LC/MS

During the reaction monitoring of the rosuvastatin intermediate synthetic step (R8) in Figure 5.1, we achieve a clear separation of the starting materials by ACQUITY UPC<sup>2</sup> utilizing a generic 2.5 minute screening method (Figure 5.18). It is common for analytical laboratories to screen high and low pH mobile phases in an effort to promote selectivity as they search for impurities within their process. When comparing the results obtained by a low/high pH reversed-phase screening, the UHPLC separation is achievable, but not ideal. The UHPLC run time may seem faster, however it should be noted that the high/low pH screening utilized a generic UHPLC screening method that was recommended by a peer at GSK. The objective was to employ screening methodology conditions which are generally used in the industry and compare it with a general screening method for UPC<sup>2</sup>. The methods were only optimized for fit for purpose and not scaled geometrically to account for the two different column formats. The experiment was purely qualitative. As the reaction continues, the product intermediate (PDT) is clearly separated from the starting materials when reviewing the UPC<sup>2</sup> results. When comparing to UHPLC, the product was co-eluted with starting material #1 (SM1). The elution of starting material #2 (SM2) is not easily identified by UPLC due to co-elution with the product intermediate (PDT), regardless of selectivity manipulations provided by pH (Figure 5.19). The improvements observed by a sub-2  $\mu\text{m}$  particle stationary phase pSFC approach aided the quantitation of the intermediate yield and purity.

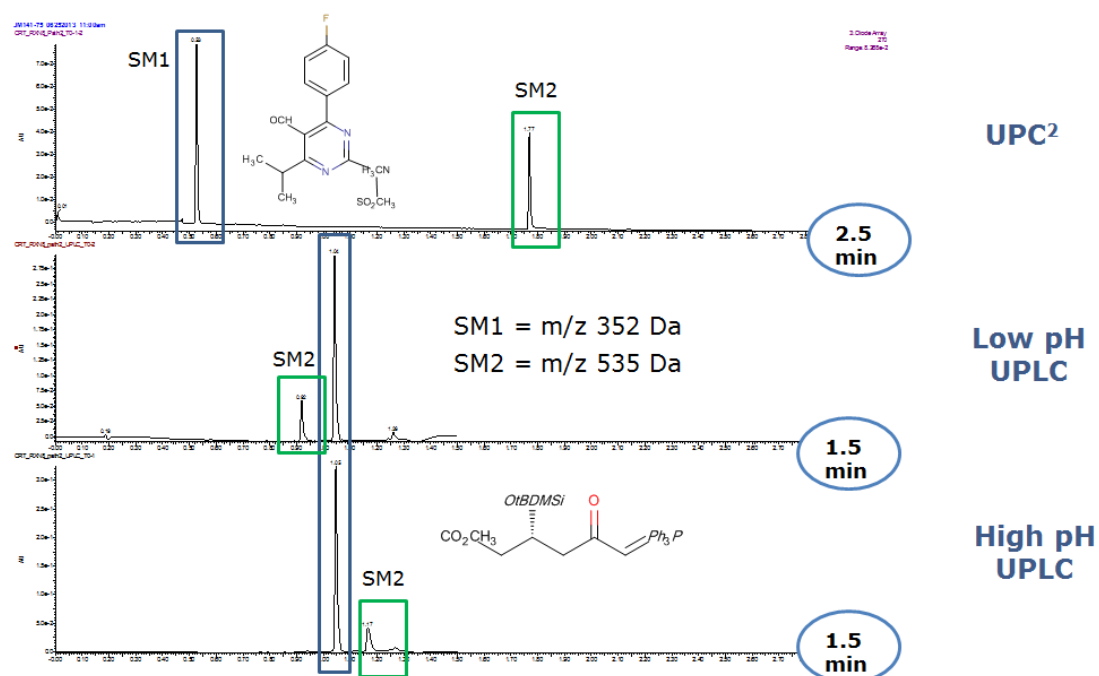


**Figure 5.18: Separations of rosuvasatin starting materials for reaction step R8 performed using ACQUITY UPC<sup>2</sup> and UPLC with high and low pH mobile phases**

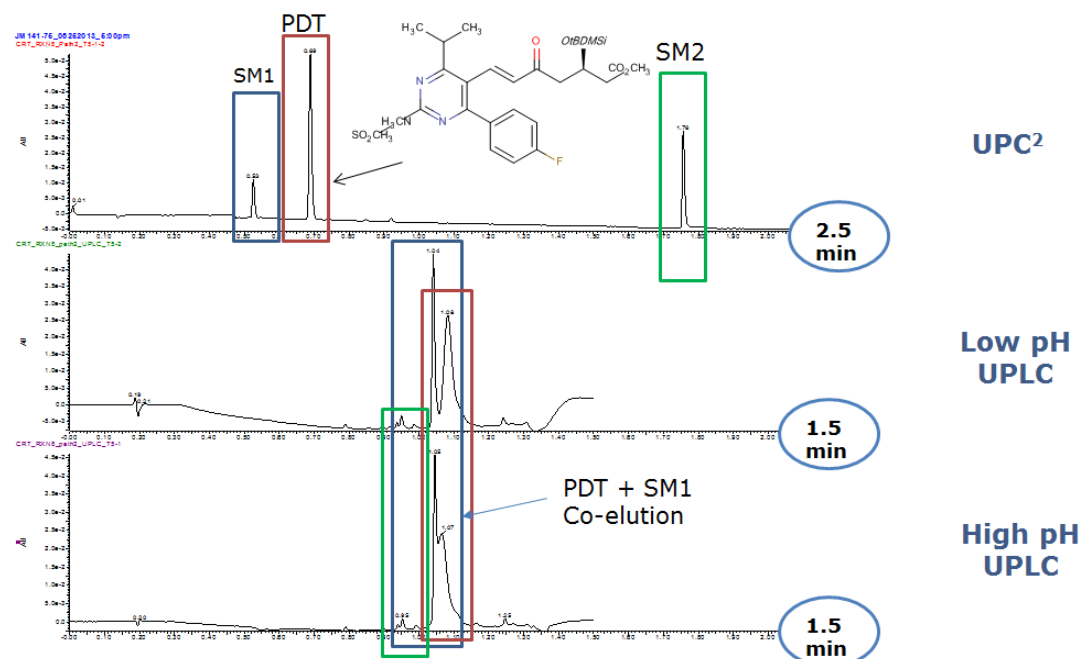


**Figure 5.19: Reaction monitoring separations of rosuvasatin R8 reaction step after 90 minutes performed using ACQUITY UPC<sup>2</sup> and UHPLC with high and low pH mobile phases**

#### 5.3.3.2 *Achiral Rosuvastatin Intermediate (R8-R11) Reactions Monitoring*

The reaction monitoring of the earlier steps indicated the presence of a variety of related impurities, most of which were purged by chemical clean-up involving simple filtering, organic washes or recrystallization of final intermediates. In Figure 5.20, the selectivity of UPC<sup>2</sup> provided a better approach for monitoring the modified HWE reaction (R8) when compared to the UHPLC reversed-phase low/high pH screening results. Upon review of the next reaction steps, some process impurities were observed during the desilylation (R9) of the intermediate, yet the final intermediates were calculated to be approximately 90% pure. The achiral chromatographic monitoring of the final stages (R10, R11) of the reaction scheme indicated the final products were relatively pure and free of major impurities, yielding 90% and 98% purity, respectively (Figure 5.20). The conversion to the calcium salt (R12) is not monitored by chromatographic techniques, but rather verified by a simple QC check to verify completion.

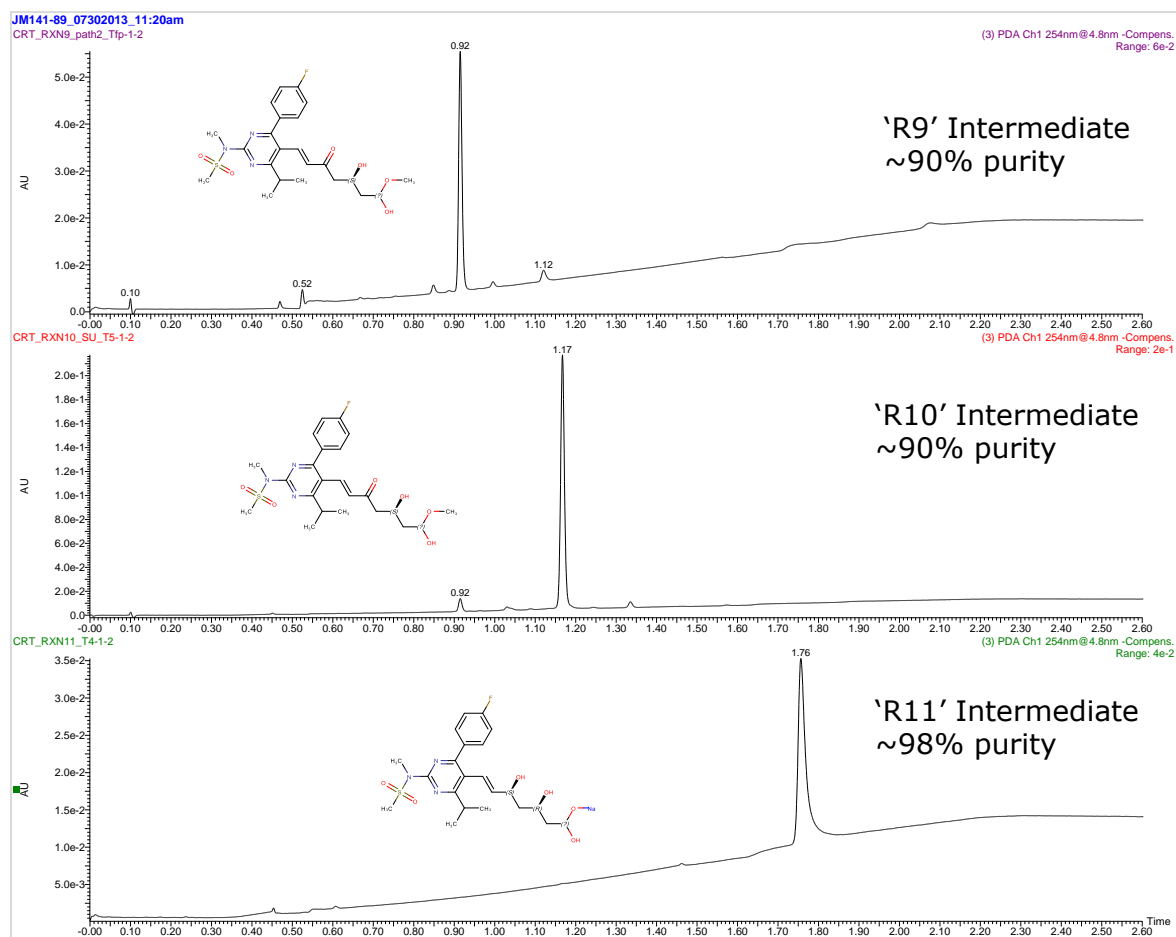


**Figure 5.20: UPC<sup>2</sup>/PDA chromatographic results overlay of intermediates R9, R10, and R11 final analysis time points. Wavelength was recorded at 254 nm.**

### 5.3.3.3 Rosuvastatin Enantiopurity Determination

Enantiopurity, often measured as percent enantiomeric excess (%ee), reflects the relative amount of one enantiomer to another of a chiral compound. In the case for diastereomers, the purity results are typically reported as a ratio of the observed diastereomers (d.r.). For stereoselective synthesis, where the configuration of the desired stereocenter is controlled using reagents and catalysts with an objective to yield a single enantiomer or diastereomer, the purity is typically reported as %ee or %de, respectively. Usually, the impurity is the less desirable enantiomer, which can alter efficacy or even toxicity. Enantiomeric determinations are a necessary analysis for all chiral drug candidates, particularly important for enantiopure

formulations. The enantiopurity of the rosuvastatin final product is expected to be relatively high, above 95% purity, based on the reaction scheme described in Figure 5.1. No major impurity peaks were observed in the chromatographic screening results of the final reactions (R11 and R12), therefore the expected risk of diastereomer impurity interferences in the final rosuvastatin product would be minimal. However, given the stereochemistry of the heptenoic side chain, a variety of diastereoisomer impurities can exist such as (3R, 5R) and (3S, 5S) including the (3S, 5R) enantiomer which requires a chiral separation. The original patent submission indicates a 10 minute normal phase method utilizing a Chiralpak IB column yielding a resolution less than 2 to detect the enantiomeric impurity [192]. In addition to the poor separation provided by the patented method, the normal phase chromatography is limited due to mass spectrometry incompatibility required for simultaneous identification and confirmation during the chromatographic separation.

A chiral chromatographic method was created to resolve rosuvastatin enantiomers using an ACQUITY UPC<sup>2</sup> Trefoil CEL1 2.5  $\mu\text{m}$  column (cellulose tris-(3,5-dimethylphenyl carbamate)). The final isocratic method composed of a mixed alcohol co-solvent with a basic additive. The resolution between the enantiomers was greater than 2.0, approximately measuring  $R_s = 4.5$ . The peaks detected by the chiral methodology were confirmed to be rosuvastatin enantiomers ( $m/z = 482.2$  Da) as determined by the mass spectrometer. The two diastereomer peaks were integrated and the percent diastereomer excess (%de) was calculated using Equation 5.1 as:

**Equation 5.1: Calculation for percent diastereomeric excess**

$$\%de = \frac{E_2 - E_1}{E_1 + E_2} \times 100\%$$

For the 2  $\mu$ L injection volumes, the d.r. was determined to be 98.7:1.3, which was above the expected 95% purity threshold. The %de was calculated to be 96.2%. The peak areas and intensities were in good agreement with the mass spectrometer signal, further confirming the results obtained (Figure 5.21). Peak identification was confirmed by spectral analysis of the QDa results (Figure 5.22).

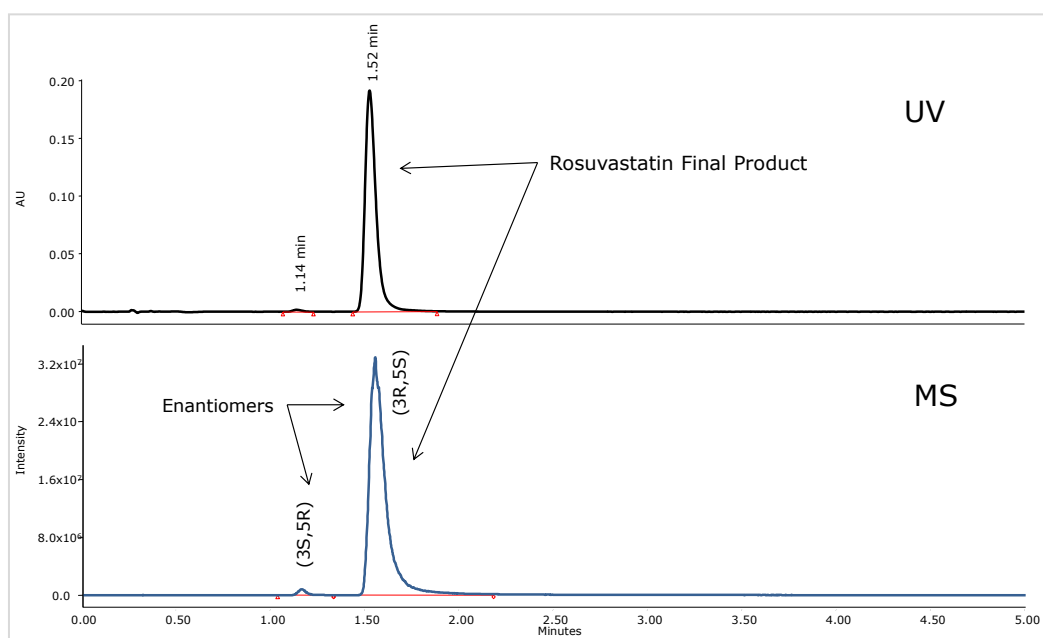


**Figure 5.21: UV and MS chromatographic traces of the Trefoil chiral separation of ‘R12’ rosuvastatin reaction product.**

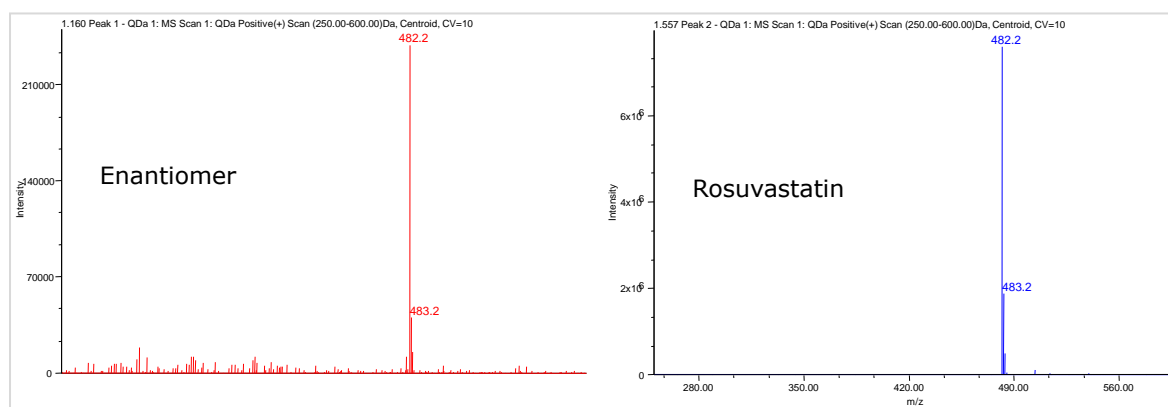


**Figure 5.22: QDa MS spectra confirmed with the resulting  $m/z = 482$  Da measurements of both peaks, rosuvastatin and the enantiomer.**



### 5.3.3.4 Exploring Strong Solvent Effects

Injection volumes from 1.0 to 9.0  $\mu\text{L}$  were injected to evaluate the injection precision and observe any possible injection solvent effects [193]. If peak distortions are observed as a result of strong solvent diluent effects, then accurate determinations of the enantiopurity would be adversely affected and further method development would be required to mediate any peak distortion. The peak area was linear (peak area  $R^2 = 0.9997$ , which is exceptional for a 10  $\mu\text{L}$  loop) with minimal distortion (peak height  $R^2 = 0.9999$ ) using 80/20 heptane/isopropanol as the sample diluent (Figure 5.23).

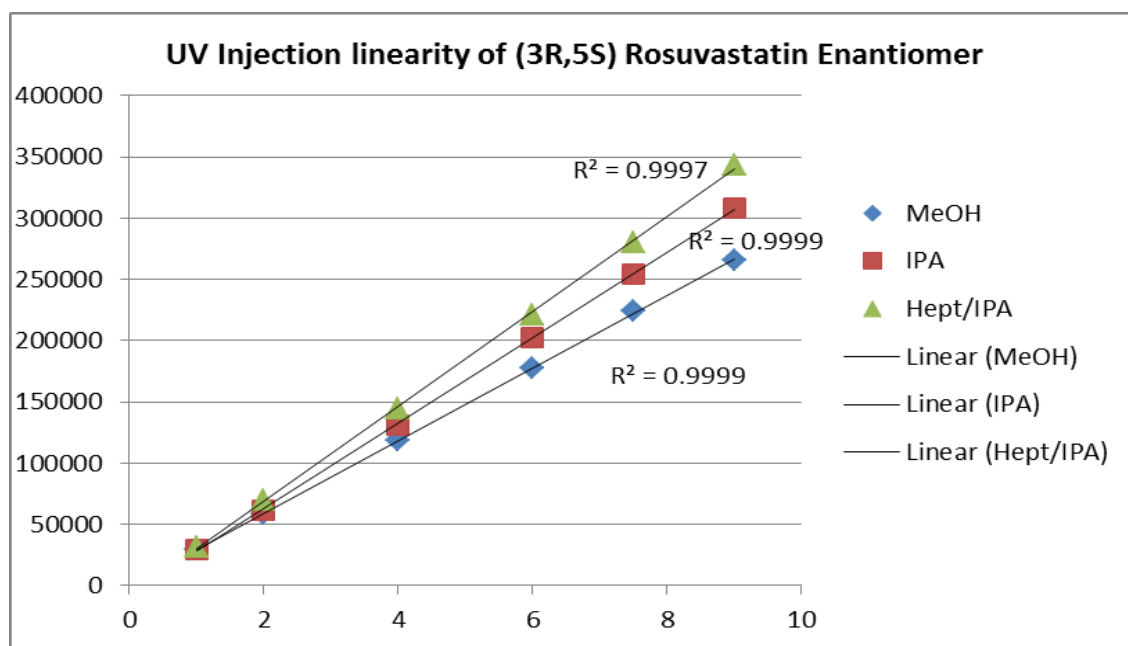


**Figure 5.23: Injection linearity exploring injection solvent effects of Rosuvastatin (3R,5S) enantiomer.**

## 5.4 Conclusions

The reaction monitoring experiments exhibited the unique beneficial orthogonality and robustness of the low volume pSFC instrument configured with sub-2 $\mu$ m particle stationary phases. The studies allowed for a variety of observations and guided decision point common to responsibilities in a synthetic chemistry and medicinal chemistry laboratory. The route synthesis monitoring of imatinib by SFC/MS guided improved decision management affecting greater yield and purity of each intermediate steps and final product. Observed benefits include 8x reduction in synthesis time and 35% higher yield for imatinib. Impurity fate was easily monitored for structurally similar compounds resulting from similar scaffold origins by performing supplemental experiments employing in-source collision induced dissociation.

The approach facilitated the re-development of the synthetic pathway for clopidogrel. The ability to easily separate the oligomer interferences was unique for the pSFC UPC<sup>2</sup> instrument. Interestingly, as this was the first chiral example performed for this investigation the ability to configure the system with chiral and achiral columns provided a stationary phase agnostic approach to the screening process. The solvent system and diluent system did not have to be altered to analyze the reactions. From a traditional LC perspective, this was proven to be a great advantage for pSFC because an instrument set-up for reversed phase LC analysis would normally have to be converted to a normal phase LC for chiral analysis. This takes either considerable amount of time or a second instrument set-up for normal phase chiral chromatography.

The chiral analysis of the asymmetric synthesis of rosuvastatin using Trefoil CEL1 columns provided a very good separation of the enantiomers, while providing improved resolution and

mass spectrometer compatibility compared to the patented methodology. Using the nominal mass confirmation, determining enantiomeric presence was achieved with high confidence. The column methodology was proven to be linear at various injection volumes free from any injection solvent effects negatively impacting the purity determinations, thus providing greater confidence in regard to the method development of the assay.

## **5.5 Acknowledgements**

I would like to thank Paula Hong, Jacob Fairchild, Sean McCarthy, Andy Aubin and John van Antwerp from Waters Corporation for participating in very fruitful discussions about supercritical fluid chromatography, open access environments, and reaction monitoring. I also thank Prime Organics Inc. for synthesizing the pharmaceutical API compounds for the reaction monitoring experiments.

## CHAPTER 6:

---

# Investigating Sub-2 $\mu$ m Particle Stationary Phase Supercritical Fluid Chromatography Coupled to Mass Spectrometry for Chemical Profiling of Chamomile Extracts.

This chapter is based partially on the following publication:

Michael D. Jones, Bharathi Avula, Yan-Hong Wang, Lu Lu, Jianping Zhao, Cristina Avonto, Giorgis Isaac, Larry Meeker, Kate Yu, Cristina Legido-Quigley, Norman Smith and Ikhlas A. Khan

*Analytica Chimica Acta*, (2014), vol. 847, p. 61-72

## CHAPTER 6

### 6 Investigating Sub-2 $\mu$ m Particle Stationary Phase Supercritical Fluid Chromatography Coupled to Mass Spectrometry for Chemical Profiling of Chamomile Extracts.

#### 6.1 Introduction

Chamomile is globally consumed in the form of various tea products. Essential oils are commonly extracted for use in soaps, candles, perfumes and a variety of consumer products. The two most popular chamomiles are Roman Chamomile (*Chamaemelum nobile*) and German Chamomile (*Matricaria chamomilla*, syn. *Chamomilla recutita*) [194], each belonging to the *Asteraceae* family. While German chamomile is more commonly used both are important medicinal plants, and despite their similar properties, differ chemically [195].

Chamomile contains a wide variety of active constituents and a variety of these have been identified differentiating the two popular chamomiles. The active constituents are contained in the essential oil of German chamomile, which comprises, e.g., spasmolytic sesquiterpene alcohols such as  $\alpha$ -bisabolol, chamazulene, farnesene, polyacetylenes and several flavonoids [196]. Roman chamomile contains, among other constituents, several SLs, the most abundant of which is nobilin, flavonoids, the allergenic  $\alpha$ -pinene, limonene and bisabolol [195, 197]. Two spirocyclic polyacetylenes, the isomeric *cis*- and *trans*-tonghaosu, have been identified from the chamomile flower extracts with the *trans* isomer being more predominant than the *cis* form [198]. The lipophilic flavone chrysosplenetin/chrysosplenols was identified from German chamomile [199]. Roman chamomile is made up mainly from esters of angelic and

tiglic acids. It also contains up to 0.6% of sesquiterpene lactones of the germacranolide type, mainly nobilin and 3-epinobilin [200].

The common constituents of German and Roman Chamomiles are based on sesquiterpene and derivatives of sesquiterpene. Sesquiterpene lactones (SLs) are bicyclic molecules consisting of a sesquiterpene backbone (15 carbon atoms) in the form of a 10-membered ring attached to a five-membered lactone Figure 6.1.

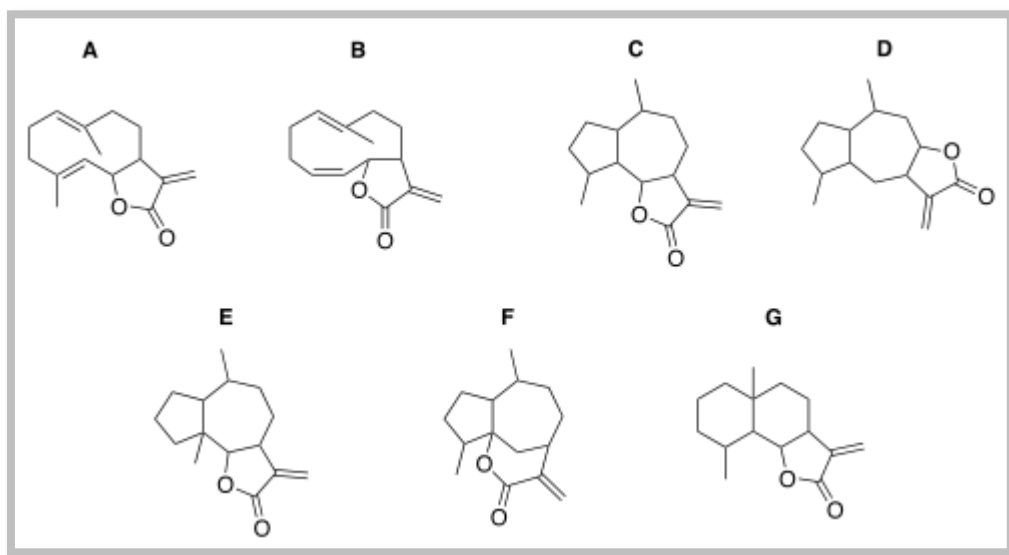


**Figure 6.1: Structures of some sesquiterpene lactones: A. Germacranolides, B. Heliangolides, C+D: Guaianolides, E: Pseudoguaianolides, F: Hypocretenolides, G: Eudesmanolides**

They represent the main allergen in the flower family *Asteraceae*. Arnica, chicory, tansy, and chamomile are some important members of this family [201]. They are important constituents of essential oils that have many applications in medical, as well as soap and perfume formulations. Often these constituents occur in trace quantities in plants. Even though chamomile extracts are widely used in herbal remedies and cosmetics, the risk of

sensitization/elicitation of dermatitis seems to be low based on published reports [202]. Presumably, cases of sensitization are primarily caused by SLs, but prolonged or repeated topical application seems necessary in order to sensitize with the tea because of its lower content of allergens [203].

Effective chromatographic techniques are required for optimal separation, identification and isolation of these components. Gas chromatography is the most efficient chromatographic technique for separating volatile mixtures, because of its high peak capacity and the availability of universal detection using flame ionization detection (FID). High performance liquid chromatography (HPLC) can be carried out when gas chromatography analysis of thermo-labile and/or non-volatile polar compounds is difficult to achieve. Supercritical fluid chromatography (SFC) and supercritical fluid extraction (SFE) have also been explored for targeted analysis and isolation of matricine in chamomile flower heads, thus streamlining the sample preparation workflow via eliminating the hydrodistillation of chamazulene and the multiple solvent-solvent extraction processes [204].

Important advances in liquid chromatography instrumentation have resulted in the worldwide implementation of sub-2 $\mu$ m particle columns, thus referencing the technique as ‘ultra’ high performance chromatography (UHPLC) [112, 205]. The enhanced instrument performance and the utilization of smaller particle size stationary phases provide practical benefits of reduced analysis time, increased resolution, and increased sensitivity [114, 206]. Historically, SFC instrumentation has lacked robustness. The previously reported results cited in the introduction of this thesis indicated poor reproducibility and poor sensitivity. The potential benefits of the technique were obvious in terms of reduced mobile phase viscosity

allowing for higher flow rates and faster analysis times. The applicability for chiral analysis was also known to be very attractive when compared to traditional normal phase LC approaches as demonstrated in Chapter 3, yet the general conclusions in recent decades suggested the technique was only suitable for use in academic research projects and never accepted as part of any sort of comprehensive workflow outside of the scope of utilizing it for unique use applications, preparatory scale isolations and chiral analysis applications.

In this study, a rapid and selective method was developed using sub-2  $\mu\text{m}$  particle columns and SFC technology coupled to photodiode array detection (PDA) and MS. The results provided insight for future botanicals profiling workflows. Liquid-liquid extraction techniques were performed on two types of authentic chamomile flowers, in which the optimal sample extraction procedure was chosen by measuring the maximum peak number and reproducibility of the chromatographic process. For comparative purposes, the orthogonality of the traditional reversed-phase approaches versus the SFC approach presented here was briefly assessed. Data was processed using multivariate statistical analysis techniques including principal component analysis (PCA) and orthogonal partial least squares-discriminate analysis (OPLS-DA) to assess differences between the authentic chamomile extracts. Reference standards were acquired and chromatographed in order to aid peak identification by comparing their retention time ( $R_t$ ), mass-to-charge ratio ( $m/z$ ), and spectral analysis of the fragment pattern of the constituents observed in the chamomile extracts. Structures of six of these compounds are shown in Figure 6.2. The methodology was applied to the authentic chamomile flowers and commercial tea products. Comparisons of the authentic flowers and commercial tea products were processed using the same multivariate statistical analysis techniques used to assess differences between the authentic chamomile extracts.



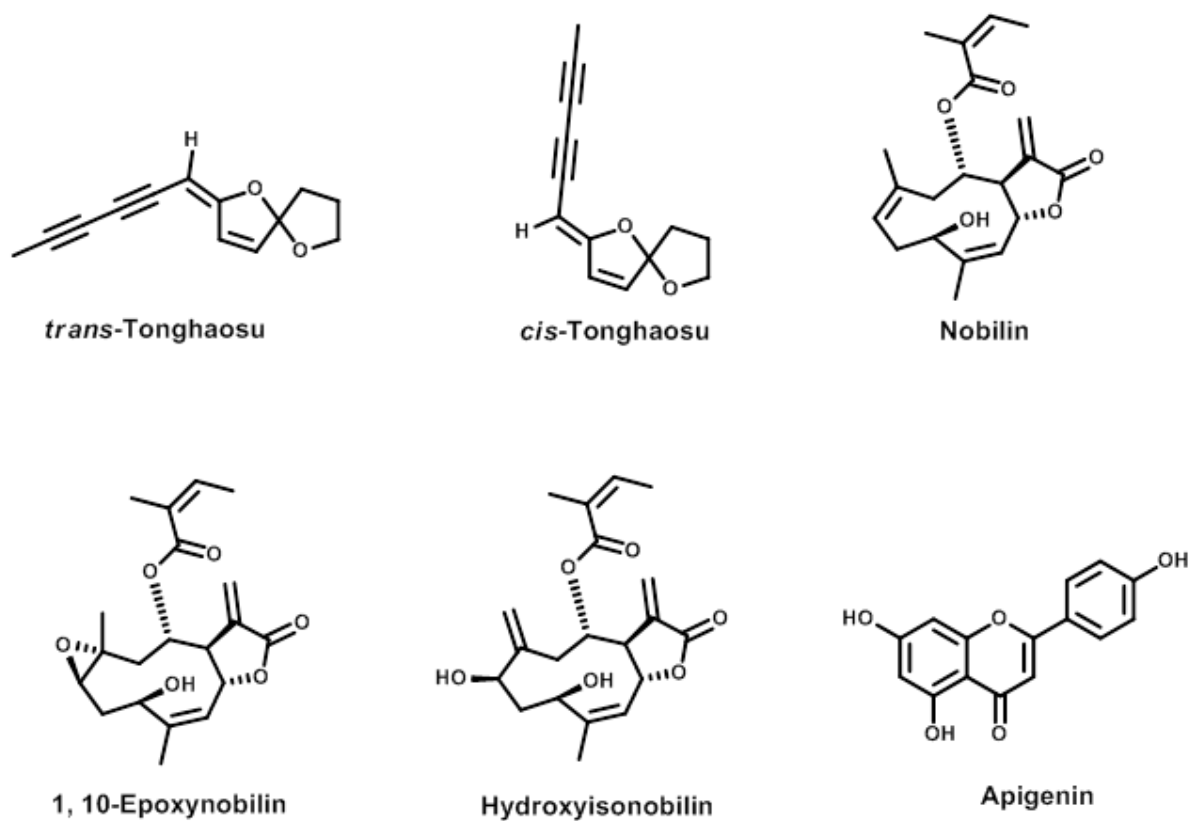


Figure 6.2: Structures of the standard reference compounds found in chamomile extracts

## 6.2 Materials and Methods

### 6.2.1 Solvents and reagents

Six standards were used as reference compounds and their structures are provided in Figure 6.2. The compounds apigenin, hydroxyisobavichalcone, 1,10-epoxyisobavichalcone, isobavichalcone, *cis*- and *trans*-tonghaosu were isolated at the National Center for Natural Products Research (NCNPR), University of Mississippi, University, Mississippi, USA. The identity and purity of these compounds were confirmed by chromatographic (TLC, HPLC) methods and spectrophotometric techniques (IR, 1D- and 2D-NMR, ESI-HRMS) by comparison with published spectral data. The purity of these isolated compounds was found to be greater than 90%. HPLC grade reagents such as acetonitrile, isopropanol, methanol, hexane, ammonium formate and formic acid were purchased from Fisher Scientific (Fair Lawn, NJ, USA). Water was purified using a Milli-Q system (Millipore).

### 6.2.2 Plant Materials

*Matricaria chamomilla* L (Syn. *Matricaria recutita* L.) (NCNPR code #9172, #11680, #11681) and *Chamaemelum nobile* (L.) All. (Syn. *Anthemis nobilis* L.) (#11577) samples were obtained from the cultivated, living collection of the NCNPR Maynard W Quimby Medicinal Plant Garden, University of Mississippi. All species were identified by Dr. Aruna Weerasooriya of the Maynard W Quimby Medicinal Plant Garden, 300 Insight Park Drive, The University of Mississippi, Mississippi, USA. Powder sample of *M. recutita* (#11781) was obtained from Missouri Botanical Garden, Missouri, USA. Powder sample of *M. recutita* (#7539) were obtained from Centre for Research in India System of Medicine (CRISM), India. Crushed flowerheads/powder samples of *M. recutita* (#2802, #9359, #9362, #9364, #9365) and *A. nobilis* (#2061, #9254) were obtained from commercial sources. Sample #9254

was identified as *A. nobilis* and samples #9172, #9359, #9362, #9364, #9365, and #2802 were identified as *M. recutita* by Dr. Vijayshankar Raman, NCNPR, The University of Mississippi, University, MS, USA. Tea bags (#9357, #9376, #9383-9391) claiming to contain chamomile were purchased online. Specimens of all samples are deposited at the NCNPR's botanical repository, The University of Mississippi, University, Mississippi, USA.

### **6.2.3 Sample Preparation**

Ten populations of German chamomile (*M. recutita*), three populations of Roman chamomile (*A. nobilis*), and eleven different commercial tea bags claimed as chamomile were used for analysis. Dry plant samples (about 500 mg) were sonicated in 2.5 mL of solvent. Four solvent mediums were evaluated: MeOH, iso-propanol, hexane and iso-propanol/hexane (50/50 v/v). Each preparation was sonicated for 30 minutes followed by centrifugation for 15 minutes. The supernatant was transferred to 20 mL scintillation vials. This procedure was repeated four times and respective supernatants combined. The samples were evaporated to dryness and reconstituted in 1.0 mL iso-propanol, vortexed, and sonicated for 15 minutes. Prior to injection, a 1 mL aliquot was passed through a 0.2 µm PTFE membrane filter and collected in 1.5 mL LC/MS certified sample vials.

## 6.2.4 Chromatography

Two chromatographic techniques were performed and compared for this chamomile profiling analysis, namely LC and SFC.

### 6.2.4.1 SFC Instrumentation

Supercritical fluid chromatography was performed using a Waters ACQUITY UPC<sup>2</sup><sup>®</sup> system (Waters Corp., Milford, MA, USA) including a binary solvent high pressure pump, a dual injector design autosampler, dual dynamic/static automatic back pressure regulator, (ABPR), column compartment with active heating and column switching control, and photodiode array detection (PDA). The experimental variables explored for the method development process are shown in Table 6.1. Concentrations and compositional mixes were varied as part of the method development investigations. All column dimensions were 100 mm × 3.0 mm ID and 1.7 µm particle size, with the exception of the UPC<sup>2</sup> HSS C<sub>18</sub> SB column which had a 1.8 µm particle size. The ACQUITY UPC<sup>2</sup> BEH 2-EP column was used for the comparisons to the UHPLC results.

**Table 6.1: Experimental variables for the method development investigation.**

Columns	Modifiers	Additives	
ACQUITY UPC <sup>2</sup> BEH	Methanol	Formic acid	Ammonium Hydroxide
ACQUITY UPC <sup>2</sup> PFP	Acetonitrile	Ammonium Formate	Isopropanylamine (IsPA)
ACQUITY UPC <sup>2</sup> HSS SB C <sub>18</sub>	Isopropanol	Ammonium Acetate	Triethylamine (TEA)
ACQUITY Shield RP <sub>18</sub>	Methanol/Isopropanol	Trifluoroacetic acid (TFA)	Diethylamine (DEA)
ACQUITY HSS Cyano	Methanol/Acetonitrile	Phosphoric acid	
ACQUITY UPC <sup>2</sup> 2-EP	Methanol/ Acetonitrile/ Isopropanol	Citric acid	Water

The final methodology for statistical analysis utilized an ACQUITY UPC<sup>2</sup> BEH 2-EP column (Waters Corp., Milford, MA, USA) with dimensions of 150 mm x 3.0 mm, and 1.7  $\mu$ m particle size. The column and sample temperature were maintained at 50 °C and 15 °C, respectively. The column was equipped with a pre-column filter and frit. The mobile phase consisted of CO<sub>2</sub> as solvent A and methanol: isopropanol (1:1) containing 0.5% formic acid as solvent B. The mobile phase flow rate was maintained at 1.7 mLmin<sup>-1</sup>. The gradient scheme was set initially at 95% A: 5% B, increasing linearly over 12 minutes to 80% A: 20% B and held isocratically for 3 minutes at 20% B. The total run time for analysis was 15 minutes. The backpressure was maintained isobarically by the automatic backpressure

regulator [referred to by the instrument manufacturer as the ACQUITY UPC<sup>2</sup> Convergence Chromatography Manager (CCM)] at a pressure of 1500 psi. The injection volume was 2  $\mu$ L. The photodiode array detection was monitored at a wavelength range from 190 - 400 nm with 2D wavelength collected at 350 nm.

#### 6.2.4.2 LC Instrumentation

The separations were performed on a 2.1 mm x 100 mm ACQUITY UPLC<sup>®</sup> 1.8  $\mu$ m HSS T3 column using an ACQUITY Ultra Performance LC Chromatography<sup>®</sup> (UPLC) System (Waters<sup>®</sup> Corporation, MA, USA). The column was maintained at 40 °C and eluted with a linear acetonitrile – aqueous gradient over 1.0 minute at 800  $\mu$ L/minute, starting at 5 % acetonitrile and rising to 95 % over the course of the gradient. The aqueous mobile phase was spiked with 0.1 % v/v formic acid. The column eluent was directed to the mass spectrometer for analysis following PDA detection.

#### 6.2.5 Mass Spectrometry

Mass spectrometry was performed using a Waters ACQUITY SQD single quadrupole mass spectrometer. The solvent flow was split post PDA detection, but prior to the MS electrospray probe. The MS electrospray ionization (ESI) source was operated in positive ionization (ESI+) mode. The capillary and cone voltages were set at 3.0 kV and 30 V, respectively. The temperature of the source and desolvation was set at 150 °C and 500 °C, respectively. The cone and desolvation gas flows were 50 and 800 L h<sup>-1</sup>, respectively. All data collected was acquired in centroid mode using Masslynx<sup>™</sup> Version 4.1 SCN 805 software (Waters Corp., Milford, MA, USA). The post PDA splitter allowed for introduction of a make-up flow used to aid ionization. The make-up flow composed of methanol with

0.1% formic acid delivered by a Waters 515 binary pump (Waters Corp., Milford, MA, USA).

### **6.2.6 Data Analysis**

The statistical analysis was performed using replicate preparations and replicate injections of each sample using the MS ESI<sup>+</sup> data. The multivariate analysis of each of the chamomile samples were facilitated using Waters MassLynx™ Software V.4.1 data acquisition whereas data processing was performed using the MarkerLynx™ XS Application Manager (Waters Corporation, Milford, USA). The software was set to analyze a retention time window of 0.5 - 12 minutes ( $\pm$  0.1 minutes) and a mass range threshold of 100-700 Da, ( $\pm$  0.02 Da). The noise elimination level was set at 10.00%. The resulting fingerprints for each sample were statistically compared by principle component analysis (PCA) to search for similar groupings. Distinctly different groupings were further compared by orthogonal partial least squares - discriminant analysis (OPLS-DA).

## 6.3 Results and Discussions

### 6.3.1 Chromatographic method development and optimization

Packed column SFC analysis of chamomile extracts or extracts of natural products with components similar to those found in chamomile extracts are rarely published [207]. General approaches to SFC method development have been previously reported by Berger *et al* for polymers as well as providing an insight into the use of additives [48, 95]. West *et al* provided an extensive set of results using Linear Solvation Energy Relationship (LSER) modeling characterizing stationary phases and mobile phases as it relates to solute retention [129, 131]. Each column used during their investigation had different combinations of physiochemical properties including hydrophobicity, silanol activity, hydrolytic stability, polarity and chemical mechanisms that will affect selectivity and retention of the solutes [128, 132, 134, 150]. Their conclusions provided insight and expectations to developing a systematic method development approach that could be applied to natural product profiling. In these experiments, method development was initially carried out using a “trial by error” approach; *yet educated by guidance from the previous citations*, to gain a better understanding of the supercritical fluid chromatographic technique and to validate previous reports by West and Berger. Chromatographic trends addressing selectivity, resolution and peak shape were identified following many experiments involving the stationary phase, modifier and additives.



#### 6.3.1.1 *Effect of Elution Solvent and Solvent Blends without Additive*

The elution solvents investigated, typically referred to as co-solvent or modifier, were neat organic solvents such as methanol, acetonitrile, iso-propanol, and compositional mixtures of each organic solvent. Injections investigating shallower gradient profiles resulted in minimal chromatographic advantages. The retention and selectivity profile of SFC dictates that the greatest selectivity changes occur within 0% modifier and 10% modifier, analogous to the profile observed for HILIC methodology, another normal phase derived technique. The modifier starting percentage at 1% versus 5% did not result in beneficial increases in resolution between peaks (Figure 6.3). Retention was observed to shift closer to the void volume marker as the starting percentage of organic modifier was increased with some gains in selectivity. Addition of a less polar elution solvent such as acetonitrile or iso-propanol to the stronger elution solvent methanol resulted in increased retentivity and general improvements in resolution between peaks eluting with greater than 10% modifier. Little to no retentivity effects were observed in the early eluting region of the chromatogram, or the ‘non-polar’ region of the chromatogram. Unfortunately, the peak shape of many of the later eluting (polar) peaks exhibited severe peak tailing for all ‘neat’ modifier experiments.

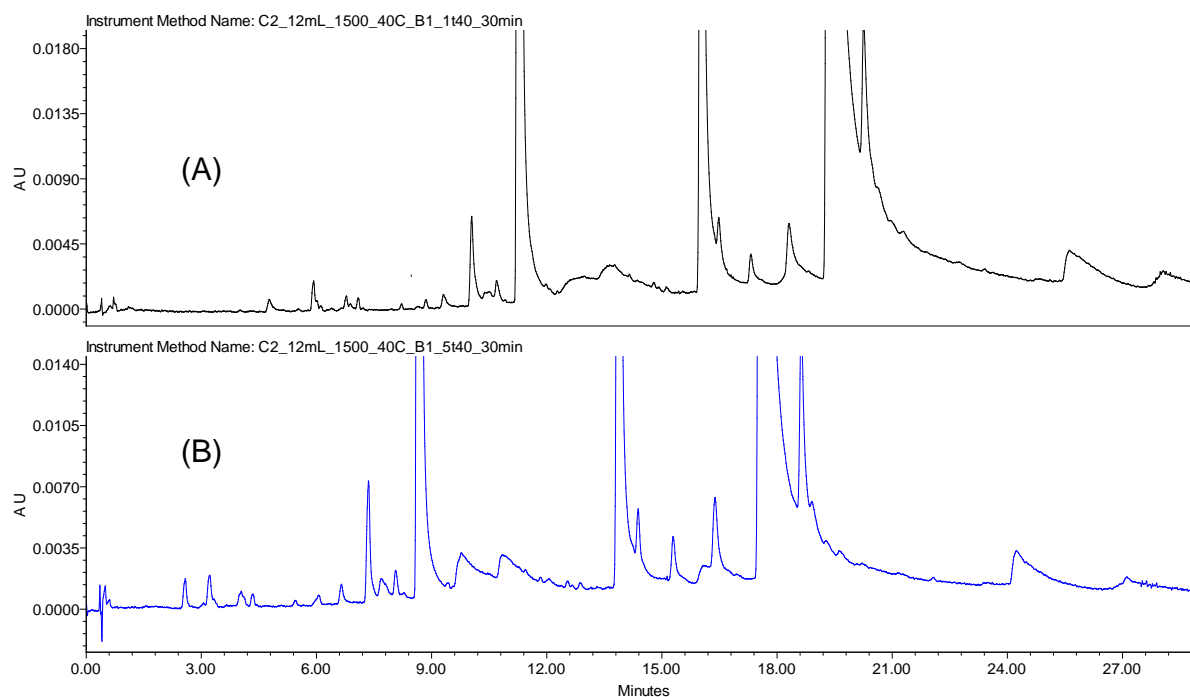


**Figure 6.3: UPC<sup>2</sup> UV chromatograms of Roman chamomile comparing different gradient profiles (A) 1% to 40% methanol modifier and (B) 5% to 40% linear gradient over minutes eluted with a methanol modifier.**

#### 6.3.1.2 Effect of Elution Solvent with Additives

The diversity of the solutes in the chamomile extract required an additive to mitigate unwanted peak tailing hypothesized as retention mechanism related. At the same time, the objective was to develop a method compatible with mass spectrometry (MS) detection. The MS compatible additives investigated were formic acid, ammonia, ammonium formate, ammonium acetate, water, and combinations thereof. The addition of formic acid visibly improved the peak shape for all the tailing peaks. Ammonium salts such as ammonium formate and ammonium acetate further improved the peak shape, however the solubility of the salt additive had to be considered when mixtures of modifier were used. For example, the system would overpressure during the equilibration segment at the start of the gradient when programmed below 8% modifier with methanol:iso-propanol (60:40) spiked with 10mM ammonium formate. Lower starting percentages of modifier can be used in the gradient

program when the composition of the weaker elution solvent in the modifier (e.g.: IPA) was decreased, thus decreasing the occurrence of salt insolubility within the flow path. Formic acid as an additive provided similar results to the ammonium formate and ammonium acetate additives without the risk of salt precipitation. During the investigation of formic acid as an additive, higher concentrations such as 0.5% rather than 0.1% provided better peak shapes. The addition of water at percentages lower than 2%, also provided good improvements in peak shape (Figure 6.4).

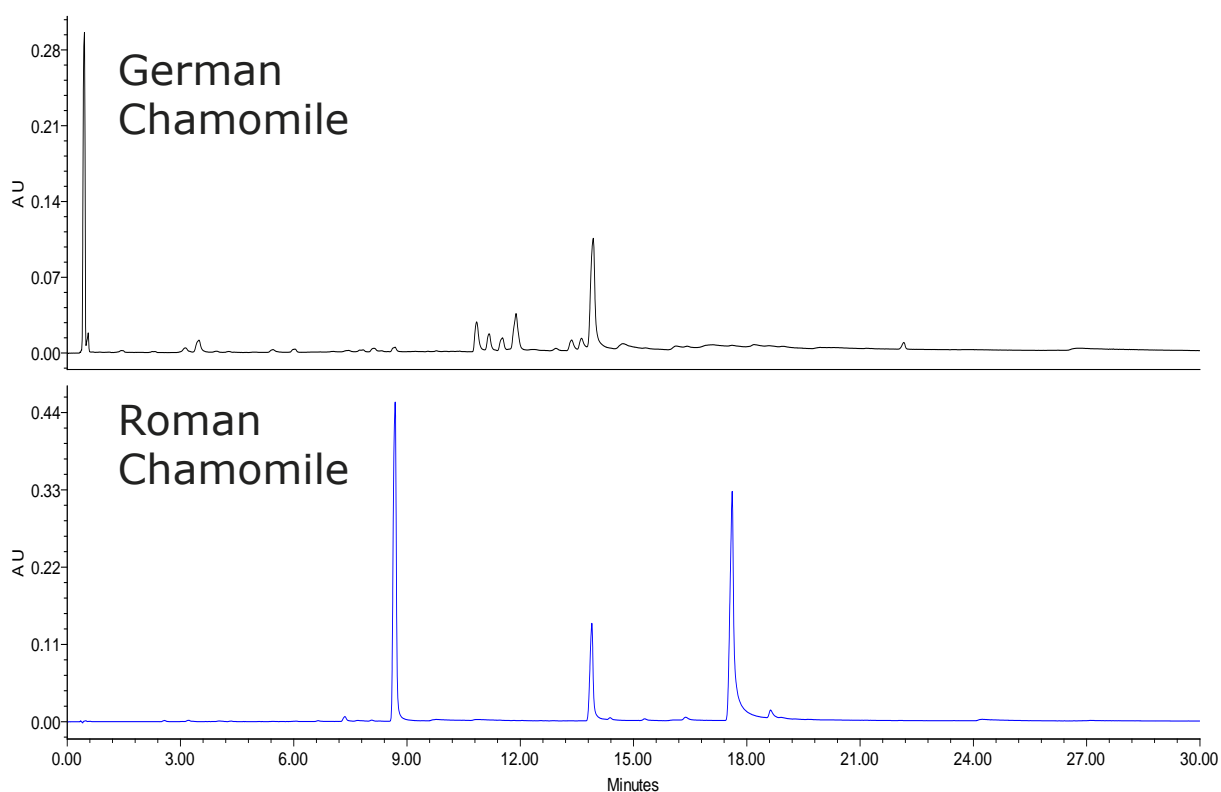


**Figure 6.4: German and Roman chamomile UPC<sup>2</sup> UV Chromatograms. Conditions: UPC<sup>2</sup> column 1.7  $\mu$ m 2-EP 2.1 x 150 mm; . Flow rate was 1.2 mL min<sup>-1</sup> at 40 °C. 1500 psi backpressure. Gradient performed with a slope profile of 5 to 40% modifier. Co-solvent was MeOH: ACN (90:10) with 0.05% H<sub>2</sub>O.  $\lambda$ =350nm.**

The water additive appeared to stabilize retention time instability for repeatable injections. Although the results with the water additive observed to be promising, peak tailing increased over time affecting the repeatability of the method (Figure 6.5). Although this phenomenon was observed from a general perspective, further investigations regarding water as an additive should be explored with controlled experiments outside the scope of this investigation to best determine the effect of water on long term column effects.

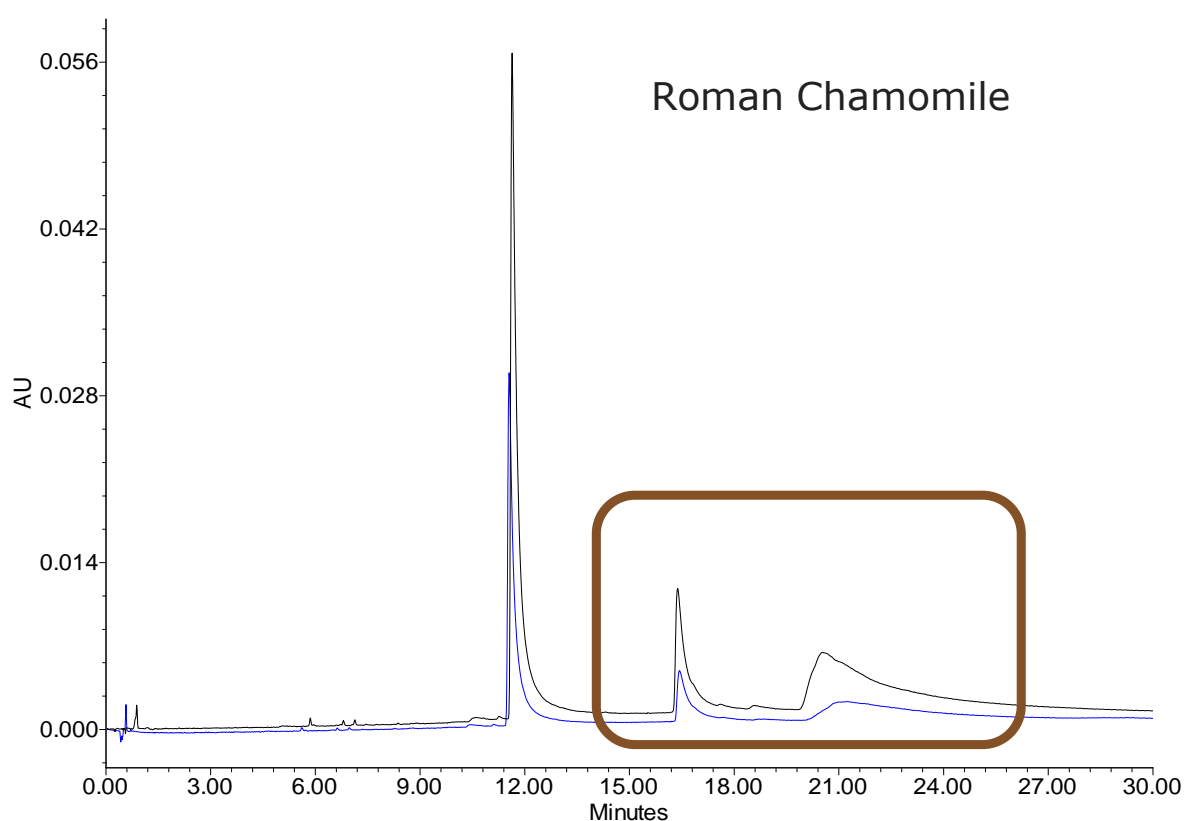


**Figure 6.5: Roman Chamomile UPC<sup>2</sup> UV Chromatogram. Evidence of increasing peak tailing over time highlighted in the rectangular box. See Figure 6.4 for conditions.**

Upon further literature reviews, research (Zhimin *et al*) showed the use of phenyl columns with ethanol elution solvent spiked with 0.05% phosphoric acid improved the peak tailing observed in their SFC separation of flavonoids extracted from Ginko Biloba leaves [208].

Additionally, the previously cited investigation of polyphenolic compounds in grape seed extracts used a diol stationary phase comparing methanol elution solvents spiked with citric acid, formic acid, and trifluoroacetic acid (TFA) [207]. A series of untypical and non-MS compatible buffers known to suppress ionization were briefly investigated, and these produced cluster ions or lacked volatility. Low concentrations of trifluoroacetic acid (0.05% to 0.1%), citric acid (5 mM to 50 mM), and phosphoric acid (0.001% to 0.1%) based additives in 100% methanol, provided improvements in peak shape and minimized peak tailing. Each of these additives have ion pairing properties and/or chelating properties sequestering secondary retention mechanisms hypothesized as effects from either residual silanol or hydrogen bonding with the solutes. Although these additives are not typically suitable for MS, knowing these additives improve chromatographic peak shape enabling UV analysis and quantitation when standards are available for the compounds previously identified by the MS compatible method. Interestingly, similar conditions to Zhinin's phenyl column and phosphoric acid conditions were performed as part of the chamomile method development screening investigation, but initially produced poor results, therefore the principles of ion pair reagents and chelating property additives for this methodology was further explored.

#### *6.3.1.3 Investigating Phosphoric Acid Additive Effects*

**During the previous screening experiments, an injection of the German chamomile using a UPC<sup>2</sup> CSH Flouro-Phenyl column with 0.05% phosphoric acid in methanol was performed with a 3  $\mu$ L injection volume. The results showed broad peaks in comparison to the other screening results (not shown) and poor resolution (Figure 6.6). Injection overload was hypothesized to be affecting the observed outcome of the observed results, therefore reduced injection volumes were performed using the flouro-phenyl and phosphoric acid conditions. The 1 $\mu$ L injections of the chamomile extracts resulted in much improved peak shapes and chromatographic resolution between peaks (**

Figure 6.7). Unfortunately, upon repeated injections and further method development, system pressure would increase over the course of a few days. A new column was introduced and repeated injections performed resulted in the same system pressure failures over less than 200 injections. The columns were not able to be regenerated with various flush sequences. System level diagnostic tests were also performed to evaluate the pump seal quality. Interestingly, the diagnostic tests indicated massive leak rates and failures. Changing the pump seals corrected the leak rate failures, thus leading to a hypothesis of phosphoric acid detrimentally affecting the integrity of the seal in presence of CO<sub>2</sub> based mobile phases. The system was set up to run just the mobile phase conditions with a union installed in place of the column. The system would eventually fail the diagnostic leak rate tests performed on the pump seals within the delivery of 2 litres of solvent. Comparisons of 0.005%, 0.01%, and 0.05% concentration of phosphoric acid each led to the same system level failures on the pump component. The issue was repeatable on a separate system and by a separate analyst as a request to better understand any localized issues. It is unclear why this particular mobile phase composition deteriorates the pump seals more rapidly. It is possible that carbonic acid is being produced and working together with the phosphoric acid to produce a more corrosive environment attacking the metal components within the system. The compositional make-up of the UPC<sup>2</sup> instrument components is not documented, therefore making it difficult to formulate an efficient investigation. The system was purged from the phosphoric acid in methanol modifier and replaced with MS compatible buffers to continue the chamomile profiling analysis. These results indicated the need for caution when developing SFC methods for use with natural product extracts. Extra considerations concerning the injection volume and loadability should be investigated.

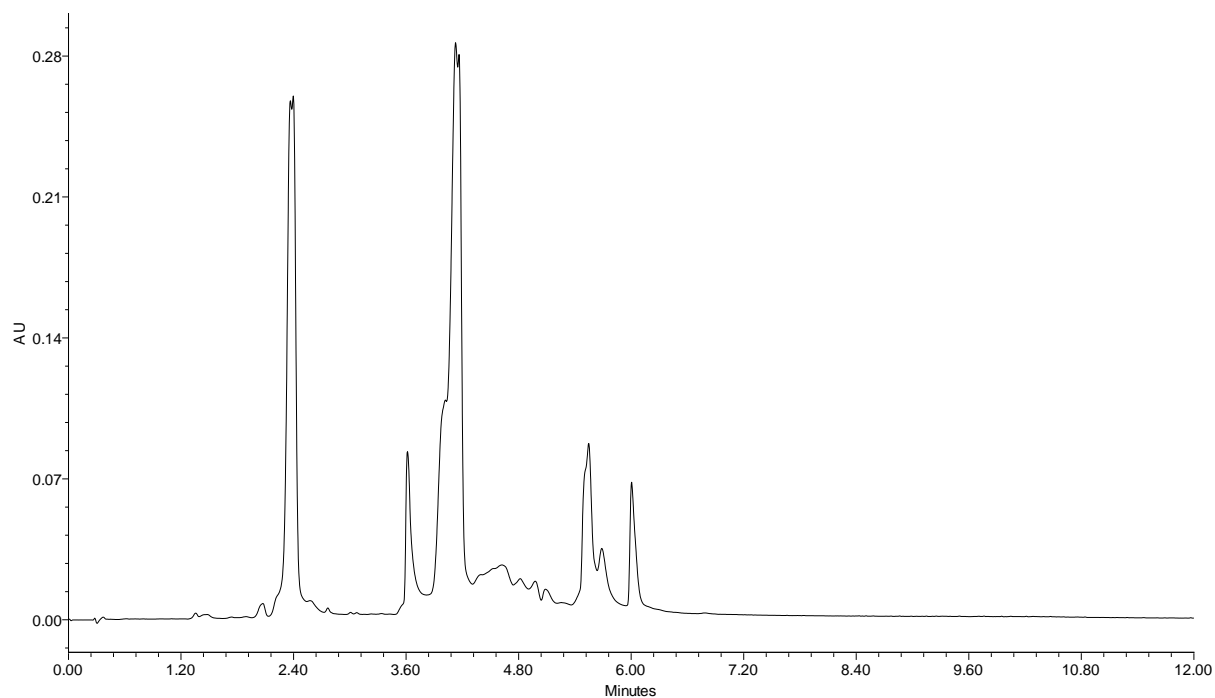


**Figure 6.6:** UPC<sup>2</sup> UV chromatogram using the 3µL injection of German chamomile extract

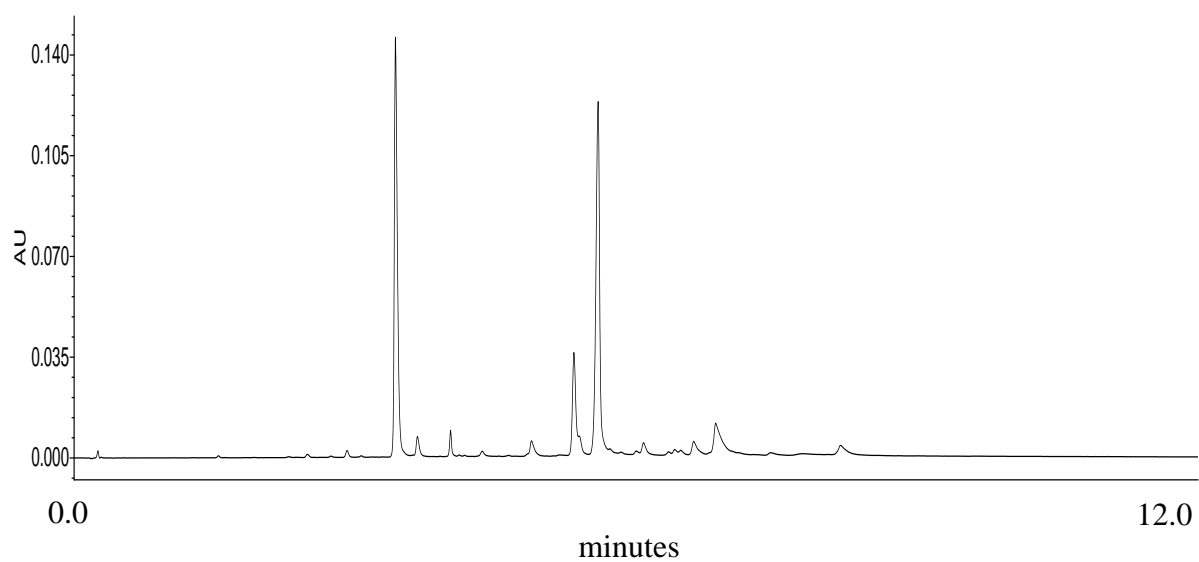


**Figure 6.7:** UPC<sup>2</sup> UV chromatogram using the 1µL injection of German chamomile extract

### 6.3.2 Effect of Column Temperature

Temperature was observed as a key factor affecting mainly retention time, peak shape and signal to noise. The optimization process investigated the effect of column temperature and backpressure as exerted by the ACQUITY UPC<sup>2</sup> CCM. Increased temperature, (*back-*) pressure, or any combination of each variable resulting in density changes did not yield major gains in resolution of the complex chamomile extract chemical profile. The increase in temperature allowed for a decrease in overall system pressure, thus allowing for increases of flow rate or column length within the allowable upper pressure threshold of the instrumentation specification of 41.4 MPa (or *6000 psi as specified by the manufacturer*). For example, the retention time shifted for the three major constituents, apigenin-7-*O*-glucoside, chamaemeloside, and apigenin, found in the authentic Roman chamomile by an average of 4 minutes later for a column temperature set to 90 °C when compared to the chromatographic results obtained when the column temperature was set to 35 °C (Figure 6.8).



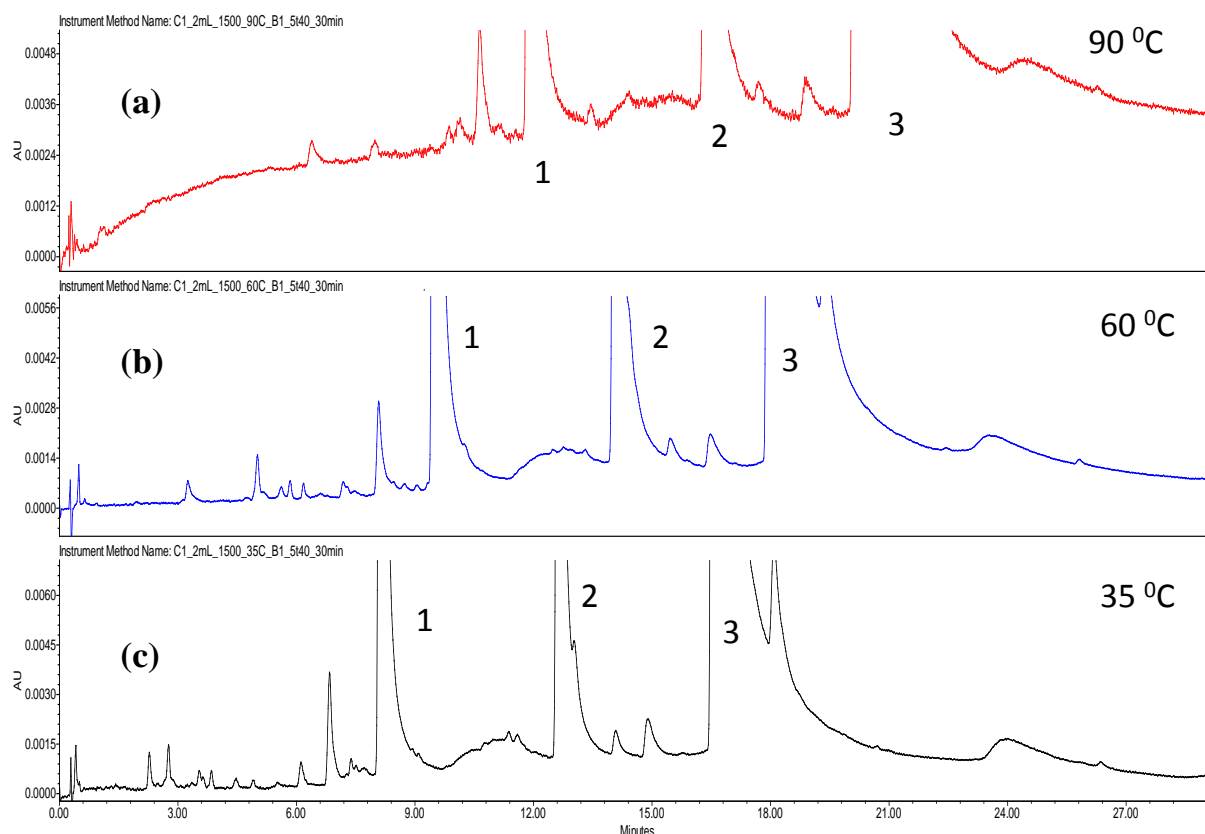


**Figure 6.8:** Chromatograms of Roman chamomile methanolic extracts labeled (a), (b), (c) show the retention time shift and the increased baseline noise with the increase of temperature for the major compounds found in roman chamomile, where peak 1 is apigenin, peak 2 is apigenin-7-O-glucoside, and peak 3 is chamaemeloside.

The increase in temperature affected the baseline noise thus reducing the measured signal-to-noise (S/N) values. This effect was believed to be the result of the rapid supercritical fluid CO<sub>2</sub> expansion as it exchanged to the gas phase thus creating a greater occurrence of CO<sub>2</sub> gas in the PDA flow cell. A column temperature of 50 °C provided the optimal choice for maintaining a similar experiment to experiment comparison of signal-to-noise across a temperature range between 35 °C and 50 °C. Therefore, 50 °C was chosen in regards to suppressing the baseline noise caused by rapid CO<sub>2</sub> expansion while maximizing the operating parameters of the instrument in terms of the upper pressure threshold.

### 6.3.3 Summary of Method Optimization

In summary, the final methodology was based on a set of conditions that provided retentivity, resolution, and suitable peak shape for the greatest number of peaks detected in the profiles while still providing compatibility with MS detection. The trends observed from the dozens of experiments performed using the variables outlined in Table 6.1, resulted in confirming the general method development workflow proposed in Chapter 3 and proved feasible for development of natural product profiling methods. It was evident that screening columns with a set of modifiers and additives maximized changes in retentivity and selectivity of the detected peaks in the chamomile extract chromatographic profile. Initially, six columns were investigated, yet the ACQUITY UPC<sup>2</sup> BEH 2-EP, provided the best option for further method optimization in terms of retention of peaks, overall number of peaks detected and optimal peak shape, specifically in the later eluting ‘polar region’ of the chromatogram. Combining iso-propanol and methanol as the modifier fine-tuned overall increases in resolution between peaks. The addition of formic acid improved peak shape without the risk of salt precipitation resulting from imbalances in salt concentration, CO<sub>2</sub> composition and insolubility with particular weaker elution solvents used in combination with methanol modifiers. Based on the optimization of the optimal operating column temperature value, the column length was increased to 150 mm allowing for an increase in overall resolution of the chemical profile.

### 6.3.4 Sample preparation optimization

Various extraction media were explored using the developed chromatographic method in order to profile the extracts. The chromatographic comparison of the different extraction procedures are shown for *M. recutita* #9172 in Figure 6.9. The solvent mixture of hexane/iso-propanol (1:1) provided the best balance of polar and non-polar solutes extracted while providing optimal peak shape. The chromatographic comparisons of the *A. nobilis* extractions (*not shown*) resulted in the same conclusions.

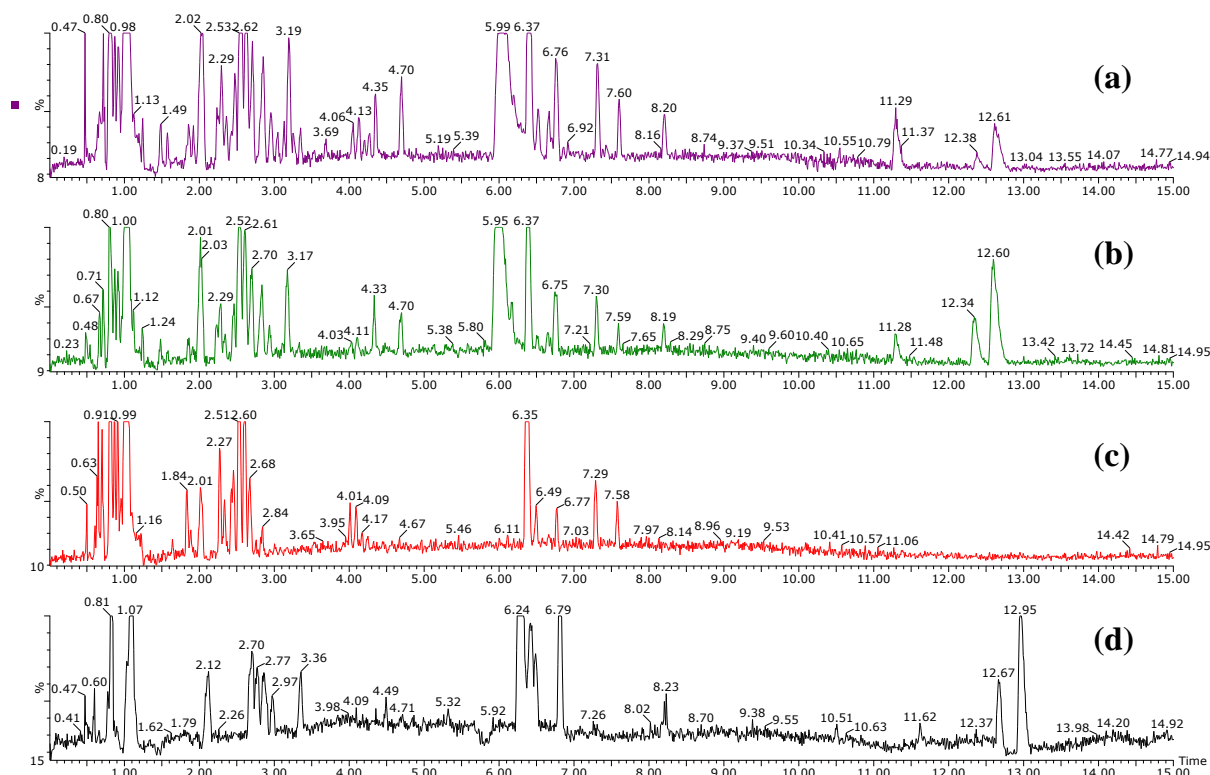


**Figure 6.9: Comparison of UPC<sup>2</sup>-MS ESI+ base peak intensity chromatogram (BPI) Roman chamomile extracts prepared using different solvents (a) isopropylalcohol/Hexane (b) isopropylalcohol, (c) hexane, and (d) methanol.**

### 6.3.5 Chromatographic Technique Comparisons

The orthogonality to reversed-phase liquid chromatography was briefly investigated. The chamomile extracts were analyzed using a generic UPC<sup>2</sup> 0 %B to 35% B gradient elution method composed of MeOH and 0.1% formic acid in solvent line B and a generic UHPLC 5 %B to 95 %B gradient elution method composed of 0.1% formic acid in water in solvent line A and 0.1% formic acid in methanol in solvent line B. Both chromatographic run times were 35.0 minutes. The orthogonality between the two chromatographic techniques was investigated by tracking the peak elution order of the solutes by UV and MS. Each peak was assigned a nominal peak ID and retention times were recorded for each UHPLC and UPC<sup>2</sup> result. The data was plotted as retention time vs. peak ID to visualize the orthogonality of the separation techniques (Figure 6.10). The UPC<sup>2</sup> elution profile showed a scattered relationship rather than a direct inverse linear relationship to that of the UHPLC technique. It is uncertain why this occurs, but the hypothesis assumes that the factors dictating the retention mechanisms in the non-polar and polar regions of the UPC<sup>2</sup> chromatogram shift from stationary phase focused to modifier focused.

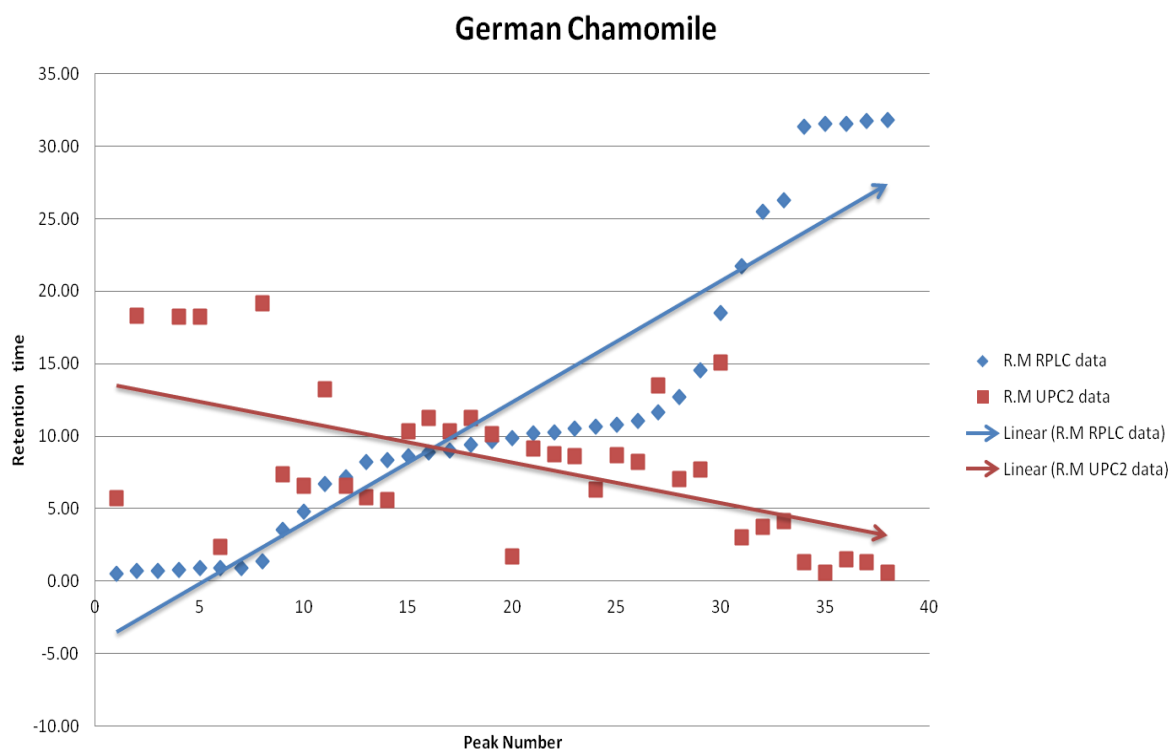


**Figure 6.10:** Comparison plot of peak ID vs. retention time for the UPC<sup>2</sup> and UHPLC chromatography results for the extracts of German Chamomile.

Further interrogation of both datasets showed better chromatographic separation of four isobaric compounds with a mass of 474.41 Da: 7-[(3-*O*-acetyl- $\beta$ -D-glucopyranosyl)oxy]-apigenin, 7-[(4-*O*-acetyl- $\beta$ -D-glucopyranosyl)oxy]-apigenin, Apigenin-7-*O*-(6'-acetyl) glucoside, and Apigenin 7-*O*-(2''-acetyl- $\beta$ -D-glucoside). The UPC<sup>2</sup> analysis of German chamomile separated the four isobaric peaks for XIC = 475 Da, whereas the UHPLC MS XIC  $m/z$  = 475 Da only separated three of the isobaric species (Figure 6.11).

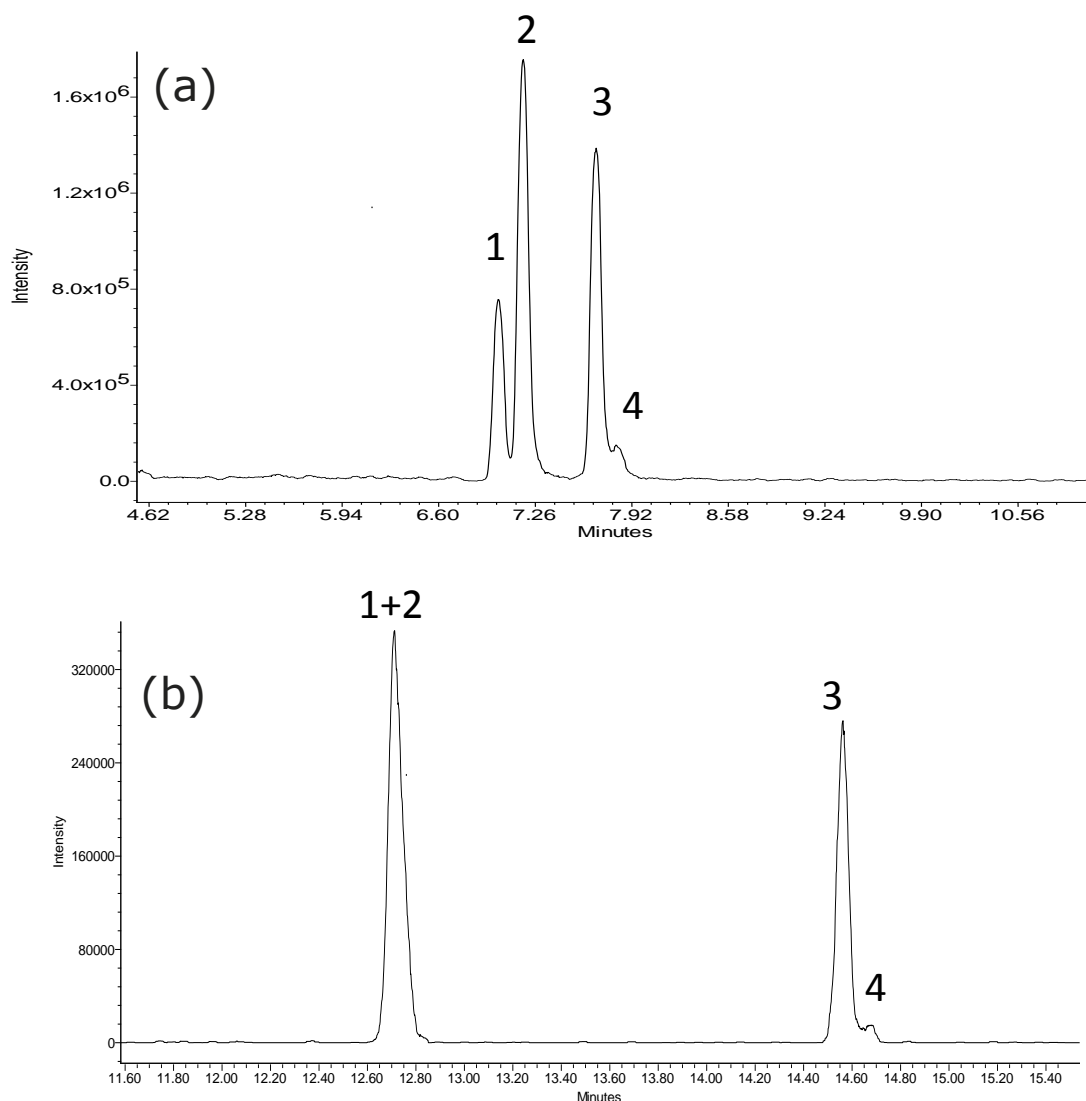


**Figure 6.11: Zoomed extracted ion chromatograms (XIC) of  $m/z = 475$  of German chamomile methanolic extract. An additional isobaric peak was identified in the UPC<sup>2</sup> trace (A) when compared to the UPLC-RP trace (B).**

### 6.3.6 Statistical Analysis

A workflow similar to that published by Plumb *et al* which outlines pattern recognition for pharmaceutical impurity profiling was followed with the exception of using nominal mass data *in substitution* for accurate mass data [209]. The data was processed in terms of pairing descriptive information such as nominal mass to charge ratios ( $m/z$ ) and retention time (Rt) thus creating a chemical ‘feature’ descriptor. All chemical features are populated into a table

for further statistical analysis. Initially two plant samples (#9172 and #9254) were checked for intra- and inter-day variations. Intra- and inter-day variation of the analysis was determined to be lower than 5%, with a maximum RSD of 4.0%. The analysis was performed three times on three different days and each run was repeated in duplicate. Multiple injections showed that the results are reproducible and displayed a low standard error. The additional samples used for the profiling experiments were prepared in the same way and injected in duplicate.

Principle component analysis (PCA) is an unbiased clustering technique requiring little prior knowledge of a data set and acts to reduce the complexity of the multivariate data without losing important information [210]. PCA generates visual plots, a scores plot and a loadings plot. The scores plot summarizes observations in terms of trends, patterns and clusters in the dataset as it separates the signal from the noise. The loadings plot correlates the variables with the observations in the scores plot. The numerical value of a loading for a given variable of a PC shows how much the variable has in common with that component.

The three authentic extracts of Roman chamomile with distinct sesquiterpenes, were distinguished from the ten extracts of authentic German chamomile as shown by the OPLS-DA scores plot in Figure 6.12, thus confirming the proof of concept that UPC<sup>2</sup>-MS methodology is reproducible and information-rich for multivariate statistical analysis. Generally, this clustering was observed using the first two principal components (**70% of the variance was explained**). Examination of the scores **and** loading plots showed as expected that the main separation from both flowers were sesquiterpene and flavonoid compounds.

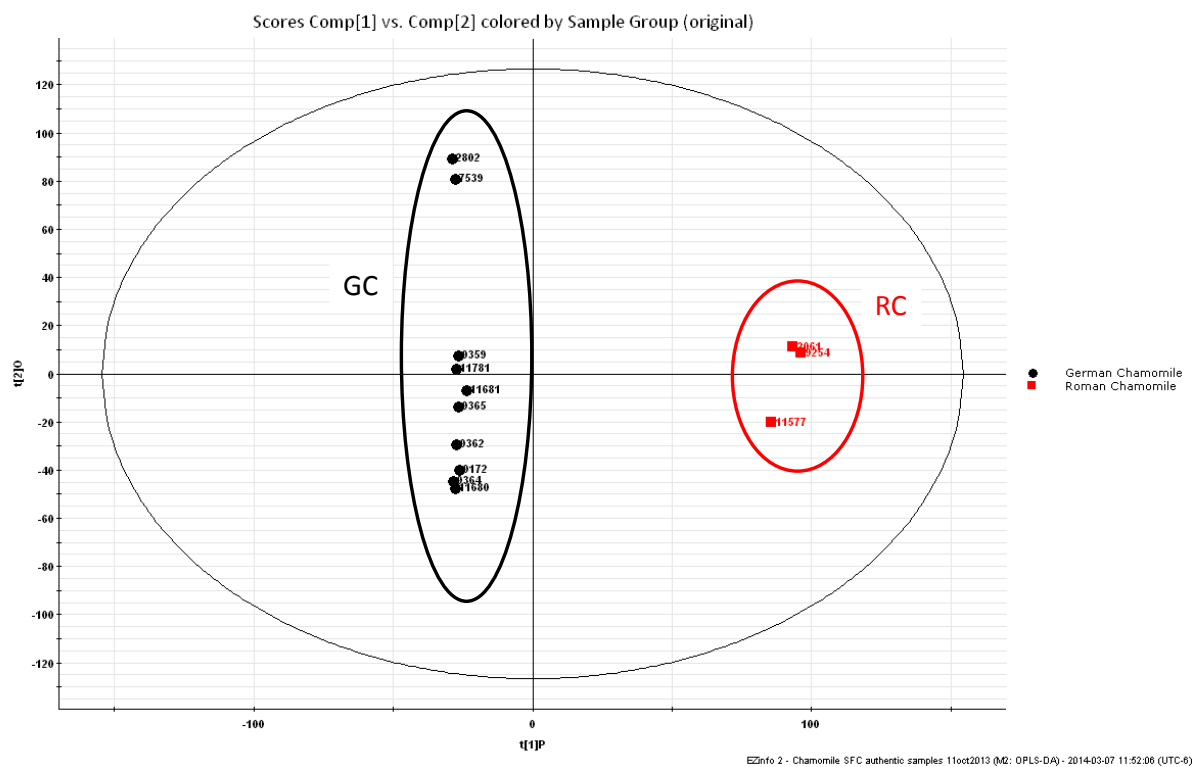


**Figure 6.12: PCA scores plot (PC-1 vs. PC-2) of the authentic German chamomile (GC) and authentic Roman chamomile (RC) extracts**

A scatter plot (S-Plot) was generated from the OPLS-DA data to further identify differences from the two sample groupings. The S-plot utilizes the mass/retention pairs to aid visualization of the variables contribution. A mass/retention pair contribution is shown in the y axis where correlation to the class or group is calculated to a maximum of 1. The S-plot for the German and Roman chamomile data set is shown in Figure 6.13.



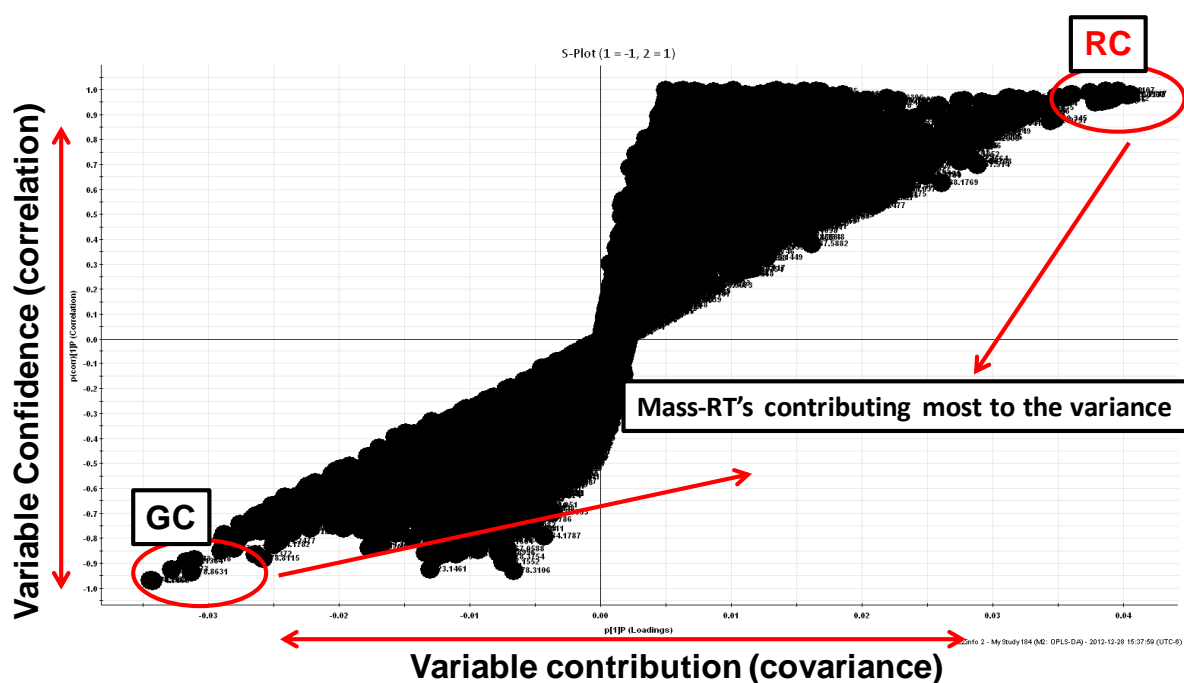


**Figure 6.13:** Scatter plot (S-plot) of German and Roman chamomile generated from the OPLS-DA statistical analysis of the dataset

### 6.3.7 Mass Spectrometry Analysis

The specificity of the MS data was sufficient in terms of interrogating the data by extracted ion chromatograms (XIC). Peaks were assigned by spiking the samples with standard compounds and comparing the retention times and mass. The UPC<sup>2</sup>-MS method was set to record  $[M+H]^+$  and  $[M+NH_4]^+$  ions typically observed in natural product profiling. Each were observed in ESI<sup>+</sup> mode with the following observed  $m/z$  and Rt values:  $m/z = 201$  Da ( $[M+H]^+$ , Rt = 0.95 min),  $m/z = 201$  Da ( $[M+H]^+$ , Rt = 1.22 min),  $m/z = 364$  Da ( $[M+NH_4]^+$ , Rt = 2.51 min),  $m/z = 380$  Da ( $[M+NH_4]^+$ , Rt = 2.85 min),  $m/z = 380$  Da ( $[M+NH_4]^+$ , Rt = 2.99 min),  $m/z = 378$  Da ( $[M+NH_4]^+$ , Rt = 3.40 min),  $m/z = 396$  Da ( $[M+NH_4]^+$ , Rt = 4.93 min),  $m/z = 380$  Da ( $[M+NH_4]^+$ , Rt = 6.18 min),  $m/z = 380$  Da ( $[M+NH_4]^+$ , Rt = 6.32 min),  $m/z = 396$  Da ( $[M+NH_4]^+$ , Rt = 8.45 min, 8.95min), and  $m/z = 271$  Da ( $[M+H]^+$ , Rt = 10.93).

The fragmentation patterns observed in the mass spectrum were useful in characterization of these compounds. Sesquiterpenes; composed of chemical markers **3** thru **10** of Table 6.2, showed the fragment ion less of 100 Da due to loss of angeloyl or tigloyl group. For example, 1,10 – epioxynobilin has the same observed  $m/z$  value as hydroxynobilin. The proposed fragmentation pathway for 1,10-epioxynobilin versus the isobaric counterpart of hydroxynobilin is shown in Figure 6.14.

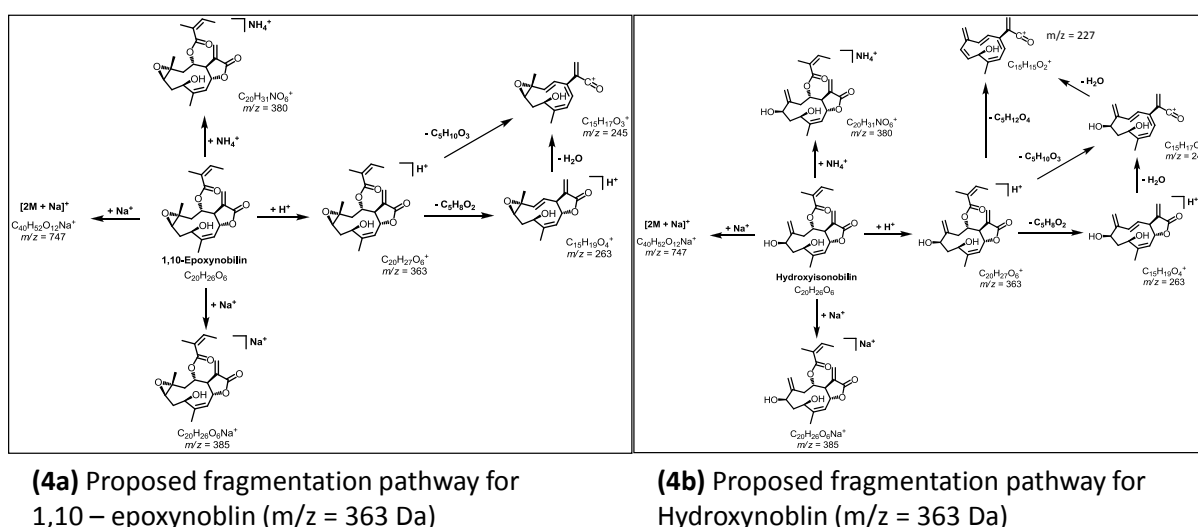


**Figure 6.14:** Proposed fragmentation pathways for the two isobaric species, (4a) 1,10-epioxynobilin and (4b) hydroxynobilin.

Components identified as a major contribution to the variance were identified as apigenin, 1,10-epioxynobilin, hydroxyisonobilin, nobilin, and other unknown compounds (Table 6.2).

**Table 6.2: Qualitative analysis of German (GC) and Roman (RC) chamomile using UPC<sup>2</sup>/MS, UPLC/MS, and GC/MS.**

#	UPC <sup>2</sup> Rt (min)	Compound Name	MS (m/z) [M+H] <sup>+</sup> or [M+NH <sub>4</sub> ] <sup>+</sup>	UPC <sup>2</sup> -MS		UHPLC-MS		GC-MS	
				M.r.	A.n.	M.r.	A.n.	M.r.	A.n.
1	1.10	<i>trans</i> -dicycloether	201	+	+	+	+	+	+
2	1.34	<i>cis</i> -dicycloether	201	+	+	+	+	+	+
3	2.56	nobilin	347/364→247	-	+	-	-	-	-
4	2.75	1,10-epioxynobilin	363/380→263	-	+	-	-	-	-
5	3.03	Unknown 1	363/380→263	-	+	-	-	-	-
6	3.58	Unknown 2	361/378→261	-	+	-	-	-	-
7	5.12	Unknown 3	379/396→279	-	+	-	-	-	-
8	5.99	hydroxyisonobilin	363/380→263	-	+	-	-	-	-
9	6.36	3-epihydroxyisonobilin	363/380→263	-	+	-	-	-	-
10	8.65	Unknown 4	379/396→279	-	+	-	-	-	-
11	9.13	Unknown 5	379/396→279	-	+	-	-	-	-
12	11.92	apigenin	271	+	+	+	+	-	-

The unknown compounds are hypothesized as stereoisomers, diastereomers and/or enantiomers related to 1,10-epioxynoblin and hydroxyisonoblin based on the common fragments observed from in-source fragmentation of the single quadrupole data. The

fragment analysis of hydroxynobilin confirms the loss of  $-C_5H_{12}O_4$  which would be inconsistent with the proposed fragmentation pathway and observed spectra for 1,10-epoxynoblin (Figure 6.14). The compounds were identified by comparing their retention times and characteristic MS spectral data for the four isobaric compounds with  $m/z = 363$  Da and the two isobaric compounds with  $m/z = 379$  Da. The three extracts of the authentic Roman chamomile showed the presence of the 6 known compounds (Figure 6.2) and the 5 new unknown compounds.

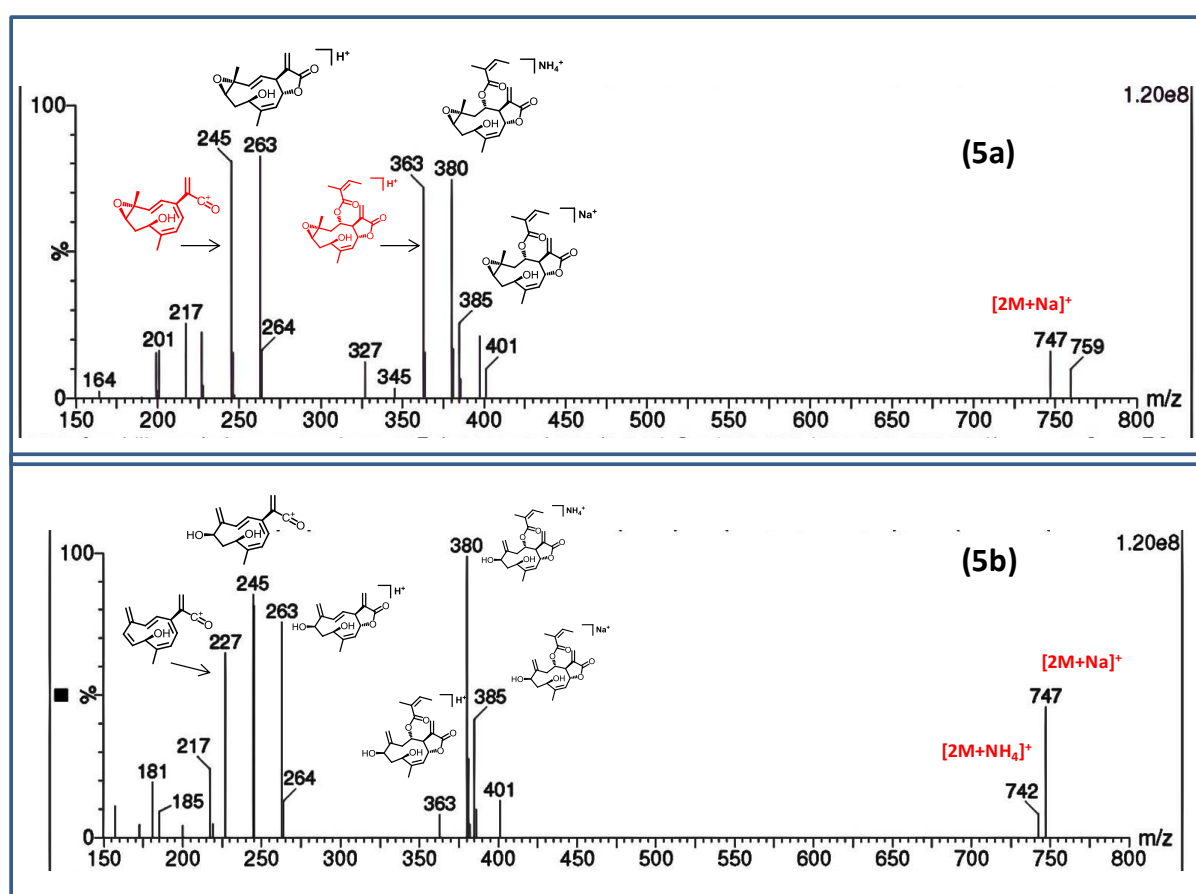


**Figure 6.15:** MS Spectral analysis of (5a) 1,10-epoxynoblin and (5b) hydroxynoblin.

Sodium adduct dimerization is identified with the  $m/z = 747$  Da fragment. Fragments for the ammonium and sodium adducts of 1,10-epoxynoblin are found at  $m/z = 380$  Da and  $m/z = 385$  Da, respectively. Angeloyl fragmentation is observed as  $m/z = 263$  Da. The ten

authenticated and eleven commercial samples of German chamomile showed the presence of compounds **1**, **2**, **11** as listed in Table 6.3. German chamomile samples also showed the presence of chrysopenetin B ( $m/z = 375$  Da,  $R_t = 6.34$  minutes) and chrysosplenol D ( $m/z = 361$  Da,  $R_t = 8.31$  minutes). These two compounds were not observed in the Roman chamomile samples. The in-source fragmentation data confirmed the suggested relationship of the unknown compounds with the sesquiterpene lactone derived compounds. The in-source fragmentation characterization of the unknown compounds has led to hypothesized elucidations of potential structures, however analysis using accurate mass data and true MS/MS analysis is required on the isolated compounds to properly identify and report these compounds as new chemical features related to chamomile. Therefore, the unknown compounds reported in Table 6.2 will be isolated via preparatory chromatography and identified by quadrupole time-of-flight mass spectrometry as future work to support the hypothesized compound elucidation data. The predicted structures are proposed in Figure 6.16

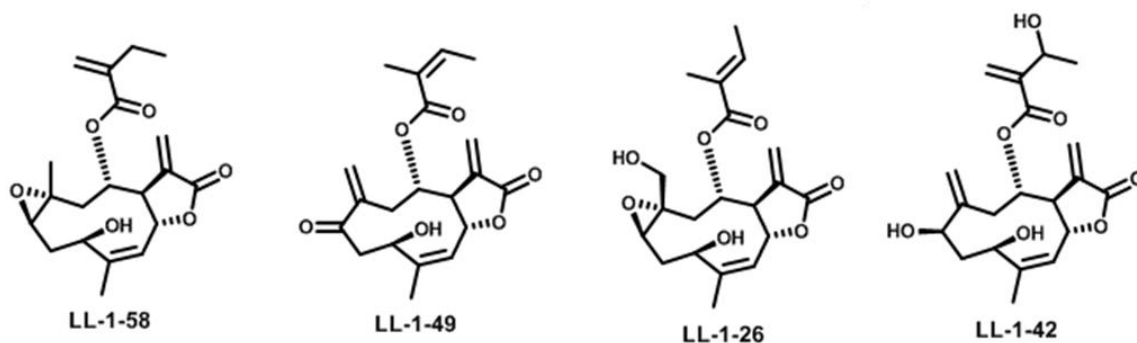


**Figure 6.16:** Predicted structures of four of the five unknown chemical entities observed in the chromatographic separation profile

### 6.3.8 Applied Investigation of Commercial Chamomile Teas

The widespread use and medicinal properties have made chamomile increasingly popular in the forms of tea. The phytochemical profile of these tea samples analyzed showed a similar

profile compared to German chamomile. None of the tea samples showed the presence of sesquiterpenes, therefore concluding that they are not authentic German or Roman chamomile. However, the PCA dataset indicates the tea samples as a variation of German chamomile. The identification of the eleven chemical markers was reported in Table 6.2; however, PCA analysis of the commercial tea sample extracts combined with the dataset of the authenticated chamomile extracts was examined. The scores plot of the entire dataset indicated clustering agreement with the qualitative findings in Table 6.3 (Figure 6.17) and some very distinct features that clustered tea from flowers in two different quadrants of the plot. This was the effect of the many compounds extracted and detected, thus reflecting the potential easily inserting sub-2 $\mu\text{m}$  particle size SFC into the workflow of fingerprinting herbal medicines.

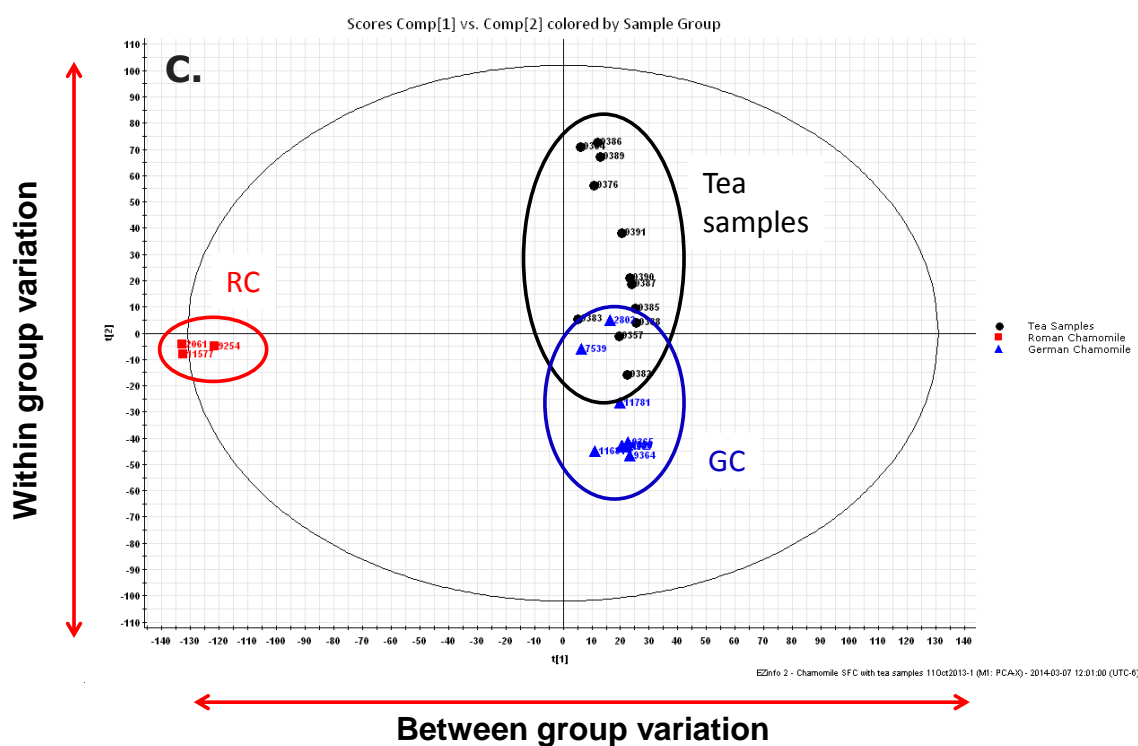


**Figure 6.17: PCA scores plot of the commercial tea samples extracts (black) and the extracts from authentic German (blue) and Roman (red) chamomiles**

**Table 6.3: Qualitative analysis of the authentic chamomile extracts and commercial tea extracts for the presence of the 11 chemical marker compounds**

Sample #	Compounds #										
	1	2	3	4	5	6	7	8	9	10/11	12
<i>A. nobilis</i>											
2061	+	+	+	+	+	+	+	+	+	+/+	+
9254	+	+	+	+	+	+	+	+	+	+/+	+
11577	+	+	+	+	+	+	+	+	+	+/+	+
<i>M. recutita</i>											
2802	+	+	-	-	-	-	-	-	-	-/-	+
7539	+	+	-	-	-	-	-	-	-	-/-	+
9172	+	+	-	-	-	-	-	-	-	-/-	+
9359	+	+	-	-	-	-	-	-	-	-/-	+
9362	+	+	-	-	-	-	-	-	-	-/-	+
9364	+	+	-	-	-	-	-	-	-	-/-	+
9365	+	+	-	-	-	-	-	-	-	-/-	+
11680	+	+	-	-	-	-	-	-	-	-/-	+
11681	+	+	-	-	-	-	-	-	-	-/-	+
11781	+	+	-	-	-	-	-	-	-	-/-	+
Tea Samples											
9357	+	+	-	-	-	-	-	-	-	-/-	+
9376	+	+	-	-	-	-	-	-	-	-/-	+
9383	+	+	-	-	-	-	-	-	-	-/-	+
9384	+	+	-	-	-	-	-	-	-	-/-	+
9385	+	+	-	-	-	-	-	-	-	-/-	+
9386	+	+	-	-	-	-	-	-	-	-/-	+
9387	+	+	-	-	-	-	-	-	-	-/-	+
9388	+	+	-	-	-	-	-	-	-	-/-	+
9389	+	+	-	-	-	-	-	-	-	-/-	+
9390	+	+	-	-	-	-	-	-	-	-/-	+
9391	+	+	-	-	-	-	-	-	-	-/-	+

In addition to the assessment of RPLC orthogonality, the specific chemical markers listed in Figure 6.2 were analyzed by UHPLC/MS, GC-MS, and UPC<sup>2</sup>/MS. The masses were extracted from the total ion chromatograms for each technique. The presence (+) or absence (-) of the compounds were recorded per each compound (Table 6.3). Using UPC<sup>2</sup>-MS, the SLs compounds were easily detected from Roman chamomile, but by the other 2 chromatographic techniques (UHPLC/MS, GC/MS) these compounds could not be easily identified.

#### 6.4 Conclusions

A sub-2 $\mu$ m packed-column supercritical fluid chromatography-mass spectrometry method was studied for the identification of sesquiterpenes and other constituents from chamomile extracts. All of the chemical marker compounds were separated within 15 minutes. German chamomile samples confirmed the presence of *cis*- and *trans*-tonghaosu, chrysopenetin, and chrysosplenols. Roman chamomile samples confirmed the presence of apigenin, 1,10-epioxynobilin, hydroxyisonobilin, nabilin, and other SLs. Various extraction techniques were evaluated on Roman and German chamomiles, yet extracts using iso-propanol/hexane (1:1, v/v) provided a good compromise in solutes extracted and optimal peak shape.

The method optimization indicated that caution should be used when investigating temperature as an optimization variable since increases in baseline noise can be observed. Increasing the backpressure in coordination with increasing the temperature will maintain the density of the mobile phase and minimize the endothermic expansion to the gaseous state, thus minimizing the gas in the flow cell contributing to the UV detector noise. The technique does not require any kind of derivatization prior to the analysis. Dual detection was achieved



in series easily by using the post UV detector splitter supplied with the instrumentation which allowed for simultaneous UV and mass spectrometry detection with ESI<sup>+</sup> data collection.

Multivariate statistical analysis approaches including principal component analysis (PCA) and partial least squares - discriminant analysis (PLS-DA) were used to correlate the data sets and visually differentiate between the chamomile samples. Sesquiterpene lactones, dicycloethers and flavonoids are key markers to differentiate Roman and German chamomiles. The PCA dataset of the tea samples indicated a relationship to German chamomile, but are not authentic German chamomile. Sub-2 $\mu$ m particle stationary phase SFC in combination with recent state-of-the-art instrumentation is an efficient tool to separate and characterize sesquiterpene lactones from chamomile. In comparison to LC and GC, it is reasonable to expect LC or GC to separate the 5 unknown compounds in Table 6.2 with extensive targeted method development; however, the separation and discovery of the 5 unknown compounds was easily accomplished using UPC<sup>2</sup>-MS methodology. In addition to the discovery of the unknown compounds, the methodology developed here will be implemented for routine quality control testing of chamomile preparations used as herbal supplements and tea at the University of Mississippi National center for Natural Product Research.

In summary, these results provide the foundation for developing a new workflow for natural product profiling using an orthogonal technique to RPLC which combines a simplified sample preparation, reliable SFC-based instrumentation capable of reproducible efficient data, a systematic method development approach, and statistical analysis that can be used as standard protocols for natural product chemical profiling.

## **6.5 Acknowledgements**

Part of this research is supported in part by “Science Based Authentication of Dietary Supplements” funded by the Food and Drug Administration grant number 5U01FD004246, the United States Department of Agriculture, Agricultural Research Service, Specific Cooperative Agreement No. 58-6408-02-1-612. I would like to thank the efforts of my co-authors of the published article, specifically Bharathi Avula and Yan-Hong Wang for supplying the plant material and assisting with the structural elucidation of the proposed pathways of the unknown components.

## CHAPTER 7:

---

# Conclusions and Future Research

## CHAPTER 7

### 7 Conclusions and Future Research

#### 7.1 Final Conclusions

New chemical entities which are developed as therapeutics resulting from natural product drug discovery represent the majority of the small molecule pharmaceutical drugs in the marketplace today. The goal of this research was designed to prove sub-2  $\mu\text{m}$  particle packed column SFC; commercially known as UPC<sup>2</sup>, as a viable technique and establish natural product drug discovery research as the field with the most to gain from its utilization. Interestingly, the technology had to advance prior to attempting chromatographic investigations because sub-2 $\mu\text{m}$  particle RPLC and HILIC columns employed by UHPLC approaches dominated the academic and innovator pharmaceutical community.

A novel instrument design capable of performing separations using today's evolution of sub-2 $\mu\text{m}$  particle size columns was developed in parallel with this research. In order to establish sub-2 $\mu\text{m}$  particle packed column SFC as a beneficial and distinct separations technique, the novel UPC<sup>2</sup> instrumentation was evaluated in terms of system performance and capability to harness the theoretical efficiencies of a of sub-2  $\mu\text{m}$  particle size column. The study showed the instrumentation was capable of achieving highly efficient separations with reproducibility exceeding those achieved on historical instrumentation configurations. Appropriate mixing of the mobile phase was critical to achieving Gaussian peak shapes, but more relevant at low flows rates and low percent modifiers. Interestingly, the study revealed observations about column efficiency and retention trends when using isobaric and isopycnic method conditions. It was noted that pressure as a function of density has a significant impact on determining an

optimal linear velocity. The van Deemter plots for the isopycnic results suggest the instrumentation pressure and flow rate upper threshold limited the ability to achieve a final determination of optimal linear velocity. If sub-2  $\mu\text{m}$  particle packed column SFC column efficiencies are being reported and compared using a van Deemter plot regardless of whether an isobaric or isopycnic approach is utilized, then the total system pressure should be reported as well in order to make the comparisons fair.

Adoption and implementation of pSFC approaches will be impacted by the amount of educational guidance provided by the scientific community. Method development knowledge and detection interfacing techniques are critical components to the education of future users, not just hypothesized for pSFC adoption but also evident from HPLC and UHPLC adoption.

In terms of discovery based analytics, the majority of metabolomics research utilizes high resolution mass spectrometry to identify new chemical features and markers. The study exploring techniques and considerations necessary when interfacing pSFC with the mass spectrometer was of critical importance prior to investigating applied approaches for synthetic chemistry reaction monitoring and natural product profiling. Issues such as probe pulsation and ionization efficiency must be explored with a critical eye. The baseline of the MS data can alert the user to spray stability. MS tune settings such as cone voltage, capillary voltage and desolvation temperatures are fairly easy to automate and investigate for optimum parameters. However, the exploration of the post-column addition make-up solvent can be significantly labor intensive and greatly impact the ionization of analytes being detected in

the final result. A mixture of water and ammonia additives in the make-up solvent resulted in the best approach to detect the most analytes.

Factors that affected selectivity in UPC<sup>2</sup> were explored and seem to have analogous behaviour to HILIC. Column screening impacted changes in selectivity the greatest; however these impacts were greater when using columns with a polar ligand and the components of interest were highly polar with longer retention times. The more neutral or non-polar compounds did not shift retention times nearly as much as their more polar structurally related compounds. The findings of Caroline West, whereas polar compounds separate well on polar columns and non-polar compounds separate well on non-polar columns was verified by these investigations. The observation of columns with  $\pi$ - $\pi$  retention mechanistic capability to separate conjugated compounds that are structurally similar was unique. The general investigations resulted in the following method development strategy:

1. Perform a generic 5 minute method column screening
2. Address peak shape with additives, preferably buffered-like additives consisting of a strong acid and conjugate base
3. Explore post-column addition solvents to enhance sensitivity in the MS detector (if used)
4. Utilize the addition of a weaker elution strength modifier to enhance resolution between critically resolved pairs
5. Optimize small selectivity variations with gradient slope, column temperature or backpressure settings

The study investigated amphipathic compounds; however mixtures of these compounds remain challenging. The benefit of the UPC<sup>2</sup> approach over HILIC or RPLC approaches resulted in moderate predictability of the retention of lipid species and class mixtures. The importance of routine use studies and system suitability methods was paramount. The routine use of the amphipathic method for lipid class separations revealed an issue with column degradation during analysis. The Consumables Group at Waters later characterized this degradation as the result of silanol group conversion to silyl ether formation (SEF) thus

resulting in a line of newly developed columns in 2014 specifically for use with UPC<sup>2</sup> applications designed to inhibit this on-column reaction[137]. This was achieved by utilizing a bonding approach which uses a hydrophilic bonding layer connecting the selector to the hybrid particle versus using a linker to bond the selector to the hybrid particle. Although these new chemistries were not available for this research, the use of buffered additives mitigated the retention drifts caused by SEF when using the hybrid sub-2 $\mu$ m particle columns. This was apparent during the system suitability method that was used as a system check during the cheminformatic investigation of structural and physiochemical attributes influence on chromatography. Little was gained from this investigation, but it did prove to be a useful approach to visualize the data in a multivariate perspective. It is difficult to conclude if the study proved or disproved perceptions relating solute physiochemical properties of logD or logP to chromatographic retention. This might be due to the basis that this study used a modifier and the perceptions of solute logD and logP influence might be in the absence of modifier.

The discovery and synthetic chemistry divisions within the pharmaceutical industry rely on the results of the analytical methodology to discover ‘hits’. Although the early discovery and medicinal chemistry scientists are not particularly concerned with traditional method development as analytical scientists are later in development, the discovery teams are cognoscente of method parameters to optimize their data collection of large compound libraries. Routine high throughput screening is driven by a selection of open access methods based on retention of the analyte for further purification. Interestingly, pSFC analytical to purification scaling strategies were published in 2014[211]. Many organic solvents, polar and non-polar, are used in the synthesis of the hits or derivations of the hits. Careful

considerations should be reviewed regarding the diluent interferences of solvents such as DMSO and DMF due to their retentivity when using UPC<sup>2</sup>.

Complex extraction techniques are performed to isolate and extract components of interest from the matrix of natural products. The extraction techniques involve many organic solvents not amenable to RPLC analysis, thus complicating the workflow to convert the extract to an aqueous based diluent better suitable for optimum peak shapes during RPLC analysis. The sample diluent conversion may alter the final sample analyzed due to solubility incompatibilities. The point of analyte solubility was a deliberate concern and point of interest in this research in terms of establishing pSFC as the appropriate separations tool for drug discovery research workflows, specifically involving natural products. The chromatographic performance from the applied use of sub-2 $\mu$ m particles columns hinged on the design and implementation of the novel low volume novel prototype pSFC instrumentation through to the final development of the commercialized UPC<sup>2</sup> instrument. The application and use of the technique for reaction monitoring of drug substance synthesis and natural product profiling provided the capability to investigate the impact of diluent systems and outputs from different extraction techniques. The impact of these sample preparation procedures were less than those observed from compound libraries that were diluted in DMSO. In fact, the impact of the resulting solutions from the reaction monitoring and natural product extracts was fairly low due in part to the dilution of the sample which was required to minimize detection saturation. In both studies, the true benefit of the UPC<sup>2</sup> approach was illustrated in the comparative data to that of the UHPLC results. New peaks were identified for the chamomile study resulting in previously undiscovered chemical entities. Cleaner separations of the starting materials and intermediate products were achieved, thus resulting in more accurate yield calculations for the reaction monitoring



studies. The general screening workflow was determined as streamlined due to the stationary phase agnostic approach that can be employed when using UPC<sup>2</sup>. When using the UPC<sup>2</sup> instrument when configured with a column switching module, chiral columns, RPLC columns, HILIC columns, NPLC columns, and all kinds of hybrid columns could be configured on the system without the need to change the mobile phase, wash solvents or diluent systems. To perform these types of separation without a general pSFC or UPC<sup>2</sup> approach, either separate dedicated HPLC instruments would have to be configured for each separation technique or timely conversion of the instrument to be compatible for each technique would have to be performed.

In conclusion, the utilization of the novel and newly commercialized option; UPC<sup>2</sup>, to achieve UHPLC-like data for an SFC-based separations technique was a breakthrough for the analytical scientific community as reported by researchers at annual conferences since 2012 to present focused on separation science and include the HPLC symposium, The SFC symposium organized by the Green Chemistry Group, Pittcon, International Symposium of Chromatography, and various US and EU SFC user group meetings held across the world. The performance evaluations, usability assessments, method development strategies and applied use examples discussed in this thesis confirm the usefulness of SFC separations and validating the need to progress the technologies that enable SFC separations. In terms of which industry would benefit the greatest from the SFC technological advancements; specifically UPC<sup>2</sup>, natural product profiling with the aim to discover new chemical entities targeted for a therapeutic purpose is recommended as the most appropriate fit. The analysis of natural products and their extracts are simplified due to the amenable diluent and solvent systems compatible with the UPC<sup>2</sup> separations approach, thus simplifying the overall preparation to final result workflow associated with complex extractions and chemical

synthesis. The column agnostic approach allows for chiral and achiral analysis on the same instrument without any changes to elution solvents and diluents. The use of polar and non-polar columns to exploit various retention mechanisms for general small molecule pharmaceuticals, structurally related compounds, and amphipathic compounds are well suited for comprehensive natural product profiling. The UPC<sup>2</sup> technology facilitates the scalability from analytical analysis to SFC purification of new chemical entity isolations enables time and cost savings that benefit high throughput discovery laboratories. This ease of scalability would also facilitate the process of small scale process development through to commercialized batch manufacturing of a lead candidate, thus completing the goal of bringing new therapeutics to the patient.

## **7.2 Summary of Thoughts, Peer Interactions and Observations about Future pSFC and UPC<sup>2</sup> Adoption**

The field of studying supercritical fluids, specifically the technique of supercritical fluid chromatography has seen ebbs and flows of research activity over the last few decades. pSFC has been explored for the analysis of pharmaceuticals, chemical materials, food research, and natural products to name a few. The pSFC application previously reported in any of the aforementioned foci of interest will usually have a major emphasis on the analysis of chiral compounds or highly lipophilic compounds. Unfortunately, aside from chiral analysis studies, the scientific community has not indicated a clear reason to use pSFC as the technique of choice when analyzing achiral molecules, never mind any mention of which field of discipline could best benefit from pSFC. It is clear that HPLC or GC will be the first option to investigate for the foci areas mentioned above. It appears that the research performed at

any given time will conclude on excellent scientific revelations, but then particular limitations inhibiting the widespread use of the technique are commonly raised, namely:

- a. pSFC technology has limitations such as performance, robustness, and ease of use.
- b. The theoretical principles that pertain to separation mechanisms and how the role of density, role of pressure, and role of temperature influence these mechanisms are very complicated and difficult to deduce.
- c. HPLC and GC utilization and analyte coverage is very high

The technology limitations stated in point (a.) are clearly addressed with the introduction of the UPC<sup>2</sup> instrument based on the findings in this thesis. Academics such as the University of Tennessee, Université d'Orléans, University of South Hampton, and University of Genève are leading the charge in characterizing the theoretical principles stated in point (b.). The utilization of HPLC and GC before the use of SFC as stated in point (c.) is a human element that takes time to overcome the barrier to change. Various factors have enabled the scientific community to defer the use of pSFC and stick to the tried and trusted technique of HPLC. An obvious factor points to technology advancements which enabled HPLC to flourish. The last 2-3 decades, separation technology advancements have primarily focused on HPLC in the form of instrumentation and column chemistry.

A common question and answer session that has been raised at each International Conference on Packed Column SFC held by the Green Chemistry Group since 2012 – 2015 throws up the following question:

*What is the universal column for pSFC which would be analogous to the C<sub>18</sub> column for HPLC?* ...The response by every presenter which is asked this question is usually similar to the following; *Well, there isn't one...yet*

The lack of an answer for a universal column is misleading. In many of the examples throughout the investigational studies of this thesis, any column used on the UPC<sup>2</sup> instrument resulted in a good separation in which additional selectivity altering approaches were applied to achieve the objectives required of the final method. These concepts of ‘method optimization’ are not unique to pSFC method development and are a necessity in RPLC method development as well. Due to the success of the separations achieved by UPC<sup>2</sup> when using a multitude of columns, the results suggest that every column is a universal column when using UPC<sup>2</sup> assuming you stick with matching the polarity of sample to the polarity of the stationary phase concepts that Caroline West recommends. Based on the column screening results from metoclopramide impurities study, lipid class – species separations study, the reaction monitoring of the pharmaceutical products study, the compound library screening study; the selection of which column could be conceived as the universal ‘SFC’ column became irrelevant. The choice of column became more of an informed judgement assessment because the chromatographic attributes that dictate a choice of column (i.e: tailing, resolution, efficiency, speed, sensitivity, etc) were not any more discerning than RPLC column selection once additives were used from the beginning to address potential peak shape issues or column stability. The practices to address better peak shapes for HPLC were the same for those to address peak shapes for SFC. In HPLC, if the molecule has a basic  $pK_a$ , the utilization of a basic additive in the mobile results in better peak shapes. In SFC, matching the additive to solute  $pK_a$  has the same benefits; however an additional option to facilitate peak shape would be to include choosing a column with  $pK_a$  properties similar to that of the solute. The ability to utilize an extra selectivity variable should not complicate it’s use, but rather simplify the achievement of a successful separation that meets the goals and objective of the method’s intended use. All in all, the time required to optimize the method for pSFC or RPLC could be perceived equivalent if normalizing the experience level of the

analytical scientist using both techniques. The application development and investigative studies towards this thesis facilitated the learning curve of SFC principles and separation expectations helped normalize these two separation experience levels, thus validating the time metrics assessment of developing methods for either separations approach.

Additionally, some of the leading practitioners tend to unknowingly complicate and confuse willing adopters of pSFC at these conferences. Statements followed by short workshops are driven by the following statement:

*“...In practice, the fluid in supercritical fluid chromatography applications is not ‘supercritical’. The fluid is sub-critical due to the use of the organic elution modifier. Based on this fact, what should we rename this technique? Sub-critical Fluid Chromatography? Convergence Chromatography? Unified Chromatography? CO<sub>2</sub>-based Chromatography?...”*

One could argue industrial agendas for scientific community recognition if the name were to change. However, for the technique to progress and be adopted by industry, efforts to make the technique sound less complicated would be a welcomed path forward.

In terms of the point of universal columns for UPC<sup>2</sup>, there seems to be a popular desire at pSFC conferences and workshops for a single column ligand for use with a single separations based technique whereas these two tools streamline the ease of use and success of that technique for >80% of the separations attempted. This perception exists as a point of benefit for RPLC, although in some ways the perception is almost counter intuitive. The use of a

single column ligand seems limiting in terms of exploring additional tools to achieve success for a challenging and complex separation. Perhaps that is why there are currently over 300 C<sub>18</sub> branded columns available in the marketplace today, and many separation scientists comment: “*Not all C<sub>18</sub> columns are the same!*”, hence perhaps further answering the question of why so many are needed. Knowing there are many C<sub>18</sub> columns available, would that not complicate the choice of C<sub>18</sub> column to use when looking to practice reversed -phase chromatography on an LC instrument? However, analytical chemists do not seem to focus on this complexity of column selection for RPLC as a point of contention for using HPLC as a technique of choice. It would be very interesting to hear a delegate in the audience of the annual HPLC Conference to ask any presenter how did they know which C<sub>18</sub> column to use? And how many C<sub>18</sub> columns were explored to get the desired separation?” The reality of the situation regarding unknown recommendations for a universal SFC column is also true when blindly applying the universal column for RPLC separation of analytes, however many times the column selection process for RPLC is not very well communicated. The method development story of a successful separation is usually never explained as to why a particular C<sub>18</sub> column was chosen from the rest of the 300 commercially available C<sub>18</sub> columns. A presentation or publication might focus on why a C<sub>18</sub> column was chosen over a phenyl column or shielded column. Solute polarity is sometimes discussed to justify why a HILIC approach was used rather than a RPLC C<sub>18</sub> approach. The scientific conversations regarding RPLC method development often focus on the pH of the mobile phase, elution solvent or temperature to alter selectivity when needed to achieve a separation. Interestingly, one important factor that is not often addressed is the solute solubility and how the solubility dictated the choice of a chromatography technique. For today’s UPC<sup>2</sup>, the practice of considering the sample solubility may increase the rate of adoption, specifically for natural product profiling and drug discovery based research of small molecules due to the range of

organic solvents used in synthesis and extraction protocols. Based on the presentations at SFC conferences such as the one held by the Green Chemistry Group, adoption is already high due to UPC<sup>2</sup> enabling the supporting analytical component to the SFC purification workflow in the pharmaceutical drug discovery divisions in companies such as Eli Lilly, Dart Neurosciences, Pfizer, Merck, Novartis and AstraZeneca.

### 7.3 On-going related research

The research within this thesis has stimulated the following additional research which is on-going and beyond the scope of inclusion:

1. Investigation of solvent-solvent extraction versus supercritical fluid extraction of *Garcinia kola* nuts. This research incorporates the comparison of extraction techniques and utilizes multivariate statistical profiling techniques based on sub-2 $\mu$ m particle pSFC high resolution mass spectrometry data to determine the coverage and overlap of each extraction approach. This research is in collaboration with Dr. Worthern and Yasah Vezele from the University of Rhode Island, Department of Pharmacy. The initial results have been presented at HPLC 2014 in New Orleans and published excerpts in Yasah Vezele's thesis submitted in partial fulfillment of the requirements for the degree of Master of Science in Pharmaceutical Science titled "*Garcinia Kola: Phytochemical, Biological, and Formulation Studies*". The research is being expanded to identify distinguishing chemical features for the main grouping of extraction procedures that are identified as unique by the principal component analysis plot.
2. Global lipidomics profiling of cotton seed oil genotypes using sub-2 $\mu$ m particle pSFC coupled to mass spectrometry. The initial results have been presented at HPLC 2013 as a poster titled: "*Application of UPC<sup>2</sup>/MS for comprehensive and targeted analysis of lipids in cotton seed extracts*". This is an ongoing collaboration with Dr. Vladimir Shulaev of the University of Northern Texas.

3. Investigating the purging of the potential genotoxic alerting structures during the synthesis of imatinib mesylate drug substance by sub-2  $\mu\text{m}$  particle pSFC and a novel miniature MS detector. Due to the emergence of the ICH M7 guidance focused on mutagenic impurities, the MS results of the imatinib reaction monitoring study will be re-investigated for the alerting and previously reported genotoxic impurities to confirm their elimination from the intermediate and final stages of the synthesis.

## 7.4 Future Research

Future research should focus on several areas to further explore the utilization of the pSFC approaches investigated within this body of work. Investigations should be expanded to incorporate CO<sub>2</sub>-based workflows inclusive of sample preparation protocols. These could include:

1. Further investigations of optimal mass spectrometry interfacing approaches. This would include investigations towards post-column addition solvents, splitter designation and design, and addition of heat to the transfer line restrictor connecting to the MS instrument.
2. Investigations of  $\pi$ - $\pi$  activated ligand bonded columns for the separation of structurally related conjugated analytes by pSFC would be a useful tool to discover new compounds or develop stronger intellectual property about the markush structure of a targeted compound. Markush structures are depicted with R groups, in which the side chain can be a structure type, e.g. 'cyclohexyl'. This more general depiction of the molecule, versus detailing every atom in the molecule, is used to protect intellectual property [212, 213].
3. Cheminformatic analysis of a targeted compound library composed of conjugated, hydroxylated, or oxygen-based functionality and peak shape should be explored. A number of compounds with these properties resulted in excessive peak broadening. The study could be designed to also explore the pi-pi influence when using a penta-fluorophenyl ligand column.



4. The multivariate statistical profiling of natural product collected by sub-2  $\mu\text{m}$  particle stationary phase supercritical fluid chromatography and compared to the sub-2  $\mu\text{m}$  reversed-phase particle stationary phase coupled to accurate mass spectrometry

## References

1. Butler, M.S., A.A.B. Robertson, and M.A. Cooper, *Natural product and natural product derived drugs in clinical trials*. Natural Product Reports, 2014. **31**(11): p. 1612-1661.
2. Shulaev, V., et al., *The genome of woodland strawberry (Fragaria vesca)*. Nat Genet, 2011. **43**(2): p. 109-116.
3. Strobel, G. and B. Daisy, *Bioprospecting for Microbial Endophytes and Their Natural Products*. Microbiology and Molecular Biology Reviews, 2003. **67**(4): p. 491-502.
4. Pharmacognosy, T.A.S.o.
5. Butler, M.S., *The Role of Natural Product Chemistry in Drug Discovery*<sup>†</sup>. Journal of Natural Products, 2004. **67**(12): p. 2141-2153.
6. Schmidt, B., et al., *A natural history of botanical therapeutics*. Metabolism: clinical and experimental, 2008. **57**(7 Suppl 1): p. S3-S9.
7. Koehn, F.E. and G.T. Carter, *The evolving role of natural products in drug discovery*. Nat Rev Drug Discov, 2005. **4**(3): p. 206-220.
8. Patridge, E., et al., *An analysis of FDA-approved drugs: natural products and their derivatives*. Drug Discov Today, 2015(0).
9. Nielsen, K.F. and J. Smedsgaard, *Fungal metabolite screening: database of 474 mycotoxins and fungal metabolites for dereplication by standardised liquid chromatography-UV-mass spectrometry methodology*. J. Chrom. A, 2003. **1002**: p. 111-136.
10. Martin, E.J. and R.E. Crichtlow, *Beyond Mere Diversity: Tailoring Combinatorial Libraries for Drug Discovery*. Journal of Combinatorial Chemistry, 1998. **1**(1): p. 32-45.
11. Newman, D.J. and G.M. Cragg, *Natural Products As Sources of New Drugs over the 30 Years from 1981 to 2010*. Journal of Natural Products, 2012. **75**(3): p. 311-335.
12. Feher, M. and J.M. Schmidt, *Property distributions: Differences between drugs, natural products, and molecules from combinatorial chemistry*. J. Chem. Inf. Comput. Sci., 2003. **43**: p. 218-227.
13. Henkel, T., et al., *Statistical investigation of structural complementarity of natural products and synthetic compounds*. Angew. Chem. Int. Ed. Engl., 1999. **38**: p. 643-647.
14. Stahura, F., et al., *Distinguishing between natural products and synthetic molecules by descriptor Shannon entropy analysis and binary QSAR calculations*. J. Chem. Inf. Comput. Sci., 2000. **40**: p. 1245-1252.
15. Lee, M.L. and G. Schneider, *Scaffold architecture and pharmacophoric properties of natural products and trade drugs: Application in the design of natural product-based combinatorial libraries*. J. Comb. Chem., 2001. **3**: p. 284-289.
16. Lipinski, C.A., et al., *Experimental and computational approaches to estimate solubility and permeability in drug discovery and development settings*. Adv. Drug Del. Rev., 1997. **23**: p. 3-25.
17. Kissau, L., et al., *Development of natural product-derived receptor tyrosine kinase inhibitors based on conservation of protein domain fold*. J. Med. Chem., 2003. **46**: p. 2917-2931.
18. Neue, U., *HPLC Columns Theory, Technology, and Practice*. 1997, NY: John Wiley and Sons.
19. Ali, M.S., et al., *Simultaneous determination of metformin hydrochloride, cyanoguanidine and melamine in tablets by mixed-mode HILIC*. Chromatographia, 2008. **67**(7-8): p. 517-525.

20. Jones, M.D. and B. William, *A UPLC Method for Analysis of Metformin and Related Substances by Hydrophilic Interaction Chromatography (HILIC)*. 2013.
21. Kirkland, J.J., et al., *Superficially porous silica microspheres for fast high-performance liquid chromatography of macromolecules*. *Journal of Chromatography A*, 2000. **890**(1): p. 3-13.
22. Weston, A., Brown, P., *HPLC and CE Principals and Practice*. 1997, CA: W.B. Saunders Company.
23. Settle, F., *Handbook of Instrumental Techniques for Analytical Chemistry*. 1997, NJ: Prentice Hall PTR.
24. Ettre, L., *Nomenclature for chromatography (IUPAC Recommendations 1993)*. *Pure and Applied Chemistry*, 1993. **65**(4): p. 819-872.
25. Cazes, J.S., R., *Chromatography Theory*. 2002, NY: Marcel Dekker.
26. Horvath, C.G. and S.R. Lipsky, *Peak capacity in chromatography*. *Analytical Chemistry*, 1967. **39**(14): p. 1893-1893.
27. Bristow, P. and J. Knox, *Standardization of test conditions for high performance liquid chromatography columns*. *Chromatographia*, 1977. **10**(6): p. 279-289.
28. Fanigliulo, A., et al., *Comparison of performance of high-performance liquid chromatography columns packed with superficially and fully porous 2.5  $\mu$ m particles using kinetic plots*. *Journal of Separation Science*, 2010. **33**(23-24): p. 3655-3665.
29. Kaczmarek, K. and G. Guiochon, *Modeling of the Mass-Transfer Kinetics in Chromatographic Columns Packed with Shell and Pellicular Particles*. *Analytical Chemistry*, 2007. **79**(12): p. 4648-4656.
30. Gritti, F. and G. Guiochon, *Mass transfer kinetics, band broadening and column efficiency*. *Journal of Chromatography A*, 2012. **1221**(0): p. 2-40.
31. Smith, R.M., *Supercritical fluids in separation science – the dreams, the reality and the future*. *Journal of Chromatography A*, 1999. **856**(1-2): p. 83-115.
32. Zekovic, Z., I. Pfaf-Sovljanski, and O. Grujic, *Supercritical fluid extraction of hops*. *J. Serb. Chem. Soc*, 2007. **72**(1): p. 81-87.
33. Katz, S.N., *Method for decaffeinating coffee with a supercritical fluid*. 1989, General Foods Corporation: USA.
34. Berche, M.H.a.R.K., *Critical Phenomena: 150 Years since Cagniard de la Tour*. *Journal of Physical Studies* 2009. **13**: p. 3001.
35. Lavoisier, A., *Dans Lequel on a pour Objet de Prouver que L'eau N'est Point une Substance Simple, Un Élement Proprement Dit, Mais Qu'elle est Susceptible de Decomposition et de Recomposition*, in *Memoire de Lavoisier, Memoires de Chemie et de Physique*. 1862: Paris. p. 351, 805.
36. Cagniard de LaTour, C., *Expose de quelque resultats obtenu par l'action combinee de la chaleur et de la compression sur certains liquides, tes que l'eau, l'alcool, l'ether sulfurique et l'essence de petrole rectifiee*. *Ann. Chim. Phys*, 1822. **21**: p. 127-132, 178-182.
37. Cagniard de LaTour, C., *Nouvelle note sur les effects qu'on obtient par l'application simultanee de la chaleur et de la compression a certains liquides*. *Ann. Chim. Phys*, 1823. **22**: p. 410-415.
38. Mendeleev, D., *Ueber die Ausdehnung der Flussigkeiten beim Erwarmen uber ihren Siedepunkt*. *Ann. Chem. Pharm.*, 1861. **119**: p. 1-11.
39. Goudaroulis, Y., *Searching for a Name: the development of the concept of the critical point*. *Revue d'Histoire des Sciences*, 1994. **47**: p. 353-379.
40. Faraday, M., *Letter to W. Whewell*. 1844.
41. Andrews, T., *The Bakerian lecture: On the continuity of the gaseous and liquid states of matter*, in *Trans. Roy. Soc*. 1869: London. p. 575-590.
42. Smith, R.M., *Nomenclature for supercritical fluid chromatography and extraction (IUPAC Recommendations)*. *Pure and Applied Chemistry*, 1993. **65**(11): p. 2397-2403.
43. Brown, L., Bursten, Burdge, *Chemistry: The Central Science*. 9th ed. 2003: Prentice Hall. 423.

44. Hannay, J.B., *On the Limit of the Liquid State*, in *Proc. Roy. Soc.* 1880: London. p. 484.
45. Hannay, J.B. and J. Hogarth, *On the Solubility of Solids in Gases*, in *Proc. Roy. Soc.* 1879: London. p. 324.
46. Hannay, J.B. and J. Hogarth, *On the Solubility of Solids and Gases*, in *Proc. Roy. Soc.* 1880: London. p. 178.
47. Williams, D.F., *Extraction with supercritical gases*. Chemical Engineering Science, 1981. **36**(11): p. 1769-1788.
48. Berger, T.A., *Packed Column SFC*, ed. R.M. Smith. 1995: The Royal Society of Chemistry.
49. Bertsch, W., *Thesis*. 1973, University of Houston.
50. White, C.M., *Modern Supercritical Fluid Chromatography*. 1988: Hüthig.
51. Lake, L.W., *Enhanced Oil Recovery*. 1989, Englewood Cliffs, NJ: Prentice Hall.
52. Taylor, L.T., *Supercritical fluid chromatography for the 21st century*. The Journal of Supercritical Fluids, 2009. **47**(3): p. 566-573.
53. Guiochon, G. and A. Tarafder, *Fundamental challenges and opportunities for preparative supercritical fluid chromatography*. J Chromatogr A, 2011. **1218**(8): p. 1037-114.
54. Lesellier, E., *Retention mechanisms in super/subcritical fluid chromatography on packed columns*. Journal of Chromatography A, 2009. **1216**(10): p. 1881-1890.
55. Lesellier, E. and C. West, *The many faces of packed column supercritical fluid chromatography – A critical review*. Journal of Chromatography A, 2015. **1382**(0): p. 2-46.
56. Klesper, E., A.H. Corwin, and D.A. Turner, *Communications TO THE EDITOR*. The Journal of Organic Chemistry, 1962. **27**(2): p. 700-706.
57. Sie, S.T., W. Van Beersum, and G.W.A. Rijnders, *High-Pressure Gas Chromatography and Chromatography with Supercritical Fluids. I. The Effect of Pressure on Partition Coefficients in Gas-Liquid Chromatography with Carbon Dioxide as a Carrier Gas*. Separation Science, 1966. **1**(4): p. 459-490.
58. Sie, S.T. and G.W.A. Rijnders, *High-Pressure Gas Chromatography and Chromatography with Supercritical Fluids. IV. Fluid-Solid Chromatography*. Separation Science, 1967. **2**(6): p. 755-777.
59. Sie, S.T. and G.W.A. Rijnders, *High-Pressure Gas Chromatography and Chromatography with Supercritical Fluids. III. Fluid-Liquid Chromatography*. Separation Science, 1967. **2**(6): p. 729-753.
60. Sie, S.T. and G.W.A. Rijnders, *High-Pressure Gas Chromatography and Chromatography with Supercritical Fluids. II. Permeability and Efficiency of Packed Columns with High-Pressure Gases as Mobile Fluids under Conditions of Incipient Turbulence*. Separation Science, 1967. **2**(6): p. 699-727.
61. Sie, S.T. and G.W.A. Rijnders, *Chromatography with supercritical fluids*. Analytica Chimica Acta, 1967. **38**: p. 31-44.
62. Giddings, C.J., et al., *High Pressure Gas Chromatography of Nonvolatile Species*. Science, 1968. **162**(3849): p. 67-73.
63. Martire, D.E. and R.E. Boehm, *Unified molecular theory of chromatography and its application to supercritical fluid mobile phases. 1. Fluid-liquid (absorption) chromatography*. The Journal of Physical Chemistry, 1987. **91**(9): p. 2433-2446.
64. Martire, D.E., *Unified Theory of Adsorption Chromatography with Heterogenous Surfaces: Gas, Liquid and Supercritical Fluid Mobile Phases*. Journal of Liquid Chromatography, 1988. **11**(9-10): p. 1779-1807.
65. Martire, D.E., *Unified Theory of Absorption Chromatography: Gas, Liquid, and Supercritical Fluid Mobile Phases*. Journal of Liquid Chromatography, 1987. **10**(8-9): p. 1569-1588.
66. Ishii, D. and T. Takeuchi, *Unified Fluid Chromatography*. Journal of Chromatographic Science, 1989. **27**(2): p. 71-74.
67. Chester, T.L., *Peer Reviewed: Chromatography from the Mobile-Phase Perspective*. Analytical Chemistry, 1997. **69**(5): p. 165A-169A.

68. Tarafder, A., et al., *Use of the isopycnic plots in designing operations of supercritical fluid chromatography: IV. Pressure and density drops along columns*. Journal of Chromatography A, 2012. **1238**(0): p. 132-145.
69. Tarafder, A., et al., *Use of the isopycnic plots in designing operations of supercritical fluid chromatography. V. Pressure and density drops using mixtures of carbon dioxide and methanol as the mobile phase*. Journal of Chromatography A, 2012. **1258**(0): p. 136-151.
70. Tarafder, A. and G. Guiochon, *Unexpected retention behavior of supercritical fluid chromatography at the low density near critical region of carbon dioxide*. Journal of Chromatography A, 2012. **1229**(0): p. 249-259.
71. Tarafder, A. and G. Guiochon, *Extended zones of operations in supercritical fluid chromatography*. Journal of Chromatography A, 2012. **1265**(0): p. 165-175.
72. Tarafder, A. and G. Guiochon, *Use of isopycnic plots in designing operations of supercritical fluid chromatography. III: Reason for the low column efficiency in the critical region*. Journal of Chromatography A, 2011. **1218**(40): p. 7189-7195.
73. Tarafder, A. and G. Guiochon, *Use of isopycnic plots in designing operations of supercritical fluid chromatography: I. The critical role of density in determining the characteristics of the mobile phase in supercritical fluid chromatography*. Journal of Chromatography A, 2011. **1218**(28): p. 4569-4575.
74. Tarafder, A. and G. Guiochon, *Use of isopycnic plots in designing operations of supercritical fluid chromatography: II. The isopycnic plots and the selection of the operating pressure-temperature zone in supercritical fluid chromatography*. Journal of Chromatography A, 2011. **1218**(28): p. 4576-4585.
75. Schoenmakers, P.J., *Open Columns or Packed Columns for SFC - A Comparison*, ed. R.M. Smith. 1988: Royal Society of Chemistry.
76. Novotny, M., W. Bertsch, and A. Zlatkis, *Temperature and pressure effects in supercritical-fluid chromatography*. Journal of Chromatography A, 1971. **61**: p. 17-28.
77. Gere, D.R., R. Board, and D. McManigill, *Supercritical fluid chromatography with small particle diameter packed columns*. Analytical Chemistry, 1982. **54**(4): p. 736-740.
78. Wasen, U. and G.M. Schneider, *Pressure and density dependence of capacity ratios in supercritical fluid chromatography (SFC) with carbon dioxide as mobile phase*. Chromatographia, 1975. **8**(6): p. 274-276.
79. Peaden, P.A. and M.L. Lee, *Theoretical treatment of resolving power in open tubular column supercritical fluid chromatography*. Journal of Chromatography A, 1983. **259**(0): p. 1-16.
80. Poe, D.P. and D.E. Martire, *Plate height theory for compressible mobile phase fluids and its application to gas, liquid and supercritical fluid chromatography*. Journal of Chromatography A, 1990. **517**(0): p. 3-29.
81. Lou, X., H.-G. Janssen, and C.A. Cramers, *Temperature and pressure effects on solubility in supercritical carbon dioxide and retention in supercritical fluid chromatography*. Journal of Chromatography A, 1997. **785**(1-2): p. 57-64.
82. Bartle, K.D., A.A. Clifford, and S.A. Jafar, *Measurement of solubility in supercritical fluids using chromatographic retention: the solubility of fluorene, phenanthrene, and pyrene in carbon dioxide*. Journal of Chemical & Engineering Data, 1990. **35**(3): p. 355-360.
83. Anitescu, G. and L.L. Tavlarides, *Solubility of individual polychlorinated biphenyl (PCB) congeners in supercritical fluids: CO<sub>2</sub>, CO<sub>2</sub>/MeOH and CO<sub>2</sub>/n-C<sub>4</sub>H<sub>10</sub>*. The Journal of Supercritical Fluids, 1999. **14**(3): p. 197-211.
84. Vesovic, V., et al., *The Transport Properties of Carbon Dioxide*. Journal of Physical and Chemical Reference Data, 1990. **19**(3): p. 763-808.
85. Fenghour, A., W.A. Wakeham, and V. Vesovic, *The Viscosity of Carbon Dioxide*. Journal of Physical and Chemical Reference Data, 1998. **27**(1): p. 31-44.
86. Chrastil, J., *Solubility of solids and liquids in supercritical gases*. The Journal of Physical Chemistry, 1982. **86**(15): p. 3016-3021.

87. Bartmann, D. and G.M. Schneider, *Experimental results and physico-chemical aspects of supercritical fluid chromatography with carbon dioxide as the mobile phase*. Journal of Chromatography A, 1973. **83**(0): p. 135-145.
88. Janssen, H.-G., et al., *The effects of the column pressure drop on retention and efficiency in packed and open tubular supercritical fluid chromatography*. Journal of High Resolution Chromatography, 1991. **14**(7): p. 438-445.
89. Janssen, H.-G., et al., *Compressibility effects in packed and open tubular gas and supercritical fluid chromatography*. Journal of High Resolution Chromatography, 1992. **15**(7): p. 458-466.
90. Bouigeon, C., D. Thiébaut, and M. Caude, *Long Packed Column Supercritical Fluid Chromatography: Influence of Pressure Drop on Apparent Efficiency*. Analytical Chemistry, 1996. **68**(20): p. 3622-3630.
91. Rajendran, A., et al., *Effect of pressure drop on solute retention and column efficiency in supercritical fluid chromatography*. Journal of Chromatography A, 2005. **1092**(1): p. 149-160.
92. Poe, D.P. and J.J. Schrodin, *Effects of pressure drop, particle size and thermal conditions on retention and efficiency in supercritical fluid chromatography*. Journal of Chromatography A, 2009. **1216**(45): p. 7915-7926.
93. Kaczmarek, K., D.P. Poe, and G. Guiochon, *Numerical modeling of elution peak profiles in supercritical fluid chromatography. Part I—Elution of an unretained tracer*. Journal of Chromatography A, 2010. **1217**(42): p. 6578-6587.
94. Zheng, J., et al., *Effect of ionic additives on the elution of sodium aryl sulfonates in supercritical fluid chromatography*. Journal of Chromatography A, 2005. **1082**(2): p. 220-229.
95. Berger, T.A. and J.F. Deye, *Role of additives in packed column supercritical fluid chromatography: suppression of solute ionization*. Journal of Chromatography A, 1991. **547**(0): p. 377-392.
96. West, C. and E. Lesellier, *A unified classification of stationary phases for packed column supercritical fluid chromatography*. Journal of Chromatography A, 2008. **1191**(1-2): p. 21-39.
97. Ghanem, A., H. Hoenen, and H.Y. Aboul-Enein, *Application and comparison of immobilized and coated amylose tris-(3,5-dimethylphenylcarbamate) chiral stationary phases for the enantioselective separation of  $\beta$ -blockers enantiomers by liquid chromatography*. Talanta, 2006. **68**(3): p. 602-609.
98. Lesellier, E., et al., *Effects of selected parameters on the response of the evaporative light scattering detector in supercritical fluid chromatography*. Journal of Chromatography A, 2012. **1250**(0): p. 220-226.
99. Hanson, M., J. Kabbara, and K. Junghans, *Packed column supercritical fluid chromatography with FID: Investigation of products from copper-catalyzed conjugate additions of trimethylaluminum to  $\alpha$ ,  $\beta$ -unsaturated aldehydes*. Chromatographia, 1994. **39**(5-6): p. 299-305.
100. Strode, J.T.B., et al., *Packed-Column Supercritical Fluid Chromatography with Chemiluminescent Nitrogen Detection at High Carbon Dioxide Flow Rates*. Journal of Chromatographic Science, 1998. **36**(10): p. 511-515.
101. Smith, R.M., et al., *Fluorescence detection in packed-column supercritical fluid chromatographic separations*. Journal of Chromatography A, 1998. **798**(1-2): p. 203-206.
102. Brunelli, C., et al., *Corona-Charged Aerosol Detection in Supercritical Fluid Chromatography for Pharmaceutical Analysis*. Analytical Chemistry, 2007. **79**(6): p. 2472-2482.
103. Xia, Z. and K.B. Thurbide, *Universal acoustic flame detection for modified supercritical fluid chromatography*. Journal of Chromatography A, 2006. **1105**(1-2): p. 180-185.
104. Mah, C. and K.B. Thurbide, *Increased flow rate compatibility for universal acoustic flame detection in liquid chromatography*. Journal of Chromatography A, 2011. **1218**(2): p. 362-365.

105. Alexander, A.J., T.F. Hooker, and F.P. Tomasella, *Evaluation of mobile phase gradient supercritical fluid chromatography for impurity profiling of pharmaceutical compounds*. Journal of Pharmaceutical and Biomedical Analysis, 2012. **70**(0): p. 77-86.
106. Smith, R.M. and D.A. Briggs, *Effect of the sample solvent and instrument design on the reproducibility of retention times and peak shapes in packed-column supercritical fluid chromatography*. Journal of Chromatography A, 1994. **670**(1–2): p. 161-171.
107. van Deemter, J.J., F.J. Zuiderweg, and A. Klinkenberg, *Longitudinal diffusion and resistance to mass transfer as causes of nonideality in chromatography*. Chemical Engineering Science, 1956. **5**(6): p. 271-289.
108. Halász, I., H. Schmidt, and P. Vogtel, *Particle size, pressure and analysis time in routine high-performance liquid chromatography*. Journal of Chromatography A, 1976. **126**: p. 19-33.
109. Endeke, R., I. Halász, and K. Unger, *Influence of the particle size (5–35  $\mu\text{m}$ ) of spherical silica on column efficiencies in high-pressure liquid chromatography*. Journal of Chromatography A, 1974. **99**: p. 377-393.
110. Halász, I., R. Endeke, and J. Asshauer, *Ultimate limits in high-pressure liquid chromatography*. Journal of Chromatography A, 1975. **112**: p. 37-60.
111. Engelhardt, H., et al., *Separations on heavily loaded small particle columns in high speed liquid chromatography*. Analytical Chemistry, 1974. **46**(3): p. 336-340.
112. Swartz, M.E., *UPLC™: An Introduction and Review*. Journal of Liquid Chromatography & Related Technologies, 2005. **28**(7-8): p. 1253-1263.
113. Mellors, J.S. and J.W. Jorgenson, *Use of 1.5- $\mu\text{m}$  Porous Ethyl-Bridged Hybrid Particles as a Stationary-Phase Support for Reversed-Phase Ultrahigh-Pressure Liquid Chromatography*. Analytical Chemistry, 2004. **76**(18): p. 5441-5450.
114. Fountain, K.J., et al., *Effects of extra-column band spreading, liquid chromatography system operating pressure, and column temperature on the performance of sub-2- $\mu\text{m}$  porous particles*. Journal of Chromatography A, 2009. **1216**(32): p. 5979-5988.
115. Neue, U.D. and M. Kele, *Performance of idealized column structures under high pressure*. Journal of Chromatography A, 2007. **1149**(2): p. 236-244.
116. Fallas, M.M., et al., *Investigation of the effect of pressure on retention of small molecules using reversed-phase ultra-high-pressure liquid chromatography*. Journal of Chromatography A, 2008. **1209**(1–2): p. 195-205.
117. Shen, Y., Y.J. Yang, and M.L. Lee, *Fundamental Considerations of Packed-Capillary GC, SFC, and LC Using Nonporous Silica Particles*. Analytical Chemistry, 1997. **69**(4): p. 628-635.
118. dos Santos Pereira, A., et al., *Green hydrophilic interaction chromatography using ethanol–water–carbon dioxide mixtures*. Journal of Separation Science, 2010. **33**(6-7): p. 834-837.
119. Pyo, D., *Temperature-controlled restrictor for UV detection in capillary supercritical fluid chromatography*. BULLETIN-KOREAN CHEMICAL SOCIETY, 2006. **27**(9): p. 1429.
120. Aubin, A. and U. Neue. *Harnessing the Power of Sub-2 $\mu\text{m}$  Chromatographic Particles in Supercritical Fluid Chromatography*. in *SFC User Meeting*. 2010. Stockholm.
121. de Villiers, A., et al., *Influence of frictional heating on temperature gradients in ultra-high-pressure liquid chromatography on 2.1mm I.D. columns*. (0021-9673 (Print)).
122. Giddings, J.C., *Unified separation science*. 1991: Wiley New York etc.
123. Keunckharian, S., et al., *Effect of sample solvent on the chromatographic peak shape of analytes eluted under reversed-phase liquid chromatographic conditions*. Journal of Chromatography A, 2006. **1119**(1): p. 20-28.
124. Layne, J., et al., *Volume-load capacity in fast-gradient liquid chromatography*. Journal of Chromatography A, 2001. **913**(1): p. 233-242.
125. Berger, T.A. and J.F. Deye, *Effect of basic additives on peak shapes of strong bases separated by packed-column supercritical fluid chromatography*. Journal of chromatographic science, 1991. **29**(7): p. 310-317.

126. Fairchild, J.N., J.F. Hill, and P.C. Iraneta, *Influence of sample solvent composition for SFC separations*. LC GC North America, 2013. **31**(4): p. 326-333.
127. Blilie, A.L. and T. Greibrokk, *Modifier effects on retention and peak shape in supercritical fluid chromatography*. Analytical Chemistry, 1985. **57**(12): p. 2239-2242.
128. West, C., S. Khater, and E. Lesellier, *Characterization and use of hydrophilic interaction liquid chromatography type stationary phases in supercritical fluid chromatography*. Journal of Chromatography A, 2012. **1250**(0): p. 182-195.
129. West, C. and E. Lesellier, *Characterisation of stationary phases in subcritical fluid chromatography with the solvation parameter model IV: Aromatic stationary phases*. Journal of Chromatography A, 2006. **1115**(1-2): p. 233-245.
130. West, C. and E. Lesellier, *Characterisation of stationary phases in subcritical fluid chromatography by the solvation parameter model: II. Comparison tools*. Journal of Chromatography A, 2006. **1110**(1-2): p. 191-199.
131. West, C. and E. Lesellier, *Characterisation of stationary phases in subcritical fluid chromatography with the solvation parameter model: III. Polar stationary phases*. Journal of Chromatography A, 2006. **1110**(1-2): p. 200-213.
132. West, C. and E. Lesellier, *Orthogonal screening system of columns for supercritical fluid chromatography*. Journal of Chromatography A, 2008. **1203**(1): p. 105-113.
133. West, C. and E. Lesellier, *Chemometric methods to classify stationary phases for achiral packed column supercritical fluid chromatography*. Journal of Chemometrics, 2012. **26**(3-4): p. 52-65.
134. West, C. and E. Lesellier, *Effects of mobile phase composition on retention and selectivity in achiral supercritical fluid chromatography*. Journal of Chromatography A, 2013. **1302**(0): p. 152-162.
135. West, C., J. Ogden, and E. Lesellier, *Possibility of predicting separations in supercritical fluid chromatography with the solvation parameter model*. Journal of Chromatography A, 2009. **1216**(29): p. 5600-5607.
136. Jacob Fairchild, J.H., Pam Iraneta, and Tom Walter. *ACQUITY UPC2: New Capabilities and Possibilities for Separations Science*. in *HPLC 2012*. 2012. Anaheim, CA.
137. Fairchild, J.N., et al., *Chromatographic evidence of silyl ether formation (SEF) in supercritical fluid chromatography*. (1520-6882 (Electronic)).
138. Lesellier, E., C. West, and A. Tchaplal, *Classification of special octadecyl-bonded phases by the carotenoid test*. Journal of Chromatography A, 2006. **1111**(1): p. 62-70.
139. Poole, C.F., *Stationary phases for packed-column supercritical fluid chromatography*. Journal of Chromatography A, 2012. **1250**(0): p. 157-171.
140. de la Puente, M.L., P. López Soto-Yarritu, and J. Burnett, *Supercritical fluid chromatography in research laboratories: Design, development and implementation of an efficient generic screening for exploiting this technique in the achiral environment*. Journal of Chromatography A, 2011. **1218**(47): p. 8551-8560.
141. Pascolutti, M. and R.J. Quinn, *Natural products as lead structures: chemical transformations to create lead-like libraries*. Drug Discovery Today, 2014. **19**(3): p. 215-221.
142. Clark, A.M., *Natural products as a resource for new drugs*. Pharmaceutical research, 1996. **13**(8): p. 1133-1141.
143. Rodrigues, T., et al., *Counting on natural products for drug design*. Nature chemistry, 2016. **8**(6): p. 531-541.
144. Lanzotti, V., *Natural products in drug discovery: from classical methods to metabolomic approaches*. Planta Medica, 2016. **81**(S 01): p. KL1.
145. Barnes, E.C., R. Kumar, and R.A. Davis, *The use of isolated natural products as scaffolds for the generation of chemically diverse screening libraries for drug discovery*. Natural product reports, 2016. **33**(3): p. 372-381.

146. Luesch, H., *18 Marine natural products as starting points for drug discovery and development*. Biochemical Pharmacology, 2017. **139**: p. 106-107.
147. Patridge, E., et al., *An analysis of FDA-approved drugs: natural products and their derivatives*. Drug discovery today, 2016. **21**(2): p. 204-207.
148. Systems, D.C.I. SMARTS - A Language for Describing Molecular Patterns. 2008; Available from: <http://www.daylight.com/dayhtml/doc/theory/theory.smarts.html>.
149. Eldridge, G.R., et al., *High-Throughput Method for the Production and Analysis of Large Natural Product Libraries for Drug Discovery*. Analytical Chemistry, 2002. **74**(16): p. 3963-3971.
150. Khater, S., C. West, and E. Lesellier, *Characterization of five chemistries and three particle sizes of stationary phases used in supercritical fluid chromatography*. Journal of Chromatography A, 2013. **1319**(0): p. 148-159.
151. Muchmore, S.W., et al., *Cheminformatic Tools for Medicinal Chemists*. Journal of Medicinal Chemistry, 2010. **53**(13): p. 4830-4841.
152. Ertl, P., *Cheminformatics Analysis of Organic Substituents: Identification of the Most Common Substituents, Calculation of Substituent Properties, and Automatic Identification of Drug-like Bioisosteric Groups*. Journal of Chemical Information and Computer Sciences, 2003. **43**(2): p. 374-380.
153. Hann, M.M. and T.I. Oprea, *Pursuing the leadlikeness concept in pharmaceutical research*. Current Opinion in Chemical Biology, 2004. **8**(3): p. 255-263.
154. Southan, C., P. Varkonyi, and S. Muresan, *Complementarity Between Public and Commercial Databases: New Opportunities in Medicinal Chemistry Informatics*. Current Topics in Medicinal Chemistry, 2007. **7**(15): p. 1502-1508.
155. Willett, P., *Chemoinformatics – similarity and diversity in chemical libraries*. Current Opinion in Biotechnology, 2000. **11**(1): p. 85-88.
156. Lipinski, C.A., et al., *Experimental and computational approaches to estimate solubility and permeability in drug discovery and development settings*. Advanced Drug Delivery Reviews, 1997. **23**(1–3): p. 3-25.
157. Grand-Guillaume Perrenoud, A., et al., *Analysis of basic compounds by supercritical fluid chromatography: Attempts to improve peak shape and maintain mass spectrometry compatibility*. Journal of Chromatography A, 2012. **1262**(0): p. 205-213.
158. Daylight Chemical Information Systems. Available from: webpage [http://www.daylight.com/dayhtml\\_tutorials/languages/smarts/smarts\\_examples.html](http://www.daylight.com/dayhtml_tutorials/languages/smarts/smarts_examples.html).
159. Coates, W.J., D.J. Hunter, and W.S. MacLachlan, *Successful implementation of automation in medicinal chemistry*. Drug Discovery Today, 2000. **5**(11): p. 521-527.
160. Godfrey, A.G., T. Masquelin, and H. Hemmerle, *A remote-controlled adaptive medchem lab: an innovative approach to enable drug discovery in the 21st Century*. Drug Discovery Today, 2013. **18**(17–18): p. 795-802.
161. Potoski, J., *Timely synthetic support for medicinal chemists*. Drug Discovery Today, 2005. **10**(2): p. 115-120.
162. Koppitz, M. and K. Eis, *Automated medicinal chemistry*. Drug Discovery Today, 2006. **11**(11–12): p. 561-568.
163. Ceglia, S., *Personal Communications*. 2015.
164. Agilent OpenLAB CDS. Available from: Agilent webpage <https://www.chem.agilent.com/en-US/products-services/Software-Informatics/OpenLAB-CDS-Automated-Purification-Software/Pages/default.aspx>.
165. Shimadzu Open Source CDS. Available from: Shimadzu webpage <https://www.ssi.shimadzu.com/products/product.cfm?product=openzol>.
166. Waters Open Access. Available from: Waters webpage [http://www.waters.com/waters/en\\_US/Open-Access/nav.htm?cid=514532](http://www.waters.com/waters/en_US/Open-Access/nav.htm?cid=514532).



167. Aurigemma, C. and W. Farrell, *FastTrack to supercritical fluid chromatographic purification: Implementation of a walk-up analytical supercritical fluid chromatography/mass spectrometry screening system in the medicinal chemistry laboratory*. Journal of Chromatography A, 2010. **1217**(39): p. 6110-6114.
168. Chan, E.C.Y., et al., *An automated LC method for the small-scale purification of organic molecules derived from combinatorial libraries*. Journal of Pharmaceutical and Biomedical Analysis, 2002. **29**(1-2): p. 139-146.
169. Pramanik, B.N., G. Bartner PI Fau - Chen, and G. Chen, *The role of mass spectrometry in the drug discovery process*. (1367-6733 (Print)).
170. Ackermann, B.L., et al., *Current Applications of Liquid Chromatography/Mass Spectrometry in Pharmaceutical Discovery After a Decade of Innovation*. Annual Review of Analytical Chemistry, 2008. **1**(1): p. 357-396.
171. Zhang, X., et al., *Development of a Mass-Directed Preparative Supercritical Fluid Chromatography Purification System*. Journal of Combinatorial Chemistry, 2006. **8**(5): p. 705-714.
172. White, C. and J. Burnett, *Integration of supercritical fluid chromatography into drug discovery as a routine support tool: II. Investigation and evaluation of supercritical fluid chromatography for achiral batch purification*. Journal of Chromatography A, 2005. **1074**(1-2): p. 175-185.
173. White, C., *Integration of supercritical fluid chromatography into drug discovery as a routine support tool: Part I. Fast chiral screening and purification*. Journal of Chromatography A, 2005. **1074**(1-2): p. 163-173.
174. Niessen, W.M.A., J. Lin, and G.C. Bondoux, *Developing strategies for isolation of minor impurities with mass spectrometry-directed fractionation*. Journal of Chromatography A, 2002. **970**(1-2): p. 131-140.
175. Ventura, M., et al., *High-throughput preparative process utilizing three complementary chromatographic purification technologies*. Journal of Chromatography A, 2004. **1036**(1): p. 7-13.
176. Matsumori, N., et al., *Stereochemical Determination of Acyclic Structures Based on Carbon-Proton Spin-Coupling Constants. A Method of Configuration Analysis for Natural Products*. The Journal of Organic Chemistry, 1999. **64**(3): p. 866-876.
177. Koehn, F.E. and G.T. Carter, *The evolving role of natural products in drug discovery*. Nature reviews Drug discovery, 2005. **4**(3): p. 206-220.
178. Echemendía, R., et al., *Highly Stereoselective Synthesis of Natural-Product-Like Hybrids by an Organocatalytic/Multicomponent Reaction Sequence*. Angewandte Chemie International Edition, 2015. **54**(26): p. 7621-7625.
179. Hanessian, S., *Approaches to the total synthesis of natural products using "chiral templates" derived from carbohydrates*. Accounts of Chemical Research, 1979. **12**(5): p. 159-165.
180. Bringmann, G. and D. Menche, *Stereoselective Total Synthesis of Axially Chiral Natural Products via Biaryl Lactones†*. Accounts of Chemical Research, 2001. **34**(8): p. 615-624.
181. Austin, J.F. and D.W.C. MacMillan, *Enantioselective Organocatalytic Indole Alkylations. Design of a New and Highly Effective Chiral Amine for Iminium Catalysis*. Journal of the American Chemical Society, 2002. **124**(7): p. 1172-1173.
182. Calter, M.A. and W. Liao, *First Total Synthesis of a Natural Product Containing a Chiral, 6-Diketone: Synthesis and Stereochemical Reassignment of Siphonarienedione and Siphonarienolone*. Journal of the American Chemical Society, 2002. **124**(44): p. 13127-13129.
183. Baumann, M. and I.R. Baxendale, *An overview of the synthetic routes to the best selling drugs containing 6-membered heterocycles*. Beilstein Journal of Organic Chemistry, 2013. **9**: p. 2265-2319.
184. Endo, A., *The origin of the statins*. Atherosclerosis Supplements, 2004. **5**(3): p. 125-130.

185. Endo, A. and M. Kuroda, *Citrinin, An Inhibitor of Cholesterol Synthesis*. The Journal of Antibiotics, 1976. **29**(8): p. 841-843.
186. Bastarda, A., R. Grahek, and M. Crnugelj, *Process for the preparation of methyl ester of rosuvastatin*. 2009, Google Patents.
187. Watanabe, M., et al., *Synthesis and biological activity of methanesulfonamide pyrimidine- and N-methanesulfonyl pyrrole-substituted 3,5-dihydroxy-6-heptenoates, a novel series of HMG-CoA reductase inhibitors*. Bioorganic & medicinal chemistry, 1997. **5**(2): p. 437-444.
188. Pandey, B., V.B. Lohray, and B.B. Lohray, *Process to prepare clopidogrel*. 2003, Google Patents.
189. Bristow, T.T., et al., *On-line Monitoring of Continuous Flow Chemical Synthesis Using a Portable, Small Footprint Mass Spectrometer*. Journal of The American Society for Mass Spectrometry, 2014. **25**(10): p. 1794-1802.
190. Browne, D.L., et al., *Continuous flow reaction monitoring using an on-line miniature mass spectrometer*. Rapid Communications in Mass Spectrometry, 2012. **26**(17): p. 1999-2010.
191. Jones, M.D. *Exploring the Use of Elevated Temperature for UPLC Applications*. in ISC 2006. 2006. Copenhagen, Denmark.
192. Hirai, K., et al., *Pyrimidine derivatives*. 1993, Google Patents.
193. Fairchild, J. *Simple Guidelines for Choosing the Right Injection Solvent for UltraPerformance Convergence Chromatography (UPC2)*. 2014; [Waters Application Note 720004981en].
194. Srivastava, M., et al., *Chamomile (Matricaria chamomilla L.): An overview*. Vol. 5. 2011. 82-95.
195. Kunde, R. and O. Isaac, *Über die Flavone der Kamille (Matricaria chamomilla L.) und ein neues acetyliertes Apigenin-7-glucosid*. Planta Med, 1979. **37**(10): p. 124-130.
196. O'Hara, M., et al., *A review of 12 commonly used medicinal herbs*. Arch Fam Med, 1998. **7**(6): p. 523-36.
197. Wilkinson, S.M., B.M. Hausen, and M.H. Beck, *Allergic contact dermatitis from plant extracts in a cosmetic*. Contact Dermatitis, 1995. **33**(1): p. 58-59.
198. Bohlmann, F. and C. Zdero, *Sesquiterpene lactones and other constituents from Tanacetum parthenium*. Phytochemistry, 1982. **21**(10): p. 2543-2549.
199. Hänsel, R., Rimpler, H., Walther, K., *Naturwissenschaften*, in *Verzeichnis der Spezialbibliotheken in der Bundesrepublik Deutschland einschließlich West-Berlin*, F. Meyen, Editor. 1970, Vieweg+Teubner Verlag. p. 56-82.
200. Srivastava, J.K., E. Shankar, and S. Gupta, *Chamomile: A herbal medicine of the past with bright future*. Mol Med Rep, 2010. **3**(6): p. 895-901.
201. Bangha, E., P. Elsner, and J.F.J. Fowler, *Occupational Contact Dermatitis Toward Sesquiterpene Lactones in a Florist*. Dermatitis, 1996. **7**(3): p. 188-190.
202. Paulsen, E., *Contact sensitization from Compositae-containing herbal remedies and cosmetics*. Contact Dermatitis, 2002. **47**(4): p. 189-198.
203. Pereira, F., Santos, R., Pereira, A., *Contact dermatitis from chamomile tea*. Contact Dermatitis, 1997. **36**(6): p. 307.
204. Jinno, K., *Hyphenated Techniques in Supercritical Fluid Chromatography and Extraction*. 1992: Elsevier Science.
205. Nováková, L., L. Matysová, and P. Solich, *Advantages of application of UPLC in pharmaceutical analysis*. Talanta, 2006. **68**(3): p. 908-918.
206. Wu, N., et al., *Effect of extra-column volume on practical chromatographic parameters of sub-2- $\mu$ m particle-packed columns in ultra-high pressure liquid chromatography*. Journal of Separation Science, 2012. **35**(16): p. 2018-2025.
207. Kamangerpour, A., et al., *Supercritical Fluid Chromatography of polyphenolic compounds in grape seed extract*. Chromatographia, 2002. **55**(7-8): p. 417-421.

- 
208. Zhimin, L., et al., *Determination of the Flavonoids from Ginkgo Biloba L. Extract by Supercritical Fluid Chromatography*. Chinese Journal of Analytical Chemistry, 1999. **27**(2): p. 214-216.
209. Plumb, R.S., et al., *A Rapid Simple Approach to Screening Pharmaceutical Products Using Ultra-Performance LC Coupled to Time-of-Flight Mass Spectrometry and Pattern Recognition*. Journal of Chromatographic Science, 2008. **46**(3): p. 193-198.
210. Eriksson, L.U.A., *Multi- and megavariable data analysis. P. 1, P. 1*. 2006, Umeå: Umetrics Academy.
211. Tarafder, A., et al., *A scaling rule in supercritical fluid chromatography. I. Theory for isocratic systems*. (1873-3778 (Electronic)).
212. Barnard, J.M., et al., *Use of Markush structure analysis techniques for descriptor generation and clustering of large combinatorial libraries*. Journal of Molecular Graphics and Modelling, 2000. **18**(4-5): p. 452-463.
213. Calcagno, M., *An investigation into analyzing patents by chemical structure using Thomson's Derwent World Patent Index codes*. World Patent Information, 2008. **30**(3): p. 188-198.

## Bibliography

### Publications

1. Salazar, C., Jones, M.D., Horn, P., Crossley, J., Chapman, K., Langridge, J., Isaac, G., Smith, N., Shulaev, V. *Application of Sub-2 $\mu$ m particle CO<sub>2</sub>-based Chromatography Coupled to Mass Spectrometry for Comprehensive and Targeted Analysis of Lipids in Cottonseed Extracts*. Rapid Communications in Mass Spectrometry (Submitted Sept. 2016)
2. Gao, J., Ceglia, S., Jones, M.D., Simeone, J., Van Antwerp, J., Zhang, L., Ross, C., Helmy, R. *A novel compact mass detection platform for the open access (OA) environment in drug discovery and early development*. Journal of pharmaceutical and biomedical analysis. 2016. **122**: p.1-8
3. Ashraf-Khorassani, M., Yang, J., Rainville, P., Jones, M. D., Fountain, K. J., Isaac, G., & Taylor, L. T. *Ultrahigh performance supercritical fluid chromatography of lipophilic compounds with application to synthetic and commercial biodiesel*. Journal of Chromatography B, 2015 **983**: p. 94-100.
4. Jones, M. D., Avula, B., Wang, Y. H., Lu, L., Zhao, J., Avonto, C, Isaac, G., Meeker, L., Yu, K., Legido-Quigley, C., Smith, N., Khan, I.A. *Investigating sub-2 $\mu$ m particle stationary phase supercritical fluid chromatography coupled to mass spectrometry for chemical profiling of chamomile extracts*. Analytica chimica acta, 2014. **847**: p. 61-72.
5. Jones, M. D., Rainville, P. D., Isaac, G., Wilson, I. D., Smith, N. W., & Plumb, R. S. *Ultra-high resolution SFC–MS as a high throughput platform for metabolic phenotyping: Application to metabolic profiling of rat and dog bile*. Journal of Chromatography B, 2014. **966**: 200-207.
6. Heaton J, Jones MD, Legido-Quigley C, Plumb RS, Smith NW. *Systematic evaluation of acetone and acetonitrile for use in hydrophilic interaction liquid chromatography coupled with electrospray ionization mass spectrometry of basic small molecules*. Rapid Communications in Mass Spectrometry. 2011 **25**(24): p. 3666-74.

### Trade Articles

1. Hong, P., Aubin, A., and Jones, M..D. *Practical Considerations for Achiral Analysis of Pharmaceutical compounds Using Convergence Chromatography*. SepSci, 2013. Europe. 5(1): p2-6.
2. Cabovska, B., Jones, M.D., Aubin, A. *Application of SFC to Leachables/Extractables Analysis*. American Pharmaceutical Review.  
<http://www.americanpharmaceuticalreview.com>

## Conference Presentations

1. Jones, M.D., *Lipid Profiling Using Sub-2 $\mu$ m Particle CO<sub>2</sub> Based Supercritical Fluid Chromatography Coupled to Mass Spectrometry*; SFC 2013
2. Jones, M.D, Salazar, C. and Shulaev, V., *Application of Sub-2 $\mu$ m particle CO<sub>2</sub>-based Chromatography Coupled to Mass Spectrometry for Comprehensive and Targeted Lipidomics*. CoSMoS 2013
3. Jones, M.D, Isaac, G., *Investigating a Lipid Analysis Method Development Approach Utilizing Sub-2 $\mu$ m particle Supercritical Fluid Chromatography Coupled to Mass Spectrometry*. HPLC 2012. \*Session Co-Chair

## Webinars

1. Jones, M. and Guillarme, D., *Increasing the Scope of Your Analytical Toolbox with UltraPerformance Convergence Chromatography (UPC<sup>2</sup>) Episode 2: Solving Complex Challenges in the Pharmaceutical Laboratory with the ACQUITY UPC<sup>2</sup> System*. LCGC North America.  
<https://event.on24.com/eventRegistration/EventLobbyServlet?target=registration.jsp&eventid=528656&sessionid=1&key=3849A510DD640A0108BACB545F46372&sourcepage=register>

## Poster Presentations

1. Jones, M.D., Vezele, Y., Worthen, D., Smith, N. *A Study Comparing SFE and Liquid-Liquid Extractions of Garcinia Kola*. paper presented at SFC2014
2. Jones, M.D., McCarthy, S., Aubin, A., Hong, P., Smith, N. *Investigating the Implementation of Convergence Chromatography for Medicinal Chemistry and Process Development Laboratories*. paper presented at SFC2014
3. Hong, P., Jones, M.D., McConville, P.; “*Chromatographic Method Development Strategies With Carbon Dioxide Mobile Phases and Sub 2- $\mu$ m Column Chemistries*”; paper presented at SFC 2013
4. Cabovska, B., Jones, M.D., Aubin, A.; “*Application of SFC to Leachables/Extractables Analysis*” paper presented at SFC2012
5. Jones, M.D., Legido-Quigley, C., Smith, N., Aubin, A. *A Critical Evaluation of Sub-2 $\mu$ m particles for Packed Column Supercritical Fluid Chromatography*. paper presented at HPLC 2011